

*This copy of the thesis has been supplied on condition that anyone who consults it is understood to recognise that the copyright rests with its author and that no quotation from the thesis and no information derived from it may be published without the author's prior consent*

---

# **FRICTION AND WEAR PERFORMANCE OF LIFEBOAT LAUNCH SLIPWAYS**

---

**BEN THOMAS**

**A thesis submitted in partial fulfilment of the requirements of  
Bournemouth University for the degree of Doctor of Philosophy**

**July 2009**

**Bournemouth University  
In collaboration with the  
Engineering and Physical Sciences Research Council  
and the  
Royal National Lifeboat Institution**



# ABSTRACT

---

The Royal National Lifeboat Institution provides a marine search and rescue service using lifeboat stations sited along the coast of the UK and Ireland. In locations where there is no natural harbour or where there is a large tidal range it is necessary to use an inclined slipway to launch a large lifeboat. Lifeboat slipway stations consist of an initial section where the boat is held on rollers followed by an inclined keelway of nickel/chromium coated steel, the lifeboat is released from the top of the slipway and proceeds under its own weight into the water. The lifeboat is subsequently recovered to the top of the slipway using a winch line. With the introduction of the new, larger Tamar class lifeboat existing boathouses are being upgraded and existing low friction coated steel slipway lining materials replaced with a low-friction jute fibre/phenolic resin composite. The composite slipway lining material was selected in part because it was able to run unlubricated or water lubricated. However the friction problems have been such that it is usual to line the slipway with grease before every launch and recovery. This adds to the number of operations involved in a launch and has safety implications. The use of grease to line the slipway results in the grease being washed out to sea with effects on the surrounding area, it is likely that there is some environmental impact due to this as the grease is non-biodegradable and not recommended for open water use according to the material data sheet. Because of these issues it is desirable to develop a set of working guidelines for crews to reduce both these risks by setting appropriate conditions for the manual application of grease along the slipway. These guidelines will also feature a method of assessing the wear of slipway panels so that panels can be replaced before they present a hazard to lifeboat operation. This thesis describes a method for assessing slipway lining materials and lubricants. Appropriate tribometer test machines are selected to assess slipway lining materials performance, the TE57 reciprocating tribometer and the TE92 rotary tribometer are used in conjunction to ascertain friction and wear performance respectively. These results are combined with detailed slipway panel surveys and case studies, and with Finite Element models to develop a method for assessing and predicting the friction and wear along a panel lined slipway. These results are used to develop slipway performance monitoring techniques for lifeboat crews and to develop design modification to combat high friction and wear on slipway panels. The adoption of a modified slipway panel and water lubrication system is proposed, this arrangement reduces panel misalignment contributions to slipway friction and wear resulting in more reliable slipway performance and is also projected to save the RNLI up to £195k annually compared with current practice.

# PUBLICATIONS RESULTING FROM THESIS

---

- Thomas, B:** 'Sustainable Design of Lifeboat Launch Systems' House of Commons: Presentations by Britain's Top Younger Engineers (2005)
- Thomas, B:** 'Experimental Wear Modelling of Lifeboat Slipway Launches' 35<sup>th</sup> Leeds-Lyon Symposium on Tribology (2008)
- Thomas, B, Hadfield, M and Austen, S:** 'Experimental Wear Modelling of Lifeboat Slipway Launches' Tribology International: 35th Leeds-Lyon Symposium on Tribology Special Issue (2009)
- Thomas, B:** 'Wear Mechanisms Applied to Lifeboat Slipway Launches' International Conference on Abrasive Processes (2008)
- Thomas, B, Hadfield, M and Austen, S:** 'Wear Observations Applied to Lifeboat Slipway Launches' Wear, Special Issue: 1st International Conference on Abrasive Processes (2009)
- Thomas, B:** 'Design of Lifeboat Slipways' Internal RNLI Document, Royal National Lifeboat Institute (2009)
- Thomas, B:** 'Design of Lifeboat Slipway Linings - Methodology' Internal RNLI Document, Royal National Lifeboat Institute (2009)
- Thomas, B:** 'Lifeboat Slipway Usage Guidelines' Internal RNLI Document, Royal National Lifeboat Institute (2009)
- Thomas, B, Hadfield, M and Austen, S:** 'Wear and friction modelling on lifeboat launch systems' Tribology Transactions (accepted) (2009)
- Thomas, B, Hadfield, M and Austen, S:** 'Reducing wear and friction on lifeboat launch slipway panels' Journal of Naval Architecture and Marine Engineering (submitted) (2009)
- Thomas, B:** 'Wear and Friction performance of lifeboat launch slipways' Tribology and Design 2010: Third International conference on Tribology and Design (abstract accepted) (2009)

# LIST OF CONTENTS

<b>1. INTRODUCTION</b>	<b>1</b>
1.1. BACKGROUND TO RESEARCH	1
1.2. AIMS	3
1.3. OBJECTIVES	3
1.4 SCOPE OF RESEARCH	4
1.5 BENEFICIARIES	4
1.6 LITERATURE REVIEW	4
1.6.1 OUTLINE	4
1.6.2 TRIBOLOGICAL CONSIDERATIONS	5
1.6.2.1 WEAR	6
1.6.2.2 FRICTION	10
1.6.2.3 LUBRICATION	12
1.6.3. FINITE ELEMENT ANALYSIS FOR WEAR PREDICTION	15
1.6.4. REVIEW OF SHIP LAUNCHING	16
1.7. PREVIOUS WORK	17
1.8. STATE OF THE ART	17
1.9 STRUCTURE OF THESIS	18
<b>2. SLIPWAY LAUNCHED LIFEBOATS OPERATIONAL ANALYSIS</b>	<b>20</b>
2.1. OVERVIEW – SLIPWAY LIFEBOATS DEVELOPMENT: 1960 - PRESENT	21
2.1.1. MODERN DESIGN AND TRENDS	22
2.2. SLIPWAY DESIGN	25
2.2.1. INITIAL SLIPWAY DESIGN OBSERVATIONS	28
2.3. SLIPWAY PANEL GEOMETRY	29
2.4. SLIPWAY LINING MATERIALS	30
2.4.1. LOW FRICTION STEEL SLIPWAY LINING	30
2.4.2. COMPOSITE SLIPWAY LINING	31
2.4.3. STEEL ROLLERS	33
2.5. SLIPWAY LUBRICANTS	34
2.5.1. MARINE GREASE	34
2.5.2. MICROBALL LUBRICANT	34
2.5.3. FRESHWATER	35
2.5.4. SEAWATER	35
2.5.5. BIOGREASE #1	35
2.5.6. BIOGREASE #2	35
2.6. SLIPWAY OPERATION	36
<b>3. CASE STUDIES</b>	<b>39</b>
3.1. CASE STUDY 1 – SELSEY	39
3.2. CASE STUDY 2 – BEMBRIDGE	46
3.3. CASE STUDY 3 – SENNEN COVE	51
3.4. CASE STUDY 4 – THE LIZARD SLIPWAY	56
3.5. CASE STUDY 5 – TENBY	60
3.6. CASE STUDY 6 – PADSTOW SLIPWAY INSPECTION	70

3.7. CASE STUDIES – SUMMARY	75
<b>4. EXPERIMENTAL WEAR MODELLING</b>	<b>83</b>
4.1 BACKGROUND OF WEAR BENCH TESTING	83
4.1.1 OVERVIEW OF SHIP LAUNCH SLIPWAY FRICTION TESTING	84
4.1.2 EXISTING SLIPWAY LINING TESTING	86
4.2 SELECTION OF TEST MACHINE	87
4.2.1 PLINT TE57 MICROPROCESSOR CONTROLLED RECIPROCATING FRICTION MACHINE	88
4.2.2 PLINT TE92 MICROPROCESSOR CONTROLLED ROTARY FRICTION MACHINE	89
4.3. SURFACE ANALYSIS	90
4.4. DESIGN OF EXPERIMENTS	91
4.5. DESIGN OF RECIPROCATING TEST RIG	91
4.5.1. RECIPROCATING TEST PARAMETER CALCULATION	93
4.6. DESIGN OF ROTARY TEST RIG	94
4.6.1. ROTARY TEST PARAMETER CALCULATION	95
<b>5. TEST METHODOLOGY</b>	<b>96</b>
5.1. TE57 RECIPROCATING TRIBOMETER: EXPERIMENTAL METHODOLOGY	96
5.2. TE92 ROTARY TRIBOMETER: EXPERIMENTAL METHODOLOGY	101
<b>6. EXPERIMENTAL RESULTS</b>	<b>104</b>
6.1. TE57 RECIPROCATING TRIBOMETER	104
6.1.1. TE57 CONTACT FORCE TESTS - RESULTS:	104
6.1.2. TE57 WEAR TESTS – RESULTS:	108
6.1.3. TE57 RESULTS: DISCUSSION	113
6.2. TE92 ROTARY TRIBOMETER	115
6.2.1. CONTACT FORCE TESTS – RESULTS	115
6.2.2. LUBRICANT TESTS – RESULTS	118
6.2.3. TE92 RESULTS: DISCUSSION	120
6.3 CONCLUSIONS	122
<b>7. FEA MODELLING – EXISTING SLIPWAY PANEL</b>	<b>123</b>
7.1. FEA MODELLING OF EXISTING SLIPWAY PANEL GEOMETRY	123
7.1.1. ONE PANEL ALIGNED CASE	124
7.1.2. TWO PANEL ALIGNED CASE	128
7.2. TWO PANEL MISALIGNMENT MODELLING	128
7.2.1. PARALLEL PANEL MISALIGNMENT	129
7.2.2 ANGLED PANEL MISALIGNMENT	130
7.2.3 SKEWED PANEL MISALIGNMENT	130
7.2.4 RESULTS	131
7.2.5. DISCUSSION	136
<b>8. FEA MODELLING – MODIFIED SLIPWAY PANEL</b>	<b>138</b>
8.1 MODIFIED SLIPWAY PANEL DESIGN	138
8.1.1. COMPARISON OF ORIGINAL VS. MODIFIED SLIPWAY PANEL GEOMETRY	143
8.2. OPTIMISATION OF MODIFIED SLIPWAY PANEL GEOMETRY	149
8.2.2. RESULTS:	151

8.2.2.1. VON MISES MAX. STRESS (SMX.)	151
8.2.2.2. MAX. FRICTION FORCE	153
8.2.2.3. MAX. WEAR RATE	155
8.2.3. CONCLUSIONS	156
8.3. KINEMATIC ANALYSIS OF SLIPWAY PANEL CHAMFER EFFECTS	157
8.3.1. EFFECTS ON WINCH LOADING DURING RECOVERY	157
8.3.2. EFFECTS ON LIFEBOAT MOUNTING THE SLIPWAY	159
8.3.3. EFFECTS OF REDUCED CONTACT AREA ON FRICTION	161
8.3. FEA CONCLUSIONS	162
<b>9. APPLIED RESULTS</b>	<b>163</b>
9.1. EXPECTED PANEL LIFESPAN FOR VARYING CONDITIONS	163
9.2. COMPARISON OF ORIGINAL AND MODIFIED SLIPWAY PANEL EXPECTED LIFESPAN	165
9.3. FRICTION COEFFICIENT BASED SLIPWAY PANEL EXPECTED LIFESPANS	167
9.4. PANEL FAILURE GUIDELINES	171
9.5. PANEL REPLACEMENT CRITERIA	173
9.5.1. WEAR – VISUAL INSPECTION FOR HIGH FRICTION PREVENTION	173
9.5.2. OTHER VISUAL WEAR FAILURE CRITERIA	174
9.5.3. UNEVEN PANEL END WEAR	175
9.5.4. OTHER VISUAL INDICATORS OF HIGH FRICTION CAUSES	176
<b>10. SUSTAINABILITY CONSIDERATIONS</b>	<b>177</b>
10.1 LIFE CYCLE ANALYSIS	177
10.2. MATERIALS BASED ENVIRONMENTAL ANALYSIS	178
10.3. LUBRICANTS BASED ENVIRONMENTAL ANALYSIS	179
10.4 WIDER SUSTAINABILITY CONSIDERATIONS	180
10.4.1 ECONOMIC ANALYSIS	180
10.4.2. SOCIAL CONSIDERATIONS	182
10.5. DISCUSSION	182
<b>11. DISCUSSION</b>	<b>184</b>
11.1. CONTACT MECHANISMS	184
11.2. LUBRICATION REGIME DETERMINATION	185
11.3. DRY WEAR	185
11.4. LUBRICATED WEAR	186
11.5. CONTAMINATED WEAR	186
11.6. REAL WORLD WEAR	187
11.7. DRY SLIDING FRICTION	188
11.8. LUBRICATED SLIDING FRICTION	188
11.9. CONTAMINATED FRICTION	189
11.10. REAL WORLD FRICTION	190
11.11. SUSTAINABILITY CONSIDERATIONS	191
11.12. IMPLICATIONS	192
<b>12. CONCLUSIONS</b>	<b>195</b>
<b>13. RECOMMENDATIONS</b>	<b>196</b>

<b>REFERENCES</b>	<b>197</b>
<b>APPENDIX A</b>	<b>201</b>
<b>APPENDIX B</b>	<b>204</b>
<b>APPENDIX C</b>	<b>205</b>
<b>APPENDIX D</b>	<b>215</b>
<b>APPENDIX E</b>	<b>216</b>
<b>APPENDIX F</b>	<b>240</b>
<b>APPENDIX G</b>	<b>244</b>
<b>APPENDIX H</b>	<b>246</b>
<b>APPENDIX I</b>	<b>249</b>

# LIST OF FIGURES

FIG 1.1: ASPERITY CONTACT	1
FIG 1.2: PLOUGHING ASPERITY	7
FIG 1.3: STRIBECK CURVE – ACTUAL FRICTION COEFFICIENT VALUES VARY BY MATERIAL	13
FIG 1.4: SLIPWAY LAUNCHING THROUGH THE YEARS	16
FIG. 2.1: LIFEBOAT LAUNCHED FROM SLIPWAY IN SUNDERLAND ~1970S	21
FIG. 2.2: OAKLEY CLASS LIFEBOAT	22
FIG. 2.3: TYNE CLASS LIFEBOAT LAUNCHING AT WICKLOW	23
FIG 2.4: TAMAR CLASS LIFEBOAT	23
FIG. 2.5: FREE BODY DIAGRAM OF SELSEY SLIPWAY: LAUNCH	26
FIG. 2.6: FREE BODY DIAGRAM OF SELSEY SLIPWAY: RECOVERY	27
FIG. 2.7: MAX. FRICTION COEFFICIENTS AT LAUNCH AND RECOVERY	28
FIG. 2.8: TYPICAL COMPOSITE SLIPWAY PANEL GEOMETRY	29
FIG. 2.9: NOMINAL LOW FRICTION STEEL COATING COMPOSITION	30
FIG. 2.10: COMPOSITE UNDER SEM	31
FIG. 2.11: COMPOSITE SLIPWAY LINING MANUFACTURE	32
FIG. 2.12: ORIGINAL COMPOSITE SURFACE PROFILE	33
FIG. 2.13: SLIPWAY LINING COMPOSITE - TENSILE TEST SPECIMEN	33
FIG. 2.14: FRESHWATER LUBRICATION JETS AT PADSTOW	35
FIG. 2.15: QUICK RELEASE SYSTEM – RINGED	36
FIG. 2.16: TYPICAL SLIPWAY LAUNCH – SELSEY	36
FIG. 2.17: LIFEBOAT ALIGNMENT AND ATTACHMENT OF WINCH CABLE	37
FIG. 2.18: HAUL STAGE	37
FIG. 2.19: RECOVERY WINCH	38
FIG. 3.1: SELSEY SLIPWAY STATION LOCATION	39
FIG. 3.2 SELSEY SLIPWAY STATION	40
FIG. 3.3: FREE BODY DIAGRAM OF SELSEY SLIPWAY	41
FIG. 3.4: FORCE CALCULATION ON SELSEY SLIPWAY	41
FIG. 3.5: SELSEY SLIPWAY ON QUARTERSTOPS WITH WINCH CABLE ATTACHED	41
FIG. 3.6: FORCES DURING RECOVERY FOR SELSEY SLIPWAY	42
FIG. 3.7: SELSEY SLIPWAY INSPECTION – ALGAE ON PANELS	44
FIG. 3.8: SELSEY SLIPWAY INSPECTION – EMBEDDED DEBRIS	44
FIG. 3.9: SELSEY SLIPWAY INSPECTION – WORN PANEL EDGES FROM RECOVERY KEEL IMPACTS	44
FIG. 3.10: SELSEY SLIPWAY INSPECTION – GOUGING WEAR SCARS	44
FIG. 3.11: SELSEY SLIPWAY INSPECTION – LIGHT PANEL END WEAR	45
FIG. 3.12: SELSEY SLIPWAY INSPECTION – EMBEDDED SHELL DEBRIS	45
FIG. 3.13: BEMBRIDGE SLIPWAY STATION LOCATION	46
FIG 3.14: BEMBRIDGE SLIPWAY STATION	46
FIG 3.15: BEMBRIDGE SLIPWAY STATION – SLIPWAY AND BOATHOUSE	48
FIG 3.16: BEMBRIDGE SLIPWAY INSPECTION – KEEL IMPACT DAMAGE	48
FIG 3.17: BEMBRIDGE SLIPWAY INSPECTION – PANEL END DAMAGE	48
FIG 3.18: BEMBRIDGE SLIPWAY INSPECTION – PANEL END ABRASIVE WEAR	49
FIG 3.19: BEMBRIDGE SLIPWAY INSPECTION – PLANE ABRASIVE WEAR	49

FIG. 3.20: SENNEN COVE SLIPWAY STATION LOCATION	50
FIG. 3.21: SENNEN COVE SLIPWAY STATION	51
FIG. 3.22: SENNEN COVE SAND	52
FIG. 3.23: SENNEN COVE SLIPWAYS	52
FIG. 3.24: SENNEN COVE SLIPWAY STATION – RECOVERY SLIPWAY	53
FIG. 3.25: SENNEN COVE SLIPWAY INSPECTION – LOWER LINED SECTION	53
FIG. 3.26: SENNEN COVE SLIPWAY INSPECTION	54
FIG. 3.27: SENNEN COVE SLIPWAY INSPECTION	55
FIG. 3.28: SENNEN COVE SLIPWAY INSPECTION	55
FIG. 3.29: SENNEN COVE SLIPWAY INSPECTION	55
FIG. 3.30: THE LIZARD SLIPWAY STATION LOCATION	56
FIG. 3.31: THE LIZARD SLIPWAY STATION	56
FIG. 3.32: THE LIZARD SLIPWAY	57
FIG. 3.33: THE LIZARD SLIPWAY INSPECTION: ROLLER SECTION	57
FIG. 3.34: THE LIZARD SLIPWAY INSPECTION: STEEL PANEL SECTION	58
FIG. 3.35: THE LIZARD SLIPWAY INSPECTION: GREENHEART WOOD SECTION	58
FIG. 3.36: THE LIZARD SLIPWAY INSPECTION: GREENHEART WOOD SECTION	58
FIG. 3.37: THE LIZARD SLIPWAY INSPECTION: GREENHEART WOOD SECTION	59
FIG. 3.38: TENBY SLIPWAY STATION LOCATION	60
FIG. 3.39: NEW TENBY SLIPWAY STATION	60
FIG. 3.40: TENBY SLIPWAY TRIALS – LOAD CELL RINGED	61
FIG. 3.41: WORN COMPOSITE SLIPWAY SECTION	65
FIG. 3.42: TENBY SLIPWAY INSPECTION: PANEL END WEAR	66
FIG. 3.43: TENBY SLIPWAY INSPECTION: GOUGING WEAR	67
FIG. 3.44: TENBY SLIPWAY INSPECTION: DELAMINATION WEAR	67
FIG. 3.45: END WEAR BEGINNING ON TENBY MISALIGNED SLIPWAY PANEL	67
FIG. 3.46: PANEL MISALIGNMENT MODELS	69
FIG. 3.47: PADSTOW SLIPWAY STATION LOCATION	70
FIG. 3.48: PADSTOW SLIPWAY STATION	70
FIG. 3.49: PADSTOW SLIPWAY	71
FIG. 3.50: PADSTOW SLIPWAY INSPECTION: PANEL END WEAR	72
FIG. 3.51: PADSTOW SLIPWAY INSPECTION: PANEL END WEAR	72
FIG. 3.52: PADSTOW SLIPWAY INSPECTION: PANEL END WEAR PROGRESSION	73
FIG. 3.53: PADSTOW SLIPWAY INSPECTION: GOUGING WEAR	73
FIG. 3.54: PADSTOW SLIPWAY INSPECTION: PLANE ABRASIVE WEAR	74
FIG. 3.55: ABRASIVE PANEL END WEAR: WEAR SCAR PROGRESSION	76
FIG. 3.56: CRACKING PANEL END WEAR: WEAR SCAR PROGRESSION	77
FIG. 3.57: CRACKING PANEL END WEAR: CRACKING BETWEEN FIXING BOLTS	78
FIG. 3.58: GOUGING WEAR FROM TAMAR PROTOTYPE	78
FIG. 3.59: 3 <sup>RD</sup> BODY GOUGING WEAR	79
FIG. 3.60: PLANE ABRASIVE WEAR	80
FIG. 3.61: DELAMINATION WEAR: WEAR SCAR PROGRESSION	81
FIG. 3.62: DELAMINATION WEAR: DETAIL	81
FIG. 3.63: EMBEDDED DEBRIS	82
FIG. 4.1: DENISON T67 RECIPROCATING TRIBOMETER PIN AND SAMPLE ARRANGEMENT	84



FIG 4.2: RV TRITON	85
FIG. 4.3: VOSPER THORNYCROFT TEST RIG	85
FIG. 4.4: COMPOSITE WEAR RATE TESTING	86
FIG. 4.5: PLINT TE57 CONTACT GEOMETRY	88
FIG. 4.6: PLINT TE57 RECIPROCATING TRIBOMETER SCHEMATIC	88
FIG. 4.7: PLINT TE92 CONTACT GEOMETRY	89
FIG. 4.8: PLINT TE92 ROTARY TRIBOMETER WITH TEST SAMPLE SCHEMATIC	89
FIG. 4.9: OLYMPUS BX60 LIGHT MICROSCOPE	90
FIG. 4.10: ZYGO INTERFEROMETER	90
FIG. 4.11: ORIGINAL TE57 CONTACT CONFIGURATION	91
FIG. 4.12: TE57 CONTACT DESIGN 1	92
FIG. 4.13: TE57 CONTACT DESIGN 2	93
FIG. 4.14: TE57 MODIFIED PIN DESIGN	93
FIG. 4.15: TE92 CONTACT DESIGN	94
FIG. 4.16: PLINT TE92 MODIFIED RING ON DISC CONFIGURATION	95
FIG. 5.1: PLINT TE57 COMPOSITE AND LOW FRICTION STEEL SAMPLE SPECIFICATION	98
FIG. 5.2: PLINT TE57 KEEL STEEL PIN SPECIFICATION	98
FIG. 5.3: PLINT TE92 COMPOSITE SAMPLE SPECIFICATION	102
FIG. 5.4: PLINT TE92 KEEL STEEL PIN SPECIFICATION	102
FIG. 6.1: TE57 COMPOSITE FRICTION COEFFICIENT VS. CONTACT PRESSURE	105
FIG. 6.2: TE57 COMPOSITE VS. LOW FRICTION STEEL FRICTION COEFFICIENT	105
FIG. 6.3. TE57 COMPOSITE CONTACT TESTS	106
FIG. 6.4. TE57 COMPOSITE DRY CONTACT TESTS	106
FIG. 6.5. TE57 COMPOSITE LUBRICATED CONTACT TESTS	107
FIG. 6.6: TE57 COMPOSITE FRICTION COEFFICIENT VS. LUBRICANT REGIME 10HRS TEST	109
FIG. 6.7: TE57 COMPOSITE STANDARD DEVIATION OF FRICTION VS. LUBRICANT REGIME	109
FIG. 6.8: TE57 COMPOSITE WEAR COEFFICIENT VS. LUBRICANT REGIME 10HRS TEST	110
FIG. 6.9: TE57 COMPOSITE WEAR COEFFICIENT VS. LUBRICANT REGIME 10HRS TEST	111
FIG. 6.10: TE57 LUBRICANT TESTS: LIGHT MICROSCOPE IMAGES	112
FIG. 6.11: TE92 JUTE/PHENOLIC COMPOSITE: WEAR VOLUME VS. CONTACT PRESSURE	115
FIG. 6.12: TE92 JUTE/PHENOLIC COMPOSITE: WEAR RATE VS. CONTACT PRESSURE	115
FIG. 6.13: LIGHT MICROSCOPE IMAGES OF TE92 CONTACT TESTS	116
FIG. 6.14: TE92 JUTE/PHENOLIC COMPOSITE: WEAR SCAR SURFACE ROUGHNESS	116
FIG. 6.15: TE92 20N, 40N, 60N AND 80N INTERFEROMETER PROFILE SCANS	117
FIG. 6.16: TE92 JUTE/PHENOLIC COMPOSITE: WEAR RATE VS. LUBRICANT REGIME	118
FIG. 6.17: TE92 MEAN SURFACE PARAMETERS	118
FIG. 6.18: TE92 LUBRICANT TESTS	119
FIG. 6.19: TE92 INTERFEROMETER WEAR SCAR PROFILES	119
FIG. 6.20: TE92: RA VS. SPECIFIC WEAR COEFFICIENT	121
FIG 7.1: PLAN VIEW OF VON MISES STRESSES ON SLIPWAY PANEL FROM FEA SIMULATION	124
FIG. 7.2: FEA SIMULATION VS. TYPICAL WORN PANEL SECTION FROM TENBY SLIPWAY	124
FIG 7.3: WEAR SCAR DEVELOPED USING FE COMPARED WITH REAL WORLD EXAMPLE	125
FIG 7.4: SIMULATION OF WEAR PROGRESSION OVER TIME ON A SLIPWAY PANEL USING FE	126
FIG 7.5: FRICTION FORCE MAP FROM FE SIMULATION OF 1 PANEL UNDER NORMAL LOADING	126

FIG 7.6: WEAR DEPTH/M SLIDING MAP OF 1 PANEL UNDER NORMAL KEEL LOADING	127
FIG 7.7: SYMMETRICAL FE WEAR SCAR DEVELOPING ON A 2 PANEL MODEL	128
FIG. 7.8: PARALLEL PANEL MISALIGNMENT MODEL	129
FIG. 7.9: ANGLED PANEL MISALIGNMENT MODEL	130
FIG 7.10: SKEWED PANEL MISALIGNMENT MODEL	130
FIG. 7.11: PARALLEL PANEL OFFSET COMPARISON	133
FIG. 7.12: ANGLED PANEL OFFSET COMPARISON	134
FIG. 7.13: SKEWED PANEL OFFSET COMPARISON	135
FIG. 7.14: WEAR MAP FOR 4MM PARALLEL OFFSET AND EQUIVALENT WEAR SCAR	137
FIG. 8.1: SLIPWAY CHAMFER PROFILE	138
FIG. 8.2: PARALLEL PANEL OFFSET COMPARISON: CHAMFERED PANEL	140
FIG. 8.3: ANGLED PANEL OFFSET COMPARISON: CHAMFERED PANEL	141
FIG. 8.4: SKEWED PANEL OFFSET COMPARISON: CHAMFERED PANEL	142
FIG. 8.5: VON MISES MAX. STRESS RESULTS	143
FIG. 8.6: VON MISES MAX. STRESS RESULTS	144
FIG. 8.7: MAX. FRICTION FORCE RESULTS	144
FIG. 8.8: MAX. FRICTION FORCE RESULTS	145
FIG. 8.9: MAX. WEAR RATE RESULTS	146
FIG. 8.10: WEAR MAP FOR 1MM PARALLEL OFFSET	147
FIG. 8.11: WEAR MAP FOR 5MM PARALLEL OFFSET	147
FIG. 8.12: MAX. WEAR RATE RESULTS	148
FIG. 8.13: SLIPWAY CHAMFER PARAMETERS	149
FIG. 8.14: MAX. VON MISES STRESS FOR VARYING CHAMFER HEIGHT (X=50, Y=1-20)	151
FIG. 8.15: MAX. VON MISES STRESS FOR VARYING CHAMFER LENGTH (Y=5, X=1-100)	151
FIG. 8.16: MAX. VON MISES STRESS FOR VARYING CHAMFER HEIGHT (X=50, Y=1-20)	152
FIG. 8.17: MAX. VON MISES STRESS FOR VARYING CHAMFER GEOMETRY INC. ORIGINAL	152
FIG. 8.18: MAX. FRICTION FORCE FOR VARYING CHAMFER DEPTH (X=50, Y=1-20)	153
FIG. 8.19: MAX. FRICTION FORCE FOR VARYING CHAMFER LENGTH (Y=5, X=1-100)	153
FIG. 8.20: MAX. FRICTION FORCE FOR VARYING CHAMFER SCALE (X,Y=0-20)	153
FIG. 8.21: MAX. FRICTION FORCE FOR VARYING CHAMFER GEOMETRY INC. ORIGINAL	154
FIG. 8.22: MAX. WEAR RATE FOR VARYING CHAMFER DEPTH (X=50, Y=1-20)	155
FIG. 8.23: MAX. WEAR RATE FOR VARYING CHAMFER LENGTH (Y=5, X=1-100)	155
FIG. 8.24: MAX. WEAR RATE FOR VARYING CHAMFER SCALE (X,Y=0-20)	155
FIG. 8.25: MAX. WEAR RATE FOR VARYING CHAMFER GEOMETRY INC. ORIGINAL	156
FIG. 8.26: FREE BODY DIAGRAM OF SELSEY SLIPWAY	157
FIG. 8.27: BEST CHAMFER EFFECTS ON WINCH LOADING	158
FIG. 8.28: FREE BODY DIAGRAM OF SELSEY SLIPWAY	159
FIG. 8.29: BEST CHAMFER $F_{MAX}$ FOR KEEL 'STICK'	160
FIG. 8.30: BEST CHAMFER EFFECTS OF REDUCED CONTACT AREA ON FRICTION FORCE	161
FIG. 9.1: EQUIVALENT NUMBER OF LIFEBOAT LAUNCHES/RECOVERIES: DRY	165
FIG. 9.2: EQUIVALENT NUMBER OF LIFEBOAT LAUNCHES/RECOVERIES: FRESHWATER	166
FIG. 9.3: EQUIVALENT NUMBER OF LIFEBOAT LAUNCHES/RECOVERIES: SEAWATER	166
FIG. 9.4: EQUIVALENT NUMBER OF LIFEBOAT LAUNCHES/RECOVERIES: BIOGREASE #1	166
FIG. 9.5: EQUIVALENT NUMBER OF LIFEBOAT LAUNCHES/RECOVERIES: MARINE GREASE	167

FIG. 9.6: EQUIVALENT NUMBER OF LIFEBOAT LAUNCHES/RECOVERIES: SEAWATER	168
FIG. 9.7: EQUIVALENT NUMBER OF LIFEBOAT LAUNCHES/RECOVERIES: FRESHWATER	169
FIG. 9.8: EQUIVALENT NUMBER OF LIFEBOAT LAUNCHES/RECOVERIES REQUIRED: BIOGREASE #1	169
FIG. 9.9: EQUIVALENT NUMBER OF LIFEBOAT LAUNCHES/RECOVERIES REQUIRED: GREASE	169
FIG. 9.10: WORN PANEL FAILURE CRITERIA BY CRACKING AROUND FIXING HOLE AREA	174
FIG. 9.11: WORN PANEL FAILURE CRITERIA – ISLANDS SHOWN ON SLIPWAY PANELS	174
FIG. 9.12: WORN PANEL FAILURE CRITERIA – ISLANDS SHOWN ON SLIPWAY PANELS	175
FIG. 9.13: WORN PANEL FAILURE CRITERIA – UNEVEN PANEL END WEAR FROM PADSTOW	175
FIG. 9.14: WORN PANEL FAILURE CRITERIA	176
FIG. 10.1: ENVIRONMENTAL IMPACTS DUE TO SLIPWAY PANEL WEAR PER YEAR	178
FIG. 10.2: SLIPWAY LUBRICANT COSTS / YEAR	180
FIG. 10.3: SLIPWAY OPERATING COSTS/YEAR – ORIGINAL PANEL VS. CHAMFER PANEL	181
FIG. 11.1: ALL SLIPWAY PANELS MISALIGNMENT HEIGHTS	187
FIG. 11.2: ORIGINAL AND MODIFIED SLIPWAY PANELS	194
FIG. A1: BEMBRIDGE SLIPWAY	201
FIG. A2: CROMER SLIPWAY	202
FIG. A3: MOELFRE SLIPWAY	203
FIG. B1: SLIPWAY PANEL SCHEMATIC	204
FIG. C1: SENNEN COVE SAND	214
FIG. D1: COMPOSITE TENSILE TEST	215
FIG. F1: TE57 RECIPROCATING TRIBOMETER: NEW PIN AND HOLDER DESIGN	240
FIG. F2: TE57 RECIPROCATING TRIBOMETER: SAMPLE SPECIFICATION	241
FIG. F3: TE92 ROTARY TRIBOMETER: PIN DESIGN	242
FIG. F4: TE92 ROTARY TRIBOMETER: SAMPLE DESIGN	243
FIG. H1: WEAR MAP FOR ALIGNED CONTACT CONDITIONS AND VARIOUS LUBRICANTS	246
FIG. H2: WEAR MAP FOR 1MM PARALLEL OFFSET	246
FIG. H3: WEAR MAP FOR 1MM ANGLED OFFSET	247
FIG. H4: WEAR MAP FOR 5MM PARALLEL	247
FIG. H4: WEAR MAP FOR 5MM ANGLED OFFSET	248
FIG. I1: REAL WORLD WEAR ASSESSMENT	249

# LIST OF TABLES

TABLE 1.1: THESIS STRUCTURE	19
TABLE 2.1: SPECIFICATION TYNE VS. TAMAR	24
TABLE 2.2: RNLI SLIPWAY STATIONS AROUND THE UK AND IRELAND	25
TABLE 3.1: LAUNCH TIMES FOR SELSEY SLIPWAY	42
TABLE 3.2: SELSEY SLIPWAY TRIALS COMPARISON	43
TABLE 3.3: BEMBRIDGE AND SELSEY SLIPWAY TRIALS COMPARISON	47
TABLE 3.4: TENBY SLIPWAY TRIAL SCHEDULE	62
TABLE 3.5: TENBY SLIPWAY TRIAL RESULTS	63
TABLE 3.6: TENBY SLIPWAY SURVEY DATA	67
TABLE 3.7: PADSTOW SLIPWAY SURVEY DATA	74
TABLE 3.8: COMBINED SLIPWAY SURVEY DATA	75
TABLE 5.1: COMPOSITE CONTACT TESTS	99
TABLE 5.2: LOW FRICTION STEEL CONTACT TESTS	99
TABLE 5.3: LUBRICANT TESTS	100
TABLE 5.4: CONTACT FORCE TESTS	103
TABLE 5.5: LUBRICANT TESTS	103
TABLE 7.1: PARALLEL PANEL OFFSET COMPARISON	131
TABLE 7.2: ANGLED PANEL OFFSET COMPARISON	132
TABLE 7.3: ANGLED PANEL OFFSET COMPARISON	132
TABLE 7.4: APPARENT FRICTION COEFFICIENT CONTRIBUTIONS FOR OFFSET SCENARIOS	136
TABLE 8.1: PARALLEL PANEL OFFSET COMPARISON: CHAMFERED PANEL	139
TABLE 8.2: ANGLED PANEL OFFSET COMPARISON: CHAMFERED PANEL	139
TABLE 8.3: SKEWED PANEL OFFSET COMPARISON: CHAMFERED PANEL	139
TABLE 8.4: ORIGINAL AND CHAMFER PANEL EQUIVALENT FRICTION COEFFICIENT	146
TABLE 8.5: CHAMFER HEIGHT VARIATIONS (Y)	150
TABLE 8.6: CHAMFER LENGTH VARIATIONS (X)	150
TABLE 8.7: CHAMFER SCALE VARIATIONS (X AND Y)	150
TABLE 8.8: BEST CHAMFER GEOMETRY COMPARISON	152
TABLE 8.9: BEST CHAMFER GEOMETRY COMPARISON	154
TABLE 8.10: BEST CHAMFER GEOMETRY COMPARISON	156
TABLE 8.11: BEST CHAMFER EFFECTS ON WINCH LOADING	158
TABLE 8.12: BEST CHAMFER $F_{MAX}$ FOR KEEL 'STICK'	160
TABLE 8.13: BEST CHAMFER EFFECTS OF REDUCED CONTACT AREA ON FRICTION FORCE	161
TABLE 9.1: EQUIVALENT NUMBER OF LIFEBOAT LAUNCHES/RECOVERIES REQUIRED	164
TABLE 9.2: HIGH RECOVERY WINCH LOADING FAILURE CRITERIA	170
TABLE 9.3: WORN PANEL FAILURE CRITERIA FOR A 1 IN 5 SLIPWAY GRADIENT	171
TABLE 9.4: WORN PANEL FAILURE CRITERIA FOR A 1 IN 5.5 SLIPWAY GRADIENT	172

TABLE 9.5: WORN PANEL FAILURE CRITERIA FOR A 1 IN 6 SLIPWAY GRADIENT	172
TABLE 9.6: WORN PANEL FAILURE CRITERIA FOR A 1 IN 5 SLIPWAY GRADIENT	173
TABLE 9.7: WORN PANEL FAILURE CRITERIA FOR A 1 IN 5.5 SLIPWAY GRADIENT	173
TABLE 9.8: WORN PANEL FAILURE CRITERIA FOR A 1 IN 6 SLIPWAY GRADIENT	173
TABLE 10.1: ENVIRONMENTAL IMPACTS DUE TO SLIPWAY PANEL WEAR PER YEAR	179
TABLE 10.2: SLIPWAY LUBRICANTS COMPARISON TABLE	179
TABLE 11.1: LUBRICANT AND PANEL MISALIGNMENT EFFECTS ON FRICTION COEFFICIENTS	190
TABLE 11.2: ASPERITY PLOUGHING CONTRIBUTION TO FRICTION	190
TABLE 11.3: CONTAMINANT CONTRIBUTION TO FRICTION COEFFICIENT	191
TABLE E1: TENBY SLIPWAY SURVEY DATA	228
TABLE E2: ALL PANELS MISALIGNMENT SCENARIOS	238
TABLE E3: PADSTOW SLIPWAY SURVEY DATA	239

# LIST OF EQUATIONS

---

<b>SPECIFIC WEAR RATE</b>	$k = V / LW$	<b>(1)</b>
<b>ARCHARD WEAR EQUATION</b>	$Q = KW / 3H_v$	<b>(2)</b>
<b>PLOUGHING BY A SINGLE ASPERITY</b>	$Q = KP / H$	<b>(3)</b>
	$K = k \tan \theta / \pi$	<b>(4)</b>
<b>PLASTICITY INDEX</b>	$\Psi = E/H (\sigma^*/r)^{1/2}$	<b>(5)</b>
<b>COMBINED ELASTIC MODULUS</b>	$1 / E' = (1 - \nu_1^2) / E_1 + (1 - \nu_2^2) / E_2$	<b>(6)</b>
<b>COULOMB FRICTION</b>	$F = \mu R$	<b>(7)</b>
<b>ADHESIVE FRICTION</b>	$A_r = W / Y_s$	<b>(8)</b>
	$F = A_r \tau$	<b>(9)</b>
<b>PLOUGHING OF A SINGLE ASPERITY</b>	$\mu_p = (2/\pi) \tan \theta$	<b>(10)</b>
<b>ELASTOHYDRODYNAMIC FILM THICKNESS EQUATION</b>	$H_0 = (4.9 \eta_0 U R_e) / w$	<b>(11)</b>
<b>FRACTIONAL FILM DEFECT</b>	$B = A_m / A_r$	<b>(12)</b>
	$A_f = A_r - A_m$	<b>(13)</b>
	$\beta = V_t / V_{mf}$	<b>(14)</b>
<b>TYPICAL SLIPWAY FRICTION LIMIT CALCULATION</b>	$Mg \sin \alpha - \mu R > 0$	<b>(15)</b>
<b>WINCH SPECIFICATION CALCULATION</b>	$C = M \mu_{\text{design}} \cos \alpha + \sin \alpha$	<b>(16)</b>
<b>OVERALL SLIPWAY FRICTION</b>	$\mu_{\text{overall}} = \mu_{\text{lubrication}} + \mu_{\text{misalignment}} + (\mu_{\text{ploughing}} + \mu_{\text{contaminants}})$	<b>(17)</b>

# ACKNOWLEDGEMENTS

---

This thesis would not have been possible without the support of a great many people. I would first like to thank Prof. Mark Hadfield for giving me the opportunity to work on this project and for continued support and encouragement throughout my research.

I would also like to thank the EPSRC for their co-funding of this project, as without this it is unlikely that a successful conclusion would have been reached.

I would like to thank the RNLI for their co-sponsorship of this project with the EPSRC and for the access and support they provided for the duration. In particular I would like to thank Steve Austen for his help and guidance throughout. I would also like to thank the coxswains of all the lifeboat slipway stations visited for allowing me to examine the slipway condition in each case and for providing honest and informed feedback on real world slipway performance.

The expertise and guidance of Phoenix tribology and FJ Engineering were invaluable in preparing the necessary test samples and designing an appropriate test rig to model such an unusual case.

My appreciation also goes to all the staff at Bournemouth University who have helped me with this project, in particular to Jo Sawyer for reminding me to keep going.

I would also like to thank Sarah Jay for all that she has done, my friends who have always been able to help relieve the stresses of research and to all at Shabby Road Studios.

Finally, I would like to thank my parents for their continued support throughout my time in Bournemouth.

# NOMENCLATURE

---

<b>K</b>	<b>Specific wear rate</b>	<b>U</b>	<b>Surface velocity</b>
<b>V</b>	<b>Wear volume</b>	<b>w</b>	<b>Load / unit width</b>
<b>L</b>	<b>Sliding distance</b>	<b>p</b>	<b>Contact pressure</b>
<b>W</b>	<b>Contact load</b>	<b><math>\beta</math></b>	<b>Fractional film defect</b>
<b>Q</b>	<b>Wear volume / Unit Sliding</b>	<b><math>A_m</math></b>	<b>Asperity contact area</b>
<b><math>H_v</math></b>	<b>Vickers hardness</b>	<b><math>A_r</math></b>	<b>Real contact area</b>
<b>k</b>	<b>Specific wear rate</b>	<b><math>A_f</math></b>	<b>Area of contact separated by</b>
<b>K</b>	<b>Wear coefficient</b>		<b>boundary lubricated film</b>
<b><math>H_b</math></b>	<b>Brinell hardness</b>	<b><math>V_t</math></b>	<b>Total wear volume</b>
<b><math>K_{abr}</math></b>	<b>Abrasive wear coefficient</b>	<b><math>V_{mf}</math></b>	<b>Wear volume for unlubricated</b>
<b><math>\mu</math></b>	<b>Coefficient of friction</b>		<b>contacts</b>
<b><math>R_a</math></b>	<b>Mean surface roughness</b>	<b><math>\alpha</math></b>	<b>Slipway angle</b>
<b><math>R_{rms}</math></b>	<b>Root mean square surface roughness</b>	<b><math>\ddot{a}</math></b>	<b>Acceleration</b>
<b><math>\Psi</math></b>	<b>Plasticity index</b>	<b>M</b>	<b>Lifeboat mass</b>
<b>E</b>	<b>Elastic modulus</b>	<b>g</b>	<b>Gravity</b>
<b><math>E'</math></b>	<b>Combined elastic modulus</b>	<b>C</b>	<b>Winch capacity</b>
<b><math>\nu</math></b>	<b>Poissons ratio</b>	<b><math>S_{max}</math></b>	<b>Max. Von Mises stress</b>
<b><math>\Theta</math></b>	<b>Mean asperity slope</b>	<b><math>D_{max}</math></b>	<b>Max. deflection</b>
<b><math>A_r</math></b>	<b>Real contact area</b>	<b><math>S_{z\ max}</math></b>	<b>Normal contact stress</b>
<b><math>Y_s</math></b>	<b>Yield strength</b>	<b>x</b>	<b>Panel chamfer length</b>
<b><math>\tau</math></b>	<b>Shear strength</b>	<b>y</b>	<b>Panel chamfer height</b>
<b><math>h_0</math></b>	<b>Minimum film thickness</b>	<b><math>\theta</math></b>	<b>Panel chamfer angle</b>
<b><math>\eta_0</math></b>	<b>Lubricant velocity</b>	<b><math>A_n</math></b>	<b>Nominal bearing area</b>
		<b><math>A_a</math></b>	<b>Actual bearing area</b>





# 1 INTRODUCTION

---

## 1.1 Background to Research

---

Lifeboats have provided a search and rescue service for the British public at sea since 1771. These lifeboats are run by the Royal National Lifeboat Institution (RNLI), a charity, since 1824 [1]. An effective rescue craft must be fast, in order to reach its destination quickly and able to deal with very severe weather conditions [2]. A number of lifeboat stations are sited around the UK, the aim is to provide a nearby rescue station for the entirety of the UK coast. Where possible these lifeboat stations are situated in natural or man-made harbours to provide calmer sea conditions for launching and recovery during a call out. However, along certain section of the UK coast there is no suitable harbour within range and the harsh conditions normally present during a call out can make conventional launching and recovery very difficult. In these cases the historical solution has been to use a slipway to launch the vessel, the boat is kept above water at the top of an inclined plane slipway and released to slide into the water under its own weight during a launch. This allows the boat to launch in almost any conditions. Recovery of the boat to the top of the inclined slipway is undertaken in calmer weather (the lifeboat will dock in the nearest harbour until conditions are suitable) and is achieved with the use of guide buoys for alignment and a winch to haul the boat back to the top. Thus slipway launched lifeboats are crucial in maintaining protection along the UK coast as they are tide and swell resistant and allow launches in conditions where a normal

launch would be impossible. The spectacular nature of inclined slipway launches has also made them an iconic image for the RNLI and very important for fundraising and public perception.

As the mass and materials in RNLI lifeboats have evolved through the years [3] however problems of high friction between lifeboat keel and slipway lining have been observed, particularly during the recovery phase where the boat is hauled up the slipway by the recovery winch [4-11]. The high friction between lifeboat keel and the slipway has resulted in high winch loads and difficulties in successfully recovering the lifeboat. The high winch loads also affect the lifespan of the winch. Wear to the slipway lining and during launch have also resulted in unpredictable surface conditions affecting launch speeds and increasing the possibility of failure to launch. To combat this problem the RNLI has installed a number of low-friction slipway lining materials including a jute/phenolic composite (hereafter, 'the composite') imbued with graphite to provide low friction and initially intended to run without lubrication. The use of marine grease along the slipway to reduce friction has also increased and this has safety implications as it is manually applied to the slipway before launch in often rough conditions and may endanger the lifeboatman on the slipway, there are also environmental implications as the grease is swept into the sea following a launch. The friction problem persists however and the new, softer lining materials are also experiencing high wear and limited life-spans. Obviously the problem of unpredictable launch and recovery friction is of great importance to the RNLI and affects the reliability of its service and the durability of its equipment. The panels are also expensive and it is estimated that at current wear rates the cost of replacing worn composite slipway panels is likely to be in the region of £5k per week once the process of upgrading slipway linings at stations across the UK is complete [12]. This translates as £260k per year which is a significant drain on the RNLI's resources, particularly as it is entirely funded by charitable donations.

Trials conducted [4-11] into the loads encountered by the winch during recovery onto the slipway at the slipway stations of Tenby, Bembridge and Selsey indicate that while the average load on the winch was within design limits, friction varied considerably along the slipway and in places exceeded the specified winch capacity. The wide variety of environmental conditions faced by slipway lifeboats makes simple analysis of this problem difficult, the wet and dry conditions, the use of greases and the presence of windblown sand are all potentially significant factors. Each slipway station is also slightly different, both in its configuration, the length and angle of slipway, the slipway lining launch practices and lubrication used, and the environmental conditions faced. This paper outlines a methodology to identify the causes of both the high friction and wear encountered.

## **1.2 Aims**

---

This research aims to develop a method for evaluating the friction and wear along lifeboat slipways with the aim of minimising these effects. It is also intended to develop general guidelines for best practice for slipway lifeboat crews based on experimental data so that friction and wear rates can be reduced and monitored more easily. Worn panel replacement criteria will also be developed so that slipway panels can be replaced before excess wear leads to launch or recovery problems. Similarly, panels with mild wear or wear unlikely to significantly affect launch and recovery conditions can be retained.

Design guidelines will also be produced in order to alert engineers to the issues raised by this research when refitting or replacing older slipways in order to reduce future slipway recovery problems. It is also intended to reduce the use of marine grease along the slipway in order to maintain low friction conditions, this grease is non-biodegradable and its repeated use may lead to grease bio-accumulating around the open water at the base of the slipway. This may have significant impacts due to the common location of lifeboat slipways on or near popular leisure beaches. This grease can be replaced with vegetable oil based greases, which have a far higher biodegradability potential, providing their function in reducing friction along the slipways is maintained. It may also be possible to switch to lubricants with a far lower environmental impact potential such as seawater or freshwater and this research aims to investigate the feasibility of this.

## **1.3 Objectives**

---

The objectives of this study are:

- To identify and minimise the causes of high friction on launch and recovery
- To predict and minimise the slipway lining wear during launch and recovery
- To develop operational guidelines for slipway crews to ensure low friction and wear
- To develop worn panel replacement criteria for slipway panels
- To develop design guidelines for future slipways and slipway linings
- To develop techniques to increase panel lifespan to reduce replacement costs to the RNLI
- To reduce the use of non-biodegradable greases on RNLI slipways

## **1.4 Scope of research**

---

This research will investigate the possible causes of high friction and wear during lifeboat launch and recovery along an inclined slipway. This research will be limited to the lifeboat slipway case and will not investigate similar friction problems during slipway ship launching or wider sustainability issues involved in the use of lifeboats.

## **1.5 Beneficiaries**

---

The project will provide a model for the performance and wear of slipway launch systems. The project will encompass product design and use of materials and will be beneficial to the RNLI and the marine industry in general, particularly with regards to marine sliding friction, slipways and marine railway applications and wear modelling.

## **1.6 Literature Review**

---

This section reviews the available literature concerning slipway launched lifeboats. The variable contact and lubrication conditions present in this case places it on the interface between various disciplines. Because of this a full literature review encompasses tribological considerations, slipway techniques including the similar case of ship launch slipways, FEA for wear and friction modelling, experimental friction and wear modelling and other related disciplines.

This involves looking at the current research and theories governing all types of slipway launches as well as the state of the art in tribology and contact modelling with regards to this subject with the aim of developing a multidisciplinary approach.

### **1.6.1 Outline**

The literature related to this subject is extensive and can be split into a number of areas. Firstly it is important to consider the tribological aspects of the contact in order to evaluate likely wear and friction mechanisms and to develop the equations that govern this behaviour. This section looks at the more theoretical aspects of slipway analysis, particularly lubrication, friction and wear mechanisms in order to ascertain the factors involved in slipway panel wear and friction with a view to developing a strategy for minimising these effects.

It is intended to combine this with a review of laboratory based friction and wear testing in order to develop an appropriate test methodology that accurately represents the real world

contact conditions to experimentally determine the wear and friction between lifeboat keel and slipway under varying lubrication and contact conditions. Experimental results will be compared with tribology theory and with the design specifications for the coefficients of friction and wear. This will help determine if environmental conditions are responsible for the increase in friction loads beyond the design capacity of the recovery winch. From this the conditions most likely to lead to high friction can be determined which will help to identify slipway stations at risk.

The third area of investigation is research directly concerned with slipway launching. It should be noted that slipways are also used for the one-off launch of large vessels from shipyards and much of the published research in this category deals with this case rather than the repeated slipway launch of search and recovery lifeboats. The basic principles and problems however remain the same and this research helps to form the technical background with regard to slipway launching.

A fourth area of study is that of wear simulation. The slipway launched lifeboat case is subject to significant variations in operating conditions, effects such as debris on the slipway, variations in lubricants and lubrication regimes encountered as well as abnormal stress concentrations resulting from panel misalignments, worn panel bearing surfaces, lifeboat keel inconsistencies and lifeboat keel misalignments are all likely. Because of this it is intended to investigate the area of wear simulation where experimental data can be used to inform a number of contact and wear models in order to fully investigate the effects of variations in slipway contact conditions and broaden the applicable conclusions resulting from the research.

### **1.6.2 Tribological Considerations**

Tribology is the science of surfaces, particularly the interactions between surfaces that produce effects like friction and wear. The concept and influence of friction on the wear and function of engineering mechanisms has concerned scientists since the time of Da Vinci, with Newton later providing some simple friction laws, but it was only with the developments that followed the industrial revolution that a real understanding of the mechanisms that underpin friction and wear became apparent. A number of theoretical models have been proposed to model the friction and wear experienced in real world contact problems and these are briefly critiqued below.

Wear and friction, although closely related, should be regarded as separate processes for analysis. An increase in wear does not necessarily infer an increase in friction though a

constant friction coefficient usually indicates a constant value of wear, any variation being indicative of a change in the lubricant regime or surface film [13].

### 1.6.2.1 Wear

When analysing wear it is common that a materials surface can be modelled as being formed of peaks and troughs termed asperities, and that the friction and wear observed derives from contact between these asperities. This approach to modelling friction and wear relies on knowing some surface properties of the materials involved and the forces between them. Models for predicting wear relevant to the slipway launched lifeboat case can be divided roughly into two categories depending on the operation of the slipway, those that model dry sliding wear and those that model lubricated sliding wear.

#### Dry Sliding Wear

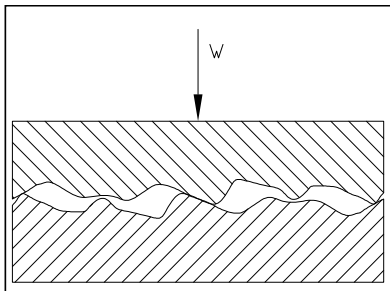


Fig. 1.1: Asperity Contact

Dry sliding wear exists where there is no lubricant between the contacting surfaces. In the case of lifeboat launch systems this is likely in the unlubricated case, and, may also be present in certain areas along the lubricated slipway where the lubricant has dried out or been washed away. The original specification for the use of the composite as a slipway lining material indicated that it could be used

unlubricated, though in real-world use it is common to lubricate the surface with either grease or running water.

#### Specific Wear Rate

Wear on the slipway panels can be expressed as a function of the contact load and sliding distance to generate the specific wear rate [14].

$$k = V / LW \quad (1)$$

Where  $k$  is the specific wear rate ( $\text{mm}^3/\text{Nm}$ ),  $V$  is the wear volume ( $\text{mm}^3$ ),  $L$  is the sliding distance (m) and  $W$  is the contact load (N).

#### Archard wear equation

A common starting point for the calculation and interpretation of dry sliding wear is the Archard wear equation [15]. Archard proposes a model based on circular contact spots and hemispherical wear particles for adhesive dry sliding wear where the contact between asperities results in the transfer of a wear particle from one material to another.

$$Q = KW / 3H_v \quad (2)$$

Where  $Q$  is the volume of material removed per unit sliding distance ( $\text{mm}^3/\text{m}$ ),  $H_v$  is the Vickers hardness,  $W$  is the normal load (N) and  $K$  is the wear coefficient ( $\text{mm}^3/\text{Nm}$ ).

This theory has been confirmed by numerous experimental results. The Archard wear equation prompts the following conclusions:

- The volume of material worn is proportional to the sliding distance
- The volume of material worn is proportional to load
- The volume of material worn is inversely proportional to the softness of the harder material

Though this appears simple, for practical applications the wear coefficient,  $K$ , depends on a number of different factors, and can vary over several orders of magnitude for a given set of materials. It is also true that while this equation is derived using adhesive wear models it cannot be used to support any particular wear mechanism as identical forms can be derived for abrasive wear [16]. The original equations also do not take into account the effects of lubricants and these can also have a very significant effect on the wear performance.

### **Abrasive wear**

Abrasive wear is the process by which a harder material abrades a softer material removing particles from the surface [17]. This can take two forms; in two body abrasion the rough surface of the harder material acts to remove material from the softer, in three body abrasion there are hard particles present between the contact area which act to abrade the surfaces. In the case of slipway launched lifeboats two body wear may be caused by imperfections in the lifeboat keel caused by floating debris or other in-service factors. Three body wear would model the case of hard abraded wear debris or wind blown sand on the slipway.

Abrasive wear can take place as plastic flow, brittle fracture or as a combination of both. In the case of three body abrasion, Hutchings indicates that if a trapped particle is significantly harder than the counterface then it will indent the surface and cause plastic flow, if the particle is less than 1.2X the hardness of the surface it will itself be blunted and not indent

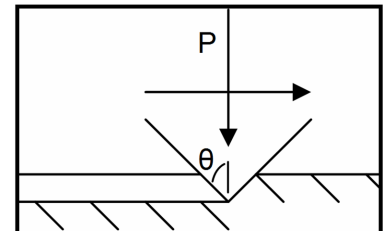


Fig 1.2: Ploughing Asperity

the counter-face [16]. This would imply that the sand present between the contact surfaces could have a significant impact on wear as the hard silica particles in sand will exceed 1.2 times the 30HB Brinell hardness of the composite.



Abrasive wear can be modelled by considering a conical asperity ploughing through a softer surface.

Ploughing by a single asperity:

$$Q = KW / H \quad (3)$$

$$K = k \tan\Theta / \pi \quad (4)$$

Where  $Q$  is the wear volume ( $\text{m}^3/\text{m}$ ),  $W$  is the total load (N),  $H_b$  is the brinell hardness of the softer surface,  $\Theta$  is the asperity slope and  $k$  is the abrasive wear coefficient.

In this derivation it is assumed that all the material displaced by the ploughing asperity becomes loose wear debris. In reality much of this material piles up along the sides of the groove and remains on the surface. This technique is also used to evaluate the contributions of larger surface imperfections such as nicks or damage to the lifeboat keel caused by floating debris or from the occasional necessity to take ground.

### **Wear of Polymers**

The Composite panels are comprised of a jute fibre mesh in graphite infused phenolic resin, the resin providing the low friction contact area and the jute fibres providing strength. Because of this it is important to consider the special case of polymer wear.

In contrast to metals and ceramics, polymers tend to exhibit lower friction coefficients, typically between  $\mu = 0.1-0.5$ . They have far lower values of elastic modulus, typically a tenth or less, strength is also lower and it is therefore appropriate to treat ceramic and metallic counterfaces as rigid bodies when sliding against polymers [18]. As almost all the deformation associated with wear takes place in the softer polymer, the surface finish of the counterface material becomes more important.

Two main wear mechanisms are observed, if the counterface is smooth, then wear may result from adhesion between the surfaces, and involve deformation only in the surface layers of the polymer. If the surface is rough, then the asperities on the counterface will induce deformation in the polymer to a significant depth, wear results from either abrasion associated with plastic deformation of the polymer, or from fatigue crack growth in the deformed region. These two wear mechanisms, involving surface and subsurface deformation respectively are termed interfacial and cohesive wear [19]. Other factors such as

surface degradation and environmental effects on fatigue crack growth may also play significant roles.

The counterface roughness values at which the transition from interfacial and cohesive wear occurs are typically in the region of  $R_a = 0.01\text{-}1\mu\text{m}$  [18]. The lifeboat keel roughness is likely to exceed these values giving a rough indication that the contact is likely to be cohesive. The nature of the contact conditions can be further investigated using the plasticity index below.

### **Polymeric Cohesive Wear**

Cohesive wear refers to the wear resulting from the deformation of surface and subsurface materials caused by protuberances of the counterface surface passing over the polymer surface. The protuberance can be a high asperity, a 3<sup>rd</sup> body abrasive particle between the two surfaces or possibly a lump of polymer debris that has attached to the counterface by the process of adhesive wear. The wear mechanisms involved depend on whether the deformation induced in the polymer is plastic or elastic, in the first case the wear mechanism is predominantly abrasion, in the second, fatigue. The distinction between these two types of mechanism is progressive, with abrasion increasingly dominating as the elastic modulus of the polymer increases. The phenolic resin used for the bulk of the composite slipway lining material has a relatively high elastic modulus compared with other polymers so abrasive wear mechanisms are likely to dominate. The relative magnitudes of these two mechanisms can be assessed using the plasticity index.

### **Plasticity Index**

The Plasticity Index is used to determine the degree to which the polymer will deform plastically under load. For  $\Psi < 0.6$  or so asperity deformation remains primarily in the elastic region, as  $\Psi$  increases the contact becomes increasingly plastic with plastic deformation becoming dominant above  $\Psi \approx 1$ . [19]

$$\Psi = E'/H (\sigma^*/r)^{1/2} \quad (5)$$

Where  $E'$  is the combined elastic modulus,  $H$  is the indentation hardness of the rough surface and the term  $(\sigma^*/r)^{1/2}$  approximates to the mean asperity slope,  $\Theta$ . The combined elastic modulus  $E'$  is derived from Young's Moduli  $E_1$ ,  $E_2$  and on Poisson's ratios  $\nu_1$ ,  $\nu_2$  for materials 1 and 2 as follows:

$$1/E' = (1 - \nu_1^2)/E_1 + (1 - \nu_2^2)/E_2 \quad (6)$$

For the composite slipway lining material and keel contact pair the plasticity index is calculated using mean asperity slope data from interferometer analysis to be 14.4, placing the contact firmly in the plastic deformation regime. This indicates that abrasive wear mechanisms will dominate over fatigue mechanisms.

### **Temperature Effects and ‘Pressure-Velocity’ Limit**

The concept of a PV (pressure, velocity) limit applies to polymer sliding contacts and represents a design limit for a given contact geometry. The theory states that the wear rate on a polymer sliding against a hard counterface will be uniform under low sliding speed and contact pressures and will remain so until the frictional heat generated at the polymer surface can no longer be adequately dispersed, at this point the friction and wear performance declines dramatically as thermal effects begin to dominate the contact. This limit can be expressed in terms of the pressure\*velocity product or PV factor.

The PV factor will vary depending on counterface roughness, lubricant conditions and contact geometry and must be derived for each new contact case; however general guideline figures are available [20]. The influence of the PV limit in the slipway launch case is likely to be found during the launch scenario where the already high contact pressures resulting from the heavy lifeboat resting on a narrow keel are coupled with launch velocities typically exceeding 12.8m/s (46kph) at the base of the slipway. PV limit implications for the preferred composite slipway lining are discussed in section 11.7.

#### **1.6.2.2 Friction**

Friction is defined the apparent force opposing the motion of two objects in contact. The understanding of friction has developed gradually with many famous early scientists and engineers contributing to the theory, including Leonardo da Vinci, Guillaume Amontons and Charles-Augustin de Coulomb. Their findings are collated into three general laws of friction [21].

- The force of friction is directly proportional to the applied load. (Amontons 1st Law)
- The force of friction is independent of the apparent area of contact. (Amontons 2nd Law)
- Kinetic friction is independent of the sliding velocity. (Coulomb's Law of Friction)

## Coulomb Friction

Coulomb friction, named after Charles-Augustin de Coulomb, is a model used to calculate the force of dry friction. It is governed by the equation:

$$F = \mu R \quad (7)$$

Where  $F$  is the friction force and  $R$  is the contact force between the surfaces.  $\mu$  is the friction coefficient. The friction coefficient can be divided into two values, the *coefficient of static friction* and the *coefficient of kinetic friction*. The static friction coefficient applies when the two bodies are at rest relative to each other and reflects the force required to induce relative motion. The *coefficient of kinetic friction* reflects the case where surfaces are in relative motion, typically  $\mu_{\text{static}}$  will exceed  $\mu_{\text{kinetic}}$ .

This relationship can be developed mathematically based on the assumption that surfaces are in atomically close contact only over a small fraction of their overall area, that this contact area is proportional to the normal force (until saturation, which takes place when all area is in atomic contact), and that frictional force is proportional to the applied normal force, independently of the contact area. Despite this the relationship is fundamentally an empirical one, the actual mechanisms governing friction are complex and varied and values for  $\mu$  are typically derived experimentally for a given contact and lubrication scenario. In the case of dry sliding this can be considered to be the sum of the friction mechanisms active, e.g:

$$\mu_{\text{overall}} = \mu_{\text{adhesion}} + \mu_{\text{abrasion}}$$

## Adhesive Friction

The adhesive component of friction is calculated by first considering the real area of contact, this is a function of the material yield strength of the softer surface and the applied load [22].

$$A_r = W / Y_s \quad (8)$$

Where  $A_r$  is the real area of contact,  $W$  is the applied load and  $Y_s$  is the yield strength.

Adhesive friction is modelled as the load required in breaking asperity adhesions and as such the shear strength of the softer material can be used to calculate the friction force:

$$F = A_r \tau \quad (9)$$

Where  $\tau$  is the shear strength of the softer material (Pa).

### **Abrasive friction**

Abrasive friction is modelled in a similar fashion to abrasive wear, with a hard asperity considered to be ploughing through the softer surface [23].

Ploughing of a single asperity:

$$\mu_p = (2/\pi)\tan\Theta \quad (10)$$

Real life asperities seldom have a slope ( $\Theta$ ) of more than  $5 - 6^\circ$  so the friction coefficient according to this equation should be  $\sim 0.04$ . In reality the pile up of material in front of the asperity means that the  $\mu_p$  is significantly higher. This technique can also be used to evaluate the friction contribution of larger surface protuberances in the same way as for ploughing wear.

### **1.6.2.3 Lubrication**

Lubricated contact describes the situation where a fluid is present between the two surfaces. This is usually added in the form of oil or grease to mechanical components in order to reduce friction and often also reduces wear. In the slipway launched lifeboat case this section covers the use of greases or water to coat the slipway prior to, and during launch and recovery.

### **Lubricated Wear**

The classic Archard wear equations do not take into account the effects of lubrication on the wear performance of contacting surfaces. To counter this, a number of attempts have been made to incorporate some aspect of lubrication into the equations. Archard and Kirk's [24] point contact experiments indicated that lubricating films can persist under low speed, lightly loaded conditions, and that at higher speeds plastic flow can occur before film breakdown. Rowe [25] introduced the concept of the fractional film defect allowing the wear to be correlated with the effectiveness of the lubrication, however this did not take into account that the total load was supported by the lubricating film and the contacting asperities and was thus subject to some variability compared with experimental results. Thompson and Bocchi [26] further developed the theory but their approach did not take into account the role of the lubricant in mitigating adhesive wear. Stolarski [27] presents a model for the adhesive wear of lubricated contacts; this is further developed to include scuffing [28] and wear prediction [29].

## Lubrication Regimes

Lubrication is used to provide asperity separation through the creation of a lubricating film, the thickness of this film is determined by the contact pressure, relative velocity of the surfaces and the lubricant viscosity. A lubricated contact will form different regimes depending on the values of these parameters and affect the friction and wear characteristics accordingly. The regime can be calculated using the elastohydrodynamic film thickness equation below [30].

$$h_0 = (4.9 \eta_0 U R_e) / w \quad (11)$$

Where  $h_0$  is the minimum film thickness (m),  $\eta_0$  is the lubricant viscosity (Pa s),  $U$  is the surface velocity,  $R_e$  is the relative radius of the contact surfaces and  $w$  is the load per unit width. Rearranging this equation to present the group  $\eta_0 U / p$  where  $p$  is the contact pressure provides the Stribeck number. The Stribeck number is used to determine the lubrication regime in place and plotted, shows the expected variation in friction as the lubrication regime changes.

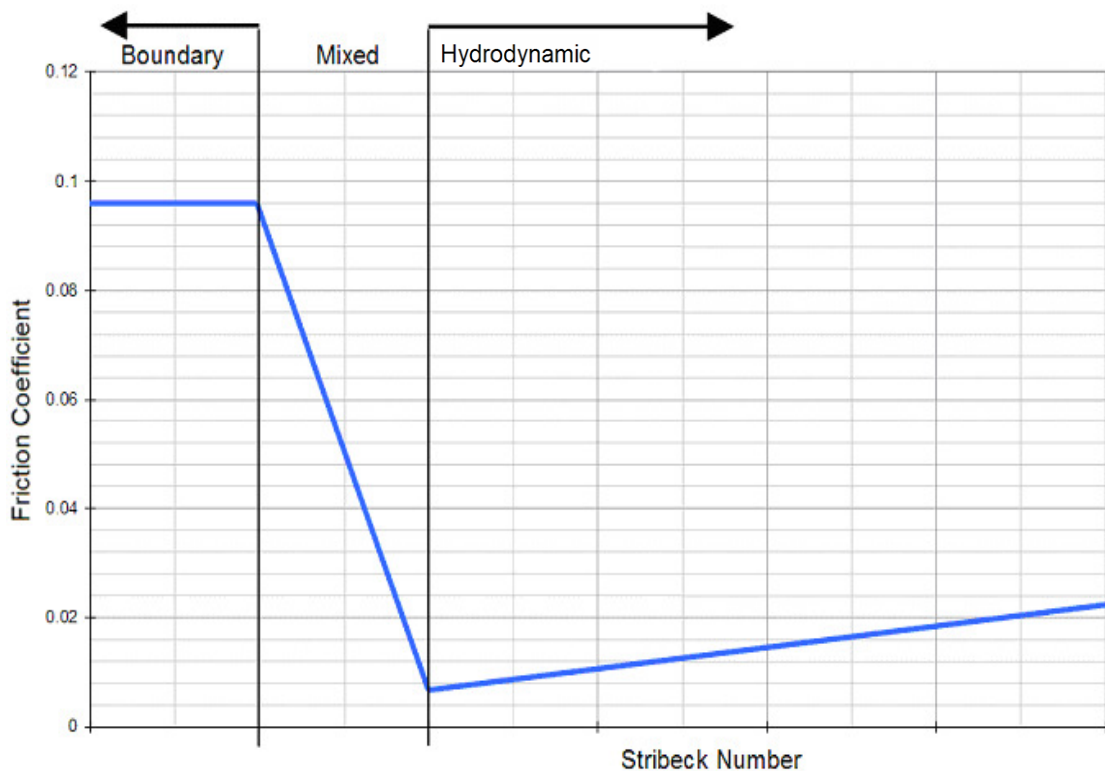


Fig 1.3: Stribeck Curve – Actual friction coefficient values vary by material

## Boundary lubrication

Boundary Lubrication occurs under high pressures or slow sliding speeds and describes the case where the hydrodynamic forces are insufficient to provide an Elastohydrodynamic film. In this instance the lubricant forms a film on the sliding surfaces limiting contact between asperities and hence asperity adhesion and junction growth. The frictional forces are thus

generally lower than the unlubricated case and although some wear occurs it is significantly less severe than in dry sliding.

### **Boundary lubrication wear**

Boundary lubrication describes any case where a lubricant film limits asperity contact although in many cases the load will be shared between the boundary film and the contacting asperities, the ratio of these is the fractional film defect [31].

Fractional Film Defect:

$$\beta = A_m / A_r \quad (12)$$

$$A_f = A_r - A_m \quad (13)$$

Where,  $\beta$  is the fractional film defect,  $A_m$  is the area of asperity contact ( $m^2$ ),  $A_r$  is the real area of contact ( $m^2$ ) and  $A_f$  is the area of contact separated by boundary film ( $m^2$ ).

Since  $A_m$  is less than  $A_r$  then  $\beta$  will be in the range 0 – 1, where  $\beta = 0$  indicates the case where there is no asperity contact and the load is carried entirely on the boundary film, and  $\beta = 1$  indicating the case where asperity contact is equal to the real area of contact, here the system will have the characteristics of dry sliding. For  $\beta$  between these two values the resultant wear volume will be the sum of the wear contributions from each of these cases, expressing this in terms of the fractional film defect gives equation (14) shown below.

$$\beta = V_t / V_{mf} \quad (14)$$

Where  $V_t$  is the total wear volume and  $V_{mf}$  is the wear volume for unlubricated contacts.

This shows the fractional film defect to be the ratio of the total wear to the wear when asperity contact is complete (dry sliding). Thus, the fractional film defect can be used to define the region between dry sliding wear and full boundary lubrication.

### **Boundary lubrication friction**

Since the friction coefficient is dependant upon the area of asperity contact and that of the film separation the friction coefficient for boundary lubrication can be expressed in terms of the fractional film defect [31].

$$\mu_{\text{overall}} = \beta\mu_{\text{dry}} + (1 - \beta)\mu_{\text{boundary}} \quad (15)$$

Where  $\mu_{\text{overall}}$  is the overall friction coefficient,  $\beta$  is the fractional film defect,  $\mu_{\text{dry}}$  is the dry sliding friction coefficient and  $\mu_{\text{boundary}}$  is the boundary lubricated friction coefficient.

### **Mixed Lubrication**

Mixed lubrication describes a transitional period where contact conditions present a mixture of boundary, elastohydrodynamic and hydrodynamic lubrication regimes.

### **Elastohydrodynamic Lubrication**

Elastohydrodynamic Lubrication is a specific case that usually occurs where counterformal surfaces result in very high lubricant pressures at line or point contacts [32]. As the keel and slipway are nominally parallel during launch and recovery this regime is unlikely. It is possible that local surface fluctuations will create local elastohydrodynamic effects but these will be very difficult to measure. It is proposed that the presence of a coherent elastohydrodynamic lubrication regime along the slipway/keel interface be discounted at present.

### **Hydrodynamic Lubrication**

Hydrodynamic lubrication defines the case where the sliding surfaces are separated by a relatively thick lubricant film [33]. This is normally the result of high sliding velocity, low contact pressure, high lubricant viscosity or a combination of all three. In contrast the slipway launched lifeboat recovery case (where problems of friction and wear are most apparent) the contact is characterised by high contact pressures and low sliding speeds. It is felt that in the case of slipway launched lifeboats these will not be sufficient to generate a hydrodynamic friction regime. Friction coefficients under hydrodynamic lubrication are in the region of 0.001 to 0.1, as the friction coefficient observed in slipway trials exceeds far this it is unlikely that there is hydrodynamic lubrication along the slipway.

#### **1.6.3. Finite Element Analysis for Wear Prediction**

In order to predict the slipway lining wear it is proposed that research be undertaken into ways to simulate and model sliding wear, particularly the use of computer simulations based on Finite Element techniques. This will involve a full literature search into the use of FEA to model wear, particularly the case of sliding wear. The aim is that by using experimental results to validate a slipway computer simulation the various angles, lengths and slipway linings adopted across the UK can be modelled by varying the computer simulation parameters rather than carry out a new bank of experiments for each slipway geometry.

The use of FE techniques to model wear and friction is relatively new but it is rapidly proving to be a valid tool for friction and wear analysis [34-42]. By using an experimentally validated



computer simulation it is possible to examine variables such as slipway angle, length and apparent coefficient of friction quickly and without the need for extensive experiment, it is hoped that this will allow extreme cases to be modelled in order to determine possible high friction problems and their solutions.

Finite Element Analysis (FEA) is software that uses complex differential equations to predict the stresses throughout a component or assembly under load. Components are modelled either in 2D or 3D on the computer and the loads likely to be encountered are applied. Modern FEA programs can account for fluctuating and stepped loads, friction, and can be used in an iterative fashion to model wear. Modelling wear using FEA is a relatively modern phenomenon though a number of useful papers citing the methodology and accuracy involved have been published [43-45]. It is intended that a combination of experimental results and FEA analysis will allow realistic predictions for the wear across the varied geometries, lifeboats and environmental conditions encountered by RNLI slipways.

#### **1.6.4. Review of Ship Launching**

Historically the primary use of large slipways has been for ship launching; consequently there is a comparatively large amount of research literature on the use of slip launch slipways compared to lifeboat launched slipways. The primary difference between the two is the need of lifeboat launched slipways to be re-used, and for the lifeboat to recover to the boathouse at the top of the slipway instead of simply proceeding down the slipway under gravity.



Fig 1.4: Slipway launching through the years, from left – Fort Carillon 1948, SS Oriana 1959, Lobo Marinho 2006

Historically, the science to model the launches began to develop in the 18<sup>th</sup> century, but was only fully applied during the following century when developments by Bouguer, Attwood and Napier of Merchiston, Simpson and Barlow enabled both the principles of naval architecture and the complex mathematics to be applied confidently to slipway launches [46]. The ‘Great Eastern’ launch debacle in 1857 where Brunel’s new ship seized on the slipway and took four months to finally launch led to increased interest in the mechanics of slipway launching, particularly for large ships and hastened interest in slipway modelling.

Great improvements in launching practice followed the introduction of petroleum based launching lubricants. These provided coefficients of friction which were low and could be accurately predicted. Two typical examples are Basekote, which was melted and applied to the slipway in order to provide a smooth, hard bearing surface, and Slidekote, a grease applied to the slipway from a barrel in a similar way to current RNLI slipway operation [47]. This highlights the need for a smooth bearing surface and low, controlled coefficient of friction along the slipway in a similar way to the lifeboat launch case. A number of techniques for assessing the friction along ship launch slipways experimentally have been developed and these are covered in later sections.

Currently most large ships are launched using the safer shiplift technique, although dynamic launching is still used occasionally where special circumstances make shiplift operation unsuitable [47].

### **1.7. Previous Work**

---

Previous work in this specific area is almost entirely confined to the on-site investigations performed by the RNLI and to research they have commissioned in the area. This includes a number of slipway trials [4-11] conducted at regular intervals for each slipway station the RNLI operates. Each trial involves the timed launch of the lifeboat, followed by recovery up the slipway while a load cell on the recovery winch records the load. Using the known lifeboat mass and the slipway angle the friction coefficient can be determined. The lifeboat is subsequently raised and lowered along the slipway by the winch with the load cell still attached in order to determine the static breakaway friction and to further investigate friction along the slipway under normal recovery hauling conditions. These are further investigated in the case studies that comprise section 3.

### **1.8. State of the Art**

---

Previous studies [48-50] commissioned by the RNLI investigated friction and wear in slipway bearing materials. The aim of this research was to investigate the feasibility of using composite rather than steel keels to reduce the weight of slipway launched lifeboats. Reducing the weight of the lifeboat would consequently reduce the force required to recover the lifeboat onto the slipway and increase the speed. The two studies compared the friction of conventional keel materials on steel slipways with some composite keel materials, namely glass reinforced phenolic, polyester, and vinyl ester (vinyl ester also tested with additives in

the surface layer, namely PTFE, MoS<sub>2</sub>, MoS<sub>2</sub> and graphite, graphite, small glass ballotini, large glass ballotini and a combination of small and large glass ballotini), carbon, kevlar and glass fibre reinforced epoxy and the initial Corten steel keel material. The study used a pin on disc style tribometer, with the pin representing the keel. Tests were performed under various conditions and the results recorded. Ultimately, though the wear rate proved acceptable in many cases, the friction generated with the new keel materials was too high to be practical and presented greater risk of 'sticking' on the slipway during launch and recovery. This appeared to be due to thermal degradation of the polymer matrix producing sticky 'tar-like' products. When cooled with sea-water the materials performed better though the report is at pains to point out that real life geometries may have very different thermal properties and it was by no means guaranteed that sufficient cooling to prevent thermal degradation could be achieved. The paper concluded by recommending large scale trials before the full scale introduction of these materials for lifeboat keels. Following this research the potential use of composite keels has been reduced.

## **1.9 Structure of Thesis**

---

The thesis has been structured as follows: Chapter 1 introduces the problem, identifies areas for further research and outlines the beneficiaries for this study. Chapter 2 is a literature review, and investigate the state of the art with regards to the research topics outlined in the introduction. This chapter also develops the aims, objectives and the scope of the research as well as developing the background to slipway lifeboats and environmental concern. Chapter 3 includes six RNLI slipway case studies including slipway winch trial data investigating winch loads on recovery as well as detailed slipway panel condition surveys to aid in identifying the causes of friction and wear along the slipway. Chapter 4 continues by investigating the current situation of experimental wear and friction modelling, looking at existing slipway friction testing, types of test machine and surface analysis techniques to determine the friction and wear regimes in place. Chapter 5 develops the test methodology for the tribometer friction and wear testing. Chapter 6 details the experimental results. Chapter 7 looks at the use of FE modelling to predict wear and friction along the slipway incorporating real world panel geometry and misalignment effects. Chapter 8 develops the FEA results by introducing panel design modifications to reduce the stress and wear concentration effects identified in chapter 7 and to increase the panel misalignment tolerance. Chapter 9 applies the data from FEA, slipway survey and tribometer testing to the real world case, developing panel wear and replacement criteria and strategies for friction based wear monitoring. Chapter 10 contains some limited sustainability performance analysis allowing environmental performance and other aspects to be incorporated into panel

design and lubricant selection. Chapter 11 summarises the results generated from all aspects of this thesis including tribological contact mechanisms, real world and theoretical wear and friction mechanisms, wear modelling and expected panel lifespans under varying contact and lubricant conditions. Also discussed here are the implications for real world slipway lubricant use and recommended best practice with regards to slipway lubricant application. Finally chapters 12 and 13 summarise the conclusions and recommendations developed from this research. The thesis structure is summarised below in table 1.1.

---

**Outline of Problem**

Chapter 1 – Introduction

---

**Requisites to address the research problem**

Chapter 2 – Slipway Launched Lifeboats Operational Analysis

Chapter 3 – Case Studies

Chapter 4 – Experimental Wear Modelling

---

**Development of Research Methodology**

Chapter 5 – Test Methodology

---

**Interpretation of Emerging Data**

Chapter 6 – Experimental Results

Chapter 7 – FEA Modelling – Existing slipway panel

Chapter 8 – FEA Modelling – Modified slipway panel

Chapter 9 – Applied results

Chapter 10 – Environmental considerations

---

**Developing a solution to the research problem**

Chapter 11 – Discussion

Chapter 12 – Conclusions

Chapter 13 – Recommendations

---

Table 1.1: Thesis structure

## 2 SLIPWAY LAUNCHED LIFEBOATS OPERATIONAL ANALYSIS

This section looks at the operational use of lifeboat launch slipways by the RNLI, the first sections begin by looking at the development of lifeboat slipway specifications and lifeboats, ending in the present day with the introduction of the new Tamar class.

Section 2.2 then looks at lifeboat launch slipway design, including some initial and previous analysis of the lifeboat launch, the use of low friction composite materials along the slipway, and the use of lubricants to lower friction. The slipway operation section then shows the lifeboat launch and recovery procedures,

## 2.1 Overview – Slipway Lifeboats Development: 1960 - Present

---



Fig. 2.1: Lifeboat launched from slipway in Sunderland ~1970s

Currently (2008) there are 126 all weather lifeboat stations, comprising 76 afloat stations, 26 slipway stations, 23 carriage and 1 station where the lifeboat is launched by davit [51].

The early 60's saw a number of significant events in the development of a new generation of fast off-shore lifeboats. This was partly in response to changes in the strategic requirements

for the RNLI to provide search and rescue cover around the UK. The target rose from providing cover to a distance of 30 miles to a distance of 50 miles with a response time of 2½ hours [52]. It became apparent that to meet these requirements a new generation of faster, more seaworthy lifeboats would be required.

The new lifeboats would still be bound to operating parameters unchanged from the original lifeboats of Greathead and Wouldhave i.e.

- To launch from carriage, slipway or afloat station
- To operate in all weathers
- To reach the casualty as fast as possible
- To have the ability to take the ground
- To have ultimate seaworthiness

In addition modern 'fast' slipway lifeboats are specified to include the following [52]:

- To have a maximum speed of 25 knots
- To have propeller protection
- To have the ability to take the ground
- To consider ease of maintenance and repair
- To launch and recover from a conventional slipway

The ability to take the ground is strategically important for a slipway lifeboat but does mean that the keel is likely to take damage and its surface may become uneven. This may well be a significant factor in the cases of high friction observed.

The need for greater speed was imperative by 1963 when the RNLI spotted the US coastguard 44'0" (13.5m) Surf Rescue Boat. A boat was bought for trials and following their successful completion 21 craft, slightly modified from the original American design and re-christened the Waveney were ordered and entered service. The new craft were fast at 16 knots and featured a hull form previously unseen at the RNLI [53].

The Waveney class lifeboat proved very successful and particularly cost-effective and this prompted the development of the Thames class lifeboat. Essentially a 50'0" Waveney with higher speed/length ratio, problems in directional stability meant only 2 were built. By this time however, work had begun on the truly radical Arun class lifeboat. The Arun was notable in featuring for the first time in an RNLI SAR Lifeboat a lightweight GRP hull and further raising the speed to 18 knots. The Arun lifeboat became the workhorse of the RNLI during the 70's and 80's with 46 built up to 1990. Following the advances of the Waveney and Arun lifeboats, the pace of change accelerated to meet the needs of the rescue service and to take advantage of the advances in composite technology and hull form.

### 2.1.1. Modern Design and Trends



Fig 2.2: Oakley Class Lifeboat

While never slow, earlier lifeboats such as the Watson, Oakley and Rother were simply not fast enough to meet these requirements. Previously, speeds of 9-11 knots had been considered adequate and weight had been considered vital for a lifeboat to succeed, limiting previous advances in lifeboat speed. From about 1960 – 80 the main slipway launched lifeboats of the RNLI were the Oakley,

Barnett and Watson class lifeboats. By 1980 however these were reaching the end of their useful lives, and many of them were self righting only when fitted with large inflatable airbags. The advances in lifeboat design described above were prompted by the need for faster boats to cover a larger area within the specified response time. Work began on a new, modern slipway launched lifeboat and the Tyne class entered service in 1983 [54].



### Tyne Class Lifeboat



Fig 2.3: Tyne Class Lifeboat launching at Wicklow

The development of this new slipway lifeboat entailed considerable constraint on the design due to the limits imposed by current slipways and slipway stations. The dimensions of the finished craft were such that it would fit into the greatest number of existing slipway stations, hence the low cabin and extendable antennae. Further operational parameters included a top speed of 18 knots, a range of 200 miles, displacement of 25.5 tonnes and space for 7 crew, 16 seated survivors and 2 stretchers [54]. The craft was also to include advanced navigation equipment and above all, to be self-righting in the event of a capsize. The Tyne entered service in 1983, further slight modifications and additional rescue equipment led to the displacement increasing slightly from the original design displacement of 25 tonnes to up to 26.5 tonnes, with the standard displacement listed as 25.5 tonnes.

### Tamar Class Lifeboat



Fig 2.4: Tamar Class Lifeboat [55]

The specification for slipway launched lifeboats was again improved with the 2006 phased introduction of the Tamar class slipway lifeboat. This was designed by JML shipyards and is adapted from an existing design. This new craft is to be phased in across the UK slipway stations and exceeds in almost every area the specification on the Tyne class lifeboat it replaces. It is also larger and heavier than the Tyne and as such many slipways and boathouses will require significant modification or even replacement to accommodate the Tamar. This places the Tamar class lifeboat at the vanguard of slipway launched lifeboat development representing the next generation of both lifeboats and the upgraded slipway



stations. Two examples of this are found in Tenby and Padstow where new boathouses and slipways have been constructed specifically for the new Tamar lifeboat.

	<b>Tyne</b>	<b>Tamar</b>
<b>Length</b>	14.3m (47ft)	16m
<b>Beam</b>	4.48m (14.8ft)	5m
<b>Draught</b>	1.26m	1.35m
<b>Speed</b>	17.6 knots	25 knots
<b>Displacement</b>	25.5 – 26.5 tonnes	Approx. 35 tonnes
<b>Construction</b>	Steel	FRP (Steel Keel)
<b>Range</b>	240n. miles	250n. miles
<b>Crew</b>	7	6

Table 2.1: Specification Tyne vs. Tamar

The design displacement for the Tamar was originally listed as 30 tonnes, however in a similar fashion to the Tyne, the further addition of rescue equipment to the original specification has led this to increase to ~35 tonnes.

## 2.2. Slipway Design

### UK Slipway Stations

Currently RNLI slipways are of various designs owing to historical developments and local conditions at each site, the main variations being due to particularly shallow shore slopes or the boat house being set back from the water line. Examples of slipways with these conditions include: Swanage, Porthdinllaen and Wicklow, which all feature rollers along the length of the slipway, and the Sennen Cove launch slipway, the recovery slipway is lined with composite but can only be used at high tide.

Boat Number	Boat Class	Station	Slipway Lining	Lubrication	Slipway Angle
47-01	Tyne	Selsey	Composite	Marine grease	1/5
47-03	Tamar	Padstow	Composite	Freshwater	1/5.5
47-05	Tyne	The Mumbles	Steel Channel	Marine grease	1/5
47-06	Tamar	Cromer	Composite	Marine grease	1/5
47-08	Tyne	Teesmouth <sup>†</sup>	N/A	Marine grease	N/A
47-11	Tyne	Angle	Composite	Marine grease	1/6
47-13	Tyne	Moelfre	Low friction steel	Marine grease	1/5.5
47-14	Tyne	Barrow	Low friction steel	Microball lubricant	1/5.5
47-15	Tyne	Porthdinllaen	Rollers	Marine grease	1/12.5
47-16	Tyne	Sennen Cove	Composite & Rollers	Microball lubricant	1/8 (Launch) 1/5 (Recovery)
47-24	Tyne	Baltimore*	Composite	Marine grease	1/5
47-26	Tyne	St. Davids	Composite	Marine grease	1/5
47-30	Tyne	The Lizard	Greenheart	Marine grease	1/6
47-32	Tyne	Douglas	Composite	Marine grease	1/5
47-35	Tyne	Wicklow*	Rollers	Marine grease	1/10
47-40	Tyne	Shoreham	Composite	Marine grease	1/5
12-23	Mersey	Swanage	Rollers	Marine grease	1/12
12-32	Mersey	Berwick-on-Tweed	Composite	Marine grease	1/5
12-35	Mersey	Arbroath	Rollers	Marine grease	1/10
16-02	Tamar	Tenby	Composite	Freshwater	1/5 (new)
47-18	Tyne	Bembridge	Composite	Marine grease	1/5

\*Ireland  
†Closed

Table. 2.2: RNLI Slipway Stations around the UK and Ireland

Lifeboat launch slipways follow a common template though the slipway angle can vary between 1 in 5 and 1 in 12. Shallower slipway angles tend to employ rollers rather than plane sliding panels to ensure low friction, with most slipway using plane sliding panels set at a gradient of 1 in 5. Schematic examples of typical slipways are shown in appendix A.

A typical slipway consists of an upper section of steel rollers and a plane lower section lined with one of the slipway lining materials mentioned below. The lifeboat is held on the rollers section inside the boathouse, when not in use. Newer slipways such as those of Tenby and Padstow also feature a see-saw arrangement at the boathouse section of the roller slipway so that the lifeboat can be stored horizontally.

The Selsey slipway is considered a typical lined slipway and is used here as an example. It has an incline of 11.4° (Approx 1 in 5) and is 53m long at mid tide. This allows the typical forces involved in a slipway launch and recovery to be calculated as follows:

$\alpha$  = Slipway angle = 11.4°

**Mg** = Lifeboat Mass X Gravity =  $25.5 \times 10^3 \times 9.81 = 250,155\text{N} = \mathbf{250.2\text{kN}}$  for **Tyne Class**

**Mg** = Lifeboat Mass X Gravity =  $35 \times 10^3 \times 9.81 = 343,350\text{N} = \mathbf{343.4\text{kN}}$  for **Tamar Class**

**R** = Reaction =  $Mg \cos \alpha = 245,219.7\text{N} = \mathbf{245.2\text{kN}}$  for **Tyne Class**

**R** = Reaction =  $Mg \cos \alpha = 336,576.1\text{N} = \mathbf{336.6\text{kN}}$  for **Tamar Class**

$\mu R$  = Coefficient of friction X Reaction (to be derived)

$\ddot{a}$  = Acceleration, derived from observed launch or winch speed

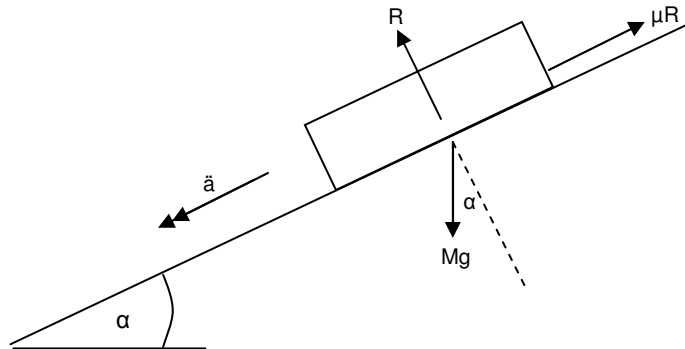


Fig. 2.5: Free body diagram of Selsey slipway: Launch

From this analysis it is seen that for a typical slipway geometry the maximum friction coefficient possible that allows the lifeboat to proceed down the slipway is present as the lifeboat begins to slip so that:

$$\mathbf{Mg \sin \alpha - \mu R > 0} \quad (15)$$

It follows that:

$$\mathbf{\mu_{max} < 0.2}$$

A significant minority of the slipway stations suitable for plane slipway panels have shallower inclines however, with the Lizard as the shallowest at 1 in 6, in this case the friction coefficient at the point of slip is:

$$\mathbf{\mu_{max} < 0.167}$$

## Recovery Scenario

During the recovery scenario the following free body diagram applies:

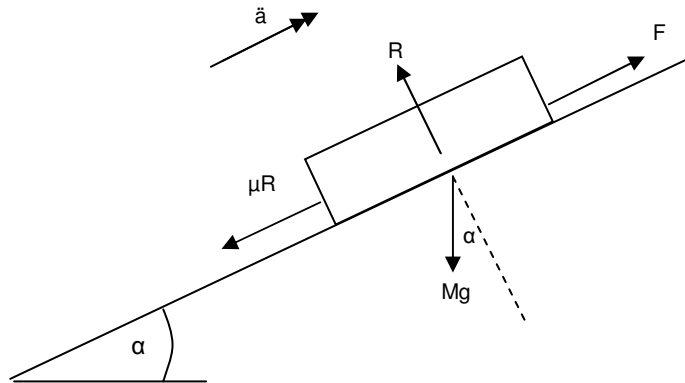


Fig. 2.6: Free body diagram of Selsey slipway: Recovery

The recovery winch is specified for a pull capacity of 12 tonnes, this means that the maximum friction coefficient during recovery that will meet this requirement on a standard 1 in 5 slipway is:

$$\mu_{\max} < 0.150$$

For a shallower slipway of 1 in 6 this is:

$$\mu_{\max} < 0.181$$

Combining all of these scenarios it can be seen that the lowest result of  $\mu_{\max} < 0.150$  therefore presents a maximum performance criterion for the friction coefficient of any slipway panels and lubrication regime considered.

## Lifeboat Keel Geometry

The Tamar keel plane sliding length is 12.8m, with a keel width of 0.15m. The keel is made from S275 Steel. The Tamar mass estimates have varied depending on the equipment fitted, initial estimates of ~30 tonnes based on the prototype have proved conservative, and a value of 35 tonnes based on in-service models is featured here [56].

## Slipway Parameter Calculation

Contact pressures for the new Tamar lifeboat are calculated as 176 kPa, derived from the lifeboat keel bearing area of 1.92m<sup>2</sup> and the Tamar in-use mass of 35 tonnes. While launch velocities can exceed 40kph at the base of the slipway, recovery is standardised to a 0.25 m/s winch line speed.

### Maintenance and service interval

Currently the slipway is being replaced as it deteriorates as the wear rate is far greater than expected. There is no fixed replacement schedule; rather, the panel is replaced panel by panel according to inspection.

#### 2.2.1. Initial Slipway Design Observations

From the above analysis it can be seen that the angle of the slipway and the line pull specification of the recovery winch are important aspects in determining an appropriate friction coefficient for successful launch and recovery. One immediate observation is that the larger the friction coefficient permissible the greater the likelihood of achieving this reliably in the real world, with this in mind the following graph is developed to investigate the relative friction coefficients for launch and recovery for a lifeboat mass of 35 tonnes and a winch specification of a 12 tonne constant load at 15m/min line speed [57] at a variety of slipway angles.

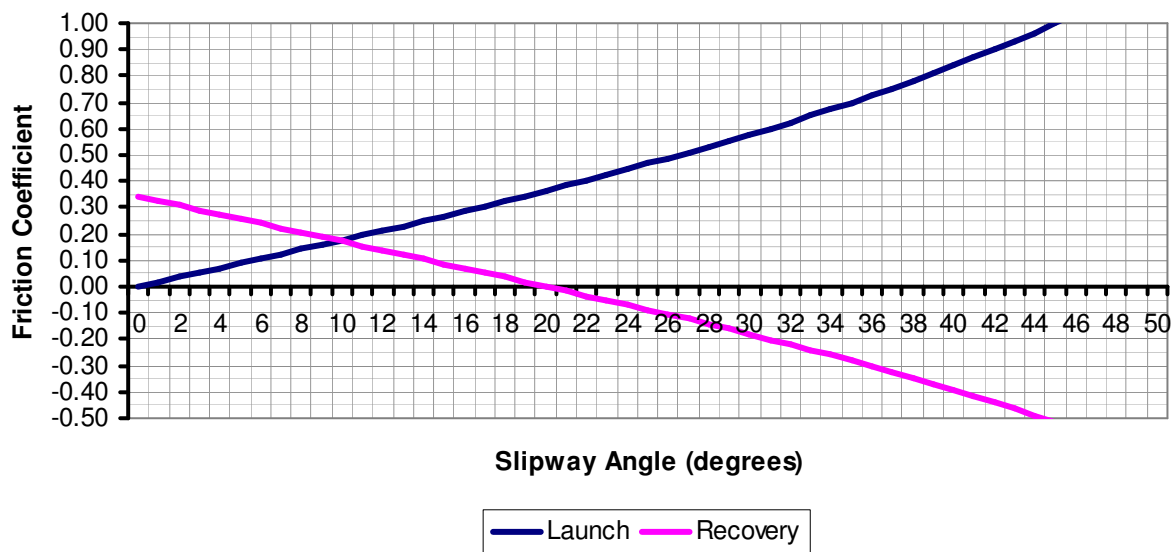


Fig. 2.7: Max. friction coefficients at launch and recovery for a lifeboat mass of 35 tonnes, winch specification of 12 tonnes vs. slipway angle

The point at which the two lines cross represents the minimum friction coefficient possible for this winch specification, this occurs at an angle of 9.87° an incline of 1 in 5.75. Obviously it may be difficult to adjust the angle of the slipway so the other variable to be considered is the winch line pull specification.

For the most common slipway incline of 1 in 5 the maximum friction coefficient permissible during launch is 0.2, during recovery this is reduced to 0.15 due to the load capacity of the winch, this value is therefore the design maximum. By increasing the load capacity of the

winch to allow the recovery friction coefficient to match the launch coefficient the design maximum also rises, allowing greater tolerance of real world conditions that may raise the friction coefficient. In the case of a 35 tonne lifeboat on a 1 in 5 gradient slipway the winch capacity to achieve this can be calculated as follows:

$$C = M ( \mu_{\text{design}} \cos \alpha + \sin \alpha ) \quad (16)$$

$$C = 13.7 \text{ Tonnes}$$

This winch specification would allow for friction coefficient of up to 0.2 along the slipway, matching the launch specification. Interestingly, in the 1 in 6 slipway incline case the launch friction coefficient maximum is lower than the recovery coefficient; by the same analysis this allows the winch specification to be relaxed slightly so that  $C = 11.5$  tonnes.

### 2.3. Slipway panel geometry

Slipway panel geometry differs between slipway stations and for differing slipway lining materials, although a standard layout has emerged in recent years for the composite slipway panels. This is shown below:

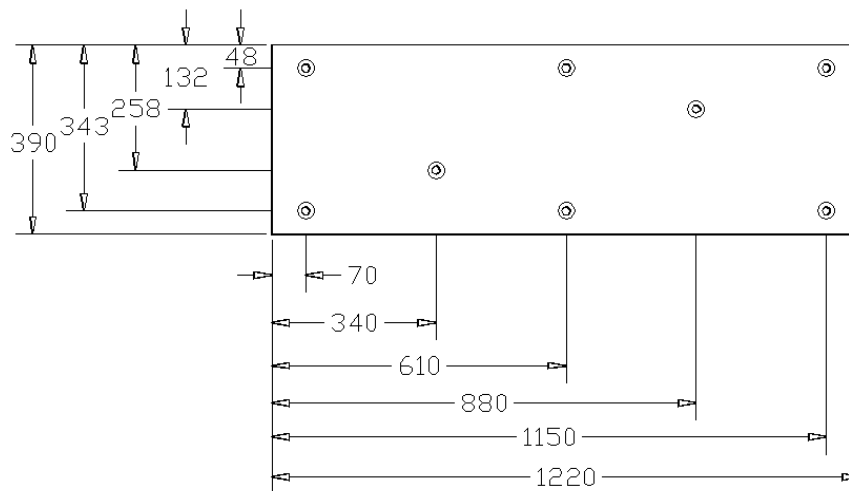


Fig. 2.8: Typical Composite Slipway Panel Geometry

The panel thickness varies with some slipways initially using a 6mm thick section while the present standard thickness is 19mm. Currently the recovery slipway at Sennen Cove is the only station to continue to use the 6mm thick composite panels.

## 2.4. Slipway lining materials

---

Slipways are currently lined with a number of different low friction materials. The original slipway lining material was Greenheart weather-treated wood and this is still used on The Lizard slipway. The Mumbles has a simple greased steel channel, Swanage, Porthdinllaen, Wicklow and the Sennen Cove launch slipway use rollers along the length of the slipway and all the remaining slipway stations use either low friction coated steel panels or composite panels. Low friction coated steel has been used successfully for several years without any significant wear problems, however, as lifeboat mass has increased with each new model there have been incidents of high friction reported. These friction problems led to a search for a more suitable, low friction material. The selected jute/phenolic composite has now been adopted on most slipways and is the preferred RNLI slipway lining. This research concerns the majority of slipway station that use either low friction steel or composite slipway panels, particularly including all slipways recently upgraded for the Tamar class lifeboat.

### 2.4.1. Low friction steel slipway lining

Low friction steel slipway linings incorporate a nickel/chromium carbide coating designed for low friction and high abrasive and corrosive wear resistance. Low friction steel coatings are applied using spray welding techniques which provides an even, smooth surface coating. Typical uses include valve seats and wire drawing capstans. The low friction layer's nominal composition is shown in fig. 2.9. Low friction steel slipway linings were originally selected because of their high wear resistance in comparison with the alternatives of Greenheart treated wood or a plain steel channel.

Carbon	0.80
Chromium	15.00
Iron	3.50
Boron	3.00
Silicon	4.00
Tungsten	16.50
Nickel	Remainder

Fig. 2.9: Nominal low friction steel coating composition [58]

A large number of slipway stations still use low friction steel coated steel panels to line their slipways but the higher contact pressures generated by the heavier Tyne class slipway have led to an increase in cases of high friction during recovery. This has led to the practice of manually applying marine slipway grease to the slipway before each launch and recovery in order to reduce friction and hence winch loading. This practice has safety implications due to the need for a crew member to scale the slipway applying the grease; in adverse weather conditions this could be dangerous. There is also an environmental implication as the grease from each launch is washed into the sea around the slipway and may accumulate over time to cause significant impacts on the local ecosystem. High friction problems are likely to remain or even worsen with the introduction of the new, heavier Tamar class slipway launched lifeboat.

#### 2.4.2. Composite Slipway lining

The composite slipway lining is a jute fibre/graphite infused phenolic resin composite designed for low friction marine dry bearing use. Typical applications include marine railways and low load bushings. The composite was selected for use as a slipway lining material due to its low friction characteristics and suitable wear and corrosion resistance.

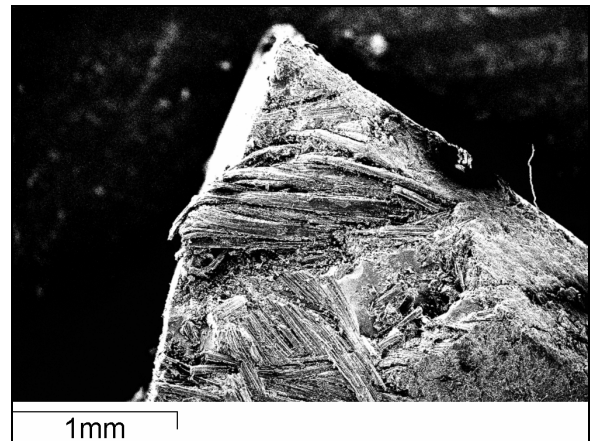


Fig. 2.10: Composite under SEM; The phenolic resin bulk and jute fibres can be seen

#### Manufacture

In manufacture, a jute fibre mesh is passed through a graphite infused hot phenolic resin and then heated until it is impregnated and partially cured. The jute mesh is then cut to an appropriate size, layered and subjected to heat and pressure until it fuses [59]. The end material is a black, hard wearing laminar composite. The composite is used on a number of slipways and as the preferred slipway lining material for the next generation of boathouses and the new Tamar class lifeboat its use is being phased in across the remaining slipway stations.

The composite is designed to run dry, or with water lubrication, though in some cases, e.g. Bembridge and Selsey it is augmented with marine grease as with the low friction coated steel lining.

Unfortunately cases of high friction have persisted with the composite lining, notably at the new boathouse and slipway for the Tamar class lifeboat at Tenby where the lining was run dry (freshwater lubrication is now used). These have manifested as winch loadings exceeding the design specification for the recovery winch with implications for its lifespan and reliability.



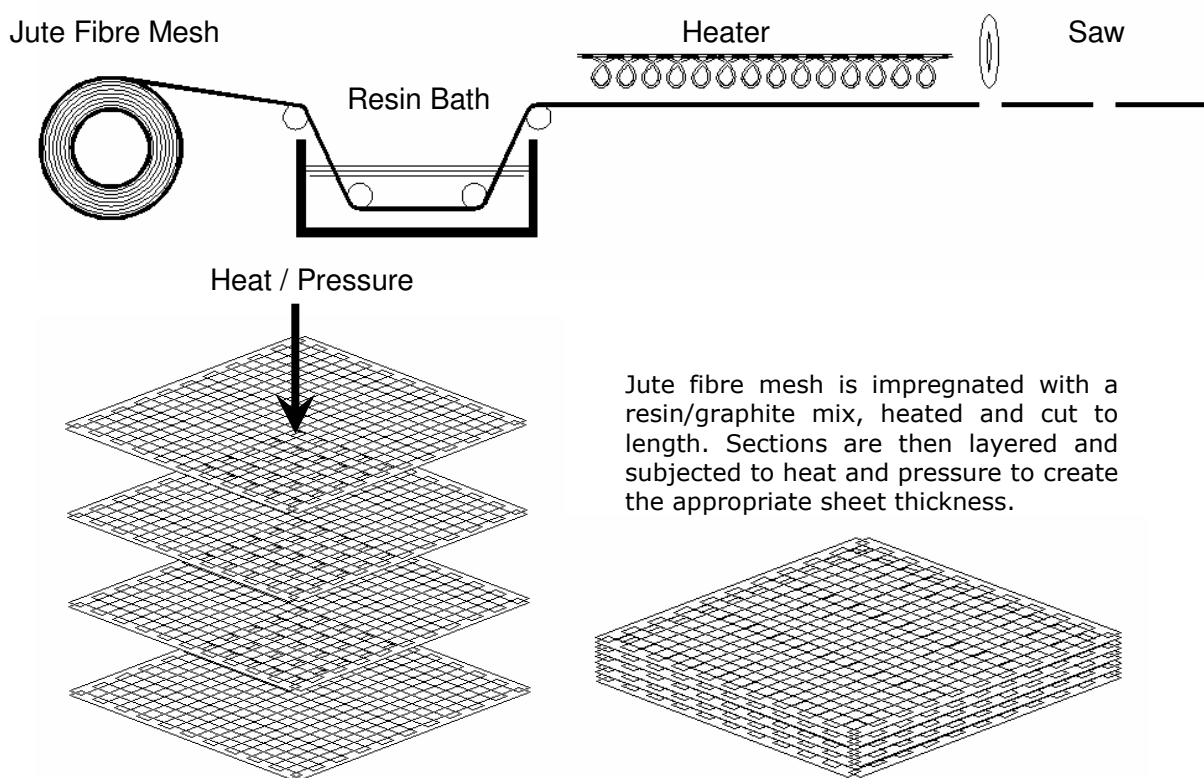


Fig. 2.11: Composite slipway lining manufacture

### **Tensile Test**

The composite slipway lining is tensile tested and is found to behave in a brittle manner with little plastic yield before failure, generating a yield stress of  $42\text{N/mm}^2$  at a yield strain of 3.49%. Full results are shown in appendix D.

### **Initial surface inspection**

The initial surface condition was measured using a Mitutoyo Surftest 301 profilometer. The profilometer provides measurements of  $R_a$  and  $R_q$ , the mean and root mean square roughness, along a sample line. The Zygo Interferometer used for later specimen scar inspection was found to be unsuitable for inspecting the initial surface condition as the asperity peak to valley height (PV) was greater than the range of the Interferometer.

### **Technique**

The profilometer is set to its maximum stroke of 2.5mm, three measurements are taken and the average used for calculation. A sample surface profile plot is shown below:

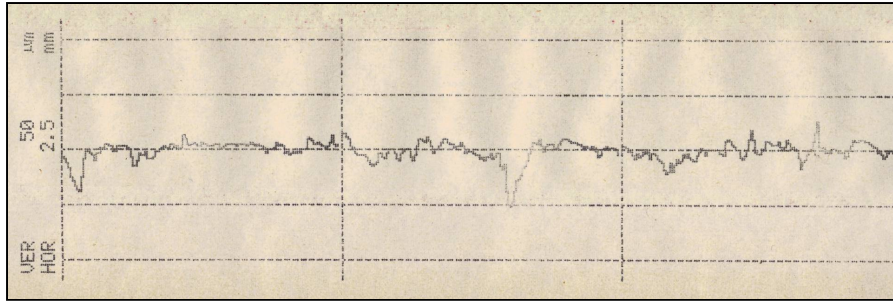


Fig. 2.12: Original composite surface profile

## Results

Consolidated results are shown below:

Ra ( $\mu\text{m}$ )	Rq ( $\mu\text{m}$ )
8.8	12.85
8.17	11.82
9.74	14.72
7.14	10.45
8.4	11.47
<b>8.45</b>	<b>12.262</b>

Fig. 2.13: Slipway lining composite - tensile test specimen

These results indicate an average surface roughness of  $R_a = 8.45\mu\text{m}$  and  $R_q = 12.262\mu\text{m}$ .

## Friction Coefficient

Friction coefficients for the composite are listed in the manufacturers literature as ranging from 0.12-0.25 with the lower limit representing the water lubricated case and the upper dry sliding. Full material specifications are shown in appendix C.

## PV Limit Considerations

The Pressure Velocity limit for phenolic resin against a hard counterface is listed in the literature [60] as between 1 and 5 depending on contact conditions; this corresponds to velocities of 5.7 - 28.4 m/s. It is known [10] that launch velocities can exceed 12.8m/s which means that the PV limit may be exceeded towards the bottom of the slipway. Because of the difficulties involved in accurately assessing the contact pressures and local condition on a real world slipway the PV limit must be inferred from the friction and wear performance for a given slipway.

### 2.4.3. Steel Rollers

Some slipways (Swanage, Mumbles, Sennen Cove launch slipway etc.) use steel rollers along the whole length of the slipway due to shallow slipway angles. This is advantageous in terms of friction performance but makes recovery more difficult as it is harder for the coxswain to 'stick' the lifeboat keel on the slipway sufficiently to allow the winch to be attached. Because of these disadvantages some slipways (e.g. Sennen Cove) use a roller slipway to launch and a separate conventionally lined slipway for recovery.

## **2.5.Slipway lubricants**

---

In order to manage the problems of high friction along the slipway, particularly during recovery with the corresponding high winch loadings various lubricants have been applied. These are often adopted on a site by site basis depending on local conditions and historical preferences. The main lubrication options in use are a marine slipway grease, freshwater, used on a number of composite lined slipways, including the Tamar operating Padstow and Tenby, and a silicon microball based cable lubricant, currently only used on the recovery slipway of Sennen Cove. Full lubricant specifications are shown in appendix C.

### **2.5.1. Marine grease**

Marine grease is a general purpose marine lubricant with applications in bearing and gear lubrication, deck winches, wire rope lubricants etc. When worked with water it forms a thick emulsion allowing it to continue lubricating and protect against corrosion. It adheres well to surfaces and is resistant to seawater washing, does not harden in cold, wet conditions and is intended to provide constant lubrication under high loading conditions. All of these characteristics make marine grease a suitable choice for a slipway lubricant; however it is intended primarily for closed systems which may include seawater contamination rather than the open environment of a lifeboat slipway.

### **Ecotoxicity & Accidental Release Measures**

The marine grease has not been tested for ecotoxicity. It is insoluble in water and non volatile at ambient temperatures, however the mineral oil component will only biodegrade very slowly and has the potential to bioaccumulate in the region around the slipway. In case of accidental release it is recommended to contain the spillage using bundling and to PREVENT the spillage from entering sewers, rivers or open water.

By their nature many lifeboat slipway stations are on or near leisure beaches (e.g. Sennen Cove, Tenby) and the regular release of grease into this environment has the potential for deleterious effects on both the local ecosystem and beach users, particularly young children.

### **2.5.2. Microball lubricant**

Microball lubricant is a 'water based thixotropic lubricant' which reduces friction by incorporating small (~0.5mm) silicon 'microspheres' which act as ball bearings between the contacting surfaces. It is primarily intended as a closed environment cable pull lubricant and not meant for the open environment of a lifeboat slipway. The silicon 'microspheres', while

non-toxic also present the strong possibility of build up between slipway panels and at the end of the slipway, affecting friction reliability and wear characteristics along the slipway panels.

### **2.5.3. Freshwater**

Freshwater is being used as a lubricant at Tenby and Padstow slipway stations and is the manufacturers recommended lubrication for the new composite slipway lining panels. The use of freshwater along the slipway obviously reduces the environmental impact of slipway launches compared with using greases and other lubricants though this could be reduced still further with the use of 'grey' water or seawater.

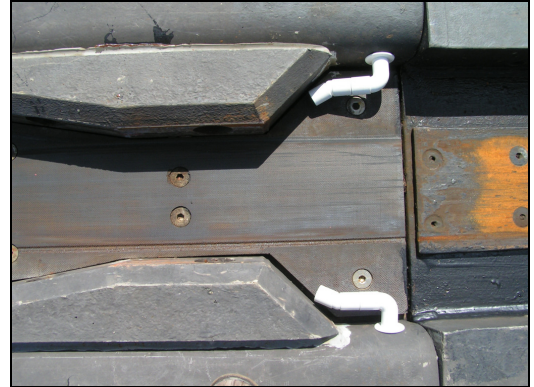


**Fig. 2.14: Freshwater Lubrication Jets at Padstow**

### **2.5.4. Seawater**

Seawater is present at the base of the slipway during every launch but its use along the length of the slipway is investigated here. Seawater would potentially have an even lower environmental impact than freshwater when the energy involved in processing drinking water to appropriate health standards is considered.

### **2.5.5. Biogrease #1**

Also considered in this study are vegetable oil based biogreases, these are selected for the ability to biodegrade in the marine environment reducing the dangers of bioaccumulation. Biogreases typically exhibit biodegradability of over 90% compared with just 20% for standard marine greases. It should be noted however that large scale release into the marine environment is still not advisable and the use of biogreases to replace current lubricants should be considered as only an incremental improvement in the environmental performance of lifeboat slipway operation.

### **2.5.6. Biogrease #2**

Biogrease #2 is the second of the biodegradeable greases tested here for their ability to be used as a direct substitute to the use of marine grease. The same caveats as for biogrease #1 described above apply.

## 2.6. Slipway Operation

---

### Slipway Launch Procedure

Before every launch it is usual for marine grease or a similar lubricant to be applied to the slipway, or for water lubrication to be activated. Prior to launch the lifeboat is held at the top of the slipway by chains attached to the front and rear of the keel, once the boathouse doors have been opened these are removed and the lifeboat is held by a quick release system on the winch cable.



Fig. 2.15: Quick release system - ringed

To launch the boat the quick release system is hit by a crewman with a hammer, the lifeboat then proceeds down the slipway under its own weight, entering the water at a speed of up to 45kph.



Fig. 2.16: Typical slipway launch – Selsey



### Slipway Recovery Procedure

Following a launch the lifeboat must be recovered to the top of the slipway. This process is considerably more difficult than launching and in rough conditions it is normal for slipway lifeboats to retire to the nearest natural harbour and wait for a lull in weather conditions that would allow it to return to the slipway.

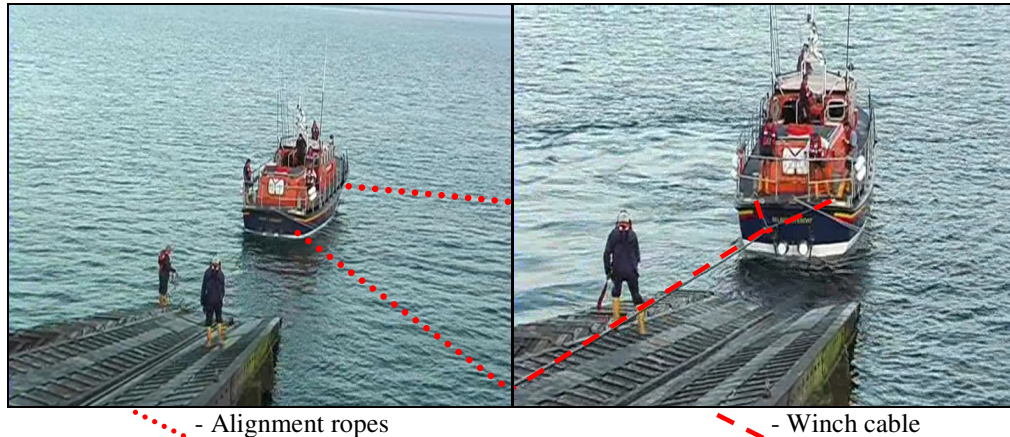


Fig. 2.17: Lifeboat alignment and attachment of winch cable – alignment ropes and winch cable indicated

First, the lifeboat is aligned with the slipway using two alignment ropes mounted on buoys. The length of these ropes is adjusted until the keel is in line with the slipway channel, indicated by a boatman on the slipway using a flag system. Once aligned the boat is manoeuvred onto the bottom of the slipway. At this point the winch cable is attached as shown and the lifeboat is hauled up the slipway [61].

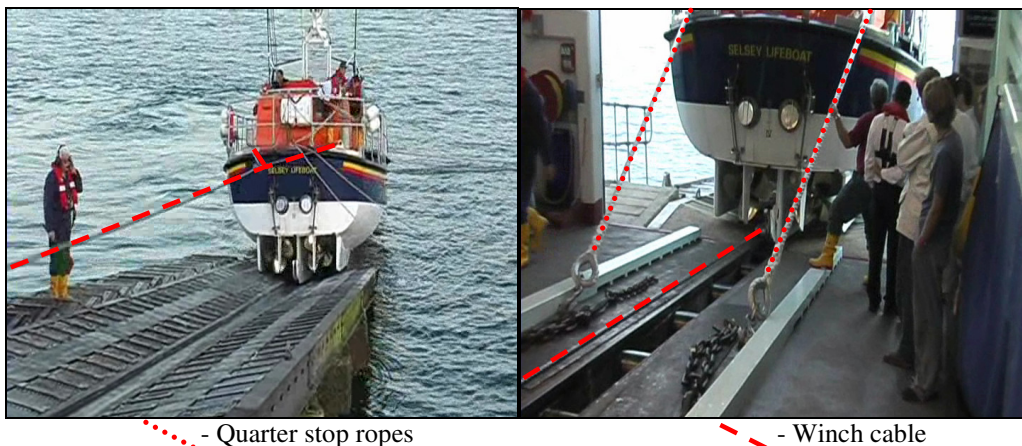


Fig. 2.18: Haul Stage – Rope quarter stops and winch cable keel attachment position shown

The lifeboat is hauled up the composite section until it reaches the boat house doors, at this point it is held by quarter stop ropes and the winch cable is attached directly to the keel of the boat. Once the cable is attached the quarter stops are removed and the boat is hauled up the

final roller section of the slipway. Prior to launch the boat is held by chains attached to the front and rear of the keel, the rear chains can be seen in fig. 2.15 (quick release system).

It is during this recovery section that most cases of high friction are experienced, these typically manifest as problems with the recovery winch, shown below:



Fig. 2.19: Recovery winch

The recovery winch is rated for a 12 tonne load at a 15m/min line pull speed, high friction incidents on the slipway can cause the load to exceed this and may require the winchman to significantly reduce the line pull speed to maintain acceptable winch loading.

# 3 CASE STUDIES

---

*The following sections detail a series of visits and winch trials performed at lifeboat slipway stations around the UK. Visits undertaken were to investigate the slipway lining for wear and high friction indicators, including a survey of the slipway panels for signs of wear and for fitting misalignments. Each slipway station has its own geographical and design characteristics and each has experienced particular problems with friction and wear.*

## 3.1. Case Study 1 – Selsey

---



Fig. 3.1: Selsey slipway station location

Selsey slipway station is located on the south coast of the UK between Portsmouth and Brighton, on the beach near the village of Selsey. Selsey lies at the southernmost point of the



Manhood Peninsula, a small island almost cut off from mainland Sussex by the sea. It is bounded to the west by Bracklesham Bay, to the north by Broad Rife, to the east by Pagham Harbour and terminates in the south at Selsey Bill. There are significant rock formations beneath the sea off both of its coasts, named the Owers rocks and Mixon rocks. Selsey beach is rocky and the slipway station is far out to sea, so there is little chance of wind blown sand on the slipway.

This section details slipway friction trials conducted at Selsey [10,11], particularly the trial of 09/10/2002. There have been lifeboats at Selsey for over 145 years and it currently operates a Tyne class all weather slipway launched lifeboat and a D class inshore boat. The original slipway was constructed in 1920 and the current boathouse dates from 1987.

## Background



Fig 3.2 Selsey Slipway Station

Selsey slipway station initially adopted a 6mm composite lining but this was soon replaced with a thicker, 19mm lining following problems with the lining cracking. Following the adoption of the thicker composite lining the performance of the Selsey

lifeboat slipway was investigated in the Selsey slipway trial [11]. The trials involved a load cell attached between the lifeboat and the winch cable, measuring the load exerted on the winch and thus enabling the friction coefficient to be defined. This is the configuration used to recover the lifeboat to the slipway once it has been positioned at the base using the alignment buoys. The trial was compared with two similar trials performed on a low friction steel slipway lining at Bembridge [7] and again at Bembridge with the new composite lining [8] with significant reductions in friction coefficient observed with the composite lining compared to the previous low friction steel lining. To ensure low friction grease is applied to the composite slipway section before each launch and recovery and the friction coefficients measured here represent the grease lubricated case.

## Slipway Design

The Selsey slipway has an incline of  $11.4^\circ$  (1 in 5) and is 53m long. The test was conducted using a Tyne class lifeboat of approximate mass 25.5 tonnes, the slipway was prepared using marine grease. The slipway is typically greased after recovery and not re-greased until

the next launch. Launches occur every 3-4 days. This allows the forces involved in the Selsey trial to be calculated as follows:

$$\begin{aligned}\alpha &= \text{Slipway angle} = 11.4^\circ \\ Mg &= \text{Lifeboat Mass} \times \text{Gravity} = 25.5e^3 \times 9.81 = 250155\text{N} = 250.2\text{kN} \\ R &= \text{Reaction} = Mg \cos \alpha = 245219.7\text{N} = 245.2\text{kN} \\ \mu R &= \text{Coefficient of friction} \times \text{Reaction (to be derived)} \\ \ddot{a} &= \text{Acceleration, derived from observed launch or winch speed}\end{aligned}$$

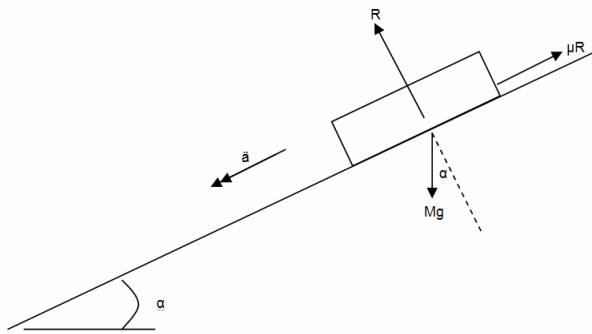


Fig. 3.3: Free body diagram of Selsey slipway

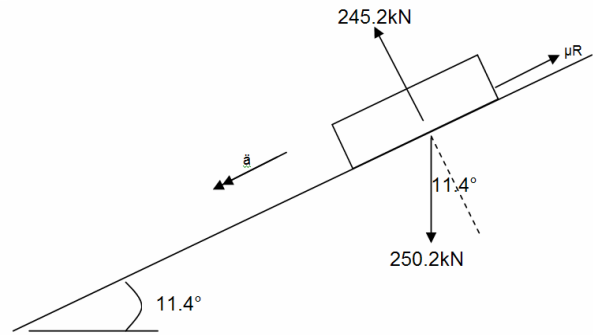


Fig. 3.4: Force calculation on Selsey slipway

During the trial the winch load was recorded at 2.5m intervals for two hauls. A launch was also recorded, giving the time and velocity as the lifeboat enters the water.

### Winch Test Procedure



Fig. 3.5: Selsey slipway on quarter stops with winch cable attached

The test was conducted in three stages. First, the launch friction was determined by launching the lifeboat and manually recording the time taken from hitting the slip hook to launch the boat to the transom of the boat reaching the end of the slipway. Times were recorded using three observers using two stopwatches and a video recorder and the average of these times was then used for calculation.

The second stage was to measure the friction as the boat was hauled up the slipway. With the slipway re-greased with marine grease following the launch of stage one, the lifeboat was recovered to the boathouse doors where it was held by quarter stop ropes allowing a load cell to be placed between the boat shoe and the winch cable. With the quarter stops released the boat was then lowered down the slipway until the bow was at the waters edge, the load on the load cell was recorded. The holding load was noted and the boat was hauled at the normal speed with the winch engine revs being kept to the recommended 1600rpm. Load cell readings were taken every 2.5m as the boat was hauled up the composite lining and onto the rollers as it entered the boathouse.

The third stage repeated stage two but also measured the load recorded as the boat was lowered down the rollers prior to the composite lined slipway section.

## Results

The following data was recorded during the first stage, a typical launch timed by two stopwatches and a video camera.

Watch 1 (sec)	Watch 2 (sec)	Video (sec)	Average (sec)
8.2	8.7	8	8.3

Table 3.1: Launch times for Selsey slipway

This data allows the launch velocity and dynamic friction coefficient to be derived:

Launch time:	8.3s	
Lifeboat mass:	25.5 tonnes	
Launch Velocity:	12.8m/s	(derived)
	46kph	(derived)
Coefficient of friction:	Dynamic – 0.07	(derived)

## Stages Two and Three

Data was recorded during stages two and three using the load cell to measure the loads along the slipway. These results are plotted in fig. 3.6. From the graph below it is clear that the friction encountered as the lifeboat is recovered is fairly constant along the composite lined section slipway and when the boat is on the rollers, with a smooth transition as the boat mounts the rollers.

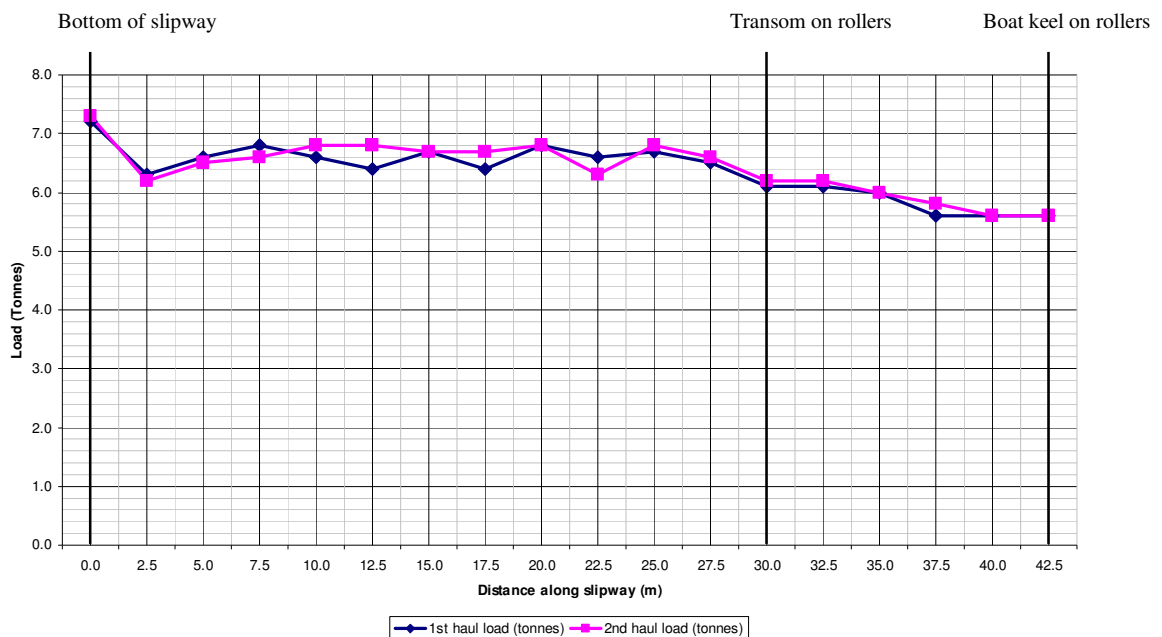


Fig. 3.6: Forces during recovery for Selsey slipway

## Conclusions

These results indicated a friction coefficient for the greased composite section of the slipway of between 0.048 and 0.07 with an average coefficient of 0.062. Previous trials conducted at Selsey on the composite section suggest similar results with an average dynamic coefficient of friction of 0.07 being recorded. However, the trial did record significantly higher values for the static friction of 0.17 compared to 0.09 in the second trial, and peak loads were also higher. This may indicate a partial breakdown of the grease boundary lubrication film in the second case so that there is asperity contact and the regime approaches dry sliding. This can be assessed by comparing the result to the manufacturer's friction coefficient values for dry sliding ( $\mu = 0.25$ ) using the fractional film defect [31]. This shows a value for the fractional film defect of  $\beta = 0.55$  in this case indicating that just over half the actual contact area is comprised of dry asperity contacts. This change in the lubricant regime may have been prompted by the lifeboat being allowed to 'dwell' on the slipway, squeezing the grease lubricant film to allow some dry asperity contact.

<b>Trial ID</b>	<b>Selsey Trial 09/10/02</b>	<b>Selsey Trial 27/02/02</b>
<b>Lining Material</b>	Composite	Composite
<b>Entry Speed (m/s)</b>	12.8	-
<b>Recovery Speed (m/s)</b>	0.25	-
<b>Max. Load (tonnes)</b>	7.3	9.2
<b>Max. Hauling load (tonnes)</b>	6.8	7.0
<b>Max Veering Load (tonnes)</b>	4.8	-
<b>Static Friction Coefficient</b>	0.09	0.17
<b>Dynamic Friction Coefficient</b>	0.07	0.07

Table 3.2: Selsey Slipway trials comparison

Despite variations between the two trials, the results for both are well within the parameters required of a slipway and indeed the trials generated similar results to those received from trials on the composite slipway at Bembridge slipway station. This would seem to indicate that the composite performs well as a slipway lining, with the only problem noted by the crew being that the lifeboat was slightly more difficult to recover to the slipway as the lower friction made it more difficult for the coxswain to 'stick' the keel to the slipway prior to hauling.

## Selsey Visit

Selsey slipway was visited on 09/10/06 at around 5pm and the slipway was inspected. The slipway lubricant regime was found to involve the use of marine grease on the composite section of the slipway. The general condition of the composite lining was good however and the coxswain indicated that there had been no real problems with either friction or durability [62]. Winch loads were said to be around 6-9 tonnes, well within limits. The main wear to the

composite lining was from the lifeboat recovery, with some impact damage to the edges of the slipway noted. In contrast to the slipway at Padstow, the Selsey slipway panels exhibited very little wear between panels and it was noted that the panels fitted together well without any significant misalignments.

Images are shown from the waters edge travelling up the slipway towards the boathouse.

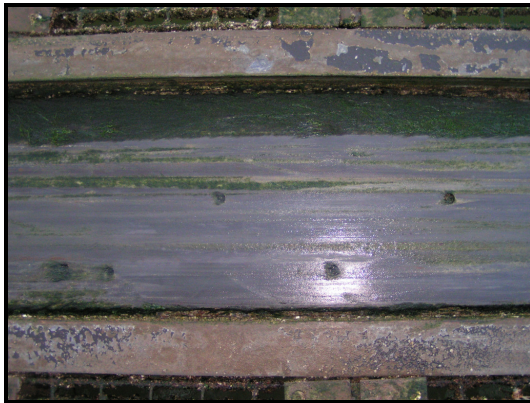


Fig. 3.7: Selsey slipway inspection – algae on panels



Fig. 3.8: Selsey slipway inspection – embedded debris

Algae was noted to be present on the lower section of the slipway and gouging wear scars were observed. One instance of embedded shell debris (ringed) was noted on the lower section of the slipway.



Fig. 3.9: Selsey slipway inspection – Worn panel edges from recovery keel impacts

Further up the slipway, damage to the side of the composite section was observed, this was attributed to keel impacts during recovery as the lifeboat initially mounts the slipway as this damage was only present on the lower section of the slipway where recovery is conducted.

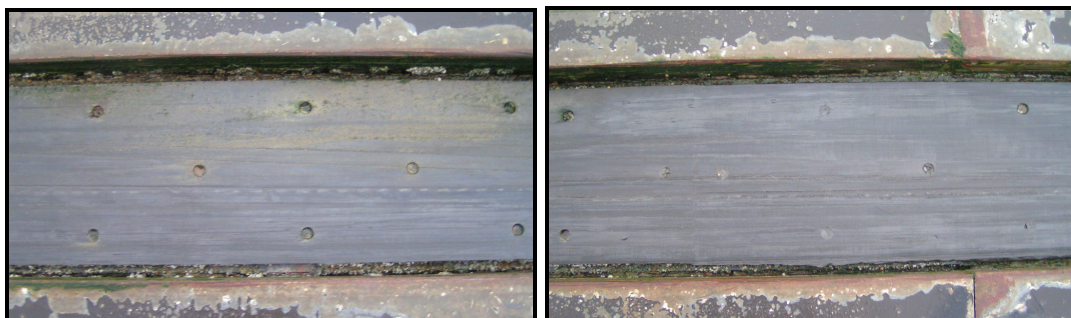


Fig. 3.10: Selsey slipway inspection – Gouging wear scars



Gouging wear was noted along the slipway with shallow wear scars indicating a raised section on the lifeboat keel or trapped 3<sup>rd</sup> body between the keel and slipway lining.

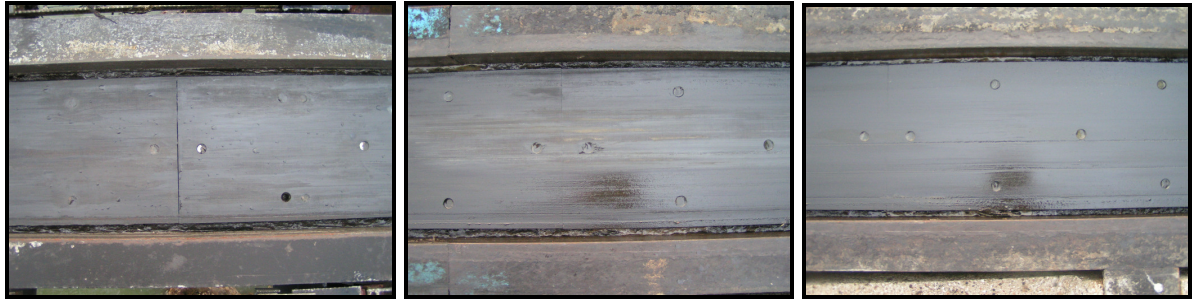


Fig. 3.11: Selsey slipway inspection – light panel end wear

Selsey slipway exhibited very little wear at the ends of the composite panels, whereas this had appeared to be the principal cause of wear at Tenby and Padstow. This may be because Selsey slipway panels are well aligned, with only small gaps between panels and no ‘step’ effects.

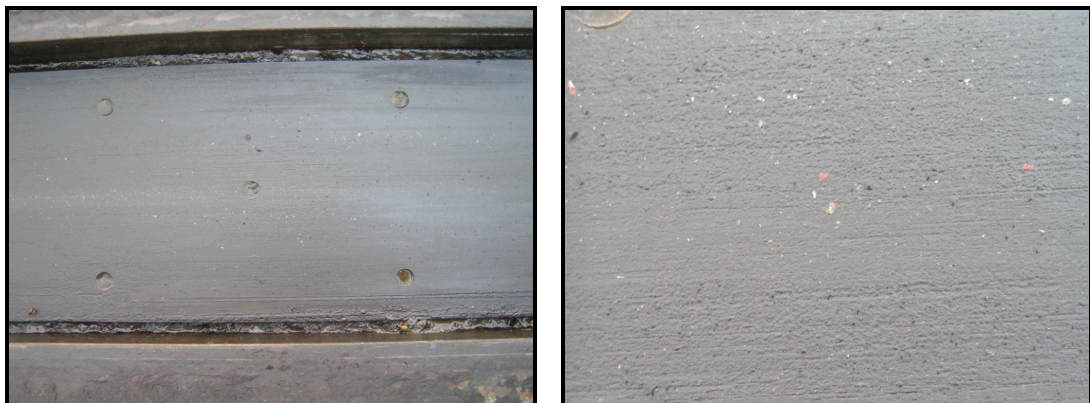


Fig. 3.12: Selsey slipway inspection – embedded shell debris

At the top of the composite slipway section there was another section of embedded debris, the coxswain believed this to be shell fragments as the slipway was used by seagulls to break the shells of hermit crabs and other molluscs [62].

### 3.2. Case Study 2 – Bembridge

---

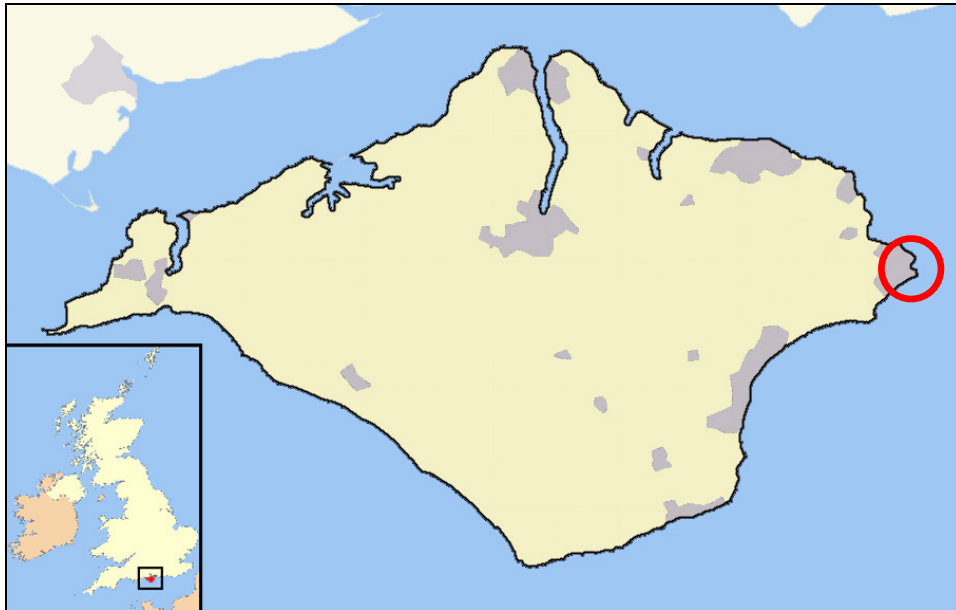


Fig. 3.13: Bembridge slipway station location

Bembridge is a village located on the easternmost point of the Isle of Wight and the lifeboat station lies to the north east of the village centre. The RNLI station is particularly important, as extending into the sea to the east of the village lies the notorious "Bembridge ledge", a large rocky outcrop which poses a major threat to passing boats. Although it is private sailing yachts which are most at risk, a wide variety of boats commonly run aground here, especially



Fig 3.14: Bembridge Slipway Station

in the often stormy weather conditions which affect the Solent during winter months. Bembridge has a sandy beach, though the boathouse is on a pier far out to sea making wind-blown sand on the slipway unlikely.

Bembridge slipway station is located on the Isle of Wight and has been in operation for over 140 years. The slipway dates from 1922 and was extended in 1989. The current boathouse was built in 1987. Bembridge currently operates a Tyne class all weather slipway launched lifeboat and a D class inshore boat with a low friction composite slipway lining. As with the Selsey slipway grease is usually applied to the composite section of the slipway prior to launch and friction results here represent the greased lubrication scenario.

### Slipway trials

Slipway trials at Bembridge [7,8] have also been conducted following the replacement of the Low friction steel lining with Composite. Results are presented below along with the Selsey trials for comparison.

### Bembridge Slipway Parameters

$\alpha$  = Slipway angle = 11.4° (1 in 5)

M = Lifeboat Mass = 25.5 tonnes

### Results

Trial ID	Bembridge 04/10/99	Bembridge 28/09/01	Selsey 27/02/02	Selsey 09/10/02
Lining Material	Steel	Composite	Composite	Composite
Entry Speed (m/s)	-	5.5	-	12.8
Recovery Speed (m/s)	-	-	-	0.25
Max. Load (tonnes)	-	-	9.2	7.3
Max. Hauling load (tonnes)	10.5	7.14	7.0	6.8
Max Veering Load (tonnes)	-	-	-	4.8
Static Friction Coefficient	-	-	0.17	0.09
Dynamic Friction Coefficient	0.16	0.07	0.07	0.07

Table 3.3: Bembridge and Selsey slipway trials comparison

The friction coefficient results from the Bembridge slipway trials are similar to results from the two Selsey trials, though the entry speed was appreciably lower. Data from trials of both lining would seem to validate the decision to replace the original low friction steel lining with the composite as significantly lower friction was encountered on the new composite lining.

### Bembridge Visit

Bembridge slipway station was visited on 02/11/06 and the slipway lining inspected. Marine grease lubricant is applied along the slipway before launch and recovery and so traces of grease were present along the slipway. The slipway is arranged with an initial roller section in the boathouse followed by a composite lined section as is common with most RNLI slipways. A photographic survey of slipway panels was conducted in order to assess wear characteristics.





Fig 3.15: Bembridge Slipway Station – slipway and boathouse

Bembridge slipway consists of a concrete substructure, with a composite lined steel keelway providing the keel bearing surface.



Fig 3.16: Bembridge Slipway Inspection – keel impact damage

Towards the base of the slipway severe cracking damage to the slipway panels it observed, this is reported by the Bembridge coxswain to be due to the impact of the lifeboat keel as the boat mounts the slipway for recovery.



Fig 3.17: Bembridge Slipway Inspection – Panel end damage: a) developing crack, b) cracked sections detached from panel

Panels are observed to be more vertically misaligned than at Selsey and panel end wear was observed at these points. This took the form of cracking, where a cantilever effect on the raised slipway panel results in a horizontal crack developing on the end of the panel. This will eventually progress through the composite until a large end section of the panel breaks away, this is seen on a worn panel at the very base of the slipway (fig. 3.17b).



Fig 3.18: Bembridge Slipway Inspection – panel end abrasive wear

If the composite remains adequately supported while still being vertically offset in relation to its neighbour then abrasive wear rather than large sections of cracking becomes dominant as seen in fig. 3.18.

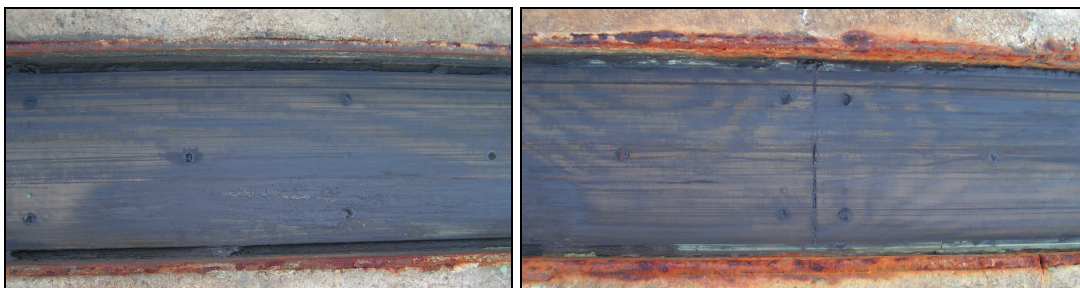


Fig 3.19: Bembridge Slipway Inspection – panel gouging wear

Abrasive gouges in the slipway lining are observed as at Selsey slipway, these are generally shallow grooves formed along the slipway panels by a raised imperfection in the lifeboat keel or by debris trapped between the keel and slipway lining. While contributing to the wear on the slipway panels these are not observed to cause panel failure, which is generally as a result of panel end cracking or abrasive wear on misaligned panels [63].

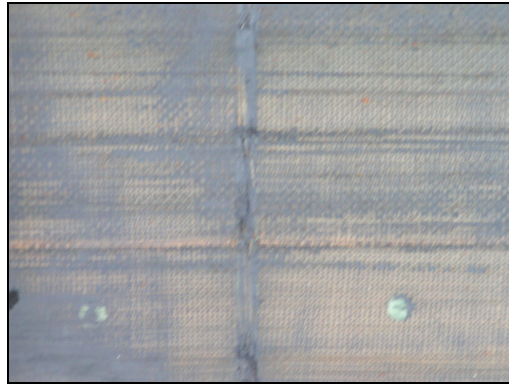


Fig 3.20: Bembridge Slipway Inspection – plane abrasive wear

Smooth abrasive wear was noted on some panels where alignment was good and the keel/slipway contact was plane and conformal, here the phenolic resin had abraded to reveal the underlying jute fibre mesh. This type of wear was observed to be very light and represents the wear that would be expected in the ideally aligned case.



### 3.3. Case Study 3 – Sennen Cove

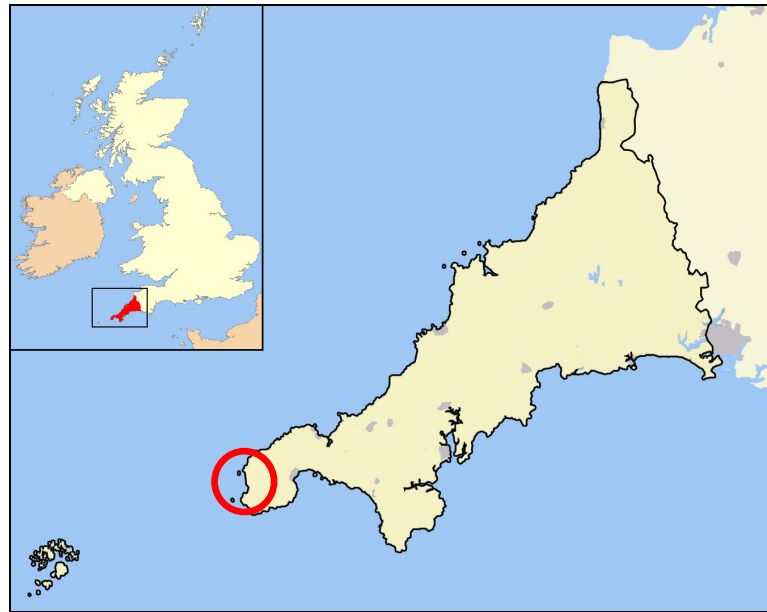


Fig. 3.20: Sennen Cove slipway station location

Sennen Cove slipway station is located near Lands End in Cornwall. Lifeboat stations at this location date from 1853 and it currently operates a Tyne class all weather slipway launched lifeboat and a D class inshore boat. At the time of its introduction in 1982 the station was not able to take the larger Tyne class lifeboat and continued with the Rother class lifeboat until the development of the lighter, Mersey class lifeboat. In 1991 the new Mersey class lifeboat, The Four Boys, arrived on station. In 1999 the boathouse was adapted to fit the larger Tyne lifeboat and the new Tyne class lifeboat arrived in January.

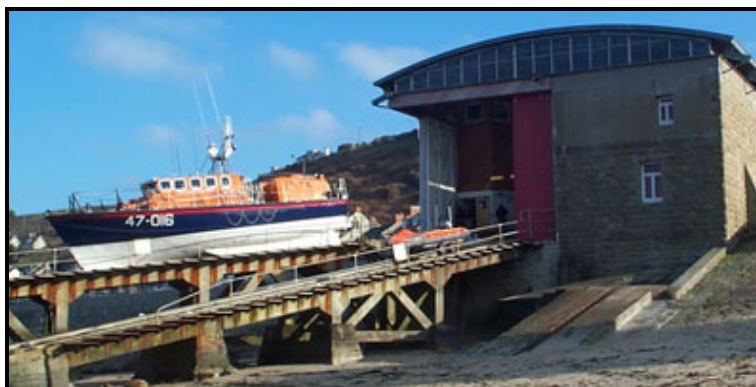


Fig. 3.21: Sennen Cove Slipway Station

Sennen Cove is notable for having two slipways, allowing the Tyne class lifeboat to be recovered in the shelter of the breakwater at high tide, or up the launching slipway at low tide. The launch slipway is shallower than usual at a gradient of 1 in 8; the recovery

slipway is the usual 1 in 5. The recovery slipway is lined with 6mm thick composite while the launch slipway, which is shallower than usual to ensure it clears the beach at low tide comprises rollers, followed by a steel channel at its furthest extent. The station also operates an inshore D class lifeboat. Inspection and analysis here focuses on the recovery slipway as this is where most friction and wear problems are reported to occur.

The crew of Sennen Cove slipway station have reported problems with high winch loading on the recovery slipway due to high friction between keel and slipway lining on recovering the lifeboat. The coxswain has suggested that this may be due to the presence of wind-blown sand from the beach depositing on the slipway, particularly when it has been greased, where it forms a 'grinding paste' increasing both friction and wear along the slipway [64]. The shallow water and sandy beach around the recovery slipway at low tide may also allow a wear effect with sand being washed up the slipway by the tide and finding its way under and around the composite lining, again causing wear and friction problems. Recently, the introduction of a microball grease, which includes suspended silicon microspheres to act as a kind of ball race has reduced the high friction problems encountered by the winch on recovery.

In order to study the effects of sand combined with grease, seawater or a combination of the two, sand samples were collected from Sennen Cove for investigation. It is this sand that is used for the sand/marine grease and sand/seawater contaminated lubricant combinations later tested on the TE57 reciprocating tribometer.

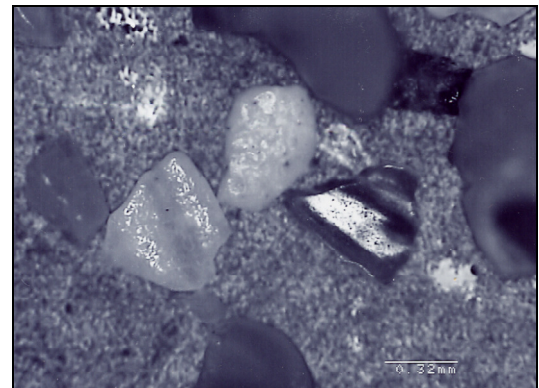


Fig. 3.22: Sennen Cove sand

### **Site Visit**

A site visit to Sennen Cove was arranged in order to investigate the recovery slipway for signs of wear and indicators to the causes of high friction on recovery.

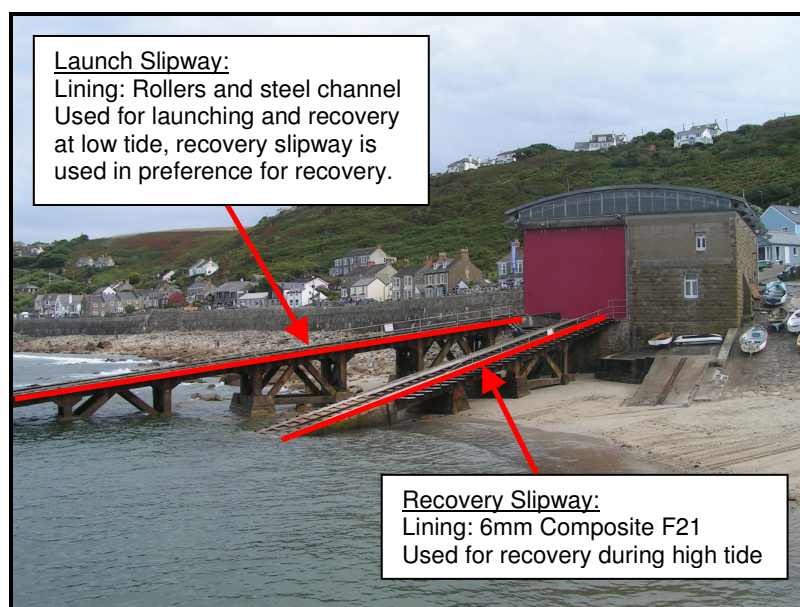


Fig. 3.23: Sennen Cove Slipways

The visit was conducted at low tide in order that the majority of the slipway was visible, and was primarily concerned with the recovery slipway as this is used for recovery wherever possible. The recovery slipway consist of a steel channel, lined with 6mm thick low friction composite at its upper reaches, this is to allow the boat keel to 'stick' when it first hits the slipway allowing the winch cable to be fitted prior to recovery. This arrangement is shown below.

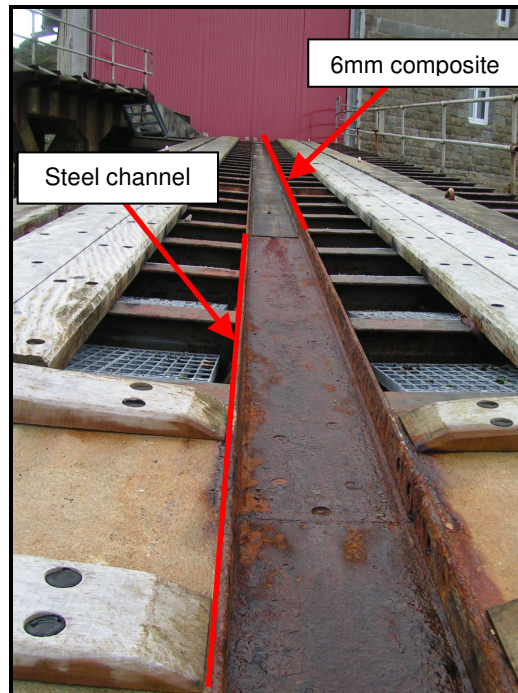


Fig. 3.24: Sennen Cove Slipway Station – Recovery Slipway (low tide)

### **Slipway Lining Inspection**

The general slipway lining condition seemed good, with little evidence of a plane keel with wear scar as expected. The majority of the damage to the slipway seemed to have come from other causes, impact or stress concentrations as the keel moved along the slip. Photos are shown with the recovery direction right to left.

#### Start of slipway Lining



Fig. 3.25: Sennen Cove Slipway Inspection – Lower lined section



The low end of the slipway has a small section of composite below the image in fig. 3.25. This section exhibited little wear apart from a couple of missing bolts (ringed) but it did show a good degree of bowing (indicated) that is likely to be from expansion due to water absorption. This problem has not been observed on slipway stations fitted with the thicker 19mm composite panels and may be in part due to the lower lateral stiffness of the thinner 6mm sections used at Sennen Cove. This section of slipway is rarely used as it is below water during high tide when recovery is most commonly attempted.

#### Second Stage of Slipway Lining



Fig. 3.26: Sennen Cove Slipway Inspection – Upper lined section, panel end wear and damage to fixing bolts

The second stage of slipway lining bears the weight of the lifeboat as it is drawn up the slipway by the winch. Again, this section is in relatively good condition with no prominent wear scar. The start of the slipway lining shows wear where an inclined section intended to smooth the step up from the unlined steel channel has worn away. Without this section the end of the slipway lining is beginning to wear in a similar fashion to the worn slipway panels observed at Selsey and Bembridge. The second slipway panel is almost unscathed with only some damage to one of the fixings observed. Wear on this section from the lifeboat keel is light and evenly distributed with the phenolic resin having worn away evenly in places to reveal the underlying jute fibre mesh in a similar way to the distributed plane sliding wear observed at Bembridge. This wear again represents the ideal case where contact is near planar and there are no stress concentrations present.



Fig. 3.27: Sennen Cove Slipway Inspection – Upper lined section, scoring and light panel edge wear

The upper section of the slipway also showed little wear, with some damage along the edges of the panels and wear on the securing screws. Light scoring was also present which is indicative of gouging wear as also found at Selsey and Bembridge. Between the panels and along the edges of the lining a dark slurry comprised of sand and grease has accumulated.



Fig. 3.28: Sennen Cove Slipway Inspection – Upper lined section, grease and sand slurry build-up

The very top of the slipway lining also exhibited some light wear, though there was one example where the edge of the panel had degraded quite significantly. Wear on this section was primarily the light plane sliding wear associated with smooth, well aligned planar contacts.



Fig. 3.29: Sennen Cove Slipway Inspection – Upper lined section, plane abrasive wear



### 3.4. Case Study 4 – The Lizard Slipway

---

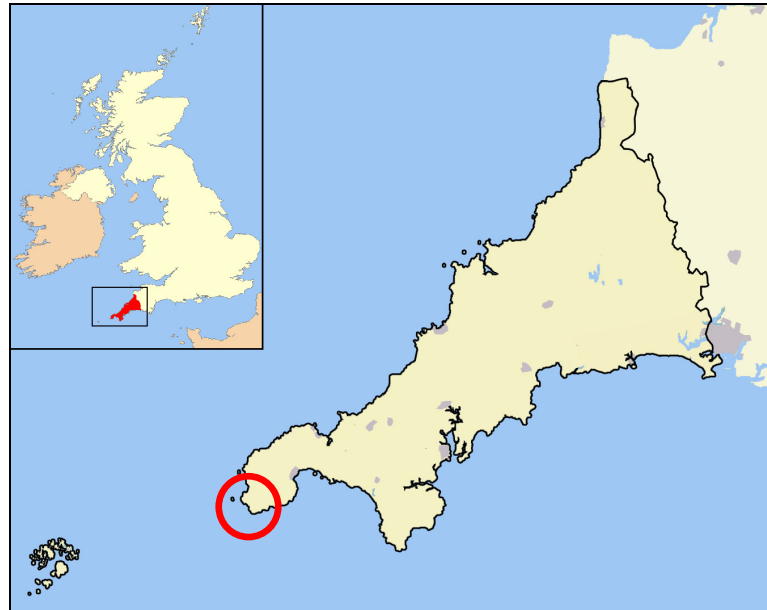


Fig. 3.30: The Lizard slipway station location

This section details the inspection of the Lizard slipway station slipway lining during a trip 23-24<sup>th</sup> August 2006. Lizard slipway station is located near Lizard point, the southernmost point in England and a notorious shipping hazard.



Fig. 3.31: The Lizard Slipway Station

The Lizard slipway station has the traditional slipway lining of Greenheart treated wood that has been in place for around 11 years although the wood panels have been rotated to present the other side as a bearing surface toward the bottom of the slipway within that time. The Station uses a Tyne class lifeboat and uses marine grease along the slipway during launch and recovery. On recovery it is reported that the

lifeboat exhibits stick/slip behaviour which is possibly more prevalent on hot days when the wood is drier [65]. As with most RNLI slipways, only the lower section of the slipway is lined, the upper section is comprised of steel rollers.

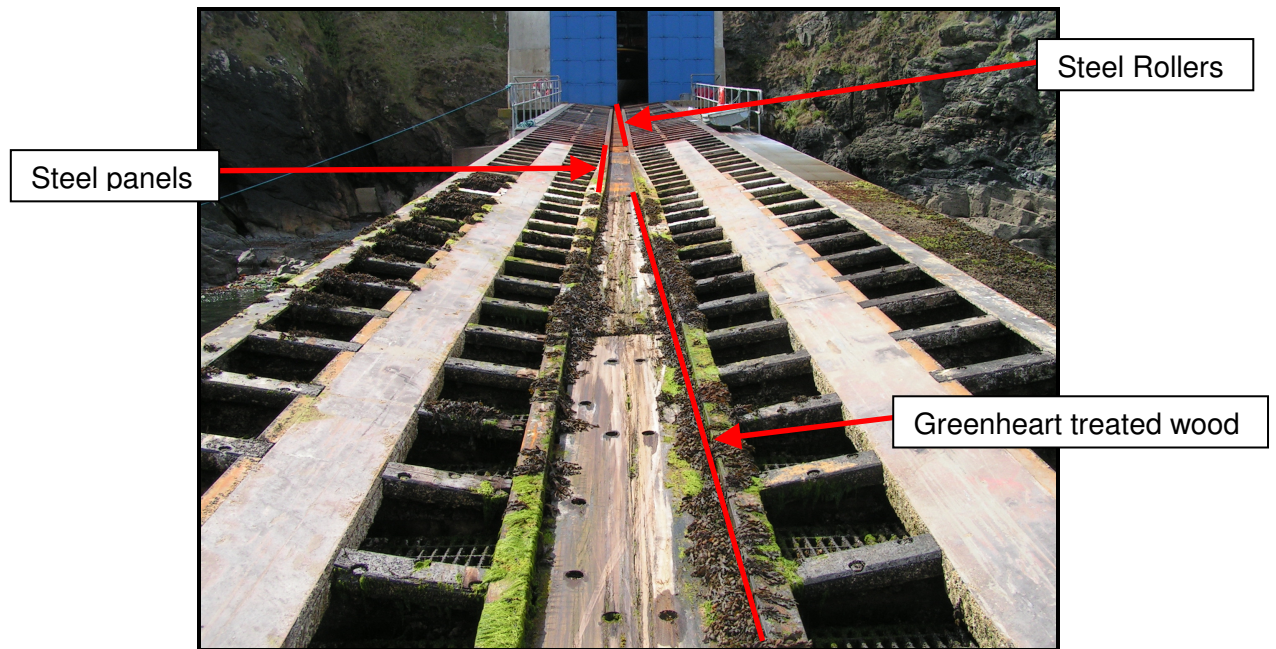


Fig. 3.32: The Lizard Slipway

### **Slipway Inspection**

The Greenheart slipway lining is observed to be deteriorating and a number of features are noticed. The slipway was inspected for its wear characteristics, pictures are shown from the boathouse doors towards the waters edge, with the direction of launch from right to left.

### **Roller Section**

The rollers are observed to be very rusty but no problems have been reported on this section of the slipway.



Fig. 3.33: The Lizard Slipway Inspection: Roller section

### **Steel Panel Section**

This section features a short length of steel panels which are greased with Marine grease for launch and recovery. These are covered in a sticky residue from the grease used and wear can be seen at the edge of sections and on the last panel, where some bowing appears to have caused the raised areas to wear. From interviewing the lifeboat station staff however, it appears that there is no real friction problem on this section of the slipway [65]. The steel section is treated with hypochlorate to remove seaweed and algae.





Fig. 3.34: The Lizard Slipway Inspection: Steel panel section

### Greenheart Wood Section



Fig. 3.35: The Lizard Slipway Inspection: Greenheart wood section

This section uses Greenheart treated wood as a bearing surface. Discussions with the crew indicate that there is a problem with high friction on this section of the slipway with the lifeboat exhibiting stick/slide characteristics as it is brought up the slipway. Seaweed and algae is left in place here as it acts as a natural lubricant and reduces the friction along the slipway. Wear on this section appears to be high, with the wood featuring cracks and heavy wear over the keel diameter.



Fig. 3.36: The Lizard Slipway Inspection: Greenheart wood section

Cracks appear to be longitudinal along the wood panel, and may be caused by swelling/shrinking of the wood as it absorbs water, cracks are more prevalent nearer the waters edge. Other wear seems to indicate gouging due to raised sections on the lifeboat keel or 3<sup>rd</sup> body particles present in the contact in a similar fashion to other slipway stations surveyed here.



Fig. 3.37: The Lizard Slipway Inspection: Greenheart wood section



### 3.5. Case Study 5 – Tenby

---



Fig. 3.38: Tenby slipway station location



Fig. 3.39: New Tenby Slipway Station

Tenby is a town in Pembrokeshire, West Wales, lying on Carmarthen Bay. Tenby slipway station is located on the easternmost point of Tenby, adjacent to the harbour and has been in operation for the past 150 years. It has both an all weather lifeboat and an

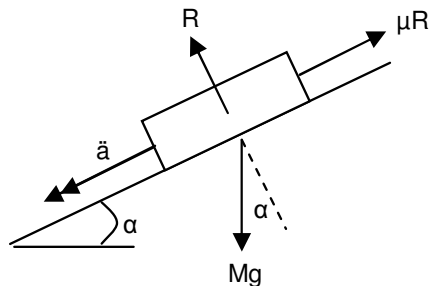
inshore D class lifeboat and was recently upgraded to be able to take the heavier Tamar class lifeboat by building a brand new boathouse next to the old one, now demolished, featuring a tilting roller section. Tenby is to be the first slipway station to receive the new Tamar class lifeboat and features a lined slipway section of 19mm thick composite with a water jet system at the top of the lined section used for lubrication.

#### **Tenby slipway trials**

The slipway trials [4,5] were conducted in a similar fashion to the trials conducted at Selsey and Bembridge with the boat recovered to the slipway as normal, held with quarter stops and a load cell placed between the boat and the winch cable. Prior to the commencement of trials it was noted that previous Tamar prototype test launches had caused the composite to

degrade and hauling loads had tended to increase. It was also noted that the friction load was higher when the slipway was dry [66].

### Slipway Parameters



$\alpha$  = Slipway angle =  $11.3^\circ$  (1 in 5)

$M$  = Lifeboat Mass = 30 tonnes

$R$  = Reaction =  $Mg \cos \alpha$

$\mu$  = Coefficient of friction

$\ddot{a}$  = Acceleration

### Instrumentation

The Tenby slipway trials were notable for using considerably more instrumentation than previous trials. The following sensors were used:

#### Winch

Three HD type pressure transducers were used to monitor hauling loads mounted on the winch motor and winch pump respectively. The Delta P Pressure across the winch motor ports is calculated from sensor readings. An infra-red RPM sensor was used to monitor the rate of drum rotation; distance travelled being a conversion based on length of rope per drum revolution.



Fig. 3.40: Tenby slipway trials – Load cell ringed

#### Load Cell

A Radiolink 25 Tonne load cell was used in line with the winch cable to monitor line pull loads; this was linked to a Telemetry base station connected to a data logger located near the winch.

#### Data Logger

Data from the load cell, pressure transducers and infra-red sensor was recorded using a MS 5000 data logger, the update interval for the load cell was set to 0.2 seconds (5 Hz) and for the pressure sensors every 50ms (20Hz).

### **Trial Schedule**

Trials were conducted according to the table below:

<b>Trial No.</b>	<b>Slipway Conditions</b>	<b>Scenario</b>	<b>Friction tested</b>
1	Wet	Haul	Dynamic
2	Wet	Haul	Dynamic
3	Wet	Haul	Dynamic
4	Wet	Haul	Dynamic
5	Wet	Haul	Dynamic
6	Semi Dry	Haul	Dynamic
7	Wet	Breakaway	Static
8	Wet	Breakaway	Static
9	Wet	Breakaway	Static
10	Wet	Breakaway	Static

Table 3.4: Tenby slipway trial schedule

In all trials hauling was undertaken over the maximum length of exposed slipway possible, up to the boat house doors which are defined as the 0m datum position. For most of the trials between 30m and 40m of slipway was exposed, as measured from the boathouse doors.

Haul trials involved hauling the boat up the slipway as in the Selsey and Bembridge trials. Breakaway trials aimed to determine a value for static friction; these involved holding the boat static on the slip under winch rope tension and collecting data as the boat was allowed to move. Under normal operating conditions recovery of the boat results in an indeterminate application of water onto the slipway as the boat is hauled in, to simulate this on all but the semi-dry trial, a hose supplying water at mains pressure was applied to the top of the composite slipway section. In the semi-dry trial the hose was removed, though residual water from the previous trials was still present.

### **Results: Dynamic Friction**

In trial 1 the load measured by the load cell increased gradually for the first 10 to 15m of the haul, this is likely to be due to the lifeboat being partially buoyant at the start of the trial with only the rear of the keel on the slipway. Due to the high waterline at the time of the trial the rear of the boat had already engaged the roller section of the slipway by 3m at the point it was fully clear of the water. This makes it difficult to calculate the friction coefficient of the composite section of the slipway as during the initial stages of the test the boat was partially supported by the water, and at the end stages it had engaged the roller section of the slipway.

Trials 2 – 5 were hauling tests with the winch running at 1400, 1600, 1800 and 2000 RPM respectively. Trial number 4 was conducted at the recommended engine speed of 1800 RPM.

Trial No.	Engine Speed (RPM)	Average Line Speed (m/min)	Average Load Condition (tonnes)	Average Friction coefficient
2	1400	16.2	8.5	0.138
3	1600	22.2	8.0	0.118
4	1800	25.0	8.0	0.118
5	2000	29.4	7.5	0.098

Table 3.5: Tenby slipway trial results

These results may imply that the line speed has an impact on the friction coefficient though any effect is slight.

These friction coefficient values contrast with the previously recorded friction coefficients in trials at Selsey and Bembridge, which indicated values of around 0.07, with a peak of 0.09. This is due to the lubrication regime in place; Selsey and Bembridge use marine grease along the slipway whereas Tenby uses water lubrication. The trial data would seem to indicate that water lubrication is not as effective at reducing friction along the slipway as grease lubrication. The friction coefficient on the rollers was recorded as approx. 0.02, matching results from the Selsey and Bembridge trials and allowing systemic recording errors to be discounted here.

#### **Trial serial no. 6**

This trial was intended to investigate whether the semi dry regime produced any changes in friction coefficient compared to the water lubricated case. In fact, no significant difference was observed, though the composite had not fully dried from the previous trials so the boundary lubrication regime may have remained in place.

#### **Static Friction: Trial serial nos. 7 – 10**

These trials were intended to investigate the static friction coefficient on the composite section of the slipway. All trials provided similar results with loads ranging from 13.0 tonnes to 15.3 tonnes with a mean of 14.2 tonnes. These correspond to a coefficient of friction of  $\mu = 0.242 - 0.320$  which is similar to values recorded during peak loads in trials 2 – 6. These values exceed the friction coefficient specification of  $\mu = 0.2$  for a 1 in 5 slipway and also approach the dry sliding friction coefficient of  $\mu = 0.25$  from the composite manufacturers in-house testing. This may be indicative of a breakdown in lubrication regime from boundary lubrication to dry sliding contact.



### **Slipway trial Conclusions**

The Tenby trials demonstrated that the recovery winch was well capable of dealing with the loads it is likely to encounter as it has achieved a peak line pull of 25 tonnes during a previous static load test, the maximum encountered during the trials was 17.4 tonnes momentarily. The winch is required to pull a load of 12 tonnes at 15m/min when running at 1800 RPM and Trial 4 indicates a line speed of 25m/min with an average load of 8 tonnes suggesting that the average loads are likely to remain within the specification. The friction encountered during the trials was far higher than that encountered on the same composite slipway lining at Selsey and Bembridge, with instantaneous friction coefficients reaching 0.392 compared to peak values of 0.070 at Selsey. Because of the low viscosity of the water lubricant used the instantaneous peak friction loads may represent a breakdown in the lubrication regime so that contact approaches the dry sliding case, and dry sliding friction coefficients of  $\mu = 0.25$  from the composite manufacturers in-house testing indicate that this is likely. It is thought that a dry sliding contact regime coupled with localised panel misalignment effects may be the cause of these friction peaks. Better instrumentation including a much higher sampling rate at Tenby may also account for some of this difference in peak values compared with other slipway stations, though the average friction coefficients recorded were also higher, at around 0.17 at Tenby, compared to 0.062 at Selsey and 0.070 at Bembridge. It should be noted that Bembridge and Selsey both use marine grease lubrication along the composite section as opposed to the water lubrication system used at Tenby, the higher viscosity of the marine grease used will reduce the susceptibility of the contact to boundary lubricant film breakdown to approach dry sliding. During the first trial it was noted that the rear portion of the boat keel was not completely flat and this almost certainly contributed somewhat to the high friction encountered. Slipway launched lifeboats occasionally need to break land and other hazards encountered in the course of duty are also likely to cause minor imperfections along the keel so this should not be considered particularly unusual, the Tamar lifeboat was new compared with the Tyne boats tested at Selsey and Bembridge, however the high friction encountered at Tenby indicates that the contribution of an uneven keel to the friction coefficient is worthy of further investigation.

### **Recovered Tenby Slipway Section**

This section looks at a section of composite slipway lining material removed some months after the Tenby trial described above. Data for the number of launches endured by the section is not available as problems of heavy wear have led to the piecewise replacement of the worn slipway lining, however the severity of the wear is evident from the removed section and it is hoped that examination of the section will allow the prevailing wear mechanisms to be identified.

The recovered section shows three distinct wear types, the most obvious is the deep scores left in the panel as a result of gouging wear by a raised keel section or 3<sup>rd</sup> body trapped between the keel- composite slipway lining contact. The second wear type present on the recovered panel is the abrasive wear present at the panel end; this is thought to be a result of panel misalignment as similar wear on real life slipway linings is noted to be far more pronounced in panels exhibiting vertical misalignment with respect to their neighbours. The third type of wear present is termed plane sliding wear and represents the abrasive wear resulting from the distributed lifeboat load under plane sliding, this wear is very light and represents the idealised sliding scenario. Plane sliding wear is also observed on other slipway panels and is characterised by an even erosion of the phenolic resin bulk of the composite material exposing the jute fibres, this is visible on slipway panels as areas of lighter colour. Algae is also present in places which may have some effect on the local friction.



Fig. 3.41: Worn composite slipway section; Abrasive wear at the panel end is clearly visible, the deep scores running along the panel are the result of gouging wear from a protruding keel section or similar and the lighter sections show plane abrasive wear where the phenolic material has been abraded away to show the lighter underlying jute fibre matrix

From measurements of the slipway gouging wear scars the theoretical ploughing friction coefficient for this contact is 0.408. Slipway trials indicate that this is seldom reached in normal operation so it can be assumed that ploughing friction is an infrequent phenomenon. In fact, subsequent investigation shows that the keel of the initial Tamar prototype was damaged forming a protruding section of the right size and shape to generate the wear scars seen after the initial slipway trials at Tenby and Padstow. The lifeboats currently in use at

these locations now have smooth keels and it is evident that the ploughing wear initially observed was an isolated incident related solely to the damaged keel of the Tamar prototype.

### **Slipway Inspection**

Following the investigation of the worn Tenby slipway section a photographic survey of the composite slipway bearing surface is conducted. The Composite slipway lining at Tenby is observed to be deteriorating rapidly. This is despite switching from the thinner 6mm to a 19mm sheet. The lining is observed to be cracking and suffering from deep gouges particularly at the edges between sheets.

### **Panel End Wear**

As in the recovered worn slipway panel it is noted that wear is most apparent at the ends of slipway panels. It is also noted that the panels exhibiting the most severe end wear show significant height misalignment with the adjacent panel. It is thought that this will have a significant effect on the stress distribution over the panel and that this may be a major contributor to wear. To further investigate this effect a panel alignment survey is conducted as described later in this section.

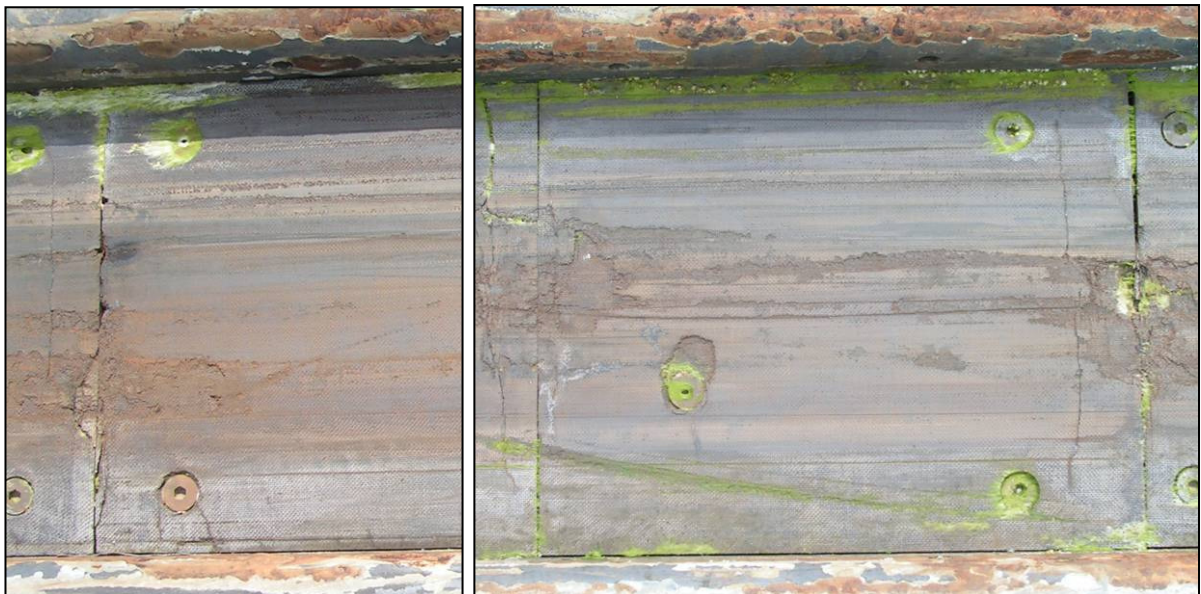


Fig. 3.42: Tenby Slipway Inspection: Panel End Wear

### **Gouging Wear**

Wear scars from a protruding section of the keel are noted in places. It is known that in early trials the prototype Tamar lifeboat keel featured some sharp protuberances and it is these that have scarred the panels. The majority of the slipway panels used with the damaged prototype keel have now been replaced; hence the gouging scars from this period are not present all the way along the slipway. The gouging scar depth is measured and matches the



gouges on the recovered section, indicating that they are both the result of the damaged prototype keel.



Fig. 3.43: Tenby Slipway Inspection: Gouging Wear

### **Delamination Wear**

Some delamination wear is seen on the better aligned panels where the load from the keel is more evenly distributed than in the end wear case.



Fig. 3.44: Tenby Slipway Inspection: Delamination Wear

### **Panel Alignment Survey**

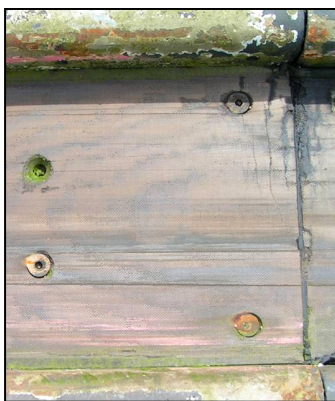


Fig. 3.45: End wear beginning on Tenby misaligned slipway panel

Photographic surveys of a number of real world slipways were conducted in order to develop a picture of the typical wear patterns developed by the slipway panels. During these investigations it was observed that there was sometime severe misalignment between slipway panels along the slipway. It was noted that the most severely worn panels seemed to coincide with the more pronounced panel misalignments and this led to more comprehensive slipway panel surveys at the new slipway stations of Tenby and Padstow to ascertain the extent of this misalignment.

Measurements of the height difference between slipway panels were taken at each corner of each panel and recorded for the extent of both slipways above the waterline - detailed results are shown in Appendix E.

These show that the panel misalignment is present and significant, reaching a peak of 3.52mm height difference between panel 18 and 19. Wear on panel 19 (raised in relation to panel 18) is observed to be primarily end wear with cracking well developed on the panel despite it having been only recently replaced. Overall the slipway shows an average height difference between panels of 0.884mm with a maximum of 3.52mm. From the composite data sheet the compressive yield strain is recorded as 1.9%. on a 19mm thick panel this would correspond to a height of 0.361mm, less than half of the average panel height difference along the slipway. This indicates that compressive deformation of the composite panels is not sufficient to accommodate the panel misalignments present, even at the maximum compressive deformation before failure.

The panel misalignments were further analysed by categorising them as one of three misalignment scenarios, angled, parallel and skewed misalignment.

This categorisation later allows FEA analysis of the effects of panel misalignment on friction and wear to be considered. The categories are as follows, Parallel misalignment, where the two panels are offset while remaining parallel as shown in fig. 3.46, i). below, Angled misalignment, where the two panels are offset by between 0 and 5mm at the panel interface due to one panel lying at an angle to the slipway bed as shown in fig. 3.46, ii). below, and Skewed misalignment, where the two panels are twisted longitudinally in relation to each other, shown in fig. 3.46, iii).

Panel No.	Average height difference to next panel (mm):
1	0.465
2	1.8
3	-0.2
4	-0.035
5	-0.27
6	0.01
7	0.87
8	-0.455
9	1.01
10	-0.9
11	-0.56
12	1.635
13	0.72
14	-0.715
15	-1.295
16	0.97
17	-0.275
18	-3.52
19	1.775
20	0.85
21	-0.225
22	No Data

Table 3.6: Tenby slipway survey data

The parallel scenario was found to be present in two thirds of all the panels surveyed (including a similar panel alignment survey conducted at Padstow), with the average offset for all panels being 0.82mm and the maximum being 4.06mm. The angled scenario accounts for around one third of all slipway panels surveyed, with the average offset angle for all panels being 0.0375° and the maximum being 0.184°. These correspond to panel interface offset heights of 0.799mm and 3.92mm respectively. The skewed scenario was present in

22% of panels, roughly equally occurring within both the parallel and angled offset scenario. Across all panels the average skewed offset angle is  $0.107^\circ$ , this corresponds to an offset height of 0.728mm. A maximum offset angle of  $0.6345^\circ$  was also recorded; this corresponds to an offset height of 4.32mm across the width of the panel.

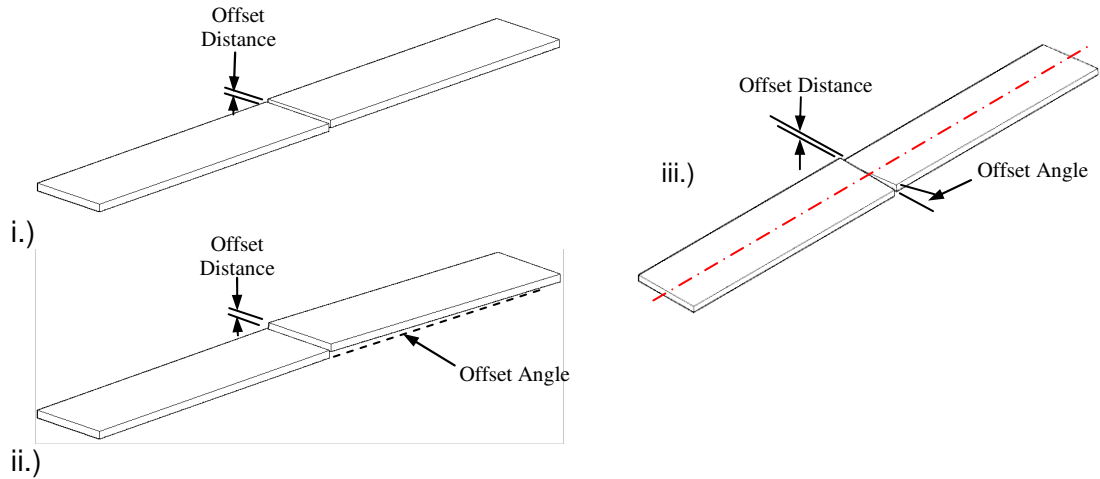


**Fig 3.46: Panel Misalignment Models; i.) Parallel Misalignment, ii.) Angled Misalignment, iii.) Skewed Misalignment**

The implications of this are discussed further in the FEA section of the thesis, here the panel misalignment data is used to construct FE models to evaluate the contribution of panel misalignment to the friction and wear on slipway panels.

### 3.6. Case Study 6 – Padstow Slipway Inspection

---

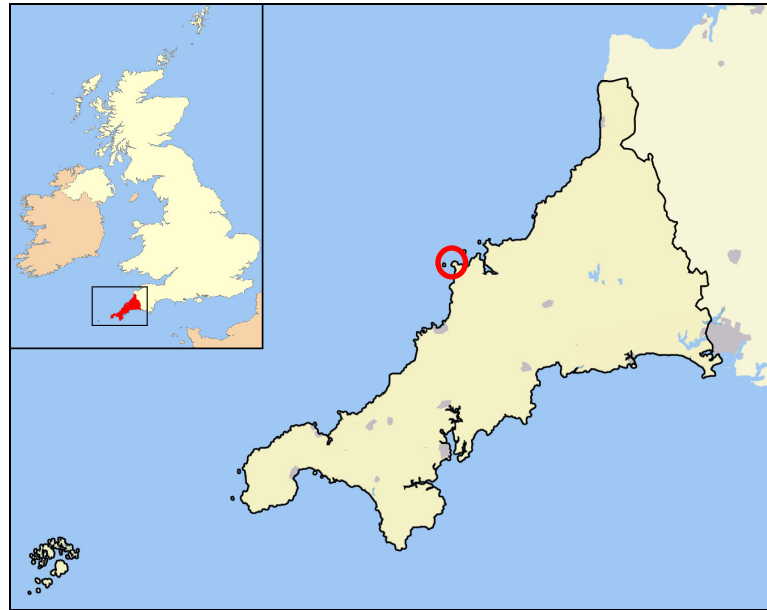


Fig. 3.47: Padstow slipway station location



Fig. 3.48: Padstow slipway station

Padstow is a small town on the north coast of Cornwall, United Kingdom, approximately 14 miles north and east up the coast from Newquay, at the mouth of the River Camel. The lifeboat station is situated on Trevoze Head and has recently been upgraded with a new slipway and boathouse to allow it to take the new Tamar class lifeboat. The boathouse features a tilting roller section similar to the one at Tenby which allows the lifeboat to be stored horizontally for maintenance. The slipway is also similar to Tenby, with a steel roller section at the top, and the lower section lined with 19mm composite panels. The slipway is either lubricated with marine grease or, more commonly, with freshwater lubricant run from nozzles at the top of the slipway. The composite lining at the time of the slipway inspection had been in place for around 30 launches.



### Dry Sliding Observations

Interviews with the coxswain [67] indicated that without any water lubrication, friction on the composite section of the slipway was ‘terrible’ with smoke being observed as the lifeboat was launched. This most likely indicates that the composite has exceeded its Pressure-Velocity limit as the high speeds present during launch mean that frictional heat build-up cannot be adequately dispersed, this results in a transition to far higher wear and friction along the slipway. The smoke observed indicates that local flash temperatures have exceeded the operating temperature limit of the composite which is listed as 130°C. With the water lubrication performance was far better as this serves not only to reduce the friction coefficient which in turn reduces friction forces and heat build-up but also aids heat dispersion; however steam was still observed during launch indicating that flash temperatures at the interface remain above 100°C.

### Slipway Inspection

The slipway lining was observed to have deteriorated significantly during use, particularly considering the few launches it had taken. The slipway was inspected for its wear characteristics in order to determine the causes of this degradation; pictures are shown from the waters edge towards the boathouse doors, with the direction of launch from right to left.

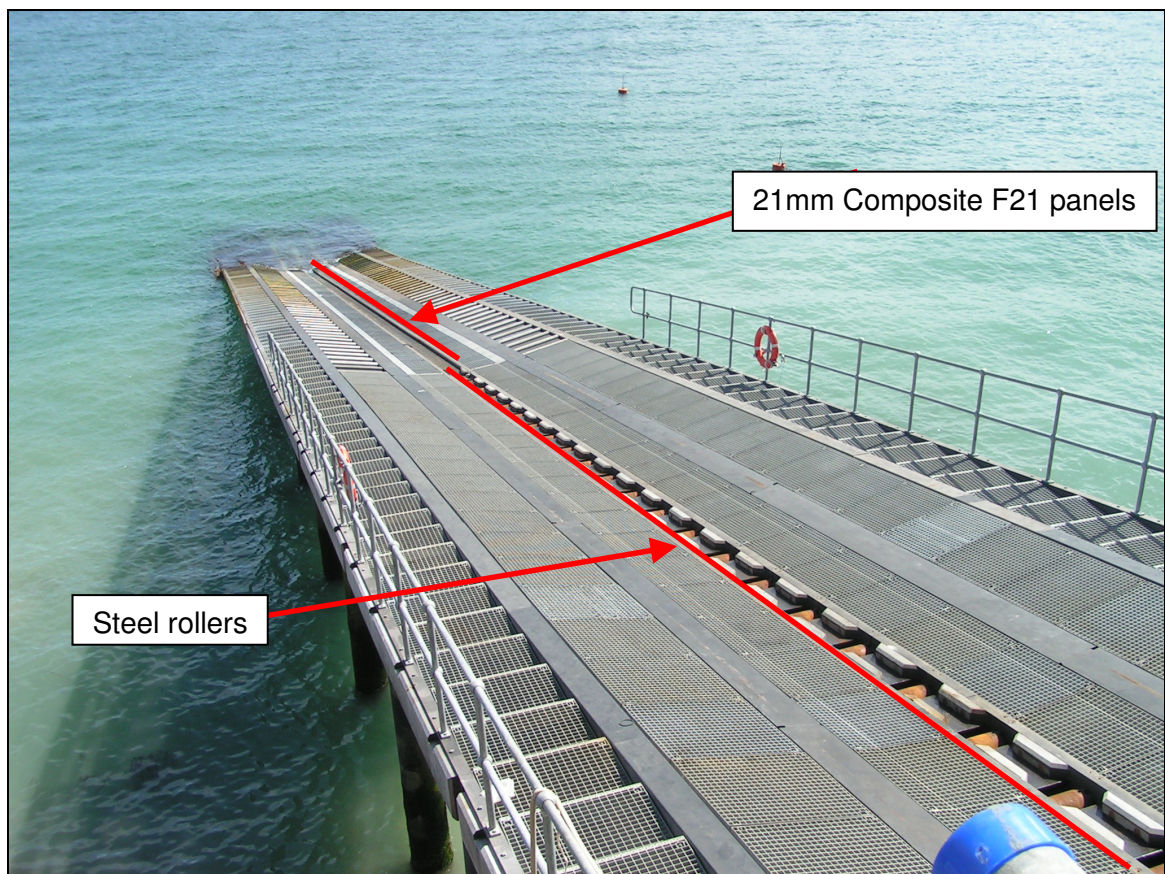


Fig. 3.49: Padstow slipway



### Panel End Wear

The composite lining shows evidence of cracking and abrasion at the panel ends in a similar fashion to the Tenby worn slipway section. As both Tenby and Padstow slipway stations are of the new boathouse design and use the new Tamar slip launched lifeboat this would indicate that this wear pattern is typical of this configuration. The effect is noted to be far more pronounced on panels featuring a vertical misalignment with their neighbours however.

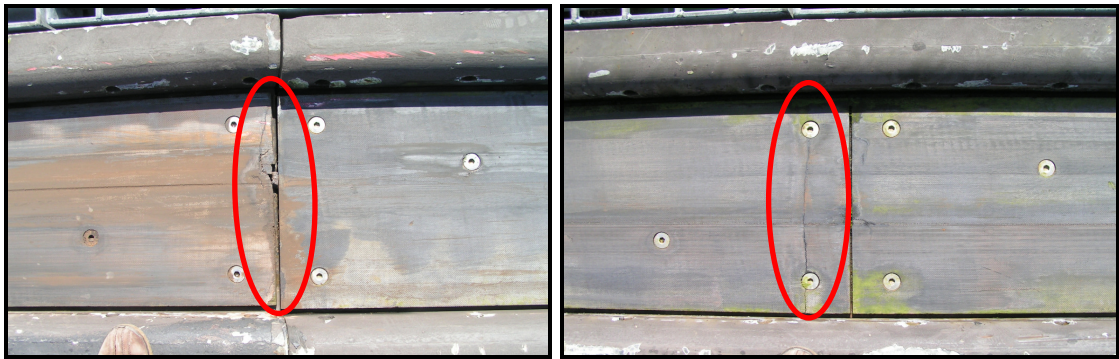


Fig. 3.50: Padstow Slipway Inspection: Panel end wear

In fig. 3.50, a vertical crack perpendicular to the launch/recovery motion is seen at the end of a panel between two fixing points, this would seem to indicate a cantilever effect with the panel sitting higher than the slipway base before cracking. This is similar to effects noted during the Tenby slipway inspection where panels that were observed to be misaligned vertically exhibited more pronounced end wear.

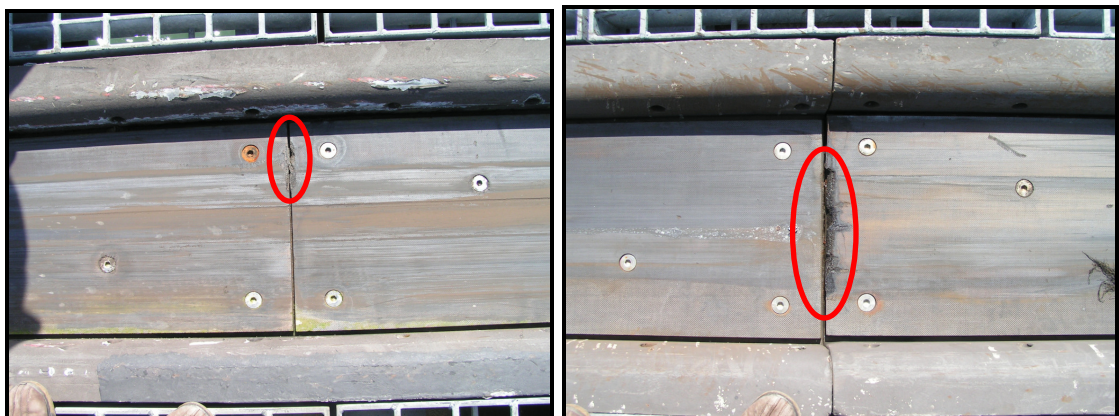


Fig. 3.51: Padstow Slipway Inspection: Panel end wear

Fig. 3.51 again shows wear developing at the panel ends of misaligned panels.



Fig. 3.52: Padstow Slipway Inspection: Panel end wear progression; i.) cracking to form panel 'islands', ii.) panel 'islands' detached from panel

Fig. 3.52 shows a typical progression of wear on the composite slipway panels, initial wear stresses cause the phenolic materials to crack leaving a panel 'island' held in place by the remaining jute fibres, this subsequently detaches reducing the bearing area of the panel.

### **Gouging Wear**

Another wear mechanism noted during slipway inspections was gouging due to keel imperfections or 3<sup>rd</sup> body particles trapped between the keel and the composite lining.



Fig. 3.53: Padstow Slipway Inspection: Gouging wear

Measurements of the gouging wear scar match those recorded at Tenby and are likely to result from keel imperfections on the Tamar prototype used in initial slipway testing as at Tenby.

### **Plane Abrasive Wear**

Plane abrasive wear is noted on the well aligned slipway panels, this is characterised by a noticeable smoothing effect along the centre of the panel where the keel passes. The wear volume is very small and this can be seen to represent the wear that would be expected from the ideally aligned contact case.



Fig. 3.54: Padstow Slipway Inspection: plane abrasive wear

Fig. 3.54 also shows the freshwater lubrication system, the two nozzles run freshwater along the slipway during launch and recovery of the lifeboat to provide a lubricated contact to reduce friction.

### Panel Alignment Survey

At Padstow it is observed that the composite panels with the most pronounced end wear are often vertically misaligned with respect to their neighbouring panels producing a raised edge which is likely to generate stress and wear concentrations. A similar effect is noted at Tenby slipway. To investigate the panel misalignment effects on friction and wear a detailed panel misalignment survey is conducted.

It is found that panel misalignment is present and significant along the slipway with an average panel height difference of 0.726mm and a maximum of 4.055mm. This compares with the maximum deflection at compressive failure of the composite for a 19mm thick panel of 0.361mm and indicates that panel misalignment

Panel No.	Average height difference to next panel (mm):
1	0.1
2	0.44
3	0.3
4	-0.05
5	4.055
6	0.135
7	0.36
8	0.605
9	0.685
10	1.525
11	0.48
12	0.515
13	0.53
14	0.53
15	-1.1
16	0.21
17	No Data
18	No Data
19	No Data

Table 3.7: Padstow slipway survey data

is a significant factor, as at Tenby. The implications of these results are discussed further in the FEA section of the thesis, here the panel misalignment data is used to construct FE models to evaluate the contribution of panel misalignment to the friction and wear on slipway panels.



### 3.7. Case Studies - Summary

---

A summary of information collected during these case studies is presented below:

#### Friction

Friction results from the slipway trial data are summarised below:

Slipway Lining Material	$\mu_{\text{static}}$	$\mu_{\text{Dynamic}}$
Composite – Greased	0.09 - 0.17	0.07
Composite – Water	0.242 - 0.320	0.098 - 0.138
Steel – Greased	-	0.16
Rollers	0.02	0.02

Table 3.8: Combined slipway survey data

These friction results show that the composite slipway lining outperforms the previous greased low friction steel linings under both greased and water lubricated conditions justifying its selection for reducing slipway friction. However the static friction coefficients are noted to significantly exceed the dynamic friction coefficients recorded and this is likely to be a contributor to stick-slip behaviour along the slipway. The breakaway friction values approach the dry sliding coefficient listed by the manufacturer of  $\mu = 0.25$  and it is postulated that the higher breakaway friction values recorded are the result of dwell effects causing the low viscosity water boundary lubrication film to break down and the contact to approach the dry sliding case.

#### Pressure-velocity Limit Considerations

At Padstow it is reported that the dry running performance of the composite slipway lining material is very poor with smoke observed during lifeboat launch. This indicates that the slipway lining material has reached its Pressure-Velocity limit where heat build up effects cannot be adequately dispersed resulting in far higher friction and wear. This may be due in part to the panel misalignment at Padstow which is noted to be more pronounced than at Tenby where the smoke effect has not been reported. Misaligned panels would result in a lower bearing area for the lifeboat keel and consequently higher contact pressures. Because of this effect and the high wear and friction associated with it the use of at least water lubrication on launch is immediately recommended. The use of other lubricants will also mitigate the effect as any action to reduce the friction coefficient along the slipway will also reduce the amount of energy lost due to frictional heating on the slipway.

## **Wear**

Wear on the slipway panels is observed to fall into four main categories: Panel end wear, Gouging wear, Plane abrasive wear and Delamination wear. A further category is keel impact wear, this is caused by the impact of the keel against the slipway as the lifeboat mounts the slipway for recovery. This wear category is dealt with separately as it is considered to be a systemic and unavoidable aspect of slipway lifeboat operation and because incidents of major lining damage from this are rare.

### **Panel End Wear**

This type of wear is reported by lifeboat crews as the main cause of panel failure. It is defined as wear that takes place at the ends of each panel and appears to be more pronounced on the raised edge of panels that are misaligned in relation to their neighbours. The actual wear can take different forms, from simple abrasion to more complex cracking effects as detailed below.

### **Panel End Abrasive Wear**

This is the most common form of panel end wear observed from the slipway surveys; it represents the case where abrasive wear has resulted in a relatively even and graded wear scar, as opposed to the larger scale panel cracking effects observed elsewhere.



Fig. 3.55: Abrasive panel end wear: wear scar progression

Fig. 3.55 above shows the typical progression of an abrasive wear scar on a misaligned panel. Initially panel end stresses cause a small region of the composite to deteriorate and fail, this initial imperfection develops until it is the width of the lifeboat keel on the panel. Further slipway operation causes this wear scar to progress into the composite panel until it reaches the level of the fixing bolts, at this point the panel is considered to have failed as it is no longer sufficiently attached to the slipway superstructure.

### Panel End Cracking Wear

Panel end stresses can also result in the formation of deep cracks in the phenolic resin of the composite, these can progress to form panel 'islands' where the phenolic resin has cracked but the jute fibre mesh retains the cracked section in place. The jute fibres eventually fail leaving the cracked material to break loose of the main panel, this results in distinctive large scale missing 'chunks' on the panel ends. This effect is noted to be more pronounced on misaligned panels and is suspected to be caused by the same stress concentration effects. Fig. 3.56 shows this process at different progressions on different panels.

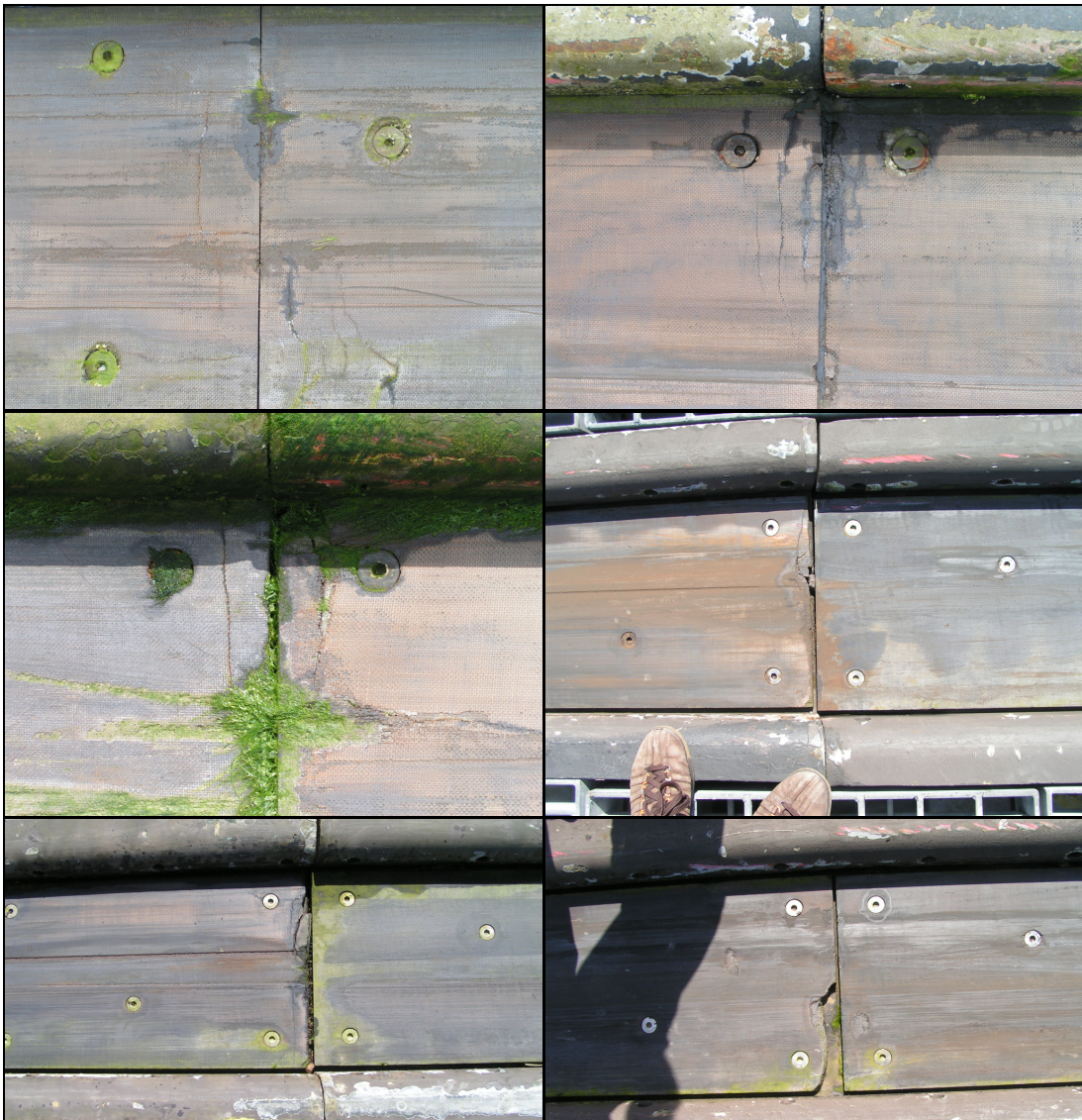


Fig. 3.56: Cracking panel end wear: wear scar progression: Initially high contact stresses due to panel misalignment cause a surface crack to develop in the phenolic resin bulk of the composite, this then develops until it reaches the other side of the slipway panel, at this point the cracked area is held in place solely by the jute fibre matrix. The jute fibres subsequently fail, allowing a large section of slipway panel to break free



A subset of the cracking to leave panel 'islands' case is where cantilever effects (where the panel is not adequately supported after the final fixing bolts) can result in cracking of the phenolic bulk materials between the fixing bolts as show below:



Fig. 3.57: Cracking panel end wear: cracking between fixing bolts

This type of wear is severe as once the cracked section separates from the main panel the holes for the fixing bolts are broken also and the panel can be considered to have failed as it is not adequately fixed to the underlying slipway structure.

### **Gouging Wear**

Gouging wear scars along the slipway indicate the presence of raised keel sections or 3<sup>rd</sup> party wear between keel/slipway lining contact. From inspection of the Tamar lifeboat slipways at Tenby and Padstow and the recovered slipway section from Tenby it is noted that the main gouging wear scars match. This ties in with the observation that the initial Tamar prototype keel was found to have a defect, this defect generated the large gouging wear scars on the Tamar slipways. From inspection of the gouging wear scar the friction coefficient contribution of the keel defect is calculated as  $\mu_{\text{gouge}} = 0.408$ .



Fig. 3.58: Gouging wear from Tamar prototype

The absence of other significant gouging wear scars on the Tamar slipways and general slipway friction performance better than that expected from ploughing indicate that once the prototype Tamar keel was repaired no other major gouging wear was encountered here. This is supported by the other slipway inspections at Selsey and Bembridge where some light gouging wear is present, though not to the severity that would be expected for the large number of launches and recoveries conducted on these slipways. This supports the proposition that significant, persistent keel damage not a common occurrence on slipways and raises the possibility that the lighter gouging wear scars on Selsey and Bembridge slipways are caused by 3<sup>rd</sup> party wear particles trapped between the contact. This is supported by the presence of diagonal and wavy gouging scars on panels, if the scars were caused solely by keel imperfections these would be expected to be in straight lines as the lifeboat does not move laterally as it proceeds along the slipway, this is shown in fig. 3.59 below:



Fig. 3.59: 3<sup>rd</sup> body gouging wear

Overall the impact of gouging wear on the slipway is unlikely to have a significant systemic effect of slipway function, the presence of straight gouging grooves on the slipway panels is an early indicator of keel damage and this should be identified and remedied before further slipway lining damage occurs. However, the low number of gouging wear scars on other composite slipways indicates that this is likely to be an infrequent problem. The presence of wavy or diagonal wear scars on the slipway indicates the presence of 3<sup>rd</sup> body particles between the keel and slipway lining, as these are not attached to either contact face they are likely to be removed from the slipway by the process of lifeboat launch and recovery. Similarly the low incidence of this type of gouging wear on the slipways surveyed indicates that this is likely to be an infrequent problem, however if these wear scars are noted to appear regularly on a specific slipway it may be necessary to inspect the slipway for debris before use. Interestingly, the diagonal wear scars indicating 3<sup>rd</sup> body wear are also present on the water lubricated Tamar slipways at Padstow and Tenby, it had been thought that a by-



product of the use of running water along the slipway would be to remove any potential wear debris from the slipway lining surface but this does not appear to be the case.

### **Plane Abrasive Wear**

Plane abrasive wear occurs when the slipway panel is well aligned and the contact with the keel is even and planar, in this case the contact pressures are relatively evenly distributed along the panel and the resulting wear is light and even. This typically results in the phenolic bulk of the composite material eroding to expose the underlying jute fibres.

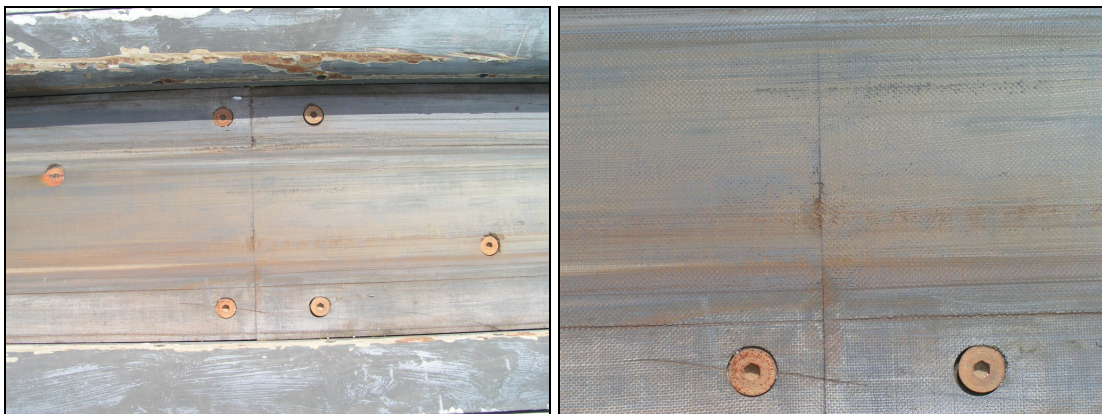


Fig. 3.60: Plane abrasive wear: exposed jute fibres

The incidence of plane abrasive wear on a panel is a sign that the panel is performing well and that the keel contact is well aligned. Under these contact conditions wear will be very light.

### **Delamination wear**

A further wear mechanism noted is the incidence of delamination, here the upper layer of the composite has separated and worn away leaving an uneven bearing surface. This kind of wear is particularly noted at Tenby. The progression of delamination wear is shown in fig. 3.61. Here the wear is shown to develop initially as small pits the depth of a composite layer, before the pits widen and join to form large areas of delamination along the slipway.



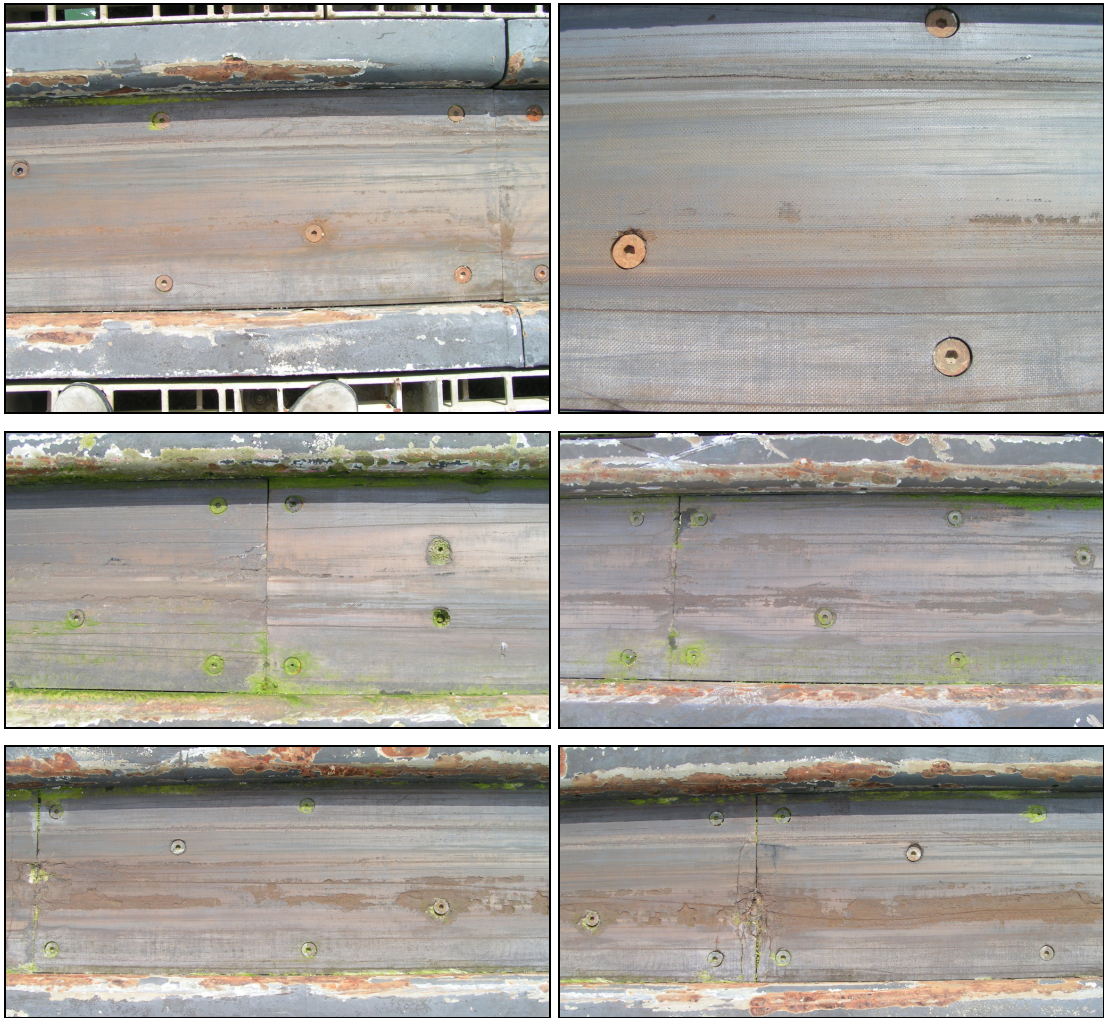


Fig. 3.61: Delamination wear: wear scar progression

Close up images of delamination wear on the composite slipway lining material are shown in fig. 3.62.

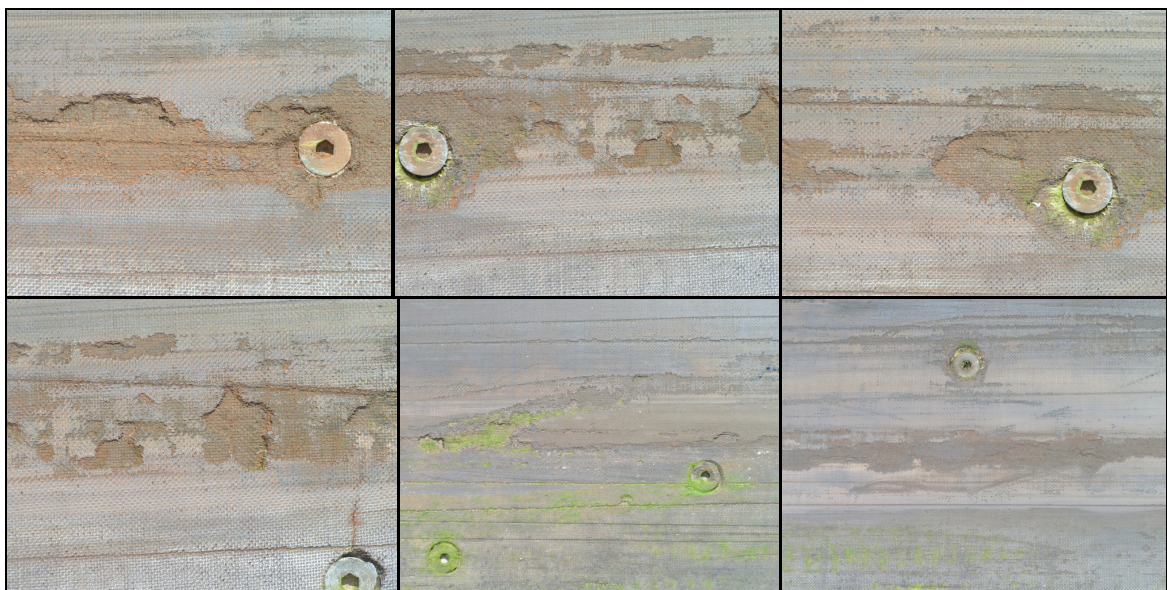


Fig. 3.62: Delamination wear: detail



### **Impact Wear**

Near the base of the slipway some lining panels were observed to have been damaged by the impact of the keel as the lifeboat mounts the slipway. The recovery technique involves the coxswain trying to 'surf' onto the base of the slipway on a wave, the water subsequently receding to leave the lifeboat sufficiently 'stuck' on the slipway to attach the winch cable. This naturally involves the keel impacting the slipway lining with some force and this can occasionally damage the slipway panels.

### **Embedded Debris**

Embedded debris is noted at Selsey slipway, conversations with the coxswain indicate that this is likely to be animal shells, this is confirmed by observation of snails and snail trails on slipway panels.



Fig. 3.63: Embedded Debris

### **Panel Misalignment**

The panel misalignment surveys conducted at Tenby and Padstow indicate that significant panel misalignment is present along the slipway in both cases. The compressive strain at failure is listed in the composite manufacturer's literature as 1.9%, for a 19mm thick slipway panel this means that the material will deflect up to 0.361mm before compressive failure. The average offset for all panels recorded from slipway surveys is 0.816mm which indicates that that panel compression will not be able to accommodate the misalignments. As the contact stresses around the raised edge of a misaligned slipway panel are likely to be high this will contribute to increased wear in the area and this is reflected by observation. The high contact forces will also have an adverse effect on friction according to the theory.

## **4 EXPERIMENTAL WEAR MODELLING**

---

In order to identify the cause and mechanisms relating to high friction on launch and recovery a full literature search relating to friction and wear testing is undertaken. This will include an examination of tribology theory and lubrication regimes to attempt to determine the governing wear and friction mechanisms at play. It is intended to combine this with a review of laboratory based friction and wear testing in order to develop an appropriate test methodology that accurately represents the real world contact conditions to experimentally determine the wear and friction between lifeboat keel and slipway under varying lubrication and contact conditions. Experimental results will be compared with tribology theory and with the manufacturers' specification for the coefficients of friction and wear. This will help determine if environmental conditions are responsible for the increase in friction loads beyond the design capacity of the recovery winch. From this the conditions most likely to lead to high friction can be determined which will help to identify slipway stations at risk.

### **4.1 Background of Wear Bench Testing**

---

It is hoped that by using tribometers it will be possible to simulate the materials, lubricants and environmental conditions encountered by the slipways and obtain wear coefficients for these conditions. This can then be used to inform slipway panel wear prediction and help to assess expected panel lifespans for varying lubrication, contact and contamination conditions.

#### 4.1.1 Overview of Ship Launch Slipway Friction Testing

---

Currently slipway ship launching tends to use friction coefficients and parameters recorded from previous launches, but as fewer ship builders launch their ships dynamically the traditional producers of slipway grease have begun to withdraw their products from the market [68]. Using previously recorded friction coefficients and parameters is valid only as long as the original conditions are replicated, with differing ship dimensions, materials and greases it is necessary to perform lubricant testing in order to more accurately predict the conditions likely to be present at launch. Dunn, Kennedy and Tibbs [68] propose using a reciprocating tribometer to test any new greases or contact materials to be used on ship launch slipways. The tribometer used is a Denison T67 Reciprocating Tribometer and the contact is arranged as shown in Fig. 4.1. The machine consists of a slipper block actuated by a hydraulic ram acting in the horizontal plane. Pairs of test specimens are positioned above and below the slipper block and loaded as shown. The velocity can vary between 1mm/s to 50mm/s and the stroke is 50mm. The clamping load can be established without motion of the slipper block to simulate a dwell time and a dwell period can also be programmed at the beginning of the stroke. A force transducer is mounted in series with the slipper block hydraulic ram to record the friction force continuously throughout the tests.

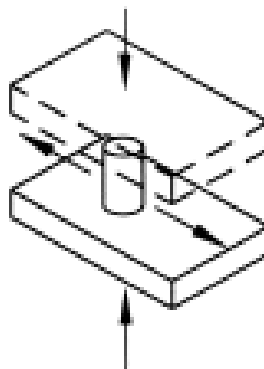


Fig. 4.1: Denison T67 Reciprocating Tribometer Pin and Sample Arrangement

Tests are run at a range of contact pressures, dwell times and velocities and the friction coefficient recorded. Each test is run until a stable friction coefficient is achieved – usually obtained in a few minutes. These tests are repeated for all keel/slipway material combinations required and with different greases, including grease degraded in the tidal environment.

Another technique for analysing the friction present during a slipway launch is outlined by Pattison, Dixon and Hodder [69] when describing problems encountered by Vosper

Thornycroft shipbuilding during the launch of the RV Triton, an experimental warship with a trimaran hull (fig. 4.2).



Fig 4.2: RV Triton

Despite the revolutionary design the ship was to be launched conventionally, with only the central hull supported. However, shortly before the launch in May 2000 it was noted that the Triton has slipped down the slipway almost 60mm of its own accord. Measures were taken to prevent further slippage and the ship was launched on schedule. Following the successful launch an investigation was launched into the causes of the slippage. It was first proposed that the friction between

the ship and the slipway blocks was sufficiently low as to cause the ship to slip but this was deemed unlikely as the friction coefficient would have to be approximately 10 times less than expected. Another theory was that the ship had moved due to a 'thermal ratchet' effect as it expanded and contracted with the daily thermal cycle, however this would not account for the low friction also observed during the launch. Suspicion fell on the low friction anti-foul paint used on the Triton and on the plastic sheet that had been used as a liner to prevent damage to the paintwork. As the Triton was washed prior to launch this liner became wet, further affecting the expected friction coefficient.

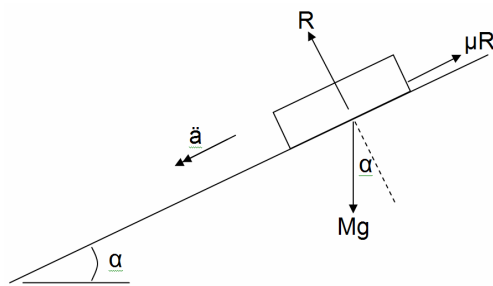


Fig. 4.3: Vosper Thornycroft Test Rig – The angle  $\alpha$  at which the sample slips down the surface is recorded

A test rig was developed to examine the static friction coefficients under different conditions, including those in the Triton case. The rig was very simple and consisted of a sample sitting on a plane plate with a separator of plastic sheet or other liners commonly used at VT shipbuilding. The samples were painted with both the low friction anti-fouling paint used on the Triton and conventional paint for comparison. The friction

coefficient was tested simply by jacking the plane plate up to an angle where slippage between the sample and the plate occurred (see Fig. 4.3). The liner was tested both wet and dry to recreate the conditions at launch where it had become wet after the hull was washed.

### 4.1.2 Existing Slipway Lining Testing

---

The makers of the composite lining used on RNLI slipways produce a range of marine bearing materials and have their own in-house testing procedures to determine static and dynamic friction and wear rates.

#### Static Friction Load Testing

A test rig similar to that used by Vosper Thornycroft is used to determine static friction, the sample is placed on an inclined plane which is raised to the point at which the sample slips, the angle at this point allows the calculation of the static friction coefficient [70]. Tests are carried out dry, with water lubricant and with additional lubrication.

#### Dynamic Friction Load Testing

A reciprocating friction machine is used by the composite material manufacturers to generate dynamic friction data for its products [71]. Tests are run for approximately 5 minutes after which time the sample is inspected to check alignment, an uneven wear scar will indicate the pin and sample are misaligned. The test is then run for a further 4 minutes and a force transducer records the average friction for this time. Again, tests are carried out dry, with water lubricant and with additional lubrication.

#### Wear Rate Testing

Wear testing is carried out using a rotating shaft, against which a sample is pressed [72]. The sample is weighed beforehand and applied to a 38mm steel shaft rotating at 700RPM with a load of 3kg. The test is run for 100hrs after observation for the first hour to ensure the material is not going to degrade before this time. Following the test the sample is weighed and the volume loss calculated.

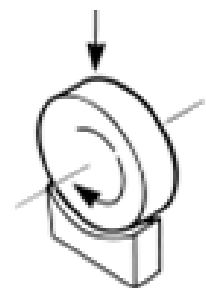


Fig. 4.4: Composite wear rate testing

#### Previous RNLI Slipway Testing

As outlined above previous slipway friction testing [48-50] has used a modified pin on disc rotary tribometer. In this a pin is loaded against a flat disc by a dead weight on the end of the loading arm, the disc is rotated by a tachometer controlled motor. The rotation of the disc forces the loading arm against a load transducer to measure the frictional force and a displacement transducer is placed against the loading arm to measure the total arm displacement during the test. The arm displacement can be used as a guide to total wear of both pin and sample as well as for assessing effects such as swelling due to water uptake and sample tilt. It is noted that while the arm displacement measurement is a convenient

monitoring tool it is unsuitable for detailed assessment of wear due to these other influencing factors.

In this case the research was to assess the performance of composite lifeboat keels on greased steel slipways. Because of the difficulty of machining a small pin from composite material without adversely affecting its internal structure the geometry was switched for testing, with a steel pin representing the slipway moving across a composite disc.

Wear was measured using weight loss techniques; however the low wear rates and large mass of the composite discs meant that this was likely to have limited accuracy in this case so profilometer traces across the wear track were used for a more accurate measurement. Four traces were taken and the average depth found, wear scar volume was then calculated by multiplying this depth by the wear track area. Friction coefficients were calculated conventionally by comparing the friction force recorded with the normal force applied.

## **4.2 Selection of Test Machine**

---

Informed by the friction and wear testing methodologies above a Plint TE57 reciprocating friction machine is selected to perform initial friction and wear tests under typical slipway conditions. This reciprocating tribometer is similar to machines used to evaluate slipway friction by Dunn, Kennedy and Tibbs, at Vosper Thornycroft and for the manufacturers in-house testing of the low friction composite slipway lining currently in use.

Although a useful tool for evaluating friction it is felt that the reciprocating contact does not mirror the slipway contact with sufficient accuracy for more detailed wear analysis. In this case a Plint TE92 rotary tribometer is selected, similar to the geometry used to assess composite keel materials above. This more accurately represents the keel-slipway contact and also allow the incorporation of dwell effects into the testing.



#### 4.2.1 Plint TE57 Microprocessor Controlled Reciprocating Friction machine

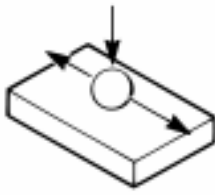


Fig. 4.5: Plint TE57:  
Typical contact geometry

The TE57 is a tribometer designed to provide an accelerated method for assessing friction and wear between pin and plate materials under various tribological conditions [73]. It was developed and subsequently modified to include a pressure chamber and a greater range of lubricant regime testing by Plint Tribology. A schematic is shown in Fig. 4.6. A pin, actuated by a motor reciprocates at up to 50Hz with a stroke length of up to 5mm. The specimen is attached below the pin and a contact force of up to 50N is applied using a spring loaded lever arrangement. The specimen sits in a bath that can be used to hold the lubricant when testing lubricated friction scenarios. The friction force on the sample is recorded using a force transducer in series with the horizontal actuating ram. The signal from the transducer is recorded throughout the stroke and in this way the friction coefficient between the pin and specimen can be calculated. The velocity of the motion and test duration is controlled by a microprocessor.

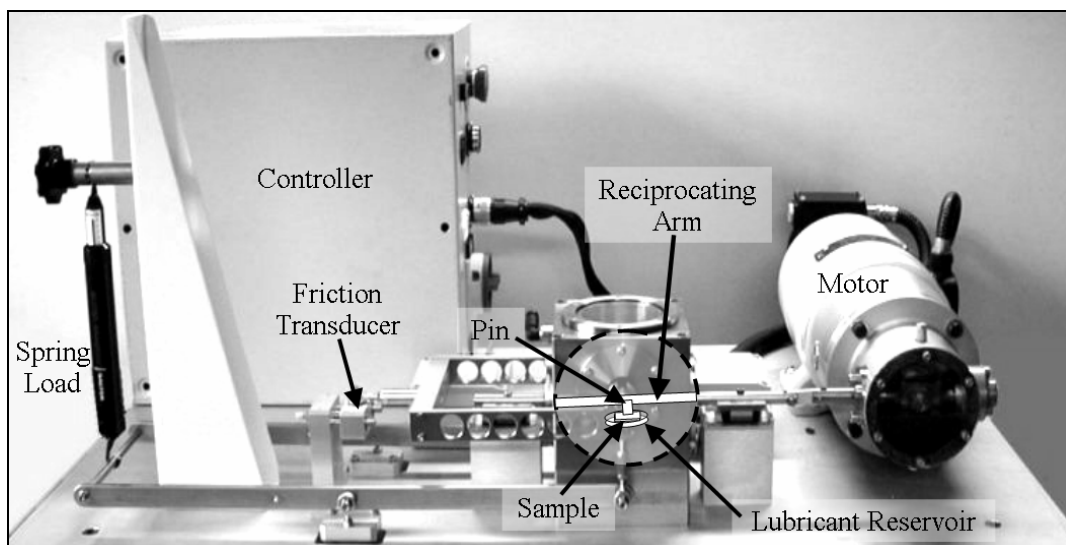


Fig. 4.6: Plint TE57 Reciprocating Tribometer Schematic

#### 4.2.2 Plint TE92 Microprocessor Controlled Rotary Friction machine

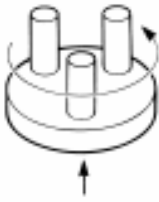


Fig. 4.7: Plint TE92:  
Typical contact geometry

The TE92 is a rotary tribometer made by Plint Tribology [74] and capable of using a number of pin/disc combinations. A schematic is shown below in fig. 4.8. The tribometer uses a pneumatic ram to bring a pin and sample into contact at a set contact pressure and then rotates the pin on the sample. The speed, contact pressure and test duration are controlled using a programmable controller CPU. The controller can also be programmed to stop the motor and restart at any time allowing the incorporation of dwell effects into the contact simulation. Following the test the sample is inspected for wear either using mass loss techniques or visual inspection.

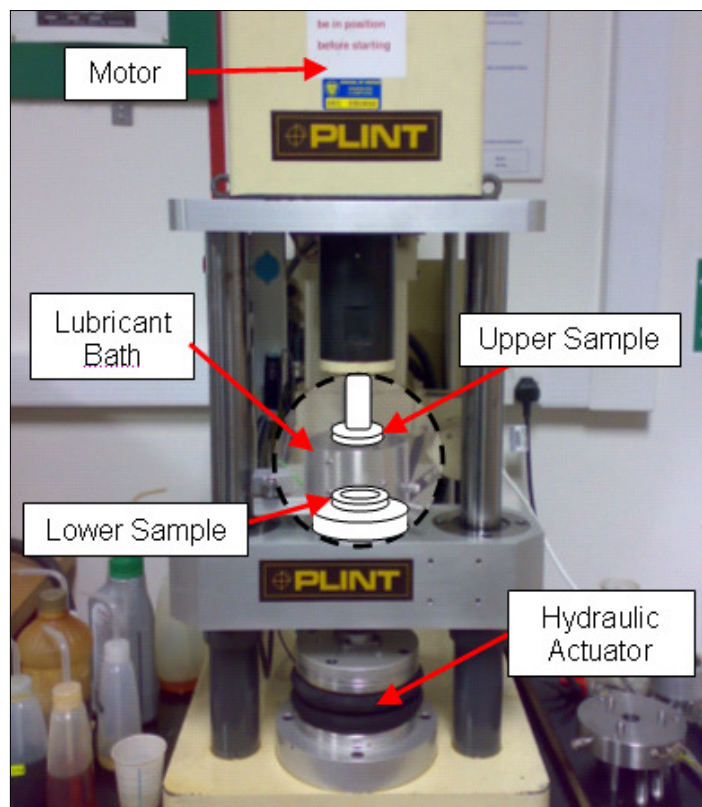


Fig. 4.8: Plint TE92 Rotary Tribometer with Test Sample Schematic

### 4.3. Surface Analysis

---

In order to determine the nature of the wear mechanisms present it is necessary to inspect the surface of the pin and sample after testing. There are a number of ways of doing this available, each with advantages and disadvantages outlined below.

#### Light Microscope



Fig. 4.9: Olympus BX60 Light Microscope

The first and simplest tool to be used to inspect the sample surface is a simple light microscope, in this case an Olympus BX60. The microscope is fitted with a digital camera to monitor and capture images and these are displayed on a monitor via a computer link. The microscope features lenses of 5, 10, 20, 50 and 100x magnification and software on the linked PC allows a scale based on the lens magnification to be added to the captured image.

#### Zygo Interferometer



Fig. 4.10: Zygo interferometer

The Zygo Interferometer uses light interferometry to generate a 3 dimensional map of a surface. This is intended to be used to investigate the surface of worn samples from tribometer experiments; it can provide useful data on the wear scar depth, profile, wear volume and on the surface finish of the wear scar area [75]. The surface finish of the original surface can also be measured. The Zygo interferometer allows the user to

perform a number of detailed scans across the surface of a sample, these can then be stitched together to create a full 3D profile of the surface and the wear scar. This may help to determine the wear mechanisms present by identifying characteristic features – e.g. grooves cause by abrasive wear.

## 4.4. Design of Experiments

---

This section looks to use the experimental techniques and surface analysis tools identified above to develop a suitable experimental programme to investigate lifeboat slipway friction and wear.

Following investigation into established slipway friction and sample friction testing it was decided to begin testing with a series of screening wear tests and friction tests using the TE57 reciprocating tribometer. More detailed wear tests using the TE92 rotary tribometer are proposed for the second stage of this research.

## 4.5. Design of Reciprocating Test Rig

---

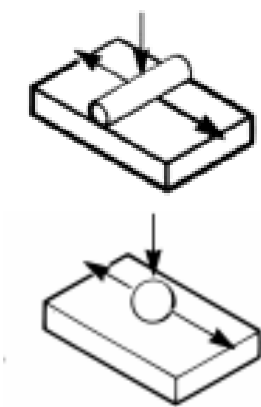


Fig. 4.11: Original TE57 contact configurations

The TE57 available at Bournemouth University has been modified from its original configuration and can now accept a range of pin/sample configurations. The configurations have been developed to investigate fretting wear and a pressure chamber allows experiments to be conducted under pressure. Previous testing [76-80] on the TE57 has used the pin/sample configurations shown on the left; here a cylindrical pin bears onto the sample with its curved edge, or a spherical pin is used. For the purposes of this research it was felt that the configuration would not be able to provide a consistent contact pressure as the curved surface would wear to a flat during the trial, increasing the contact area between pin and sample and reducing the contact pressure. The geometry also bears little resemblance to a slipway/keel situation.

A test rig that will better model the slipway/keel interface is proposed; this section details the development of the final design.

### Pin and Holder Design

In a real life slipway launch the contact pressure between keel and slipway remains constant for the majority of the launch, only varying as the boat enters the composite section of the slipway and as it leaves. The pin and sample design currently used would not provide this. In order to provide constant contact pressure throughout the test as the pin wears the contact area must stay the same, this implies that a parallel sided pin must be used. Two pin designs were proposed before a final selection was made.

## TE57: Contact Geometry Design #1

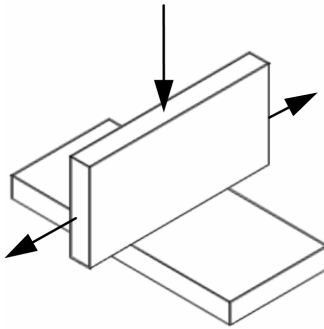


Fig. 4.12: TE57 contact design 1

The first design proposed aimed to replicate the geometry of a slipway launch with a rectangular pin as shown below. The pin overlaps the sample edges so as not to provide an edge to generate ploughing wear. The contact stresses at the sample edge are expected to be larger and this is designed to simulate the conditions at the end of each composite panel on the slipway. As seen above in the inspection of the worn composite section from Tenby, wear at the ends of each panel appears higher than in the centre.

A design was drawn up and tested using FEA to evaluate its performance prior to use. The FEA results are shown below and indicate the expected stress concentrations at the edge of the sample.

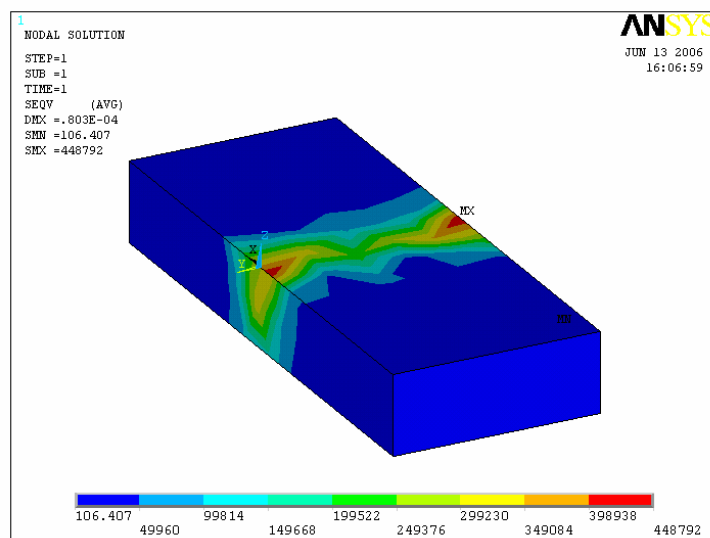


Fig. 4.12: Pin and Pin Holder design 1 – FEA showing stress concentrations

It was felt that the stress concentrations present in this design would be likely to distort the true friction and wear results, the wear scar would also be difficult to measure as it would be uneven. As a result of this initial analysis the design was abandoned and a new contact geometry design developed.

## TE57: Contact Geometry Design #2

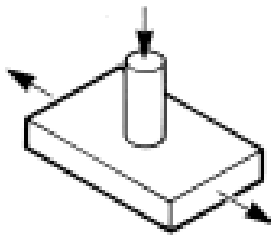


Fig. 4.13: TE57 contact design 2

Following the difficulties encountered with design 1, a new variation was proposed, this would feature a parallel sided cylindrical pin bearing on its flat end as shown. As the pin is parallel sided the contact area should remain the same regardless of pin wear resulting in stable contact pressure as experienced on real world slipways. To avoid ploughing friction the pin edge is broken with a chamfer. Previous testing has highlighted difficulties with the alignment of pin and sample, if the alignment is not square the contact area and wear scar become unpredictable and calculations are required to compensate if an uneven wear scar is detected. To minimise this it was proposed to adopt a degree of self compensation into the pin holder ensuring the pin remained flat to the sample. This was to be achieved by machining a slight point on the top of the pin and fitting a thin o-ring inside the pin holder, this arrangement is shown below. It is hoped that this design will give the pin some flexibility to align with the sample surface.

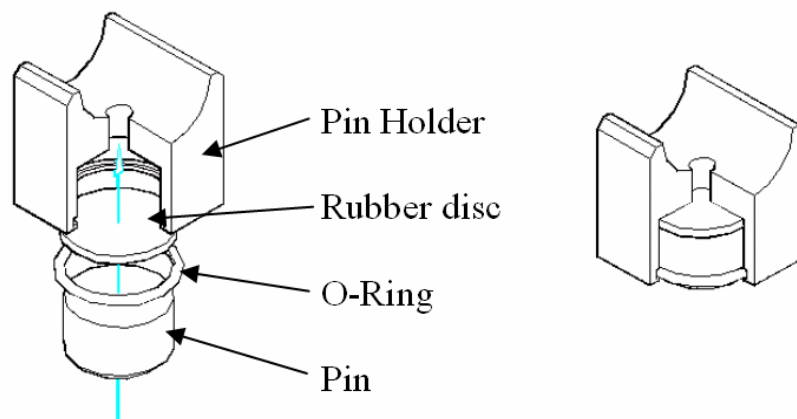


Fig. 4.14: TE57 Modified Pin Design

This design was adopted for the TE57 screening tests; the pin diameter is calculated as shown below.

### 4.5.1. Reciprocating Test Parameter Calculation

For these tests pin diameter, frequency and stroke must all be calculated to mirror the real life situation. Using the Tamar lifeboat mass of 30 tonnes a keel contact area of  $1.95\text{m}^2$  and a typical slipway angle of  $11.4^\circ$  (1 in 5) the contact pressure is calculated as 148kPa. The TE57 can apply a contact force of 0 to 50N so the pin contact area will be calculated to deliver a contact pressure of 148kPa within this range. Using a pin diameter of 10mm a force of 11.6N will deliver 148kPa. The stroke is set to its maximum value of 5mm so as to better model the slipway situation. From previous experience the majority of high friction and wear events are reported occur during the recovery of the lifeboat to the top of the slipway, and

this manifests as very slow recovery speed and possible overloading and damage to the recovery winch. Because of this it is decided to concentrate on this aspect for the tribometer tests. For the recovery scenario the frequency is based on the RNLI specified recommended winch line speed of 15m/min. The TE57 is set so that the root mean square average speed matches this, corresponding to a frequency of 25Hz. The speeds encountered during the launch scenario fall outside the range of the TE57 and it is intended that these be investigated at a later stage using the TE92 rotary tribometer. It is worth noting that the majority of high friction and wear incidents occur during the lifeboat recovery.

#### 4.6. Design of Rotary Test Rig

---

The TE92 Rotary tribometer is to be used for detailed wear testing to more accurately model real life slipway wear over an extended period.

In order to develop a suitable test geometry for more detailed slipway panel wear modelling it is necessary to incorporate real-world effects such as the dwell time between launch and recovery, the nature of the plane sliding contact and the geometry of the slipway panels themselves. It is decided to investigate these using a specially modified TE92 rotary tribometer.

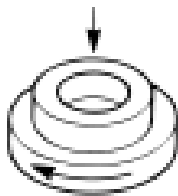


Fig. 4.15: TE92  
contact Design

Following consultation with Plint Tribology, the makers of the TE92 it was decided to adopt a ring-on-disc configuration for the experiments, with the upper ring representing the lifeboat keel and the lower ring representing the slipway lining. This will allow the simulation of a square, flat keel running on a flat slipway lining within the laboratory environment. By running the tribometer for a set time, then allowing a dwell time, then repeating, the real world launch scenario can be modelled. The dwell time allows the heat generated in sliding to dissipate, as in real life. The contact length of the Tamar class lifeboat keel is measured as 12.8m, so by running the disc for an appropriate number of revolutions this can be replicated so that each point on the sample will see 12.8m travel of the disc per pass. In order to model the life of the slipway lining it is proposed that 1000 launches will be modelled, involving 1000 passes and dwells, and the surface wear scar recorded. Based on one lifeboat launch / recovery per week this represents 10 years of use (this extended test period is derived from initial very low wear rates recorded during TE57 screening tests). The test is to be repeated for a variety of lubrication regimes as with the TE57 tests, and with notch and hole features added to model the geometry of the Composite panels as they are fitted.



### Contact Geometry Design

The contact geometry was chosen to most closely mirror the real-world case and is based on a ring on disc geometry. This effectively mimics the conditions of plane sliding on the real-world slipway.

In order to incorporate the effects of the geometric features present on the slipway panels into the test, these features are included on the test specimen. A small slot is cut radially in the sample to simulate the edge stresses present in the panel interfaces and a small 2.5mm dia. hole is drilled in the specimen to mimic the geometric stresses present around the fixing holes of the slipway panels.

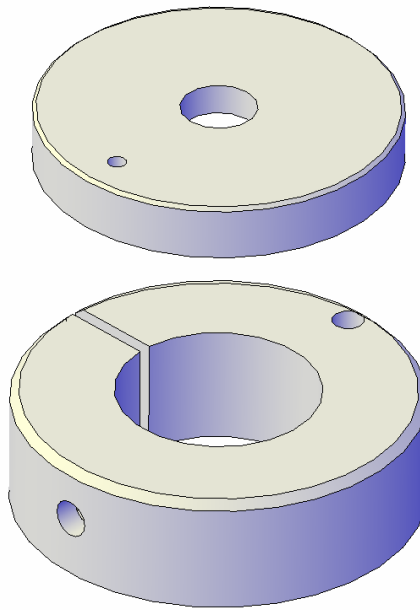


Fig. 4.16: Plint TE92 Modified Ring on Disc Configuration

#### 4.6.1. Rotary Test Parameter Calculation

For these tests the appropriate contact force and rotational speed must be chosen to match the real-world case, here, a contact force of 20N generates the same contact pressure as the 35 tonne Tamar lifeboat resting on a  $1.92\text{m}^2$  keel contact area and a rotation speed of 176RPM corresponds to the recommended 15m/min line speed of the recovery winch.

The interval between launch and recovery is simulated by programming a dwell time into the tests. This consists of a pause in rotation of 30 seconds after every 12.8m pass of the entire Tamar keel length. This pause not only simulates the dwell between launch and recovery but also allows the dissipation of heat build-up effects in the sample. Tests are conducted for a total of 1000 passes, corresponding to roughly 10 years of use (based on a weekly launch/recovery). The test is extended beyond the slipway panel design life in order to generate significant wear to ensure accurate measurement following the indications of very low wear coefficients from the reciprocating tribometer tests.

# 5 TEST METHODOLOGY

---

## 5.1. TE57 Reciprocating Tribometer: Experimental Methodology

---

An experimental methodology drawing on the previous work mentioned above is devised. It is proposed to use a Plint TE57 reciprocating friction machine to evaluate the performance of slipway lining materials in a similar fashion to previous work in this area [48-50,68,69,71,72].

### Tests Schedule

Tests are conducted in two stages, first a series of long tests are performed to mimic the wear generated on the slipway lining after the expected total sliding distance during the scheduled 2 year lifespan of the slipway lining. This is calculated as 50 launches/year, with both launch and recovery this equates to two passes over the slipway lining per launch, the average length of slipway lining contacted by the keel during launch is 45m so this equates to a total sliding distance during the expected 2 year life of the slipway lining panels of 9km. On the TE57 machine at a frequency of 25Hz this equates to a 10 hour continuous test.

These tests are conducted for a number of common and proposed lubrication scenarios as detailed below in table 5.1. Friction is recorded using the in-built force transducer at intervals of 10 seconds and wear is examined after the tests conclusion using optical interferometry

techniques to determine wear scar depth and wear volume, and thus the wear coefficient for the tested conditions.

Secondly, a series of shorter tests are run for varying lubrication regimes and contact pressures in order to investigate the effects on the friction coefficient. These tests are run until stable friction is achieved. The aim of the tests is to check the relationship between the friction coefficient and the applied load in each case as this may be indicative of contact conditions. These tests are also used to compare the lubrication regimes at varying normal loads such as might be experienced when the slipway lining is uneven, damaged or misaligned, or the lifeboat keel does not sit flat on the slipway i.e. during the initial stages of recovery from the water, due to tilting during launch or recovery or due to unevenness in the lifeboat keel. The aim is to investigate whether higher contact pressures will affect the lubrication regime, possibly causing a transition from boundary lubrication towards dry sliding asperity contact and the effect this may have on friction.

Tests are performed under a number of lubrication regimes to provide a broad picture of the real world case. The lubricants tested are chosen to encompass those currently in use on existing slipways, i.e. no lubricant (dry), marine grease as used on the majority of slipways of both lining materials, a silicon microsphere infused lubricant as used at Sennen Cove and proposed for possible use elsewhere, seawater and freshwater. In addition, two biodegradable greases are selected in order to evaluate their feasibility for slipway use, this would reduce the environmental impact of the accumulated grease around the end of the slipway.

Also tested are scenarios where the lubricant is contaminated with sand, this has been proposed as a possible reason for the increased friction during recovery at Sennen Cove; a seawater/sand mix, a freshwater/sand mix and a marine grease/sand mix are tested. Finally, a marine grease/seawater mix is also tested to investigate the case near the bottom of the slipway where mixing may have occurred.

### **Test Procedure**

Suitable pins and specimens are prepared to represent the keel and the slipway lining respectively. The pin is S275 J2G3 steel as used on the Tamar class keel, while specimens are made from the graphite infused jute fibre/phenolic resin composite that is the preferred slipway lining material for the RNLI and the low friction coated steel it replaces.

### Sample Properties

Samples are constructed as indicated below. The initial surface finish of the virgin composite material is measured as  $R_a = 8.45\mu\text{m}$  and  $R_q = 12.262\mu\text{m}$ .

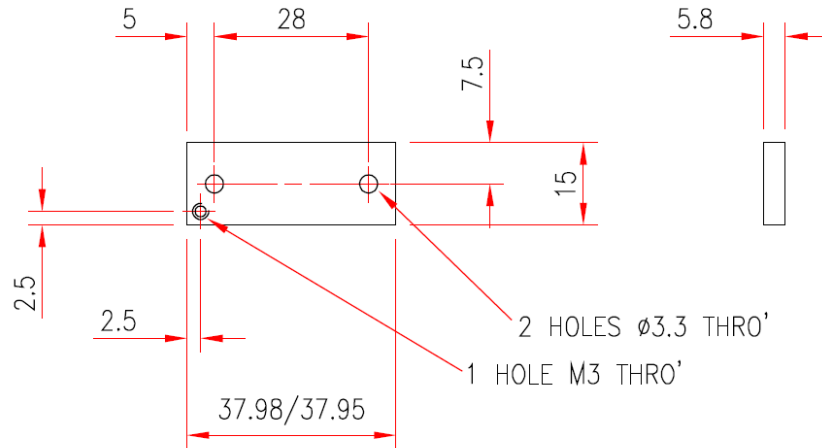


Fig. 5.1: Plint TE57 Composite and low friction steel sample specification

### Pin Properties

Pins representing the lifeboat keel are constructed as indicated below. The contact surface finish of the pins is measured as  $R_a = 0.858\mu\text{m}$ ,  $R_q = 1.065\mu\text{m}$ .

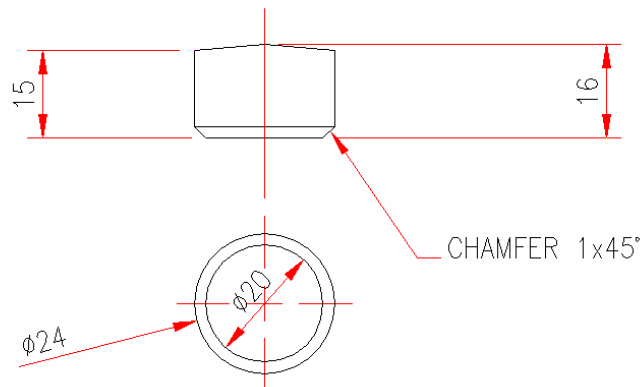


Fig. 5.2: Plint TE57 Keel steel pin specification

### Sample Preparation

Prior to testing samples are cleaned using acetone cleaning fluid and an ultrasonic bath. The lubricant bath, pin, and fixing screws are also cleaned to remove any trace debris that may be present. The sample is then fitted to the lubricant bath and attached to the force input rod, after checking that the machine is unloaded the pin is fitted to the feedback rod.

### Addition of Lubricant

Where lubricated conditions are to be tested the specimen sits in a bath of lubricant throughout the test. In such cases the sample is fitted first, the bath is then filled to the rim with lubricant for each test which leaves a depth of 2mm above the sample. The pin is then fitted as for unlubricated testing. For sand contaminated testing approx. 30mm<sup>3</sup> of collected Sennen Cove sand is thoroughly mixed with the lubricant prior to application. For the water / grease contaminated case the grease lubricant is mixed with an equal volume of seawater before application.

### Contact Force Tests:

Tests are conducted on the jute fibre/phenolic resin composite at contact forces of 5, 10, 15, 20, 25, 30, 35, 40, 45 and 50N for the following lubrication regimes:

Contact Force (N)	Lubricant							
	Dry	Fresh water	Sea water	Marine Grease	Silicon Microball Lub.	Biogrease #1	Biogrease #2	Marine Grease/Water
5	C1	C11	C21	C31	C41	C51	C61	C71
10	C2	C12	C22	C32	C42	C52	C62	C72
15	C3	C13	C23	C33	C43	C53	C63	C73
20	C4	C14	C24	C34	C44	C54	C64	C74
25	C5	C15	C25	C35	C45	C55	C65	C75
30	C6	C16	C26	C36	C46	C56	C66	C76
35	C7	C17	C27	C37	C47	C57	C67	C77
40	C8	C18	C28	C38	C48	C58	C68	C78
45	C9	C19	C29	C39	C49	C59	C69	C79
50	C10	C20	C30	C40	C50	C60	C70	C80

Table 5.1: Composite contact tests

In addition the same test sequence is performed using the previously used low friction coated steel slipway material under dry and marine grease lubricated sliding conditions (test ID C81-100) for comparison.

Contact Force (N)	Lubricant	
	Low friction Steel - Dry	Low friction Steel - Marine Grease
5	C81	C91
10	C82	C92
15	C83	C93
20	C84	C94
25	C85	C95
30	C86	C96
35	C87	C97
40	C88	C98
45	C89	C99
50	C90	C100

Table. 5.2: Low friction steel contact tests

Ideally aligned real world contact conditions are represented by contact forces of 10-15N here, with higher contact forces replicating cases of increased contact pressures due to panel or lifeboat keel misalignments.

### **Wear Tests:**

Tests are conducted for the following lubrication regimes for a duration of 10 hours in order to simulate the total sliding experienced by the lining during its expected use-life of 2 years.

ID	Lubricant	ID	Lubricant
W1	Dry	W7	Biogrease #2
W2	Seawater	W8	Dry/Sand
W3	Freshwater	W9	Seawater/Sand
W4	Marine Grease	W10	Freshwater/Sand
W5	Silicon Microball Lub.	W11	Marine Grease/Sand
W6	Biogrease #1	W12	Silicon Microball/Sand

Table 5.3: Lubricant Tests

### **Post Test Analysis:**

Following the tests the samples cleaned using acetone in an ultrasonic bath to remove any debris or lubricant traces. Samples are then inspected using light microscope and surface profile interferometry techniques to examine the wear scar area. Due to lubricant absorption by the composite and the low wear rates experienced in some cases it is difficult to assess the wear volume using solely mass loss, profile interferometry is used here to assess the wear scar volume and determine the wear coefficient.



## **5.2. TE92 Rotary Tribometer: Experimental Methodology**

---

### **Tests Schedule**

Tests are conducted in two stages, first a series of contact force tests are conducted under dry sliding conditions. The slipway panel wear behaviour at high contact pressures is of particular interest as observations from slipway station case studies has indicated a significant increase in wear around areas of panel misalignment where edge stress effects act to increase the apparent pressure on the slipway lining panel.

Secondly, a series of tests using different lubricants are conducted. These aim to evaluate the effects of lubricant choice on minimising the wear on the composite slipways. The lubricants tested are chosen to encompass those currently in use on existing slipways, i.e. no lubricant (dry), marine grease as used on the majority of slipways and a silicon microsphere infused lubricant as used at Sennen Cove and proposed for possible use elsewhere.

Also tested are lubricants selected for their environmental performance in order to evaluate their feasibility for slipway use, these are seawater, freshwater and a biodegradable marine grease. It is hoped that if these eco-friendly greases exhibit sufficient friction and wear performance they may be adopted in place of the lubricants currently used, this would significantly reduce the environmental impact of the accumulated grease around the end of the slipway.

### **Test Procedure**

Suitable pins and specimens are prepared to represent the keel and the slipway lining respectively. The pin is S275 J2G3 steel as used on the Tamar class keel, while specimens are made from the graphite infused jute fibre/phenolic resin composite that is the preferred slipway lining material for the RNLI and the low friction coated steel it replaces.

### **Sample Preparation**

Prior to testing samples are cleaned using acetone cleaning fluid and an ultrasonic bath. The lubricant bath, pin, and all fittings are also cleaned to remove any trace debris that may be present. With the main power off the sample is then fitted to the lubricant bath and the pin to the pin shaft. After fitting the safety guard the power is turned on and the pneumatic piston is actuated by computer control. The test then commences with the pin rotating on the sample for 48.8 seconds, a distance of 12.8m, equal to the bearing length of the lifeboat keel, before stopping for a dwell period of 30 seconds as detailed above.

## Sample Properties

Samples are constructed as indicated below. The initial surface finish of the virgin composite material is measured as  $R_a = 8.45\mu\text{m}$  and  $R_q = 12.262\mu\text{m}$ .

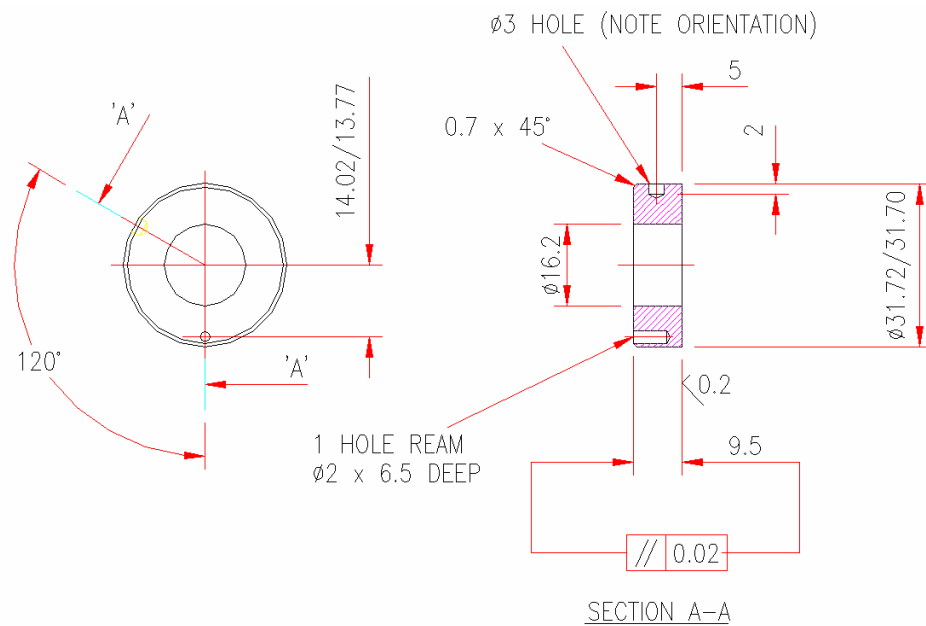


Fig. 5.3: Plint TE92 Composite sample specification

## Pin Properties

Pins representing the lifeboat keel are constructed as indicated below. The contact surface finish of the pins is measured as  $R_a = 0.398\mu\text{m}$ ,  $R_q = 0.586\mu\text{m}$ .

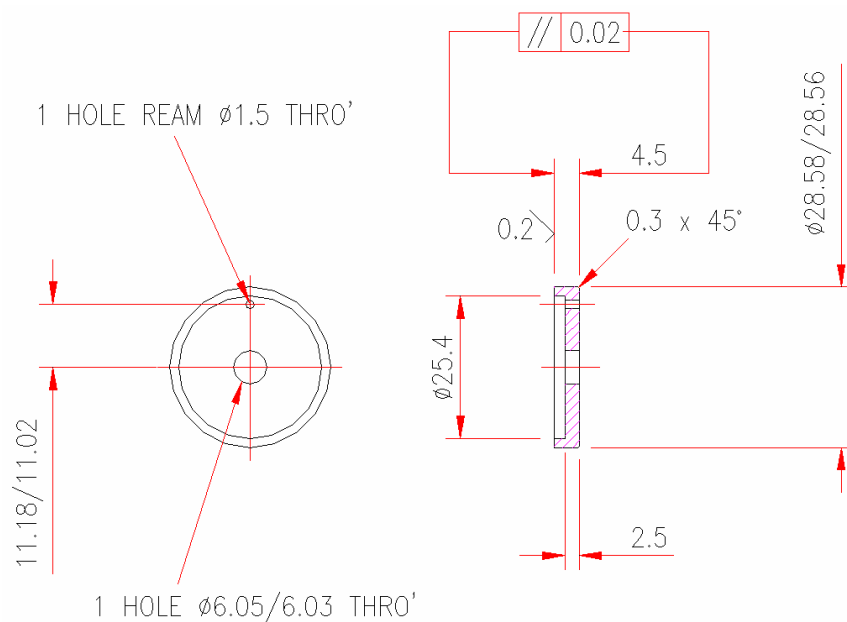


Fig. 5.4: Plint TE92 Keel steel pin specification

### Addition of Lubricant

In lubricated tests the lubricant is added to the lubricant bath with the sample fitted, for low viscosity lubricants such as seawater and freshwater the whole bath is filled until the lubricant level reaches 2mm above the sample surface, for viscous lubricants such as greases the lubricant is applied directly to the sample to a depth of 2mm. The pin and safety guard are then fitted to the machine and the pneumatic piston actuated in the same way as above.

### Contact Force Tests:

Tests are conducted on the jute fibre/phenolic resin composite at contact forces of 20, 40, 60 and 80N under conditions of dry sliding:

Test ID	Lubricant	Test Duration (#passes)	Contact Force (N)
CR1	Dry	1000	20
CR2	Dry	1000	40
CR3	Dry	1000	60
CR4	Dry	1000	80

Table 5.4: Contact Force Tests

### Lubricant Tests:

Tests are conducted for the following lubrication regimes for a duration of 1000 passes corresponding to the expected total sliding experienced by the lining during 10 years of service.

Test ID	Lubricant	Test Duration (#passes)	Contact Force (N)
LR1	Dry	1000	20
LR2	Seawater	1000	20
LR3	Freshwater	1000	20
LR4	Marine Grease	1000	20
LR5	Silicon Microsphere Lub.	1000	20
LR6	Biogrease #1	1000	20

Table 5.5: Lubricant Tests

### Post Test Analysis

Following the tests the samples cleaned using acetone and an ultrasonic bath to remove wear debris and lubricant contamination, Samples are then inspected using light microscope and surface profile interferometry techniques to examine the wear scar area. Due to lubricant absorption by the composite and the low wear rates experienced in some cases it is difficult to assess the wear volume using solely mass loss, profile interferometry is used here to assess the wear scar volume and determine the wear coefficient.

# 6 EXPERIMENTAL RESULTS

---

## 6.1. TE57 Reciprocating Tribometer

---

### 6.1.1. TE57 Contact Force Tests - Results:

The results from the friction force tests are shown below. These results show a good direct proportionality to  $W$ , the applied load which would indicate that the abrasive friction is the dominant contact regime. It is also noticeable that the addition of lubricants significantly reduces the friction force encountered, particularly at the most likely contact force region of 10-25N. This would seem to indicate that the presence of a lubricant is indeed beneficial to the friction coefficient, though the benefits of seawater or freshwater lubrication are lower than with the greases tested. The dominant lubricated friction regime for all lubricants would appear to be boundary lubrication as the friction coefficient remains constant for varying loads as indicated in the boundary lubricated region of the Stribeck curve. The high contact pressures, plastic contact as determined by the plasticity index and relatively rough composite surface all also suggest that boundary lubrication is likely to dominate. The consistent friction coefficients recorded here also indicate that the lubrication regime remains constant, even as contact pressures exceed three times the expected distributed contact load.

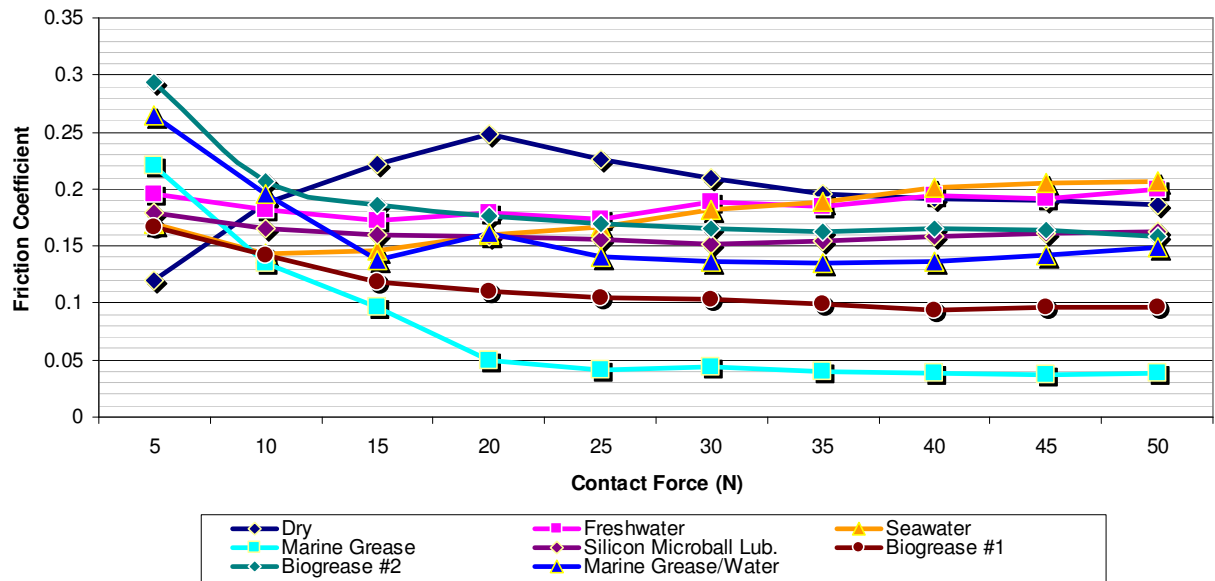


Fig. 6.1. TE57 Composite tests: Friction Coefficient vs. Contact Pressure

### Comparison with previous slipway lining

Comparing the new jute/phenolic composite slipway lining material with the previously used low friction coated steel shows the dry sliding friction coefficient for the composite is on average just 27% of the coated steel result. Even when the steel lining is greased as intended the jute/phenolic composite still performs well in comparison and when the composite is run greased the friction coefficient is far lower. This significant reduction in friction would seem to justify the introduction of the new slipway lining material and highlight the dangers of sections of steel lined slipways losing grease to approach the dry sliding scenario.

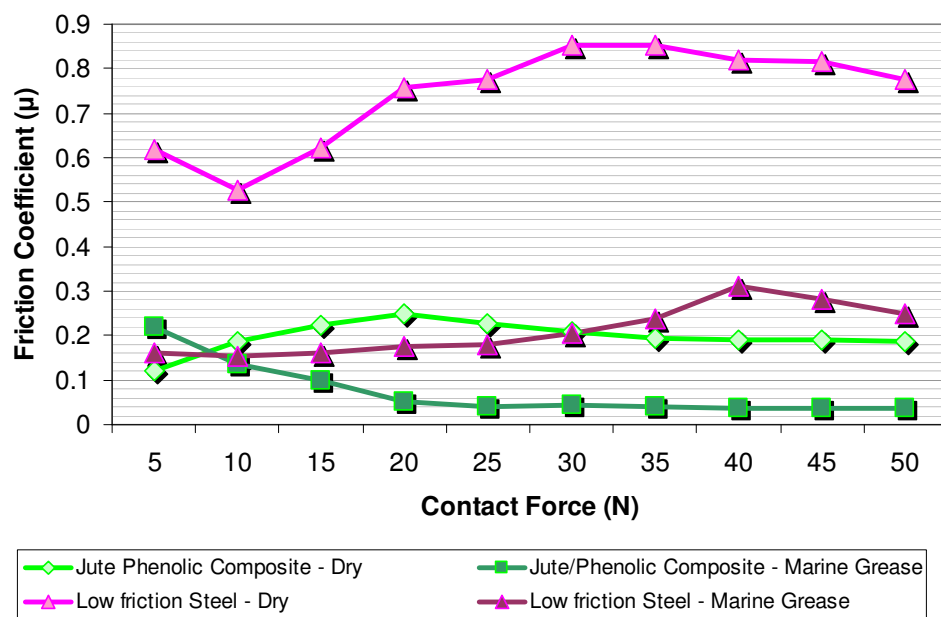


Fig. 6.2. TE57 Composite vs. Low friction steel friction coefficient at various contact pressures

A marine grease/water mix was tested to investigate conditions near the base of the slipway where water and grease are likely to be mixed.

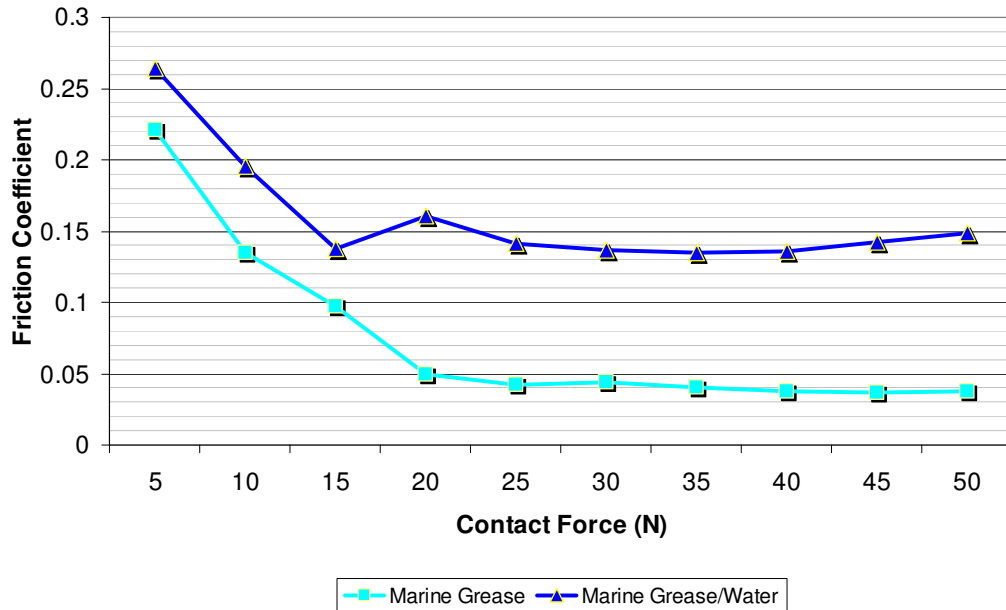


Fig. 6.3. TE57 Composite contact tests: marine grease vs. marine grease/water lubrication

The results show that the presence of water in a marine grease lubricated contact is detrimental to the friction performance, though the friction performance still remains within specified limits.

### Contact load proportionality

Plasticity index calculations indicate that the sample will deform plastically under the applied loads tested so that cohesive wear mechanisms will dominate, this can be further tested by comparing the friction force proportionality to the applied load. Contact test results vs. the contact load,  $W$  and vs.  $W^{-1/3}$  are presented below, with correlation representing cohesive and adhesive contact mechanisms respectively. These show a direct proportionality between the friction force and the applied load, this indicates that cohesive, abrasive contact mechanisms are present [81]. For comparison the friction force vs.  $W^{-1/3}$  is shown.

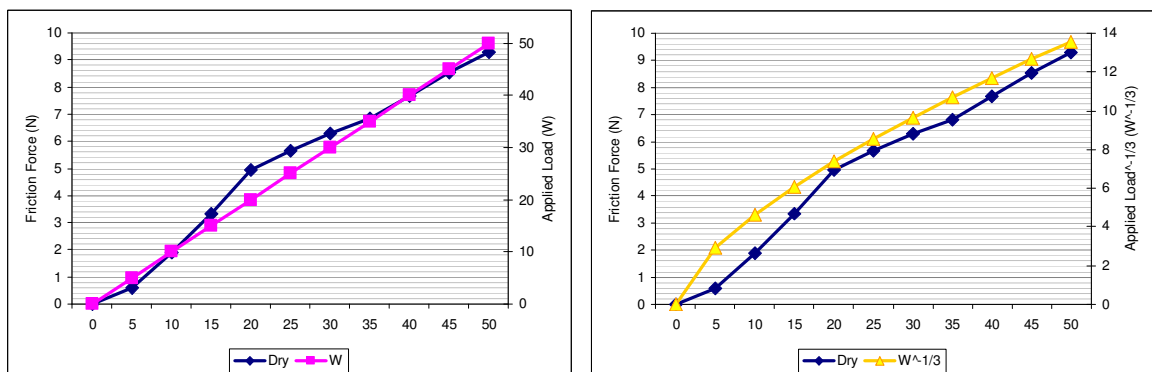
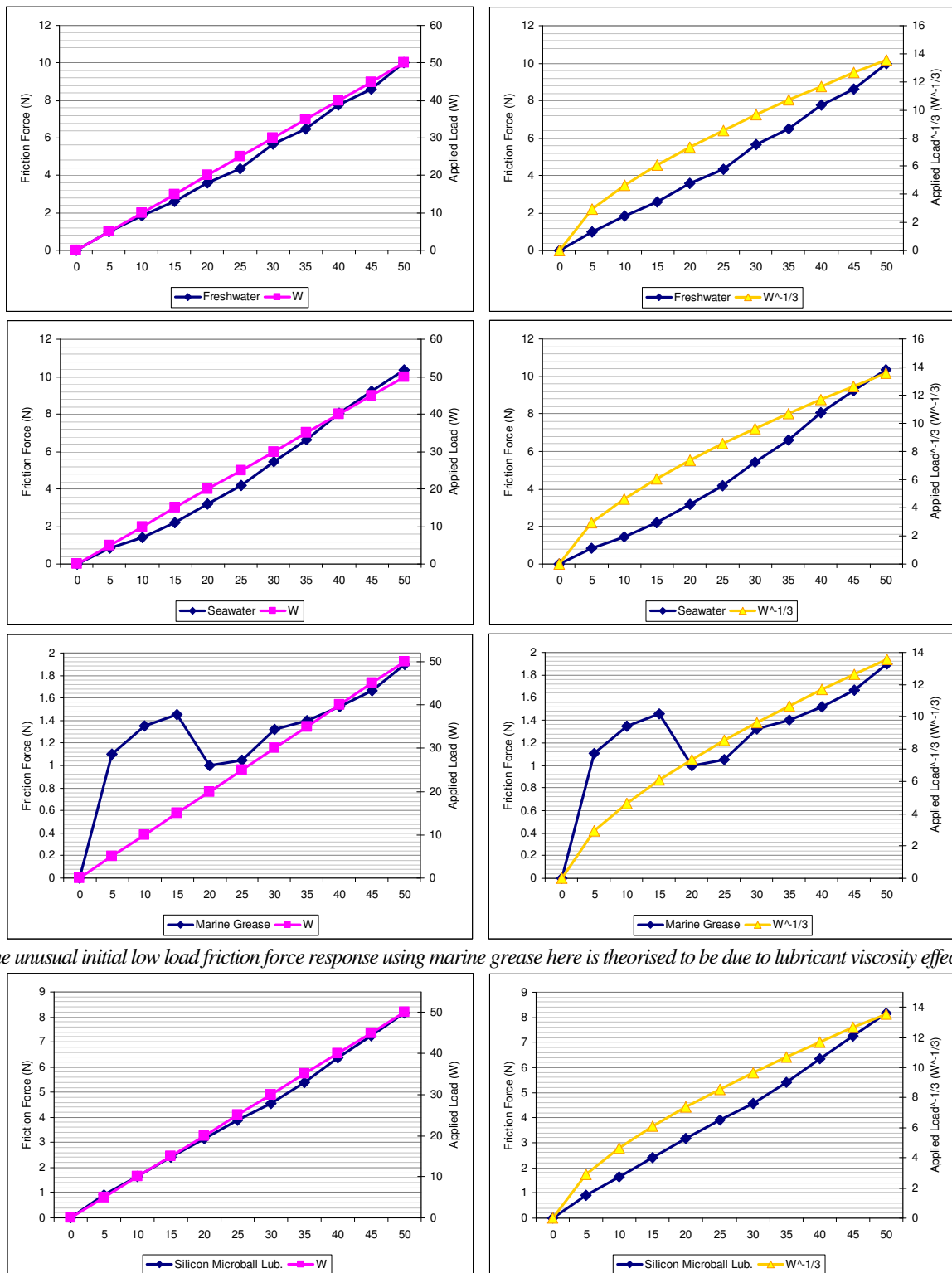


Fig. 6.4. TE57 Composite dry contact tests: proportionality to contact load,  $W$  and  $W^{1/3}$



This correlation is also noted under lubricated conditions, again indicating cohesive contact conditions.



*The unusual initial low load friction force response using marine grease here is theorised to be due to lubricant viscosity effects*

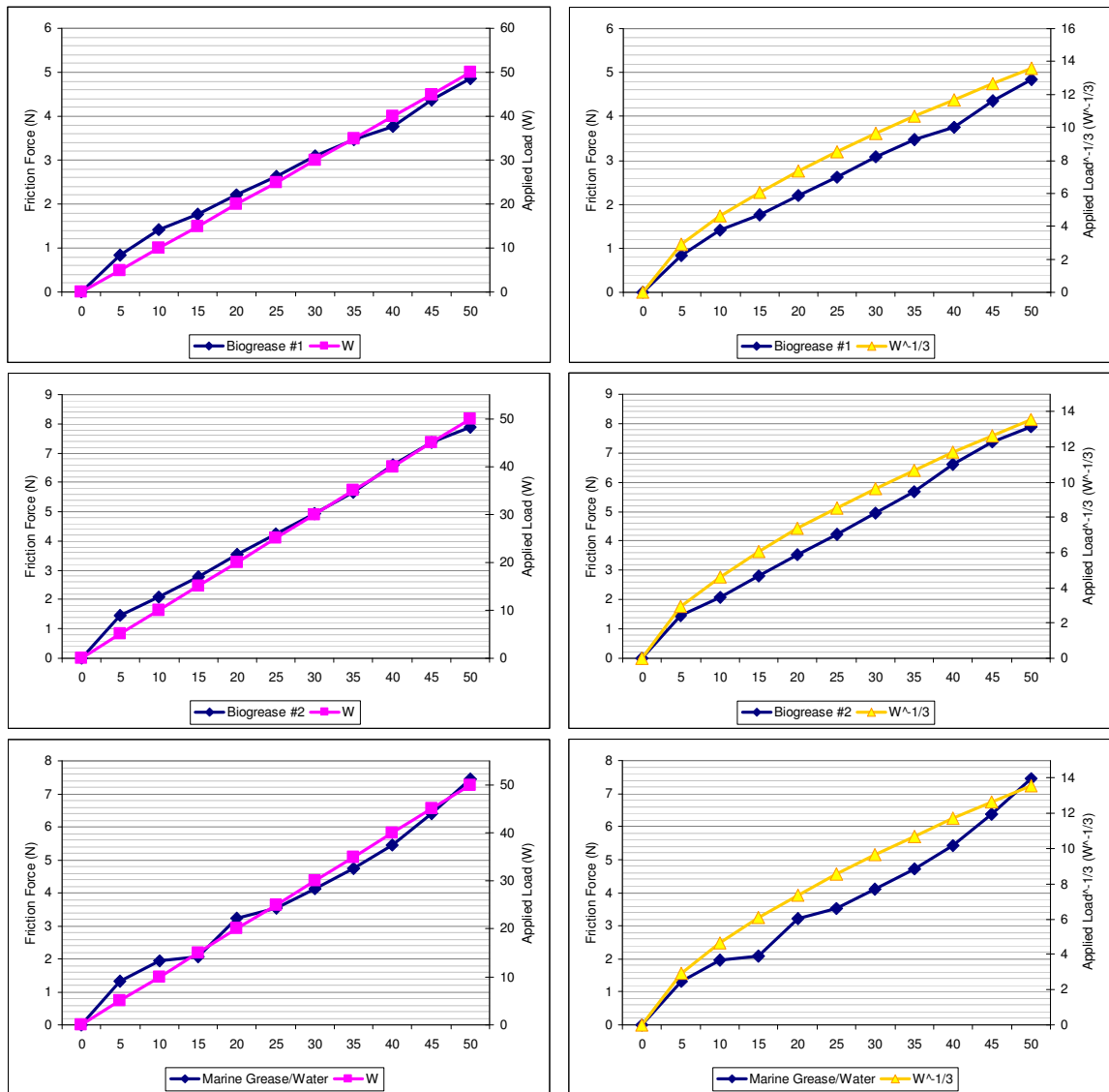


Fig. 6.5. TE57 Composite lubricated contact tests: proportionality to contact load,  $W$  and  $W^{1/3}$

### 6.1.2. TE57 Wear Tests – Results:

The results from the wear tests conducted are shown below. Shown are the average friction coefficient recorded during the duration of the 10 hour test, the standard deviation of the friction coefficient during the test and the dimensional wear coefficient for the samples as determined using light interferometry techniques to investigate the wear scar volume of the cleaned sample after the test.

These results are compared with the maximum  $\mu$  specification of  $\mu=0.2$  for a 1 in 5 slipway, and  $\mu=0.167$  for a 1 in 6 slipway. These indicate that the phenolic composite will not meet either specification without the addition of a lubricant. All lubricants except biogrease #2 are shown to be suitable for reducing the friction coefficient to below the specification.

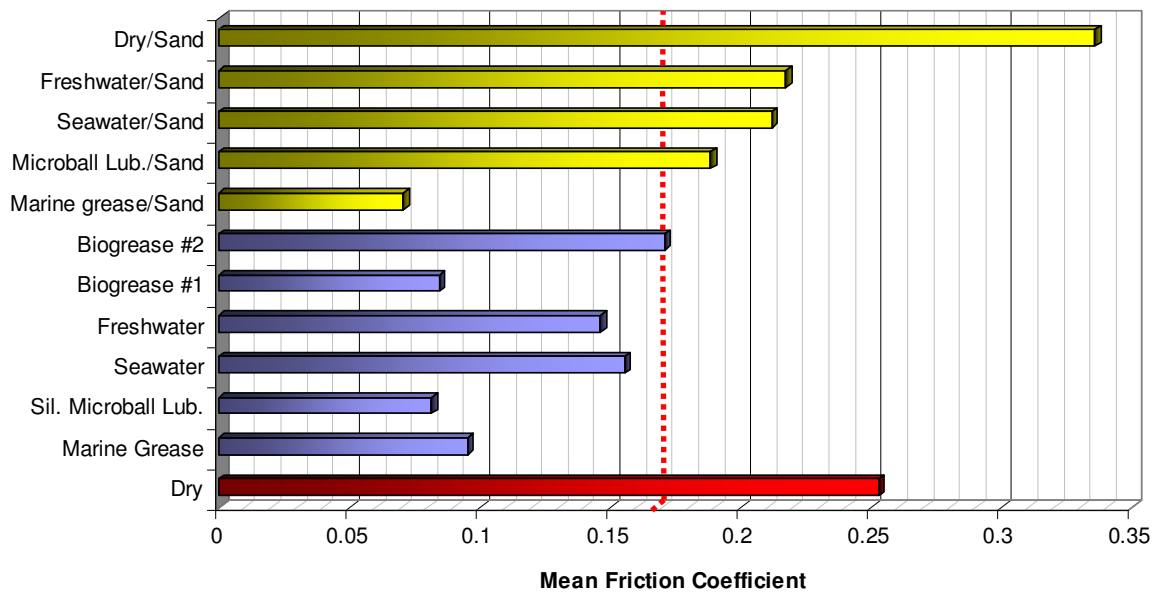


Fig. 6.6: TE57 Composite Friction Coefficient vs. Lubricant Regime 10hrs Test

The addition of sand contamination to the contact has a detrimental effect of the friction coefficient causing all lubricants tested except the marine grease lubricated case to exceed the friction specification. This would indicate that marine grease lubrication is suitable for use at slipways where sand contamination is present. Water lubrication is shown to be feasible for both 1 in 5 and 1 in 6 slipways with freshwater providing a slightly lower friction coefficient.

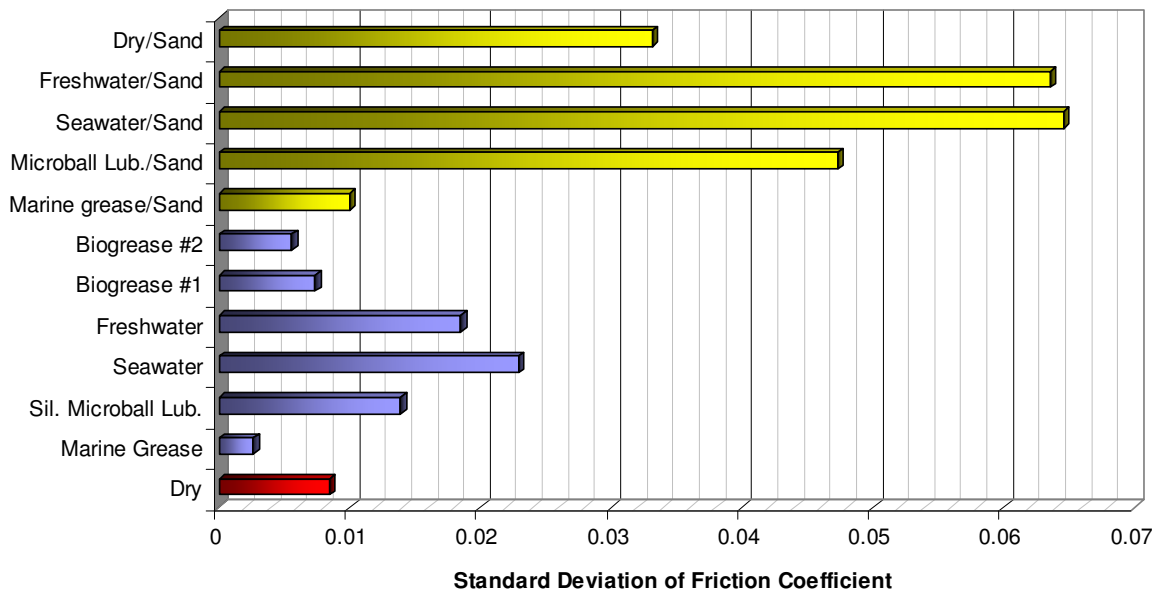


Fig. 6.7: TE57 Composite Standard Deviation of Friction vs. Lubricant Regime 10hrs Test

The standard deviation of friction results are shown above in fig. 6.7. This can be seen as an indicator of the variability of the friction from the average result under the different lubrication regimes tested. The results show that for lubrication under normal conditions the friction

variability is generally low, exceptions to this rule are the seawater and freshwater lubricated cases and the silicon microball lubricant which show a marked increase in friction variability compared with the grease lubricated case. In the case of the microball lubricant this is due to the presence of silicon microballs in the contact, these act as 3<sup>rd</sup> bodies and increase the variability of both the friction and wear. In the water lubricated case the friction variability may indicate a partial breakdown of the lubricant boundary film to allow some unlubricated asperity contact. This effect is more prevalent in the water lubricated cases than the grease lubricated tests due to its relatively low viscosity. The difference between the seawater and freshwater cases can be explained by the presence of impurities in the seawater.

The friction variability increases significantly with the addition of sand contamination as would be expected due to the changing geometry and placement of the sand particles in the contact zone, as mentioned above however; the addition of grease lubrication does mitigate this effect.

### Wear Coefficient

The wear coefficients recorded for the same experiments are shown below. As can be seen, the wear rates are uniformly low under ideal conditions and would present no particular problems during the expected use-life of the lining. However, when environmental contamination in the form of sand is introduced, the wear rates increase dramatically and could generate significant problems if this situation is commonly encountered.

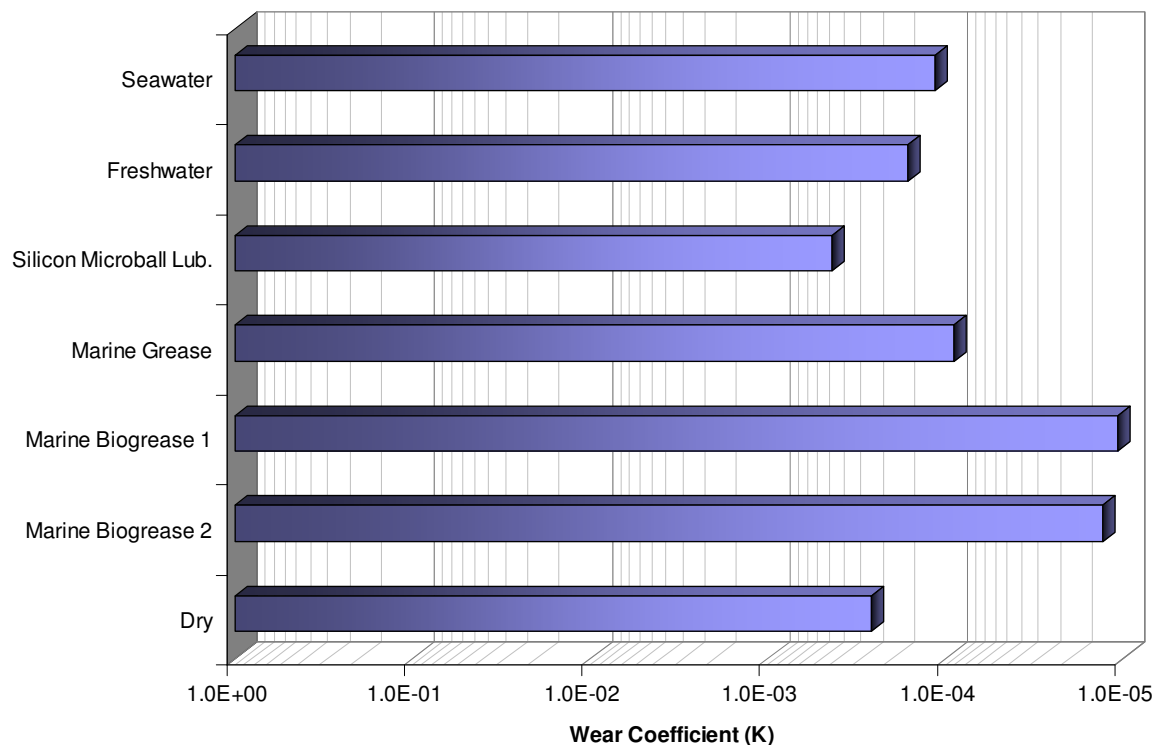


Fig. 6.8: TE57 Composite Wear Coefficient vs. Lubricant Regime 10hrs Test

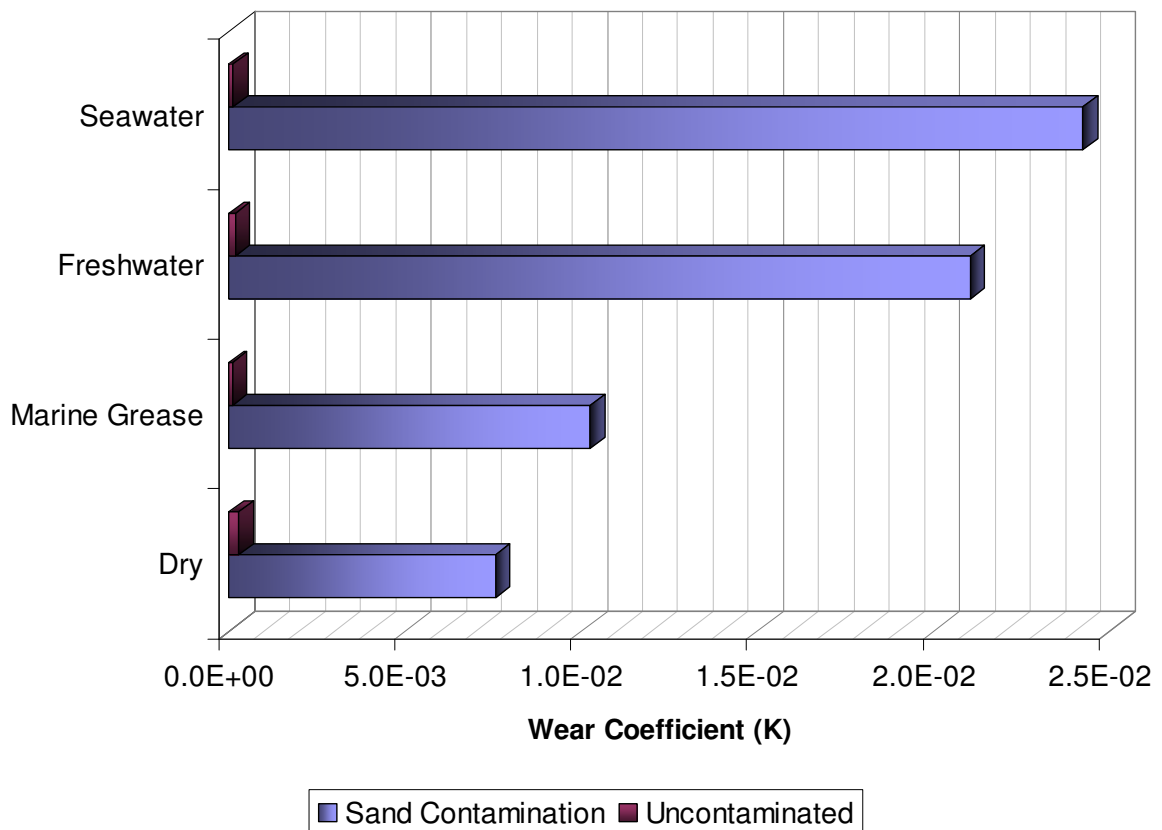


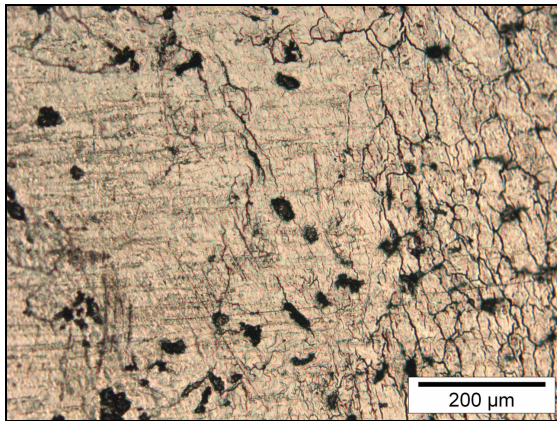
Fig. 6.9: TE57 Composite Wear Coefficient vs. Lubricant Regime 10hrs Test

It should be noted that because the TE57 reciprocating geometry differs significantly from the real world case the wear coefficients recorded here represent screening tests rather than necessarily accurate figures for wear prediction. The TE92 rotary tribometer experiments are intended to more accurately develop wear coefficients for real world wear prediction.

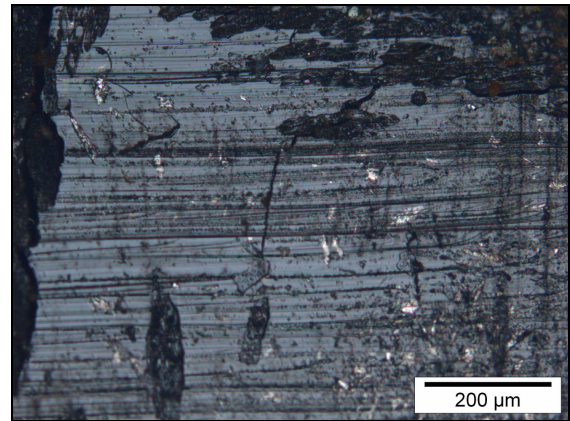
### Post Test Analysis

Following the lubricant tests the samples are inspected using a light microscope. This shows a smoothing of the composite surface under all conditions with this effect being the most pronounced on the dry sliding test sample. The surface scar surface is noted to be reflective and dark, which prompts the observation that this may be a graphite transfer film formed from the abraded debris of the graphite infused phenolic resin. Such transfer layer are often formed when a polymer slides against a hard counterface and usually form on the counterface surface, however in this case they form on both the polymer surface and the counterface, a feature also noted for thermosetting polymers in previous literature [82]. A transfer layer usually acts to reduce both the friction and wear in a contact pair and is also noted to have a smoothing effect on the worn surface as abraded debris fills cavities in the sample surface [82].

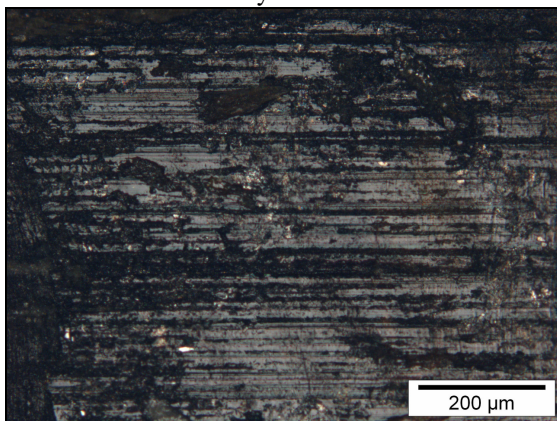




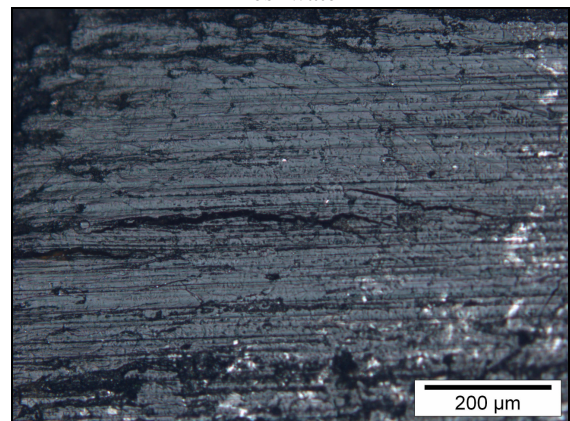
Dry



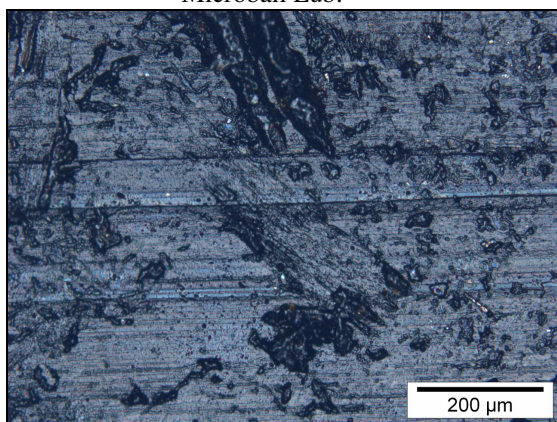
freshwater



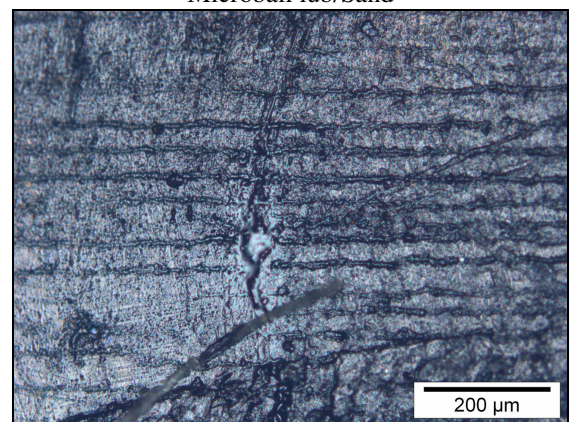
Microball Lub.



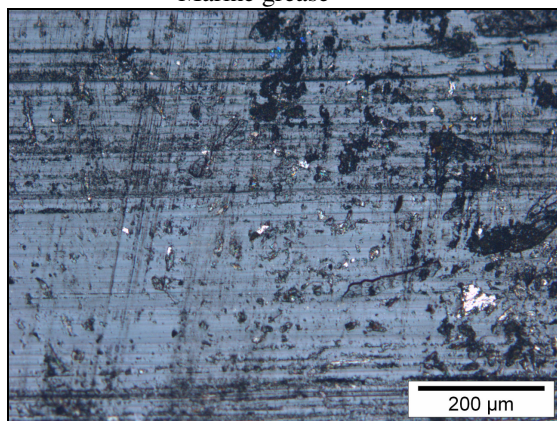
Microball lub/Sand



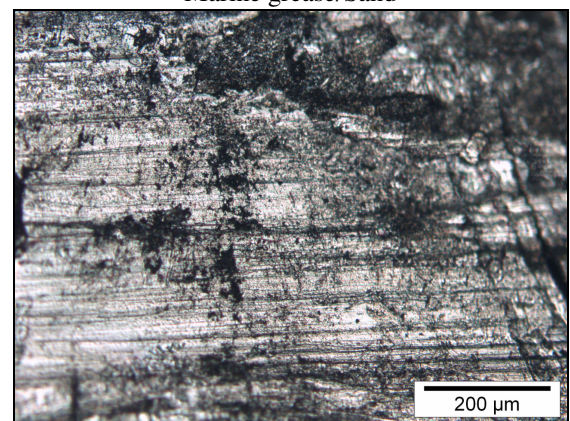
Marine grease



Marine grease/Sand



Seawater



Seawater/Sand

Fig. 6.10: TE57 Lubricant tests: light microscope images



It is known [83] that the addition of lubricants to a contact can impede the development of a transfer film and it is noteworthy that the smoothing effect seen on the dry sliding composite sample under the light microscope is less pronounced on the lubricated test samples.

Also noticeable is an increase in the grooves characteristic of abrasive wear with all lubricated tests, this indicates that the wear regime has changed from one borne by the graphite transfer layer to more conventional abrasive wear, again indicating that the presence of lubricants may have an adverse effect on transfer layer formation.

### **6.1.3. TE57 Results: Discussion**

This study shows that the selection of a jute/phenolic composite to replace the existing low friction coated steel slipway lining presents significant benefits in reducing the friction coefficient along the slipway. This is particularly true in the unlubricated case where the friction coefficient of the jute/phenolic composite records an average friction coefficient of  $\mu = 0.252$  whereas the low friction steel has an average friction coefficient of  $\mu = 0.74$  – far too high for reliable launch or recovery. It is likely given this research that the majority of cases where very high friction and winch loading was encountered in the past using the low friction coated steel are due to a breakdown in the lubrication so that the friction coefficient will increase from the average of  $\mu = 0.27$  for low friction steel with boundary marine grease lubrication to the unlubricated case of  $\mu = 0.74$ . Using the jute epoxy composite the range between the marine grease lubricated case and the unlubricated case is  $\mu = 0.07 - 0.19$  according to the contact tests and  $\mu = 0.09 - 0.252$  according to the extended tests which will allow far more reliable launch conditions even if the lubrication regime should break down. These results also closely mirror those recorded during the slipway trials indicating that the testing method used here is appropriate for assessing slipway lining friction performance.

The use of lubricants with the jute/phenolic composite to further reduce friction to the ideal level of  $\mu = 0.167$  is possible with all lubricants tested except biogrease #2 approaching this value. However the use of marine grease, the silicon microball lubricant and the biogreases still presents the problem of applying the grease to the slipway manually in high seas. The use of seawater or freshwater could circumvent this problem by using water jets mounted at the top of the slipway to run water along it, this would also help to ensure consistent friction with the case near the bottom of the slipway where seawater contamination is present. These test show that water lubrication is sufficient to meet friction specifications under good conditions.

Environmental impacts from the use of lubricants near an open environment can be reduced in two ways: firstly the lubricants themselves could be substituted with biodegradable greases such as biogrease #1 and #2 tested here. These have been shown to be effective in reducing the friction from the dry sliding case and would reduce the impact of the grease being washed into the sea on launch. Of the two biogreases tested, biogrease #1 is the most effective, exhibiting lower wear and friction than biogrease #2 and meeting the more stringent friction coefficient specification of  $\mu = 0.167$  necessary for a 1 in 6 slipway. The second approach would be to switch to a seawater or freshwater lubrication system; this is shown here to be effective in reducing friction to below the  $\mu = 0.167$  specification. This approach would have negligible environmental impact and would also remove the danger of manually applying the grease to the slipway in hazardous conditions.

The use of the silicon microball lubricant is shown to be effective but doubts exist as to its suitability in this case. This is primarily due to the dangers of microball build up with repeated use, the longer wear tests revealed a hard residue of dried lubricant and microballs around the wear scar and this could present problems if allowed to build up in the full size case, this would be a particular problem if the lubricant were left on the slipway to dry during the sometimes long intervals between launch and recovery. The silicon microballs also present an environmental impact if they are allowed to accumulate at the bottom of the slipway. The performance of the lubricant was good, but was matched by the other lubricants tested leaving little reason to favour its use.

The wear rates for all uncontaminated lubricant regimes are shown to be low, and this would indicate that this is not a particularly important variable in selecting a suitable lubricant for real world use. When sand contamination is introduced the wear rates increase dramatically though would still present little real problem during the 2 year scheduled lifespan of the lining. One possible solution to the presence of sand along the slipway is to use a seawater or freshwater lubrication system as described above, this would run water down the slipway prior and during launch and recovery which would wash away any sand or other environmental debris present.

Subsequent research has shown that slipway panel wear is predominantly caused by panel misalignment and keel impacts during the locating of the keel to the keelway during the initial stages of the recovery of the lifeboat, rather than the idealised plane contact modelled here. Contact tests show that the friction force is proportional to the contact stress and this is increased in regions of panel misalignment where the contact moves away from the plane sliding case.

## 6.2. TE92 Rotary Tribometer

### 6.2.1. Contact Force Tests – Results

Results from the contact force tests (CR1-4) are shown below.

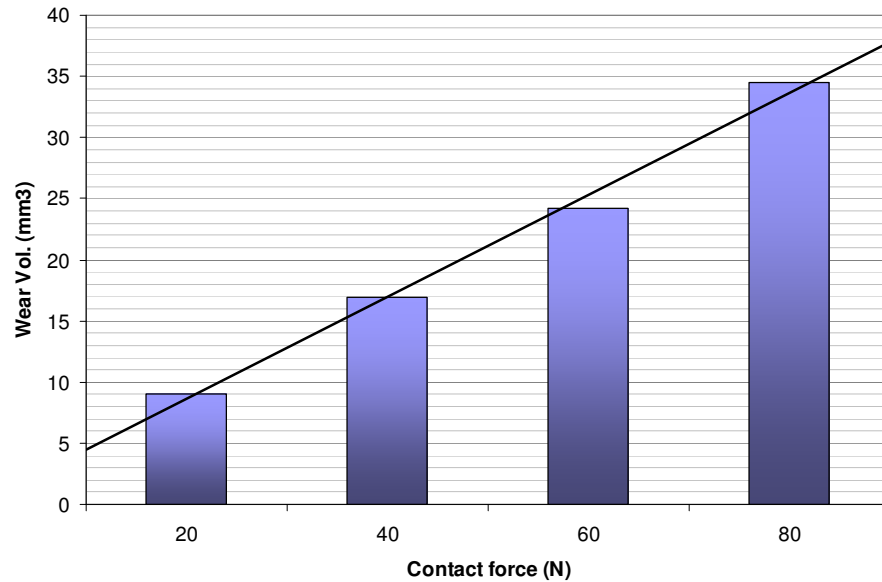


Fig. 6.11: TE92 Jute/Phenolic Composite against keel steel: Wear Volume vs. Contact Force

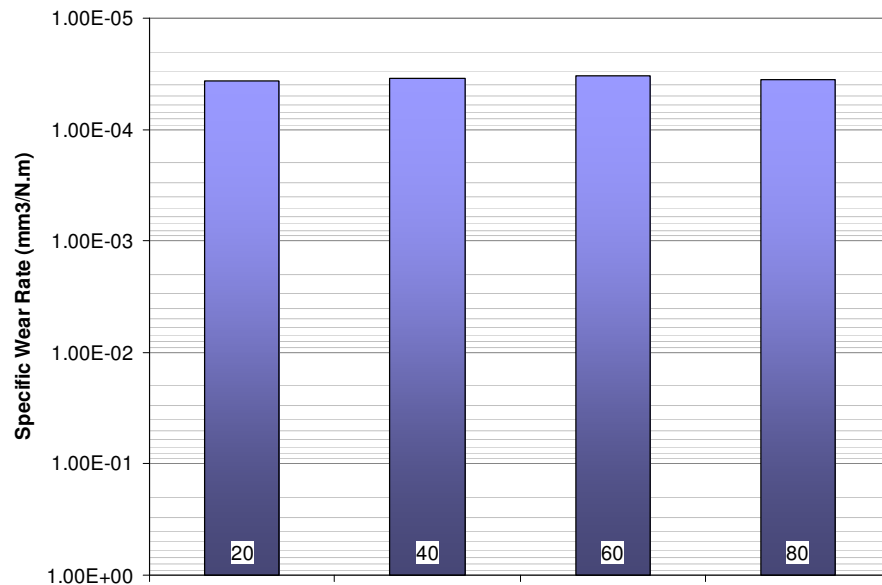


Fig. 6.12: TE92 Jute/Phenolic Composite against keel steel: Wear Rate vs. Contact Force

These results indicate a direct proportionality with the applied load  $W$ , confirming observations from earlier reciprocating tribometer tests that the contact is cohesive rather than adhesive with significant contact stresses present below the contact surface. The wear rates also confirm earlier test results indicating that under aligned contact conditions the wear is unlikely to cause panel failure even for an extended panel lifespan of 10 years.

### Contact Force Tests – Surface Analysis

Light microscope images of the worn sample surface are shown below, interferometry is also used to investigate the worn surface and to record surface roughness parameters, results are shown below:

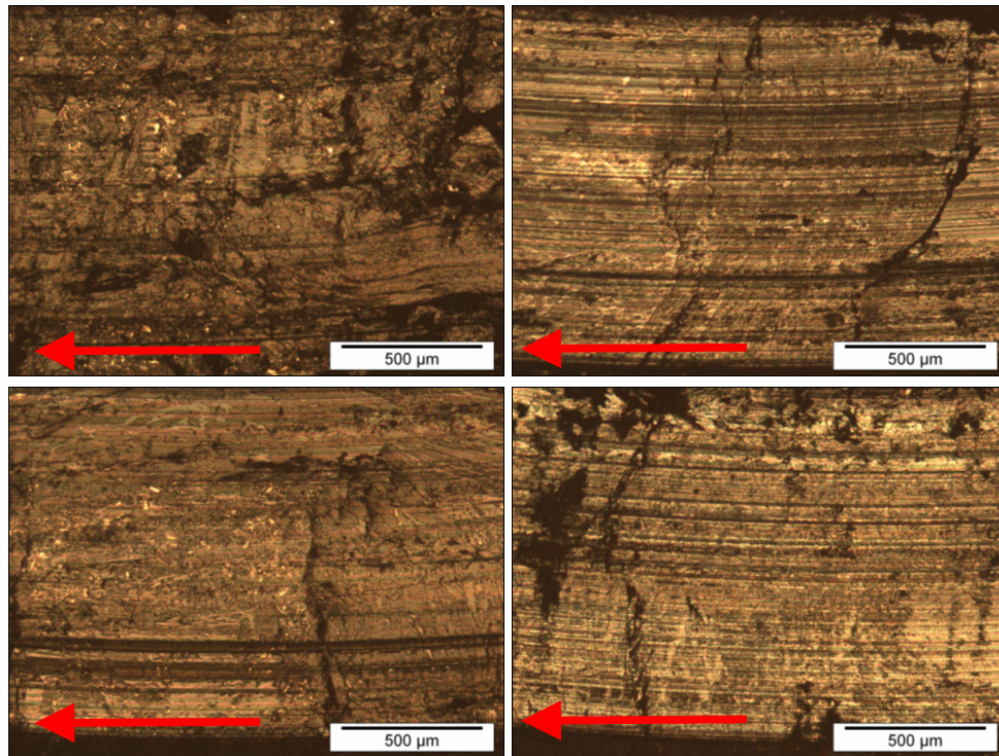


Fig. 6.13: Light Microscope Images of TE92 Contact Tests: Dry 20N, 40N, 60N, 80N

These images show a smooth, reflective surface becoming more pronounced with increasing contact pressure as with earlier reciprocating tests.

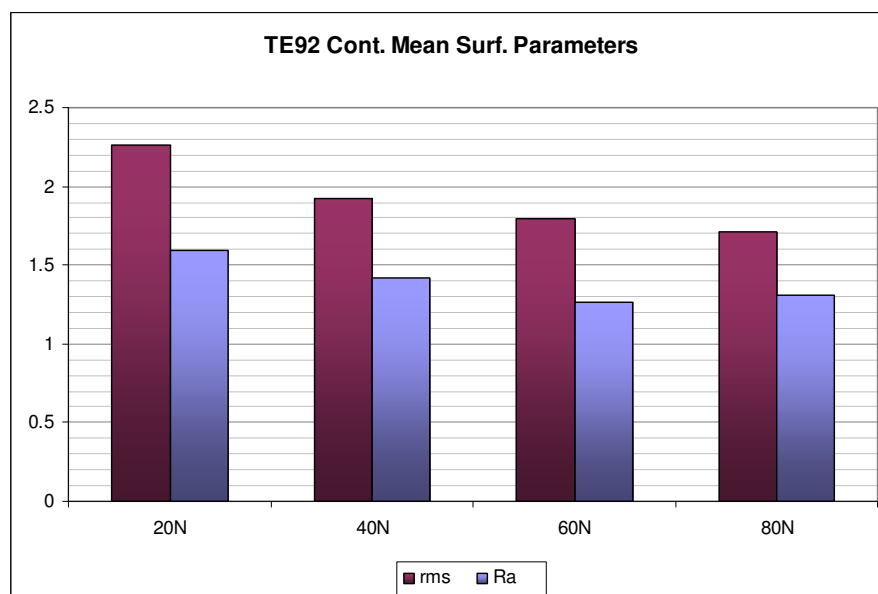
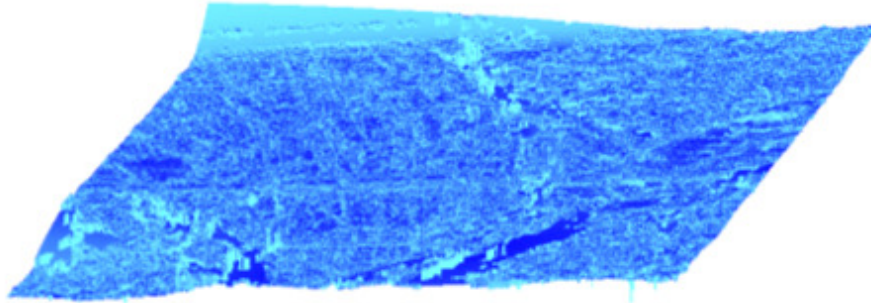
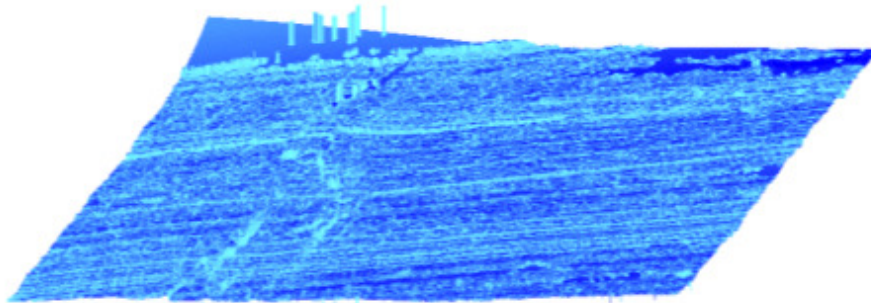


Fig. 6.14: TE92 Jute/Phenolic Composite: wear scar surface roughness

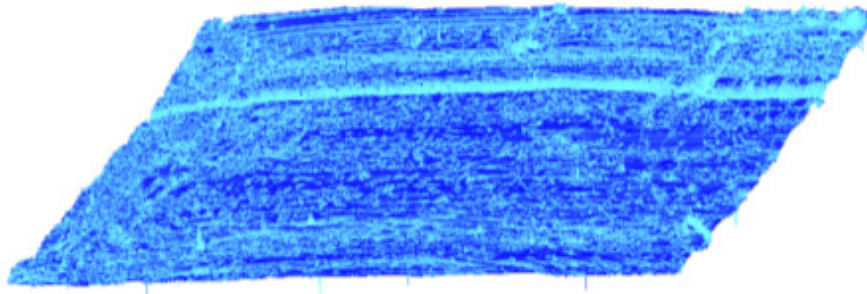
These results confirm the earlier observation that there is smoothing present on the worn sample surface and that this effect is proportional to the load. Interferometer scans of the worn surfaces showing this effect are shown below.



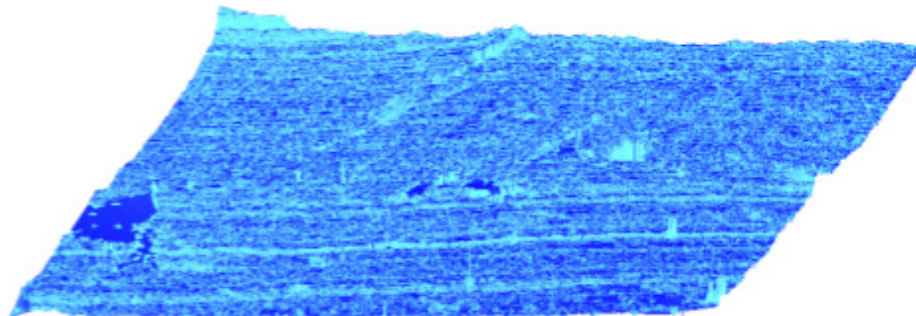
i). TE92 20N test interferometer profile scan



ii). TE92 40N test interferometer profile scan



iii). TE92 60N test interferometer profile scan



iv). TE92 80N test interferometer profile scan

Fig. 6.15: TE92 interferometer profile scans: Shows increasing smoothing with contact pressure (and wear volume)

### 6.2.2. Lubricant Tests – Results

Results from the TE92 rotary tribometer lubricant tests are shown below:

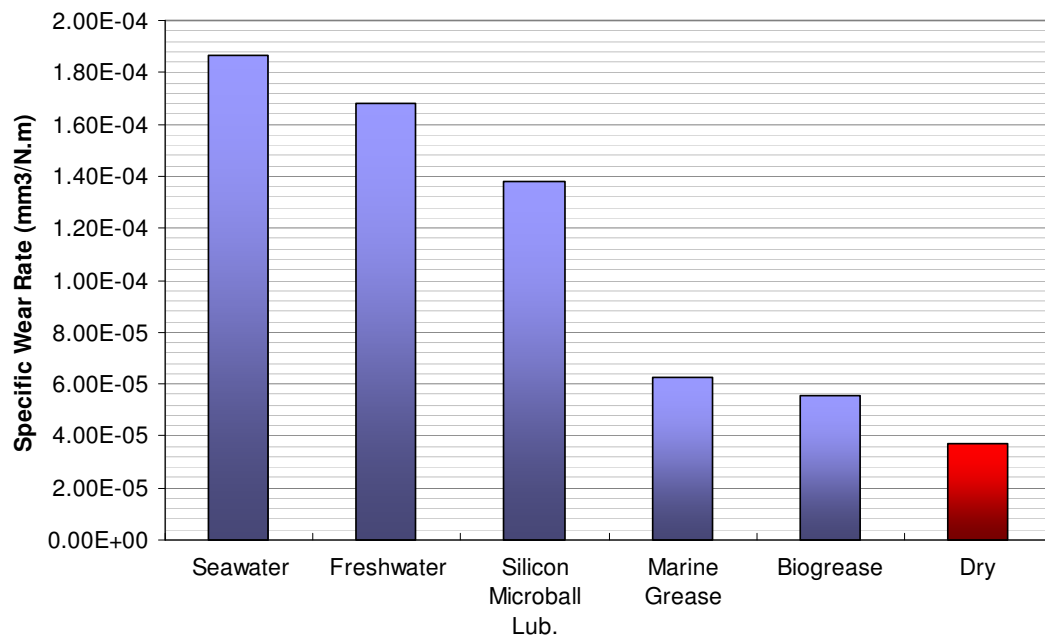


Fig. 6.16: TE92 Jute/Phenolic Composite: Wear Rate vs. Lubricant Regime

These show wear rates increasing with lubricant use compared to the dry sliding case. This result is unexpected as lubricants usually act to reduce both friction and wear in a contact.

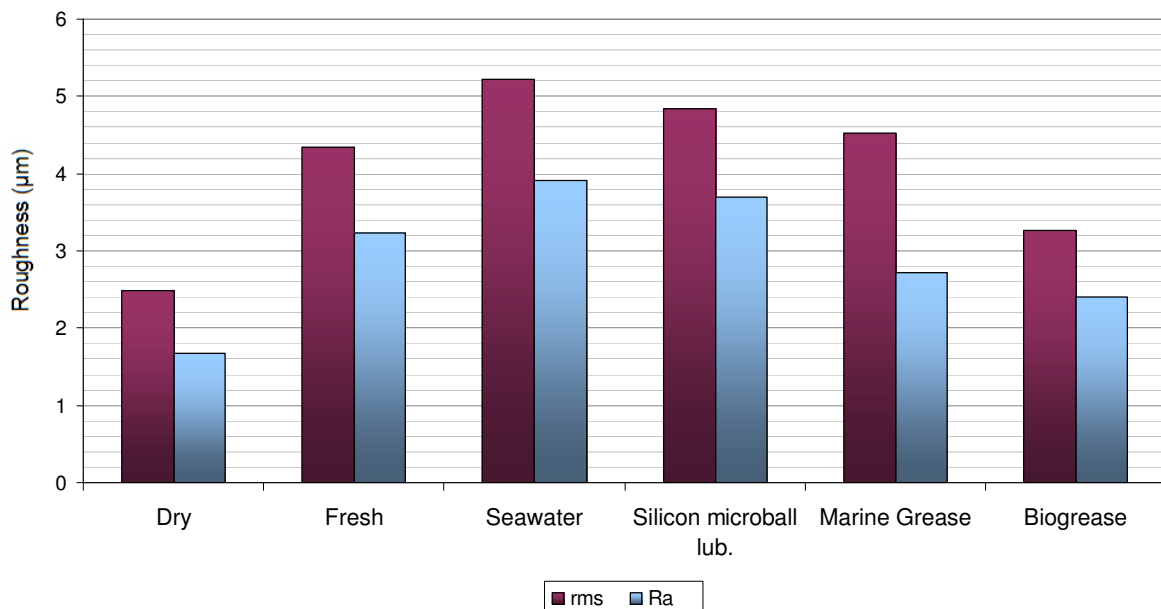


Fig. 6.17: TE92 mean surface parameters

Surface roughness results are also surprising with increasing roughness observed with lubricant use. This is unexpected as the greater wear rates found with lubricants would imply that the wear scar surface would be smoother as high asperities are abraded away.



## Lubricant Tests – Surface Analysis

Surface analysis of lubricant test wear scars is shown below:

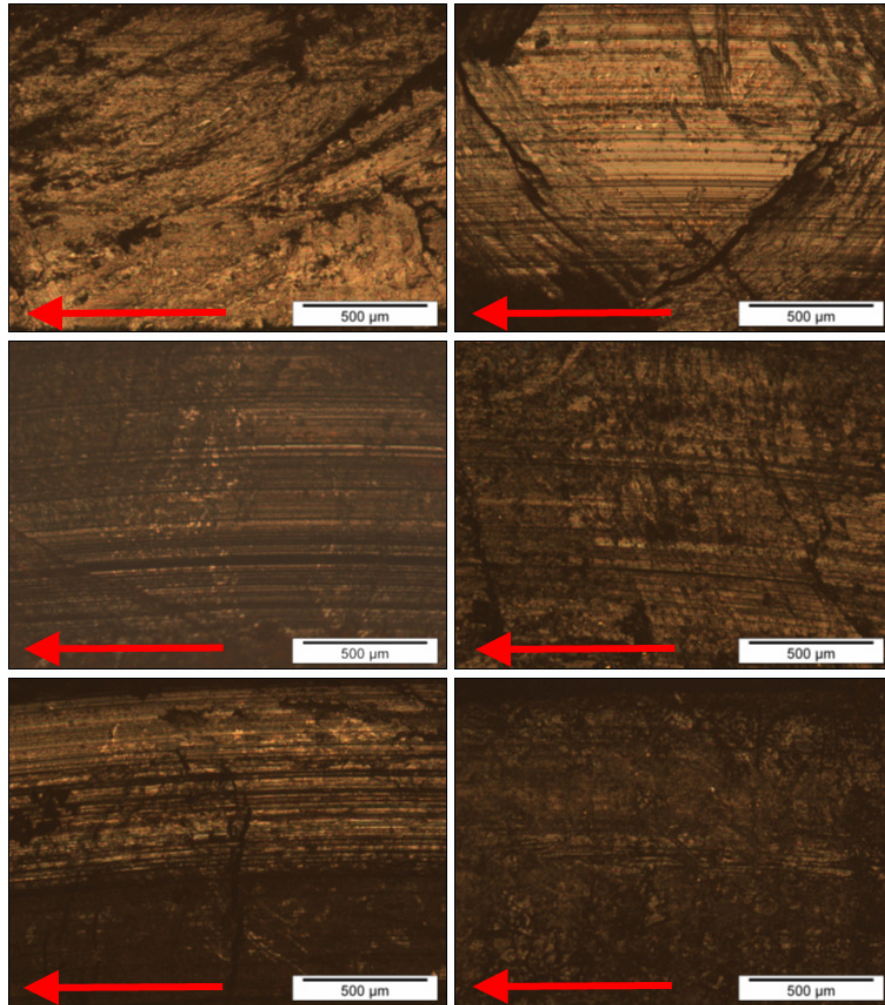


Fig. 6.18: TE92 Lubricant Tests: Dry, Freshwater, Seawater, Marine grease, Si Microball, Biogrease #1

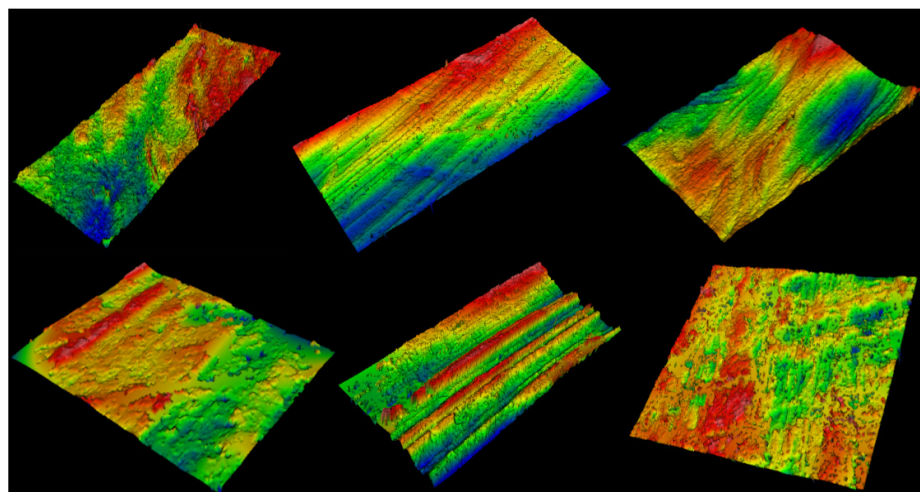


Fig. 6.19: TE92 Inframeter Wear Scar Profiles: Dry, Seawater, Freshwater, Marine grease, Si Microball, Biogrease #1

These results again show the dry sliding case to be smoother than the lubricant cases. Lubricant use also shows greater evidence of the wear tracks usually found in abrasive wear.

### 6.2.3. TE92 Results: Discussion

---

#### Contact Force Tests

The experimental results show a linear increase in wear volume with increasing contact force and a steady wear rate. These indicate that the composite material wears in direct proportion to the applied load and thus behaves according to Archard's laws. This generates the expected result that a real-world increase in contact pressure will correspond to an increase in wear. The mean specific wear rate from the experiment data is calculated to be  $3.50\text{E-}05 \text{ mm}^3/\text{Nm}$  for dry sliding conditions. No consistent increased wear effects were noted around the slot and hole features in the sample due to the very low wear rates recorded.

Observed wear coefficients are uniform and very low, indicating that abrasive sliding wear under normal contact pressures would not be sufficient to cause panel failure, even in the case of the composite panels far exceeding their original 2 year lifespan. Even for contact pressures at four times the distributed load case the expected wear over 10 years would not be sufficient to cause panel failure.

The microscope pictures indicate a smooth, reflective surface has been formed, becoming more pronounced with increasing contact load, this is confirmed by interferometer roughness results which also show a reduction in surface roughness with increasing contact pressure. It is proposed that this is the result of abraded graphite wear debris forming a transfer layer between the two surfaces. This contrasts with the larger flakes and chunks observed when fatigue wear mechanisms dominate. The presence of a transfer layer acts to reduce the wear rate and this is reflected in the low wear volume observed during the experiments.

#### Lubricant Tests

The lubricant tests show that the wear observed on the composite samples is greater with the addition of lubricants. This effect is most marked when seawater or freshwater lubrication is used, with only a minor increase in the wear coefficient observed with the marine grease and biogrease lubrication. Again wear rates and wear scars were low and no consistent wear effects were noted around the slot and hole features in the sample. Initially the variation in wear rates seen here would seem to suggest that the choice of lubrication is of high importance for minimising the wear along the slipway, however the actual distributed wear scar generated on the slipway in the ideal real world case due to the sliding wear would be less than 1mm deep in all cases, suggesting that the 19mm thick composite panel is very unlikely to fail due to abrasive sliding wear regardless of the lubricant used under ideal conditions.

The microscope images again show a smooth transfer layer, though this varies in extent across the lubricants used. This impression is confirmed by the interferometer data which also shows variation in the surface roughness. It is proposed that the roughness recorded is reflective of the development of a graphite transfer layer as this will act to fill valleys in the sample surface, creating a smoothing effect [82].

It is known that the presence of lubricants [83] in sliding contacts can interfere with the formation of a transfer film resulting in higher wear rates than if the film is allowed to develop. It is suggested that this process is the reason for the increase in wear rates, rather than the expected decrease in wear rates under lubricated conditions, observed when using lubricants compared to dry sliding. If this was the case we would expect to see a correlation between the wear scar roughness and the wear rate for a given sample, with higher roughness corresponding to a less developed transfer film and higher wear rates. Fig. 6.20 below shows the specific wear rate vs. the recorded wear scar roughness for the lubrication regimes tested, this shows a distinct correlation, with the lower roughness values corresponding to lower wear rates for the lubrication regimes tested.

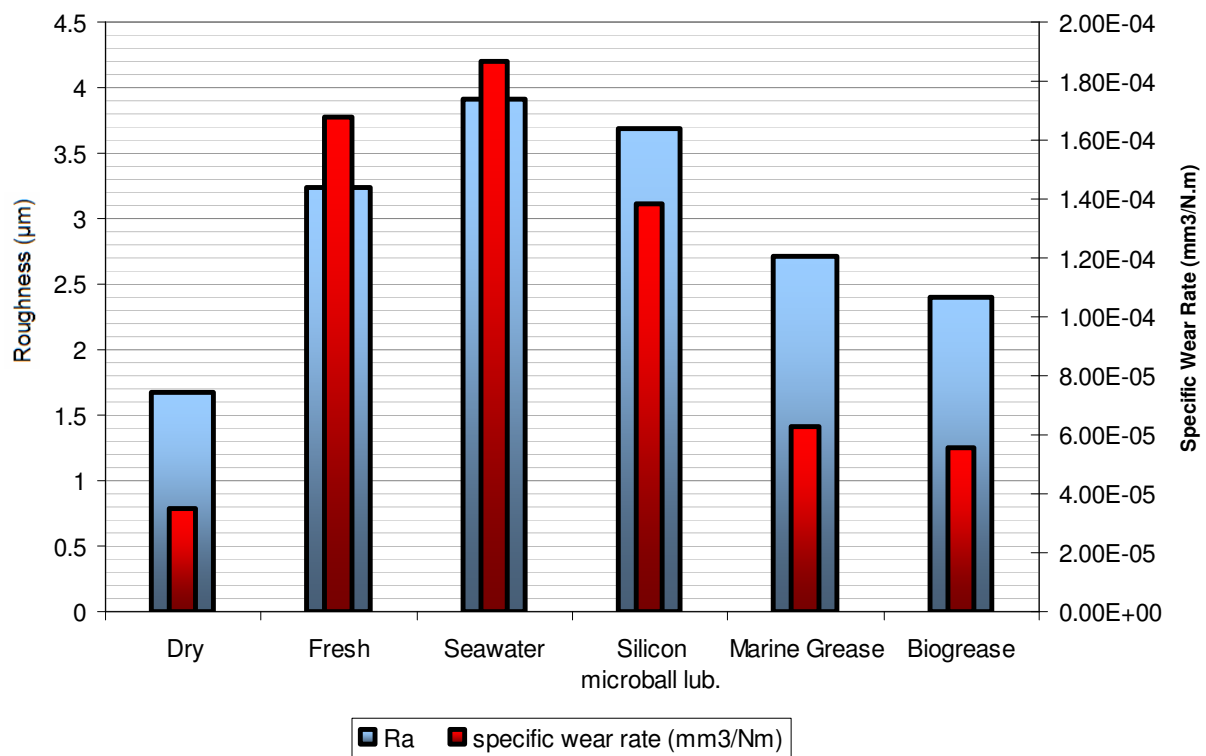


Fig. 6.20: TE92: Ra vs. specific wear coefficient

This hypothesis is further supported by the light microscope observations of increased 'grooving' when lubricants are added to the contact. This is a characteristic of abrasive wear and indicates that the protective effect of the transfer layer has been lost.

### 6.3 Conclusions

---

The experimental results indicate that the wear rate on the composite panels is dependant on the development of a graphite transfer layer, the addition of lubricants to the contact, while beneficial in reducing friction, can interfere with the development of this film and lead to higher wear rates on the composite. This hypothesis is supported by sample roughness measurements and by light microscope observations of decreasing smoothness and an increase in wear grooves with lubricated contacts. These indicate that the wear is no longer mitigated by the presence of a developed transfer layer and this is reflected in the increased wear coefficients recorded for the lubricated tests.

It is seen from the results that the use of lubricants can dramatically affect the wear rate of the composite lining material; however the wear rate remains insufficient to cause panel failure over the expected lifespan of the slipway lining and the frictional benefits resulting from the use of lubricants along the slipway outweigh the increase in wear rates.

The rotary tribometer tests conducted here ultimately show that even with the variations in wear rates encountered when using lubricants the abrasive sliding wear generated under normal conditions would not be sufficient in isolation to cause failure of the slipway panels. Despite this wear is noted as a serious problem on some slipways, particularly the two new boathouses and slipways at Tenby and Padstow. Following this research a closer inspection was made of the slipways in question including a panel wear survey and panel misalignment measurements to attempt to identify the prevailing real-world wear mechanisms and the factors affecting wear severity.

# **7 FEA MODELLING – EXISTING SLIPWAY PANEL**

---

## **7.1. FEA Modelling of Existing Slipway Panel Geometry**

---

Following tribometer testing the friction and wear rates for the composite against steel under various lubrication regimes are determined. However, the wear scars generated bear little resemblance to the real world case and the friction is also observed to be far more stable. From investigation of the worn Tenby slipway panel it is noted that wear occurs, not evenly across the keel/panel contact area as expected from an evenly distributed load on a flat surface, and as generated by the tribometer tests, but unevenly, and particularly at the panel edge and area surrounding the fixing holes. This would imply that the evenly distributed load/flat surface assumption does not hold entirely for the length of the lifeboat keel in the real world case. Site surveys undertaken at Tenby and Padstow to determine the extents and nature of the uneven wear observed found that there was significant misalignment present between panels, the nature of which could be roughly categorised into three misalignment scenarios. It is thought that this deviation from the evenly distributed load/flat surface contact may be a cause of the higher than expected friction and wear observed on real world lifeboat slipways. In order to assess the impact of the panel geometry and alignment on the wear rate it is proposed to use FE methods in ANSYS coupled with the friction and wear data derived experimentally from tribometer testing.

### 7.1.1. One Panel Aligned Case

Finite Element techniques are used to model the static case of an evenly distributed load along the lifeboat keel on a composite slipway panel using a beam with a coupled upper surface to model the lifeboat keel; results are shown below for the Von Mises stresses on the panel.

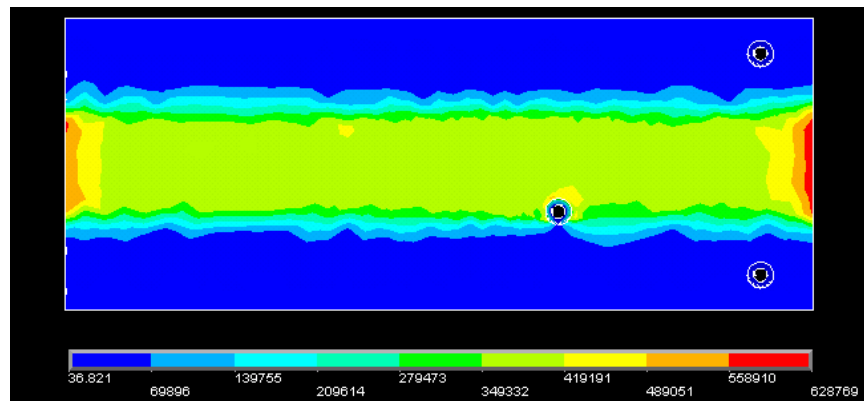


Fig 7.1: Plan view of Von Mises Stresses on slipway panel from FEA simulation

It is found that the areas of high stress concentrations correlate well with the worn regions observed on composite panels during slipway surveys and on the damaged slipway panel recovered from Tenby slipway station as shown in fig. 7.2.

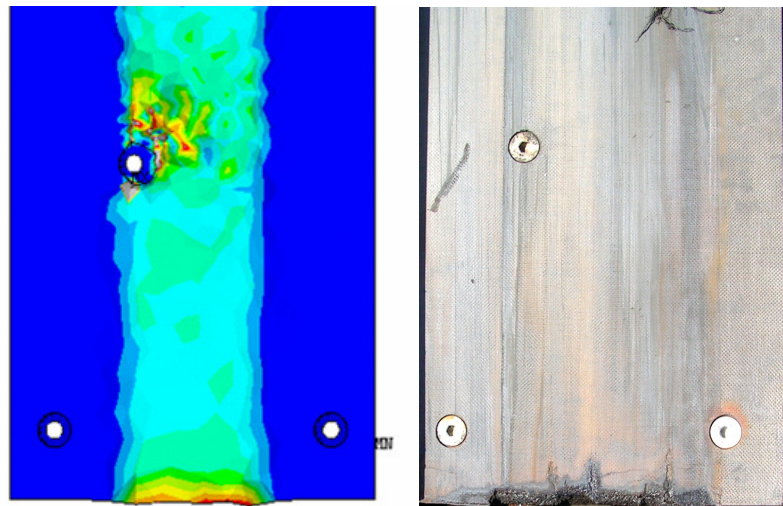


Fig. 7.2: FEA simulation vs. typical worn jute fibre/phenolic resin composite lining panel section from Tenby slipway

The stress concentrations on the FEA model are seen to occur around areas close to geometric features, particularly the panel edge and fixing hole areas. This would indicate that geometric considerations are an important factor in determining the likely local wear rate and friction on a slipway panel due to the stresses concentrated in these areas.



## Wear Simulation

Using element death techniques and appropriate element failure criteria a wear scar can be developed within the FEA model. This is done by using a fine element mesh around the expected wear concentrations, elements exhibiting stresses above the material failure criteria are 'killed' and removed from the analysis, generating a wear scar. Using iterative techniques this wear scar can be modelled over time to show the likely progression of wear on the slipway panel. The wear scar generated is shown to correlate well with the real world case as shown below.

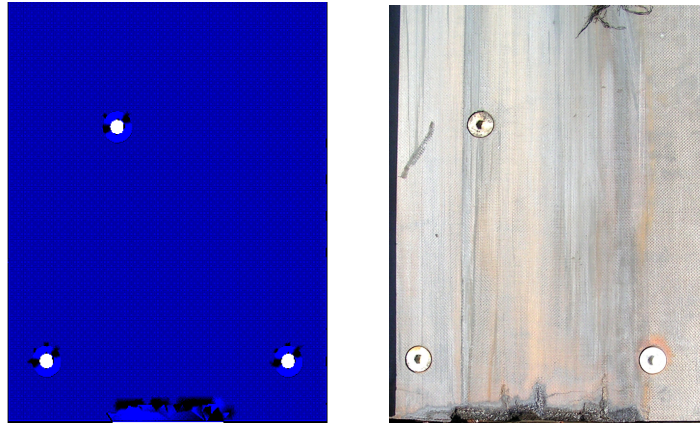


Fig 7.3: Wear Scar developed using FE iterative element death techniques compared with real world example

Using this technique the wear progression on the composite slipway panel can be modelled beyond the current subjective visual replacement criteria as shown below. This data indicates that the initial edge wear will develop over time into more serious progressive wear, a feature also observed during slipway surveys where panels exhibiting different stages of edge wear indicated the same progression. The wear modelling below also shows the development of delamination, predicting that this type of wear will be more pronounced around geometric features such as panel fixing holes, this again confirms observations from real world slipway panel surveys (e.g. fig. 3.61-2).

Another aspect of this simulation of wear progression is that the panel bearing area is progressively reduced as the composite material is abraded with a consequential increase in the apparent contact pressure as the lifeboat mass load is distributed over a reduced area. This will lead to an increase in both the wear rate, which is shown from rotary tribometer testing in section 6.2 to be directly proportional to the applied load, and also in the friction force, which is shown by reciprocating tribometer testing to be proportional to the applied load in section 6.1.

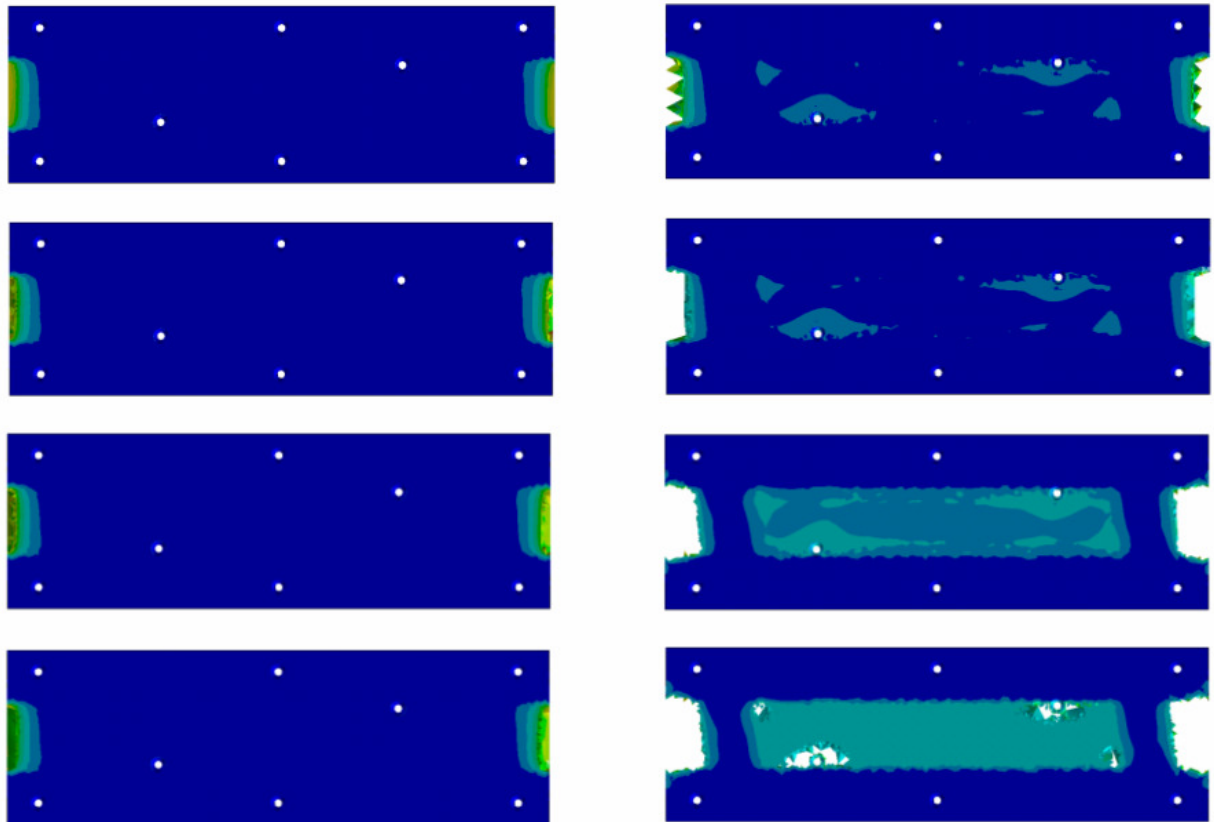


Fig 7.4: simulation of wear progression over time on a slipway panel using FE iterative element death techniques

### Wear and Friction Map Generation

Wear and friction maps are generated from the FE solution data to indicate the likely wear and friction across the surface area of the present panel design. The friction map is generated directly from the FE solution data which incorporates the friction coefficient of 0.252 recorded during dry sliding tribometer trials. Similarly, the wear map incorporates the wear coefficient data from tribometer testing to produce a realistic wear expectation under the various lubrication regimes tested. Presented here is the dry sliding case, see appendix H for full wear and friction maps for each lubrication regime tested.



Fig 7.5: Friction force map from FE simulation of 1 panel under normal keel loading. Friction force is shown in Newtons and is based on a friction coefficient of 0.252 from tribometer dry sliding tests

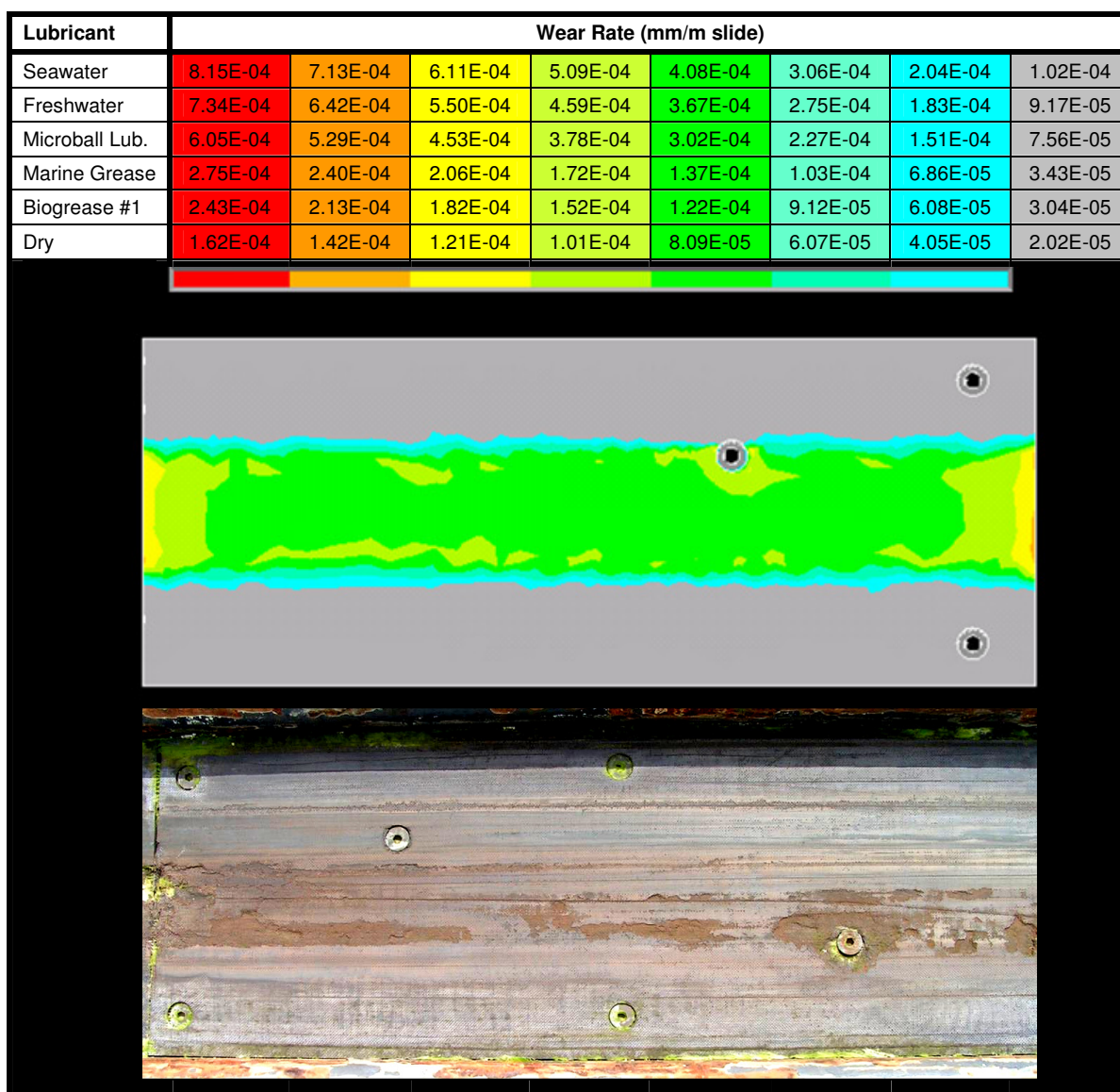


Fig 7.6: Wear Depth/m sliding map from FE simulation of 1 panel under normal keel loading. Wear Depth is shown in mm and based on a wear coefficient of 3.7e-5 derived from rotary tribometer dry sliding tests. A worn panel from Tenby is shown for comparison

Fig. 7.8 again shows a good correlation between the wear predicted by the FEA model and real world wear. This result indicates that the most severe panel wear is concentrated at the panel ends, followed by wear around the panel fixing holes and along the keel contact track, a result also seen on composite panels from slipway surveys.

This wear map represents the aligned contact case and mirrors the slipway survey observations of light panel end wear and delamination wear on slipway panels that were noted to be reasonably well aligned (less than 1mm height difference) with respect to neighbouring panels, full slipway survey data is shown in appendix E.

### 7.1.2. Two Panel Aligned Case

---

The one panel case is expanded to a 2 panel case to examine the stresses at the panel/panel interface. It is found that the 2 panel case closely mirrors the 1 panel case when the panels are modelled as being perfectly lined up with one another, with the wear on each panel similarly mirrored.

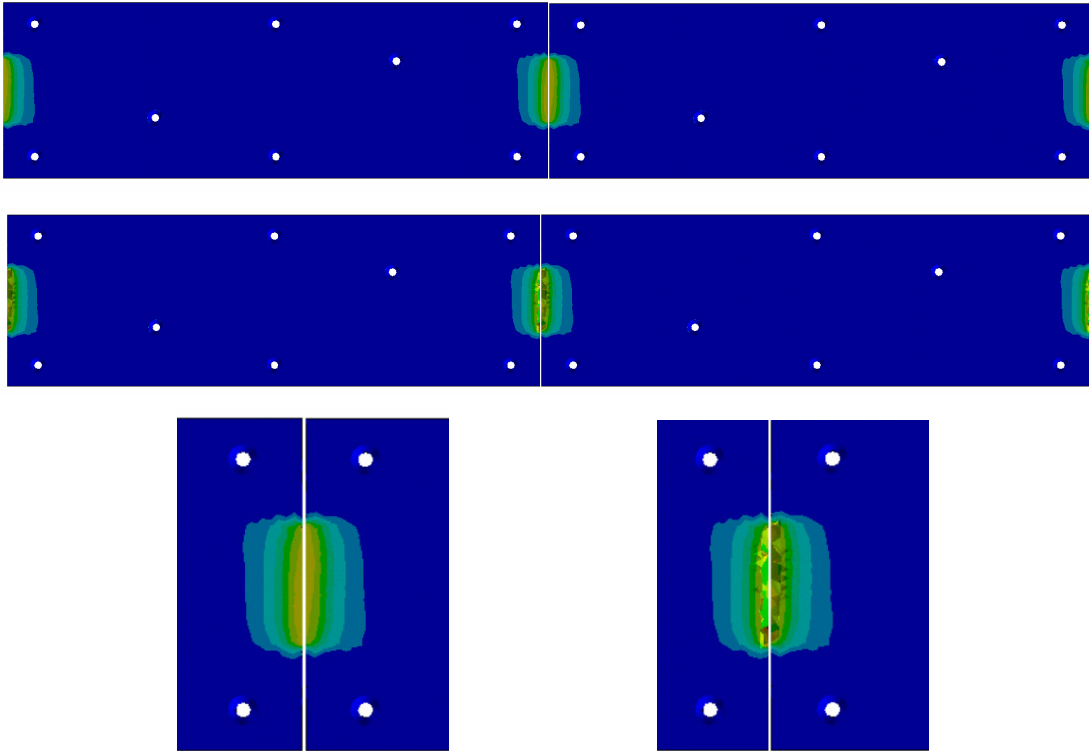


Fig 7.7: Symmetrical FE Wear Scar developing on a perfectly aligned 2 panel model

It is now possible to expand this case to include some of the panel misalignment effects encountered on real world slipways.

### 7.2. Two Panel Misalignment Modelling

---

From slipway site panel surveys it is seen that the height difference between panels can be up to 4mm, this may be an important influence on the wear and friction rates of slipway panels and so a number of simulations are run to model these misalignments between 0 and 5mm in height.

Three misalignment scenarios are modelled, one in which the slipway panels are assumed to have a parallel offset, both remaining in the same plane, and one where an angled offset is used, with the second panel angled in such a way as to give a panel height difference of 0 to 5mm at the panel interface. Site surveys indicate that both of these scenarios are present

between slipway panels with the parallel panel offset scenario predominating, making up a total of 67% of the slipway panel interfaces surveyed. The remaining 33% of panels fit the angled offset scenario. A third scenario in which the second panel is skewed longitudinally with respect to the first is also modelled, survey data indicates that this scenario is present in 22% of cases, roughly equally occurring within both the parallel and the angled offset scenarios.

Small offsets of 0-1mm are modelled for the parallel case to further investigate the effects of panel misalignment, initial screening simulations indicate that results for both parallel and angled misalignment scenarios are similar for these small offset distances.

In order to reduce analysis computation times the panel models are simplified by removing the fixing holes, the stresses around these features have already been modelled in the previous 1 and 2 panel analyses (section 7.1-2) where it is shown that wear at these features, although still significant, is far less than at the panel interfaces and that the related contact stresses which contribute to friction forces are also far lower.

#### **7.2.1. Parallel Panel Misalignment**

The parallel panel misalignment scenario assumes that the two panels are offset while remaining parallel by between 0 to 5mm as shown in the diagram below:

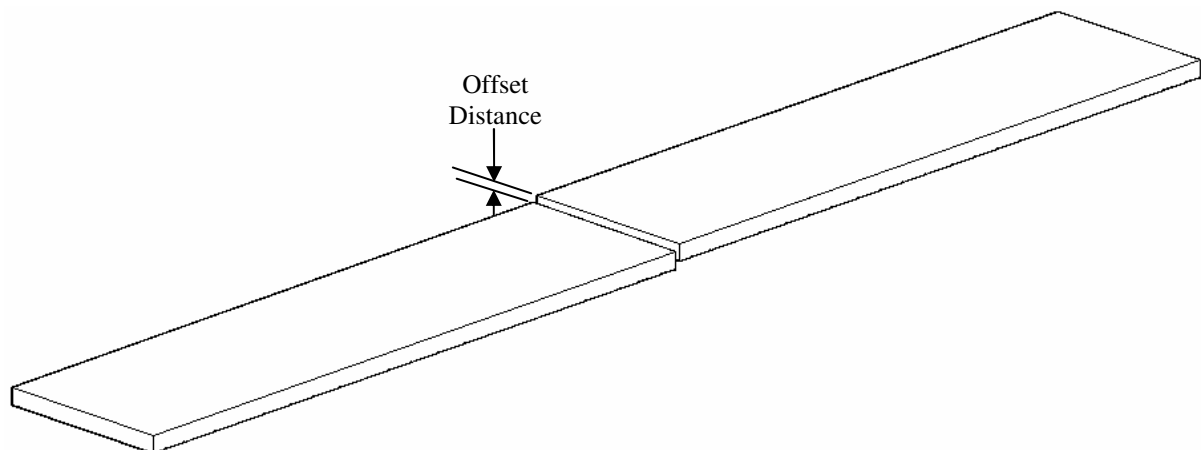


Fig. 7.8: Parallel Panel Misalignment Model

This model accounts for two thirds of the panels surveyed, with the average offset for all panels being 0.816mm and the maximum being 4.055mm. Panel offsets of 0-1mm are also modelled for this scenario to further clarify the panel interface behaviour for these small offset distances.

### 7.2.2 Angled Panel Misalignment

The parallel panel misalignment scenario assumes that the two panels are offset by between 0 and 5mm at the panel interface due to one panel lying at an angle to the slipway bed as shown below:

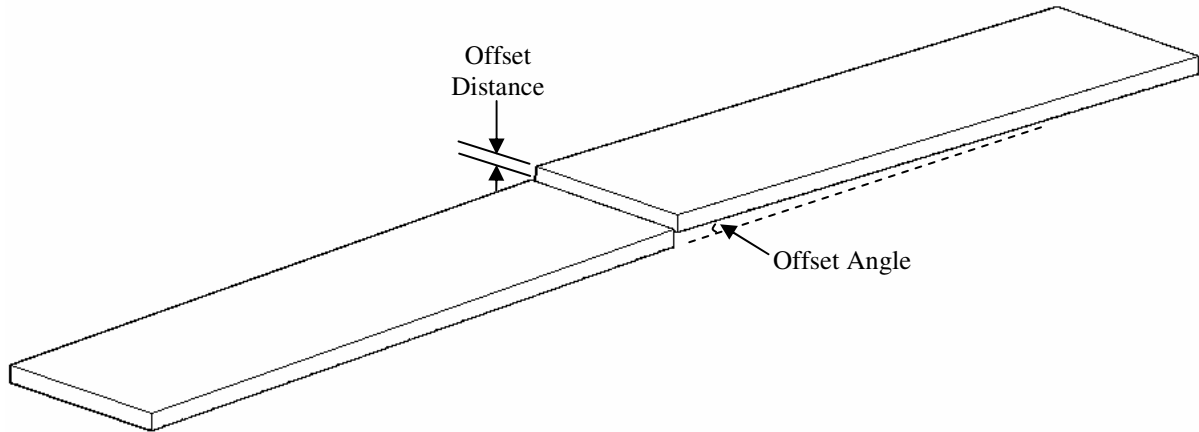


Fig. 7.9: Angled Panel Misalignment Model

Site surveys indicate that this model accounts for around one third of slipway panels surveyed, with the average offset angle for all panels being  $0.0375^\circ$  and the maximum being  $0.184^\circ$ . These correspond to panel interface offset heights of 0.799mm and 3.92mm respectively.

### 7.2.3 Skewed Panel Misalignment

The skewed panel misalignment assumes that the two panels are twisted longitudinally in relation to each other as shown in the diagram below:

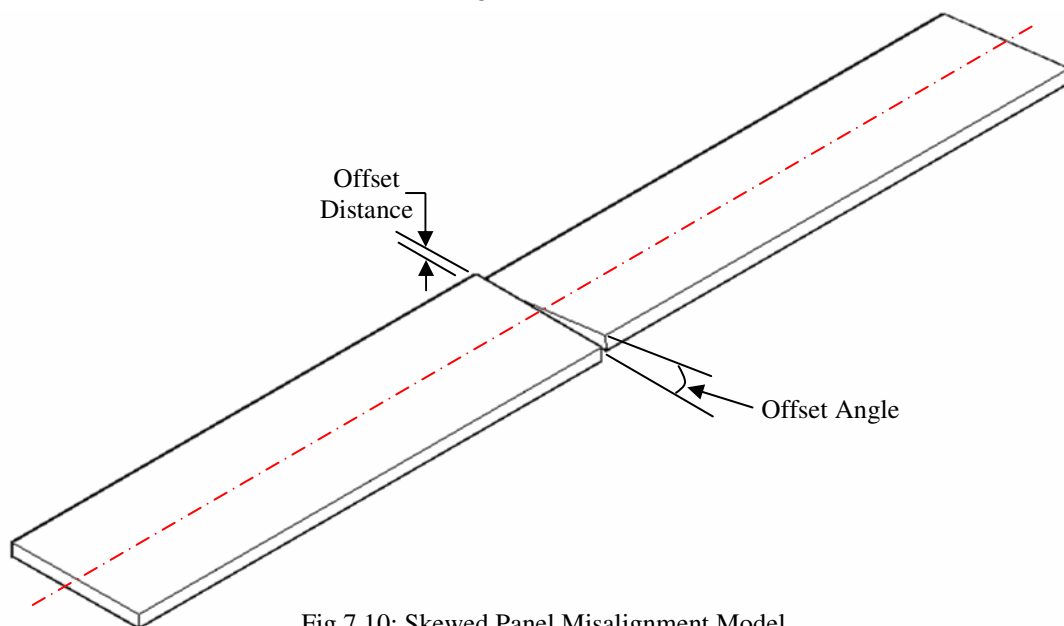


Fig 7.10: Skewed Panel Misalignment Model

Site survey data indicates that this type of misalignment is present in 22% of panels, roughly equally occurring within both the parallel and angled offset scenario. Across all panels the



average skewed offset angle is  $0.107^\circ$ , this corresponds to an offset height of 0.728mm. A maximum offset angle of  $0.6345^\circ$  was also recorded; this corresponds to an offset height of 4.32mm. FE simulations are conducted using an offset height of 0-5mm as indicated by site survey data.

## 7.2.4 Results

Models are generated and simulations are completed for the three offset scenarios using simplified panel models for equivalent panel interface offsets of 0-5mm. The Von Mises maximum shear stress  $S_{\max}$  is recorded as an indicator of the general load on the panels, as is the maximum deflection  $D_{\max}$ .

### Results – Parallel Offset

Offset dist. (mm)	Von Mises Stress: $S_{\max}$ (Pa)	Von Mises Stress vs. aligned case (%)	Max. Deflection: $D_{\max}$ (mm)	Max. Friction Force (N)	Vertical Stresses: $S_{z \max}$ (Pa)	Max. Wear/m Sliding: (mm)
0	2.15E+05	100.00%	1.261E-03	9.590E+03	2.352E+05	1.009E-04
0.1	8.53E+05	396.40%	4.922E-03	1.195E+04	1.080E+06	4.633E-04
0.2	1.18E+06	548.10%	6.749E-03	2.804E+04	1.280E+06	5.490E-04
0.3	1.43E+06	664.22%	8.104E-03	4.536E+04	1.550E+06	6.649E-04
0.4	1.64E+06	761.76%	9.209E-03	6.300E+04	1.770E+06	7.592E-04
0.5	1.81E+06	840.73%	1.015E-02	8.096E+04	1.970E+06	8.450E-04
0.6	1.97E+06	915.04%	1.098E-02	9.887E+04	2.140E+06	9.179E-04
0.7	2.11E+06	980.07%	1.174E-02	1.172E+05	2.300E+06	9.866E-04
0.8	2.24E+06	1040.46%	1.242E-02	1.352E+05	2.450E+06	1.051E-03
0.9	2.36E+06	1096.20%	1.306E-02	1.534E+05	2.580E+06	1.107E-03
1	2.48E+06	1151.93%	1.366E-02	1.717E+05	2.710E+06	1.162E-03
2	3.35E+06	1556.04%	1.803E-02	3.534E+05	3.710E+06	1.591E-03
3	3.98E+06	1848.67%	2.102E-02	5.344E+05	4.430E+06	1.900E-03
4	4.60E+06	2136.65%	2.447E-02	5.984E+05	5.120E+06	2.196E-03
5	5.05E+06	2345.67%	2.655E-02	7.492E+05	5.640E+06	2.419E-03

Table 7.1: Parallel Panel Offset Comparison

### Results – Angled Offset

Offset Angle ( $^\circ$ )	Offset dist. (mm)	Von Mises Stress: $S_{\max}$ (Pa)	Von Mises Stress vs. aligned case (%)	Max. Deflection: $D_{\max}$ (mm)	Max. Friction Force (N)	Vertical Stresses: $S_{z \max}$ (Pa)	Max. Wear/m Sliding: (mm)
0.0000	0	2.15E+05	100.00%	1.261E-03	9.590E+03	2.352E+05	1.009E-04
0.0470	1	2.69E+06	1249.48%	1.499E-02	8.428E+04	2.950E+06	1.265E-03
0.0939	2	3.78E+06	1755.77%	2.079E-02	1.681E+05	4.150E+06	1.780E-03
0.1409	3	4.58E+06	2127.36%	2.495E-02	2.534E+05	5.050E+06	2.166E-03
0.1879	4	5.25E+06	2438.57%	2.838E-02	3.360E+05	5.810E+06	2.492E-03
0.2348	5	5.82E+06	2703.33%	3.134E-02	4.150E+05	6.450E+06	2.767E-03

Table 7.2: Angled Panel Offset Comparison

### Results – Skewed Offset

Offset Angle (°)	Offset dist. (mm)	Von Mises Stress: $S_{max}$ (Pa)	Von Mises Stress vs. aligned case (%)	Max. Deflection: $D_{max}$ (mm)	Max. Friction Force (N)	Vertical Stresses: $S_z$ max (Pa)	Max. Wear/m Sliding: (mm)
0.0000	0	2.15E+05	100.00%	1.786E+02	1.261E-03	9.590E+03	2.352E+05
0.1469	1	2.06E+06	956.85%	3.081E-02	9.992E-03	5.587E+04	1.990E+06
0.2938	2	3.49E+06	1621.07%	3.787E-03	1.488E-02	1.256E+05	2.480E+06
0.4407	3	4.32E+06	2006.60%	8.700E-04	1.802E-01	1.989E+05	3.030E+06
0.5876	4	4.99E+06	2317.80%	2.190E-04	1.153E-01	2.825E+05	4.020E+06
0.7345	5	5.96E+06	2768.36%	9.680E-05	2.358E-02	3.560E+05	4.040E+06

Table 7.3: Angled Panel Offset Comparison

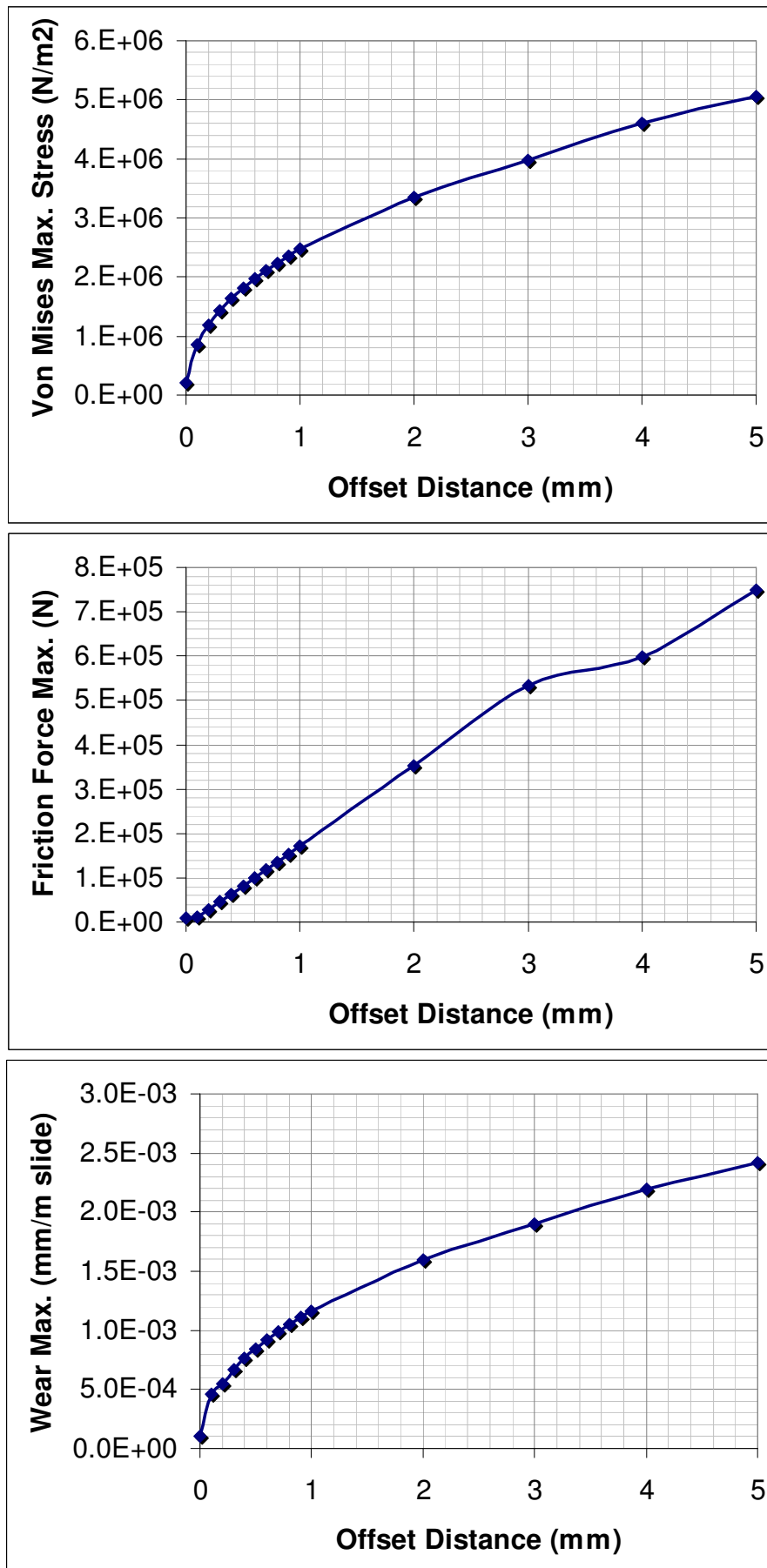


Fig. 7.11: Parallel Panel Offset Comparison

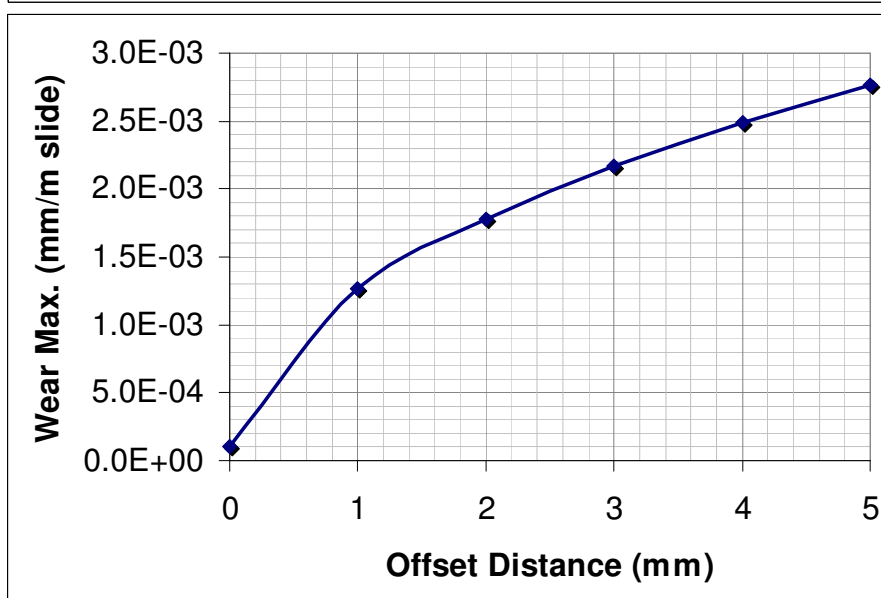
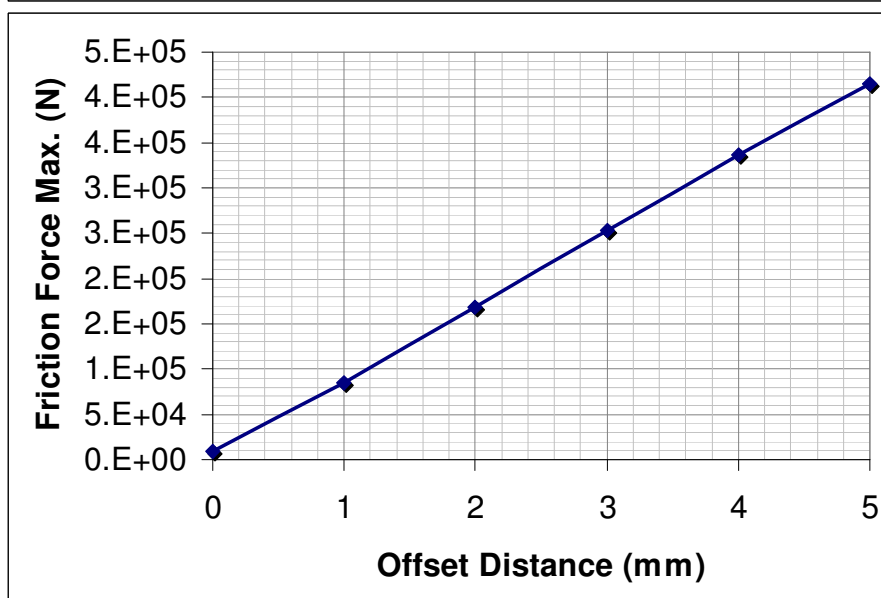
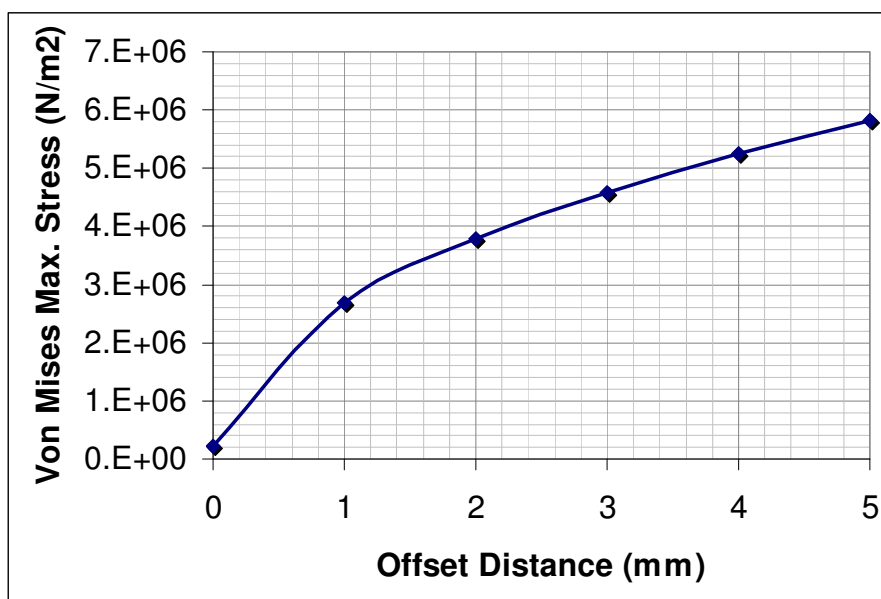


Fig. 7.12: Angled Panel Offset Comparison

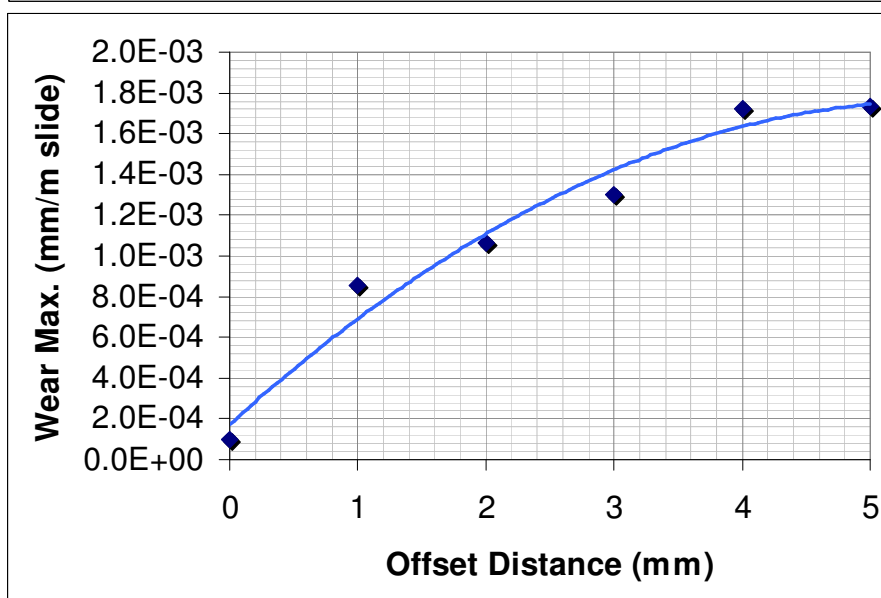
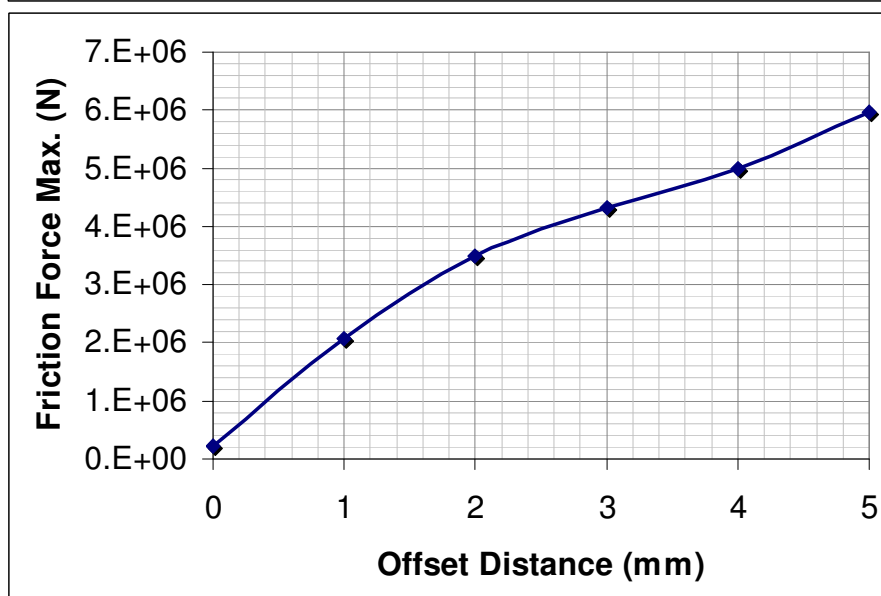
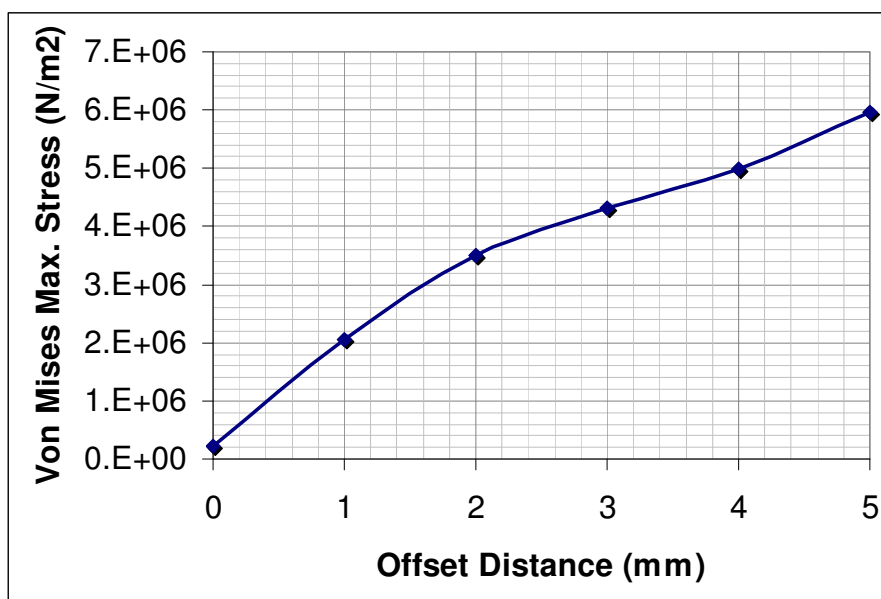


Fig. 7.13: Skewed Panel Offset Comparison

### 7.2.5. Discussion

From the simulations it can be seen that there is a significant increase in the maximum Von Mises stresses, Friction forces and wear rate encountered as the height difference between panels increases. This effect can be very significant, rising to 27 times the original stress and wear rates, and up to 78 times the original friction force for the perfectly aligned case compared with a 5mm angled offset and the 5mm parallel offset scenarios respectively. Maximum offsets of around 4mm have been observed on real world slipways for both parallel and angled scenarios, these would correspond to wear rates of 25 times the perfectly aligned case and friction forces of 62 times for the angled and parallel cases respectively. Even at an offset of 1mm, close to the mean offset observed for all slipway panels the stresses rise to over 11 times, wear rates to 12 times and friction rises to 18 times the perfectly aligned case. These results are extremely significant and could account for a good deal of the high wear and friction experienced during lifeboat recovery in the real world. The data from the skewed scenario also shows a significant effect with stresses at the panel interface reaching almost 28 times the perfectly aligned case.

### Apparent Friction Coefficient Contribution

The contribution of panel misalignments to the apparent friction coefficient are shown in table 7.5 below for all offset scenarios tested.

#### Parallel Offset

Offset dist. (mm)	Friction Force Max.	Friction Coefficient Contribution
0	9.590E+03	0.028
0.1	1.195E+04	0.035
0.2	2.804E+04	0.082
0.3	4.536E+04	0.133
0.4	6.300E+04	0.184
0.5	8.096E+04	0.237
0.6	9.887E+04	0.290
0.7	1.172E+05	0.343
0.8	1.352E+05	0.396
0.9	1.534E+05	0.449
1	1.717E+05	0.503
2	3.534E+05	1.035
3	5.344E+05	1.565
4	5.984E+05	1.752
5	7.492E+05	2.194

#### Angled Offset

Offset dist. (mm)	Friction Force Max.	Friction Coefficient Contribution
0	9.590E+03	0.028
1	8.428E+04	0.247
2	1.681E+05	0.492
3	2.534E+05	0.742
4	3.360E+05	0.984
5	4.150E+05	1.215

#### Skewed Offset

Offset dist. (mm)	Friction Force Max.	Friction Coefficient Contribution
0	9.590E+03	0.028
1	5.587E+04	0.164
2	1.256E+05	0.368
3	1.989E+05	0.582
4	2.825E+05	0.827
5	3.560E+05	1.042

Table 7.4: Apparent friction coefficient contributions for modelled offset scenarios

These friction coefficients represent the apparent friction that would be indicated by winch loads calculated under the assumption of the lifeboat mass being evenly supported by the



slipway panels. These do not represent an increase in the *actual* friction coefficient of the contact, but rather a consequence of the misrepresentation of the contact case as an evenly distributed load.

The results in table 7.5 indicate that panel misalignment is likely to have a significant adverse effect on local friction coefficients; with apparent friction exceeding unity at a panel offset distance of 2mm for the parallel alignment case and of 5mm for the skewed and angled misalignment scenarios. This may explain the stick-slip behaviour noted to occur during winch trials at Tenby and Padstow. These simulations thus confirm the hypothesis that panel misalignment on real world slipways could be a major factor in understanding the discrepancies between real and theoretical friction and wear rates on lifeboat slipways. Survey data also confirms that such panel misalignments are present to the extent that they may contribute significantly to the wear and friction observed along the whole slipway. Panel misalignments are common to all slipways surveyed and are likely a result of the fitting techniques involved, however, for large outdoor structures such as slipways it may well be impractical to reduce alignment tolerances to wholly eliminate misalignment effects.

With these results in mind it is proposed to investigate the slipway panel geometry for possible modifications to reduce the effects of panel misalignment. Focussing on the raised panel edge where most stress, wear and friction are concentrated under normal loading it is proposed that a chamfered edge would reduce the geometrical stress concentrations. In order to test this hypothesis a chamfered panel is modelled and simulated under load for the offset scenarios shown above using similar FE techniques.

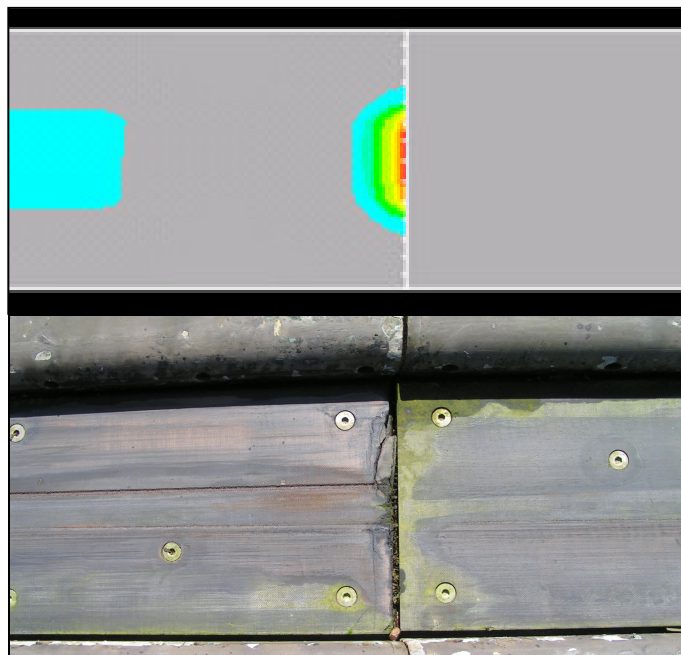


Fig. 7.14: Wear map for 4mm parallel offset and equivalent wear scar on real world slipway section

## 8 FEA MODELLING – MODIFIED SLIPWAY PANEL

---

### 8.1 Modified Slipway Panel Design

---

The maximum stress, wear rate and friction forces are all observed to occur along the interface edge of the raised panel, it is proposed that a design modification to this edge will allow for a more evenly distributed load and thus lower friction and wear forces. A chamfer is designed with a depth of 5mm to allow for a corresponding panel offset of up to 5mm, chamfer length is set to 50mm in order to present a shallow 1:10 chamfer gradient to the lifeboat keel on recovery to reduce sticking between panel chamfers.

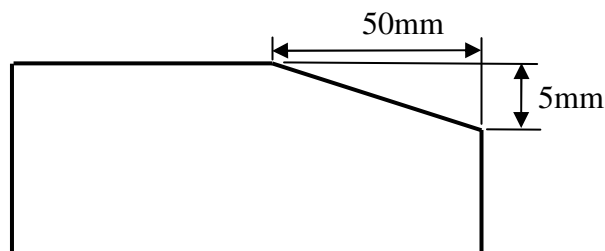


Fig. 8.1: Slipway Chamfer profile

The effects of this chamfer on reducing the friction and wear on misaligned slipway panels is investigated for the parallel and angled offset scenarios in a similar fashion to the analysis in section 6.2. Offsets of 0-5mm are modelled and the results presented below.

### FEA Modelling of Modified Slipway Panel Geometry – Parallel Offset

Offset dist. (mm)	Von Mises Stress: $S_{\max}$ (Pa)	Von Mises Stress vs. original panel (%)	Max. Deflection: $D_{\max}$ (mm)	Max. Friction Force (N)	Vertical Stresses: $S_{z \max}$ (Pa)	Max. Wear/m Sliding: (mm)
0	2.16E+05	100.39%	1.076E-03	1.833E+04	3.251E+05	1.395E-04
1	1.29E+06	52.02%	4.784E-03	3.736E+04	1.670E+06	7.163E-04
2	1.78E+06	53.13%	6.672E-03	7.158E+04	2.290E+06	9.823E-04
3	2.14E+06	53.77%	8.155E-03	1.068E+05	2.730E+06	1.171E-03
4	2.43E+06	52.83%	9.427E-03	1.424E+05	3.070E+06	1.317E-03
5	2.67E+06	52.87%	1.056E-02	1.771E+05	3.350E+06	1.437E-03

Table 8.1: Parallel Panel Offset Comparison: Chamfered Panel

### FEA Modelling of Modified Slipway Panel Geometry – Angled Offset

Offset Angle (°)	Offset dist. (mm)	Von Mises Stress: $S_{\max}$ (Pa)	Von Mises Stress vs. original panel (%)	Max. Deflection: $D_{\max}$ (mm)	Max. Friction Force (N)	Vertical Stresses: $S_{z \max}$ (Pa)	Max. Wear/m Sliding: (mm)
0.0000	0	2.16E+05	100.39%	1.076E-03	1.833E+04	3.251E+05	1.395E-04
0.0470	1	1.14E+06	42.38%	4.962E-03	7.740E+04	1.520E+06	6.520E-04
0.0939	2	1.62E+06	42.86%	6.982E-03	1.586E+05	2.130E+06	9.136E-04
0.1409	3	1.97E+06	43.01%	8.192E-03	1.776E+05	2.590E+06	1.111E-03
0.1879	4	2.27E+06	43.24%	9.149E-03	2.262E+05	2.950E+06	1.265E-03
0.2348	5	2.55E+06	43.81%	1.063E-02	3.836E+05	3.250E+06	1.394E-03

Table 8.2: Angled Panel Offset Comparison: Chamfered Panel

### 8.1.3. FEA Modelling of Modified Slipway Panel Geometry – Skewed Offset

Offset Angle (°)	Offset dist. (mm)	Von Mises Stress: $S_{\max}$ (Pa)	Von Mises Stress vs. original panel (%)	Max. Deflection: $D_{\max}$ (mm)	Max. Friction Force (N)	Vertical Stresses: $S_{z \max}$ (Pa)	Max. Wear/m Sliding: (mm)
0.0000	0	2.15E+05	100.39%	1.076E-03	1.833E+04	3.251E+05	1.395E-04
0.1469	1	8.15E+05	39.58%	3.461E-03	3.645E+04	1.030E+06	4.418E-04
0.2938	2	1.23E+06	35.24%	5.272E-03	9.033E+04	1.460E+06	6.263E-04
0.4407	3	1.40E+06	32.41%	5.556E-03	1.314E+05	2.420E+06	1.038E-03
0.5876	4	1.80E+06	36.07%	8.519E-03	2.070E+05	2.150E+06	9.222E-04
0.7345	5	1.69E+06	28.36%	8.095E-03	2.752E+05	2.460E+06	1.055E-03

Table 8.3: Skewed Panel Offset Comparison: Chamfered Panel

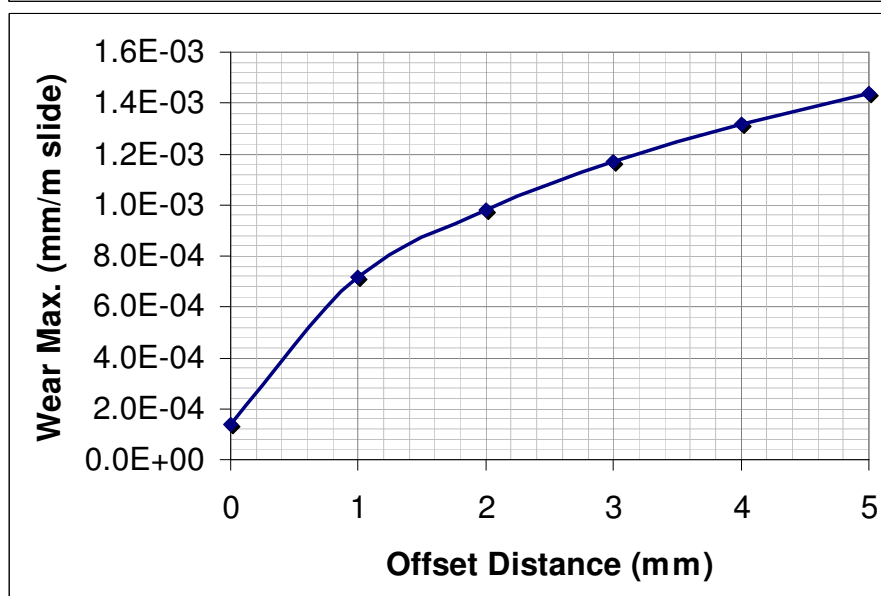
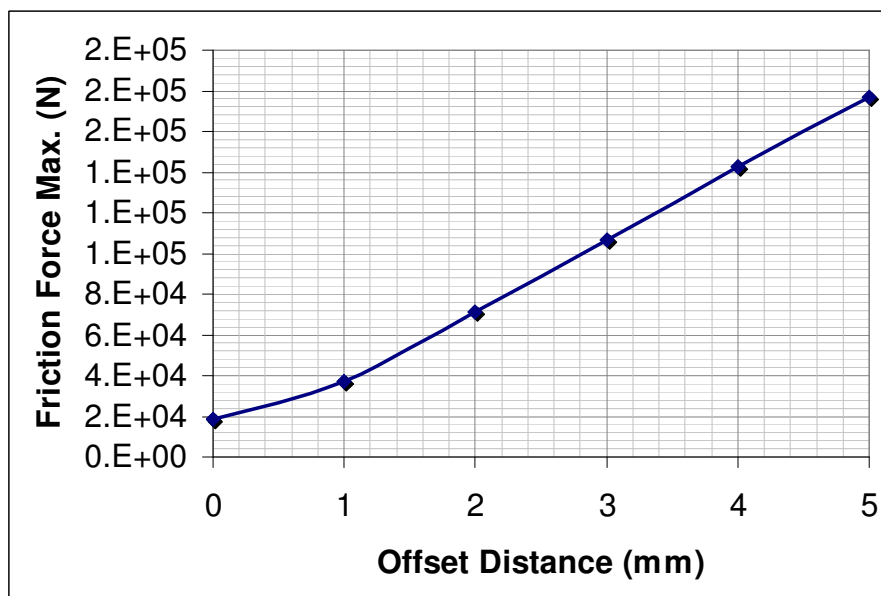
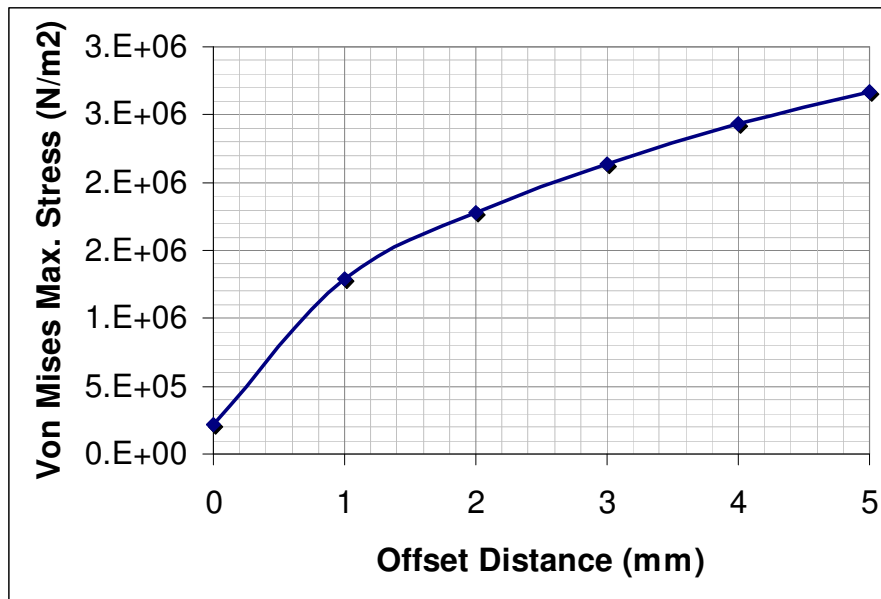


Fig. 8.2: Parallel Panel Offset Comparison: Chamfered Panel

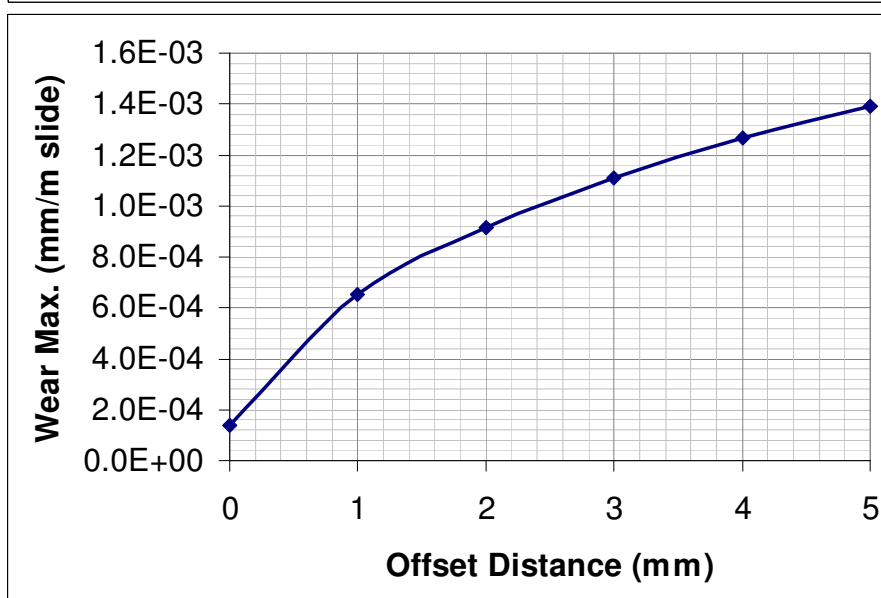
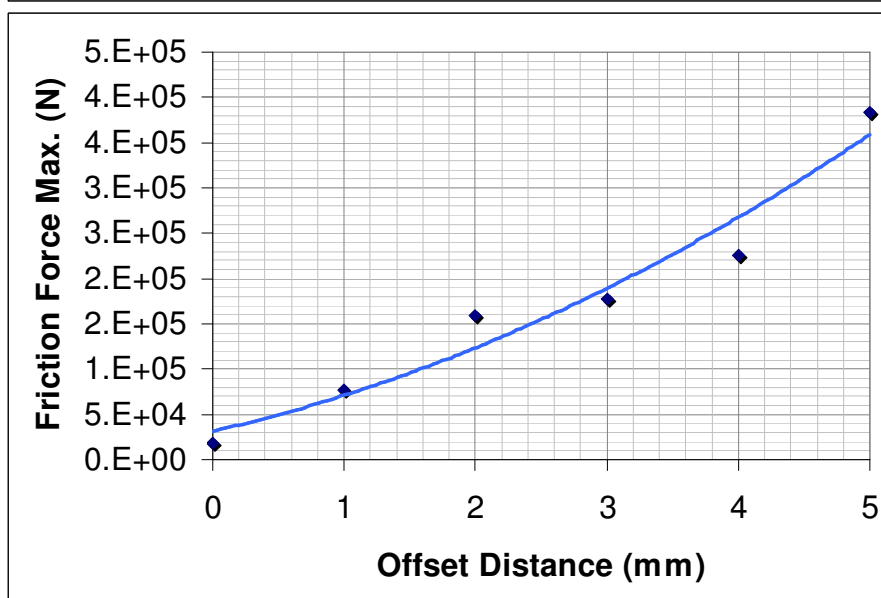
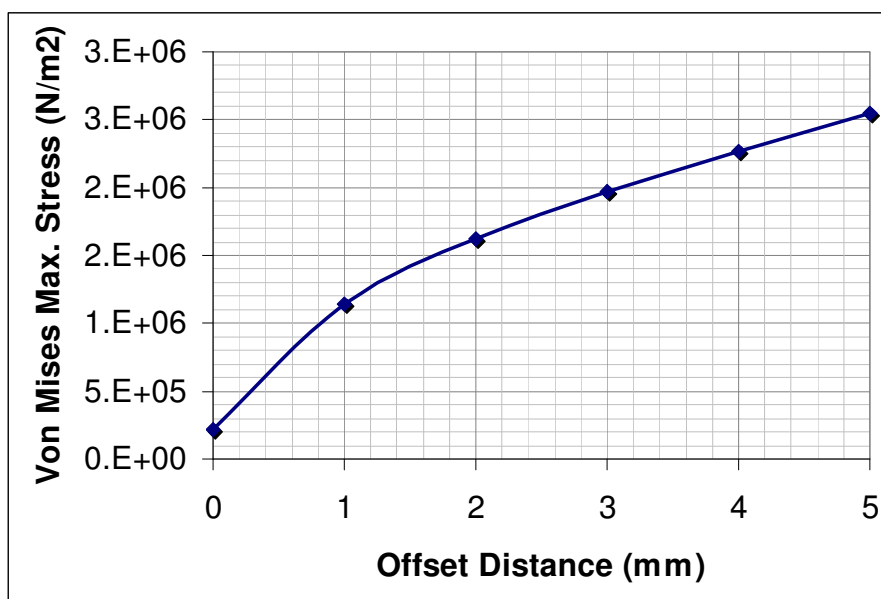


Fig. 8.3: Angled Panel Offset Comparison: Chamfered Panel

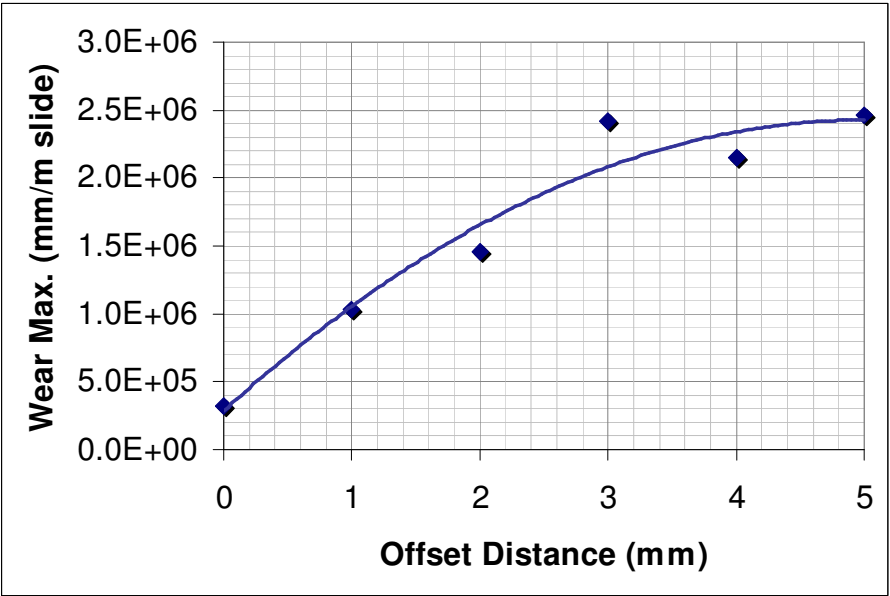
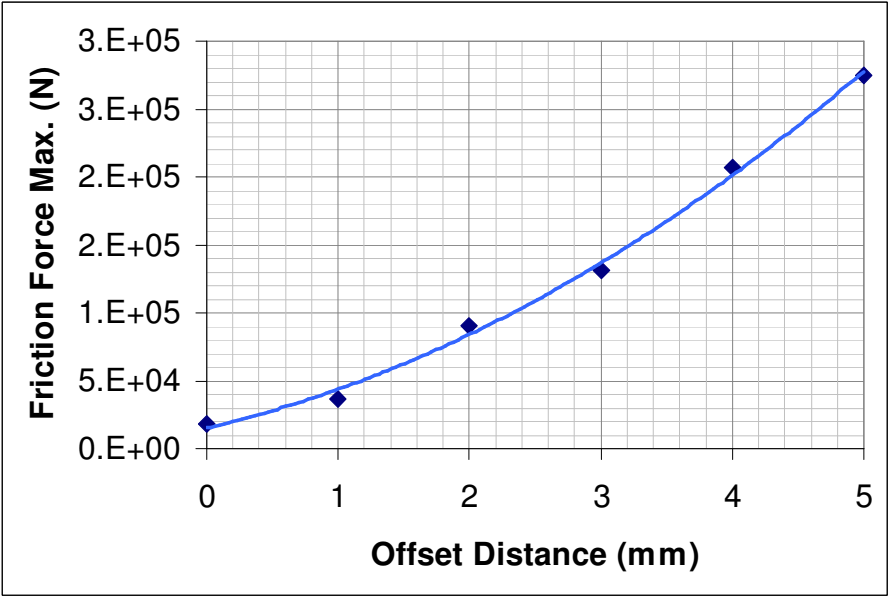
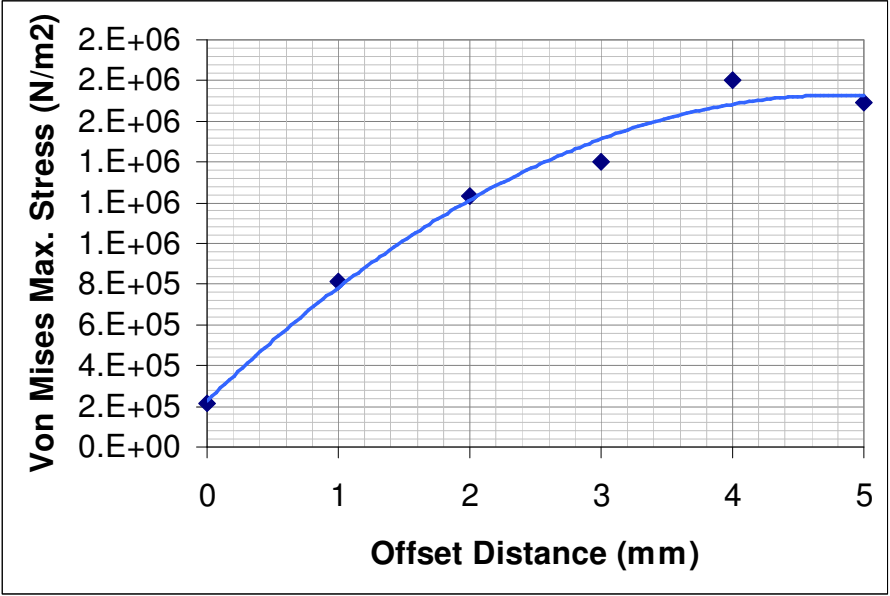


Fig. 8.4: Skewed Panel Offset Comparison: Chamfered Panel



### 8.1.1. Comparison of Original vs. Modified Slipway Panel Geometry

The modified slipway panel geometry shows significant reductions in peak stress, wear rates and friction forces when compared with the original panel. In an ideal perfectly aligned case the chamfered exhibits slightly higher values for wear rates and friction forces due to the reduced contact area, however as a panel offset is introduced, the friction force and wear rates are considerably less than in the original panel geometry as shown in the graphs below:

#### Stress Effects

The Maximum Von Mises stresses recorded in the chamfered panel are roughly 50% of the stresses in the original panel under both the angled and parallel offset scenarios. This appears to indicate that the panel interface edge chamfer modification is effective at reducing the overall load borne by the slipway panel at this point.

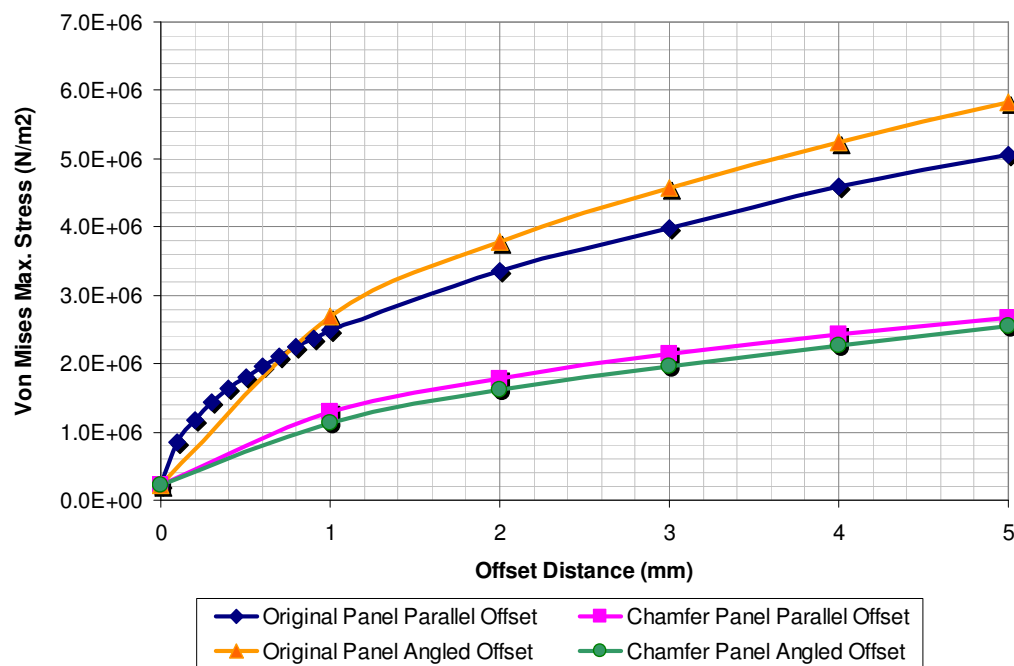


Fig. 8.5: Von Mises Max. Stress results for original and chamfered panel geometry vs. offset distance for parallel and angled misalignment scenarios

The skewed scenario also shows a significant reduction in the Von Mises stress using the chamfered panel, though the gains are less than the angled or parallel offset case, typically between 30-40% of the stresses in the original panel, results are presented below:

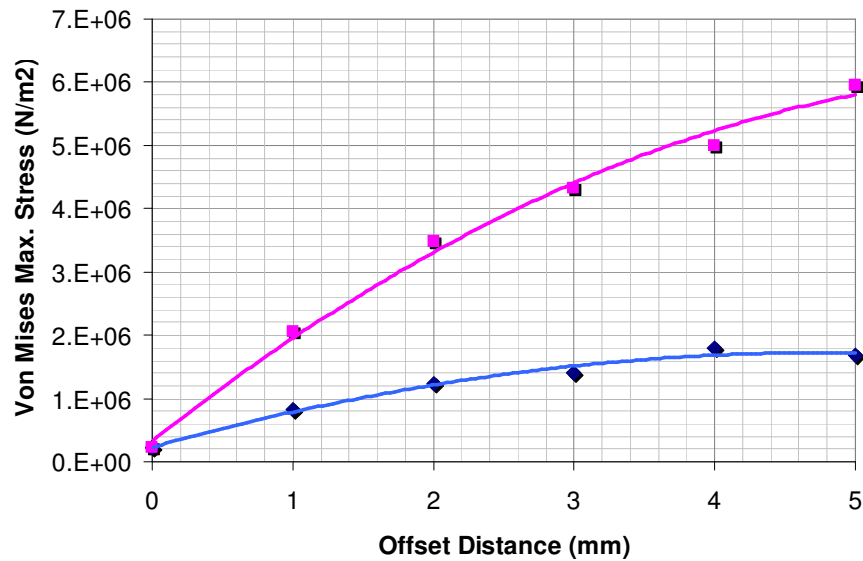


Fig. 8.6: Von Mises Max. Stress results for original and chamfered panel geometry vs. offset distance for skewed misalignment scenario

### Friction Force Effects

The modified panel exhibits far lower friction forces than the original panel under the parallel offset scenario, at around 20% of the original as the offset is brought in. The angled case is slightly less clear with friction force savings of between 10-30% compared with the original. It is worth noting that from survey data the parallel offset scenario accounts for 2/3 of all slipway panels, so the greater savings with this scenario should predominate.

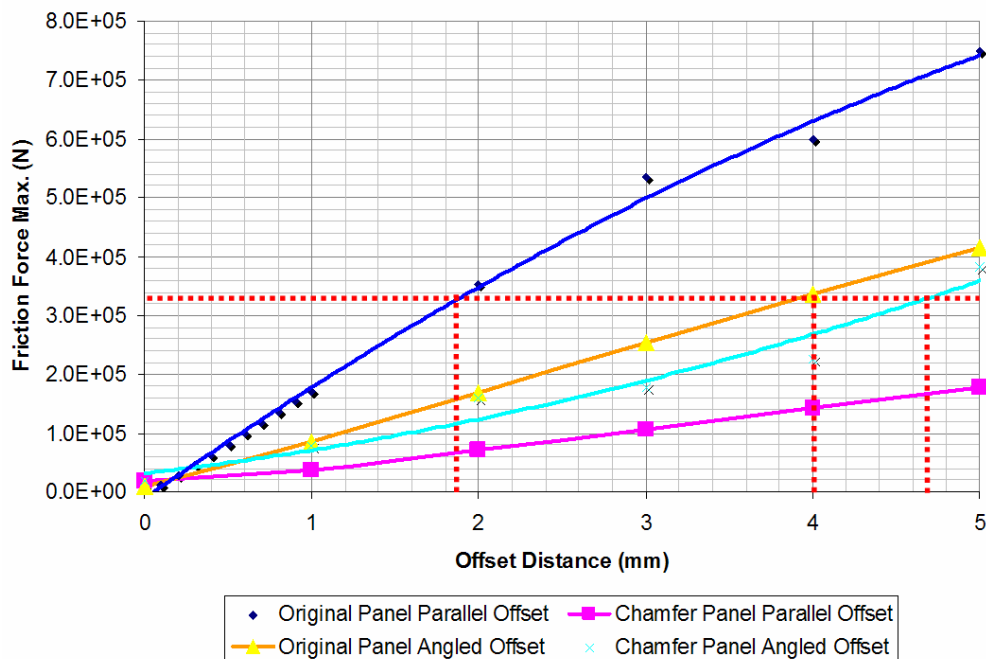


Fig. 8.7: Max. Friction force results for original and chamfered panel geometry vs. offset distance for parallel and angled misalignment scenarios

### Skewed Panel Misalignment Scenario Effects on Friction force

The skewed scenario again shows slight reductions in the friction forces using the chamfer panel compared to the original panel, results are presented below:

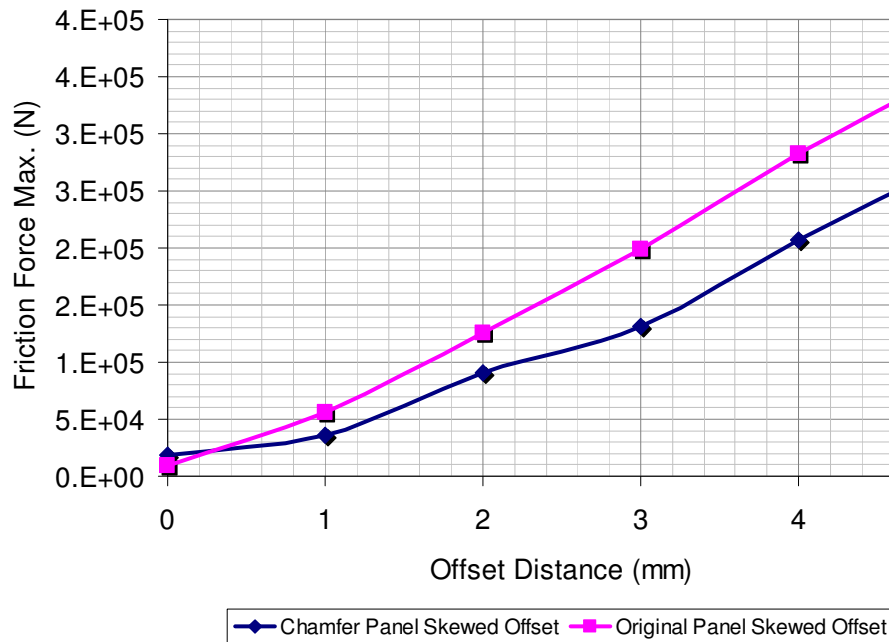


Fig. 8.8: Max. Friction force results for original and chamfered panel geometry vs. offset distance for skewed misalignment scenario

### Friction force effects on apparent friction coefficient

The friction forces presented by a 1mm parallel offset would manifest as an apparent friction coefficient of 0.5 on the slipway if the perfect alignment scenario has been assumed. This is not due to an increase in the actual friction coefficient, but rather a misrepresentation of the contact case, contact pressures at areas of panel misalignment greatly exceed the evenly distributed load case. The graph shows that under panel misalignment condition the friction force can exceed the reaction force on the slipway of  $3.35 \times 10^7 \text{ N}$  calculated using the simple free body diagram model, at this point the apparent coefficient of friction would approach unity. According the FE data this point would occur at a parallel offset of 1.87mm and an angled offset of 3.95mm with the original panel geometry, the modified panel geometry would reach this value at an offset height of 4.68mm under the angled offset scenario, and would not reach this value at all for parallel offsets up to 5mm. This obviously allows for far greater tolerances in panel misalignments, indeed, no panel in the surveyed slipways had sufficient misalignment to generate an apparent friction coefficient of unity if the chamfer panels had been fitted.

## Apparent Friction Coefficient Comparison

Table 8.4 shows the apparent friction coefficients for the original and modified chamfer panels for the alignment scenarios tested, these show a reduction in apparent friction using the chamfer panel for all misalignments.

Parallel Misalignment			Angled Misalignment			Skewed Misalignment		
Offset dist. (mm)	Friction Coefficient Contribution		Offset dist. (mm)	Friction Coefficient Contribution		Offset dist. (mm)	Friction Coefficient Contribution	
	Original	Chamfer		Original	Chamfer		Original	Chamfer
0	0.028	0.054	0	0.028	0.054	0	0.028	0.054
1	0.503	0.109	1	0.247	0.227	1	0.164	0.107
2	1.035	0.210	2	0.492	0.464	2	0.368	0.265
3	1.565	0.313	3	0.742	0.520	3	0.582	0.385
4	1.752	0.417	4	0.984	0.662	4	0.827	0.606
5	2.194	0.519	5	1.215	1.123	5	1.042	0.806

Table 8.4: Original and chamfer panel equivalent apparent friction coefficient comparison

## Wear Rate

The FE data indicates that the maximum wear rates are far lower with the modified panel geometry at around 60% of those found in the parallel offset case and 50% of those in the angled offset case. Selected wear maps for the original and chamfered panel geometry are presented for comparison below.

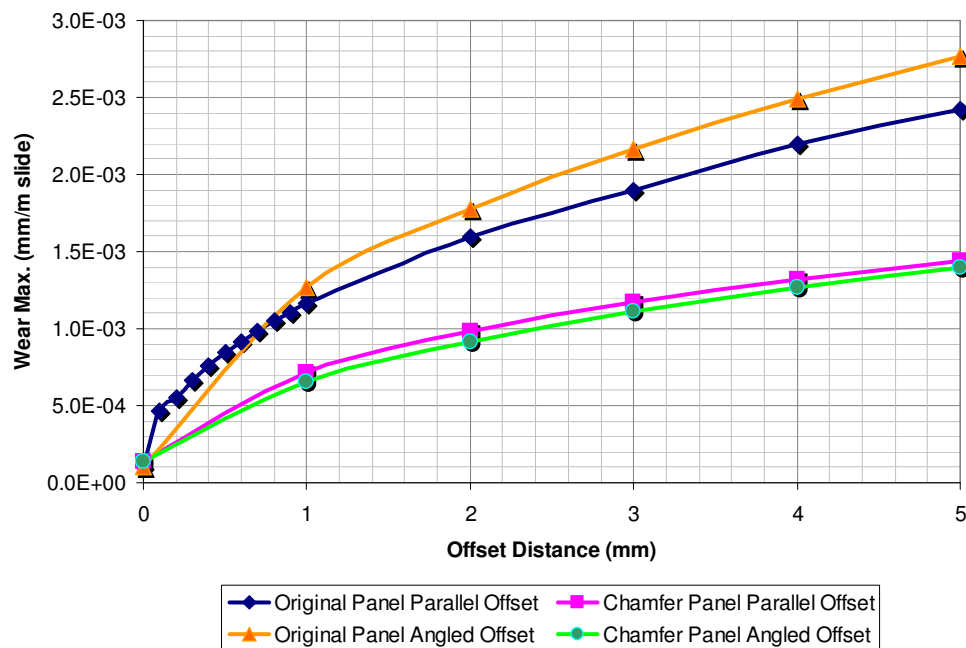


Fig. 8.9: Max. Wear Rate results for original and chamfered panel geometry vs. offset distance for parallel and angled misalignment scenarios

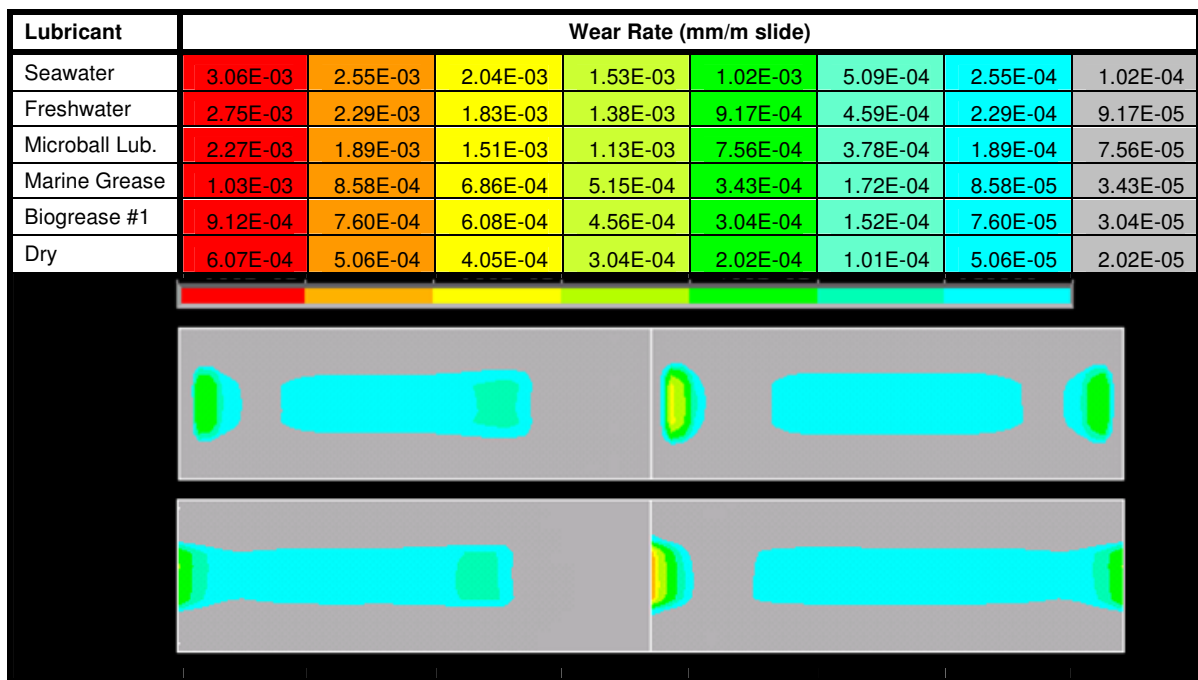


Fig. 8.10: Wear map for 1mm parallel offset – Chamfer panel (top), Original panel (bottom)

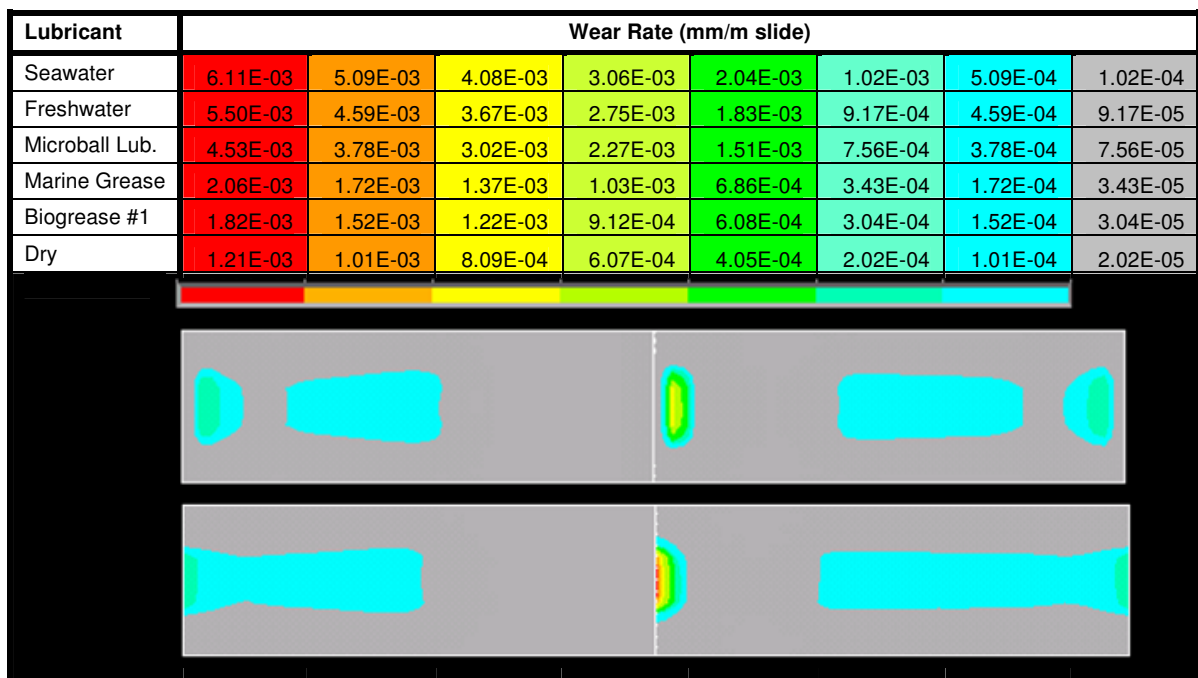


Fig. 8.11: Wear map for 5mm parallel offset – Chamfer panel (top), Original panel (bottom)

### Skewed Panel Misalignment Scenario Effects on Wear Rates

The skewed scenario also shows a reduction in the wear rate with wear rates between 50-80% of the original panel in the same offset scenario. These results are shown in fig. 8.12.

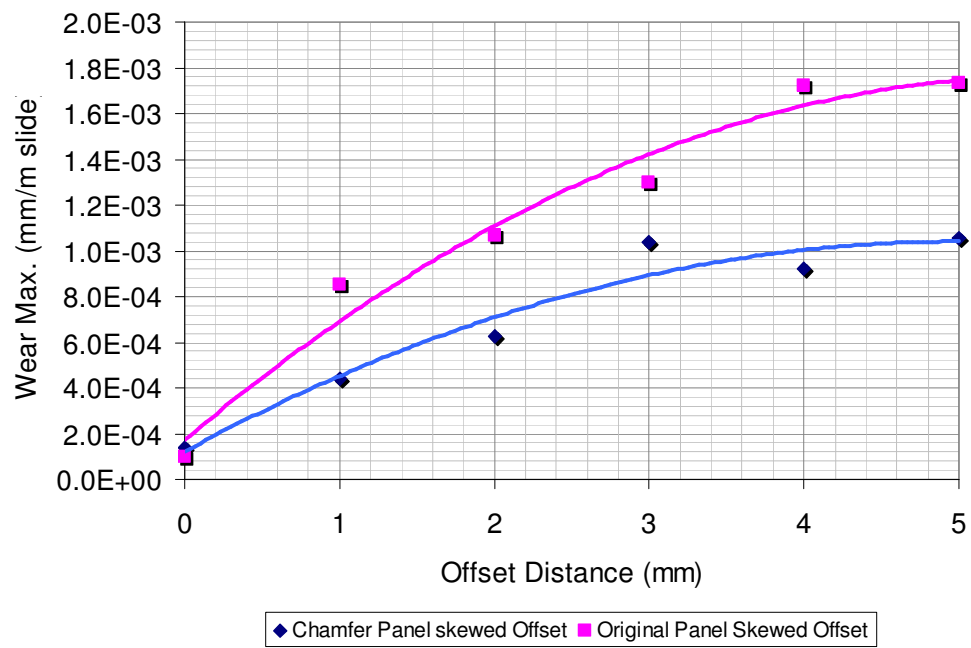


Fig. 8.12: Max. Wear Rate results for original and chamfered panel geometry vs. offset distance for skewed misalignment scenario



## 8.2. Optimisation of Modified Slipway Panel Geometry

Following the improved results for a slipway panel with a 50x5mm chamfer a series of simulations are run to investigate the optimum chamfer geometry in order to further reduce wear rates and friction along the slipway. From survey data of composite slipway panels at the new boathouses of Tenby and Padstow it is found that the average panel offset is 0.88mm for Tenby and 0.73mm for Padstow, with the parallel offset scenario accounting for the majority (67%) of cases. Based on this data a standard slipway panel scenario of a 1mm parallel offset is used for the chamfer optimisation tests.

Tests for optimising the chamfer geometry are conducted in 3 stages investigating the depth, length and size of the panel chamfer. The most successful chamfers from this stage of the analysis are then investigated for their possible impact on the kinematics of recovering a lifeboat to the slipway and the winch loading involved. Larger or higher angled chamfers may have an adverse effect here as they may allow the lifeboat keel to catch between panels with a subsequently increased initial load on the winch. The effects of the chamfer on encouraging the desired 'keel stick' as the lifeboat mounts the slipway are also evaluated, as are the possible effects of the reduction in panel contact area associated with large chamfer lengths.

### 8.2.1. Chamfer Geometry:

The slipway chamfer is defined as follows:

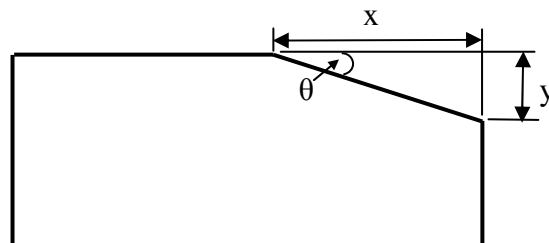


Fig. 8.13: Slipway Chamfer parameters

Simulations are conducted in 3 stages, first the depth of the chamfer,  $y$ , is varied between 0-20mm the upper limit defined by the thickness of the Composite panel. Secondly the length of the chamfer,  $x$ , is varied between 0-100mm. Thirdly, the effects of the chamfer scale are investigated by varying the size of a uniform  $x=y$  ( $45^\circ$ ) chamfer between 0-20mm the upper limit again defined by the thickness of the Composite panel. The Von Mises maximum shear stress  $S_{\max}$  is recorded as an indicator of the general load on the panels, as is the maximum deflection  $D_{\max}$ . Friction forces are again recorded, based on the friction coefficient of 0.251 obtained from tribometer dry sliding tests. Wear rates are similarly developed using the dry sliding wear coefficient derived from tribometer tests.

### Height Variations (y)

Y	X	Chamfer Angle (°)	Von Mises Stress: $S_{max}$ (Pa)	Von Mises Stress vs. original panel (%)	Max. Deflection: $D_{max}$ (mm)	Vertical Stresses: $S_z$ max (Pa)	Max. Wear/m Sliding: (mm)	Max. Friction Force (N)
0	50	0.0000	2.48E+06	100.00%	2.710E+06	1.162E-03	6.775E+05	2.48E+06
1	50	1.1458	8.10E+05	32.66%	1.280E+06	5.490E-04	3.200E+05	8.10E+05
2	50	2.2906	1.05E+06	42.34%	1.390E+06	5.962E-04	3.475E+05	1.05E+06
3	50	3.4336	1.22E+06	49.19%	1.620E+06	6.949E-04	4.050E+05	1.22E+06
4	50	4.5739	8.87E+05	35.76%	1.290E+06	5.533E-04	3.225E+05	8.87E+05
4.5	50	5.1428	8.71E+05	35.14%	1.300E+06	5.576E-04	3.250E+05	8.71E+05
5	50	5.7106	1.29E+06	52.02%	1.670E+06	7.163E-04	4.175E+05	1.29E+06
10	50	11.3099	1.19E+06	47.98%	1.580E+06	6.777E-04	3.950E+05	1.19E+06
15	50	16.6992	1.09E+06	43.95%	1.500E+06	6.434E-04	3.750E+05	1.09E+06

Table 8.5: Chamfer height variations (y)

### Length Variations (x)

Y	X	Chamfer Angle (°)	Von Mises Stress: $S_{max}$ (Pa)	Von Mises Stress vs. original panel (%)	Max. Deflection: $D_{max}$ (mm)	Vertical Stresses: $S_z$ max (Pa)	Max. Wear/m Sliding: (mm)	Max. Friction Force (N)
5	0	90.0000	2.48E+06	100.00%	2.71E+06	1.162E-03	6.775E+05	2.48E+06
5	1	78.6901	2.64E+06	106.45%	2.94E+06	1.261E-03	7.350E+05	2.64E+06
5	2	68.1986	2.44E+06	98.39%	2.78E+06	1.192E-03	6.950E+05	2.44E+06
5	3	59.0362	2.48E+06	100.00%	2.82E+06	1.210E-03	7.050E+05	2.48E+06
5	4	51.3402	2.08E+06	83.87%	2.86E+06	1.227E-03	7.150E+05	2.08E+06
5	5	45.0000	2.17E+06	87.50%	2.17E+06	9.308E-04	5.425E+05	2.17E+06
5	10	26.5651	1.25E+06	50.40%	1.73E+06	7.421E-04	4.325E+05	1.25E+06
5	15	18.4349	1.40E+06	56.45%	1.74E+06	7.464E-04	4.350E+05	1.40E+06
5	20	14.0362	1.47E+06	59.27%	1.84E+06	7.892E-04	4.600E+05	1.47E+06
5	25	11.3099	1.44E+06	58.06%	1.82E+06	7.807E-04	4.550E+05	1.44E+06
5	30	9.4623	9.58E+05	38.63%	1.50E+06	6.434E-04	3.750E+05	9.58E+05
5	40	7.1250	1.19E+06	47.98%	1.41E+06	6.048E-04	3.525E+05	1.19E+06
5	50	5.7106	1.29E+06	52.02%	1.67E+06	7.163E-04	4.175E+05	1.29E+06
5	60	4.7636	8.10E+05	32.66%	1.08E+06	4.633E-04	2.700E+05	8.10E+05
5	70	4.0856	8.87E+05	35.76%	1.30E+06	5.576E-04	3.250E+05	8.87E+05
5	80	3.5763	8.12E+05	32.73%	1.13E+06	4.847E-04	2.825E+05	8.12E+05

Table 8.6: Chamfer length variations (x)

### Scale Variations (x,y)

Y	X	Chamfer Angle (°)	Von Mises Stress: $S_{max}$ (Pa)	Von Mises Stress vs. original panel (%)	Max. Deflection: $D_{max}$ (mm)	Vertical Stresses: $S_z$ max (Pa)	Max. Wear/m Sliding: (mm)	Max. Friction Force (N)
0	0	0.0000	2.48E+06	100.00%	2.71E+06	1.162E-03	6.775E+05	2.48E+06
1	1	45.0000	3.05E+06	122.98%	3.23E+06	1.385E-03	8.075E+05	3.05E+06
2	2	45.0000	2.60E+06	104.84%	2.71E+06	1.162E-03	6.775E+05	2.60E+06
3	3	45.0000	3.13E+06	126.21%	3.37E+06	1.446E-03	8.425E+05	3.13E+06
4	4	45.0000	2.41E+06	97.18%	2.29E+06	9.823E-04	5.725E+05	2.41E+06
5	5	45.0000	2.17E+06	87.50%	2.17E+06	9.308E-04	5.425E+05	2.17E+06
10	10	45.0000	1.73E+06	69.76%	1.92E+06	8.236E-04	4.800E+05	1.73E+06
15	15	45.0000	1.71E+06	68.95%	1.96E+06	8.407E-04	4.900E+05	1.71E+06
20	20	45.0000	1.52E+06	61.29%	2.04E+06	8.750E-04	5.100E+05	1.52E+06

Table 8.7: Chamfer scale variations (x and y)

### 8.2.2. Results:

Results from the FE simulations regarding Von Mises maximum stress, friction forces and wear rates are presented below:

#### 8.2.2.1. Von Mises Max. Stress (Smx.)

This can be seen as an indicator of the general load on the panel geometry.

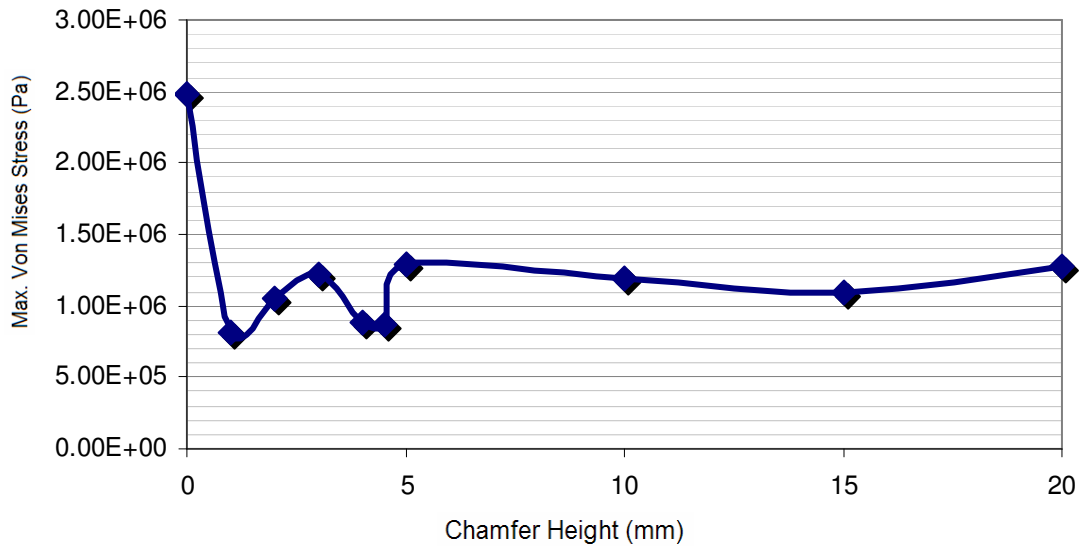


Fig. 8.14: Max. Von Mises Stress for varying chamfer height (x=50, y=1-20)

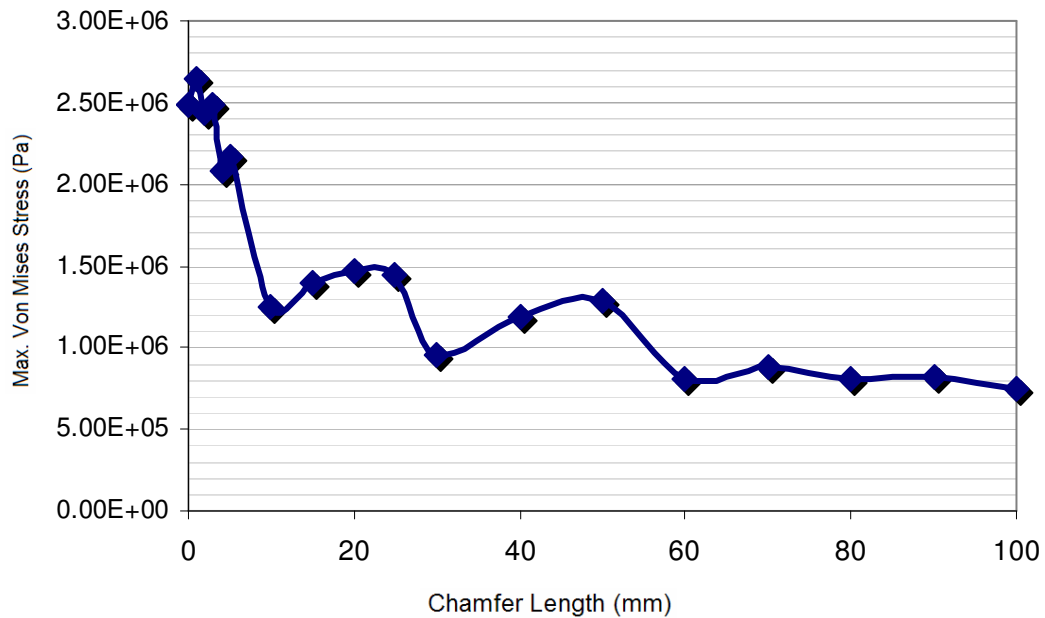


Fig. 8.15: Max. Von Mises Stress for varying chamfer length (y=5, x=1-100)

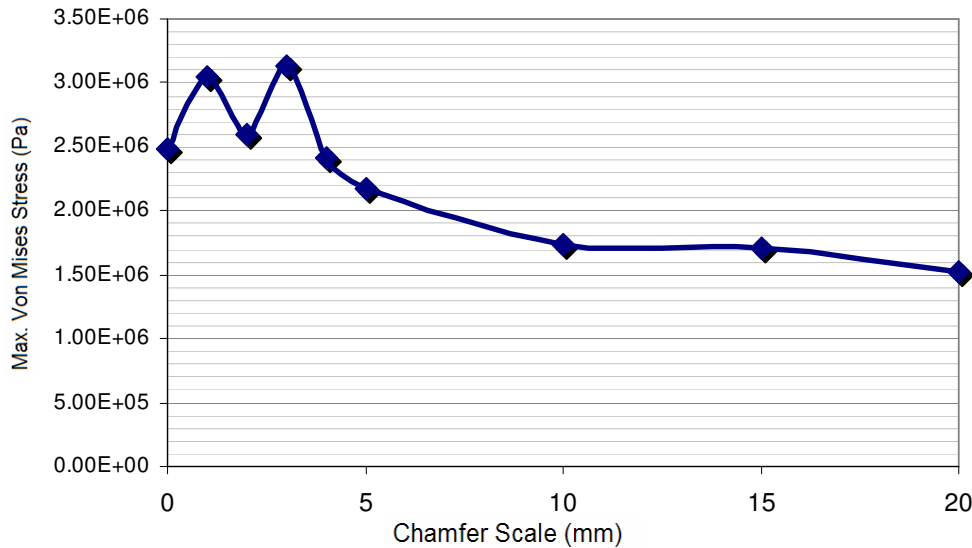


Fig. 8.16: Max. Von Mises Stress for varying chamfer scale (x,y=0-20)

From these results it can be seen that the lowest stress concentrations are found with the longer, shallower chamfers, in particular those with a geometry of  $y=5$ ,  $x=60-100$  which show significantly lower maximum Von Mises stresses compared with deeper and shorter chamfers. These also show a significant reduction compared with the  $50 \times 5$  chamfer originally proposed with Von Mises stresses down to around 1/3 of the original panel geometry. Comparisons of the best performing chamfer geometries for maximum Von Mises stress reductions are shown below along with the original panel geometry.

y	x	angle	area	Smx	% Original
0	0	0	0	2.48E+06	100.00%
5	50	5.710593	125	1.29E+06	52.02%
5	60	4.763642	150	8.10E+05	32.66%
5	70	4.085617	175	8.87E+05	35.76%
5	80	3.576334	200	8.12E+05	32.73%
5	90	3.17983	225	8.15E+05	32.85%
5	100	2.862405	250	7.47E+05	30.11%

Table 8.8: Best Chamfer Geometry comparison

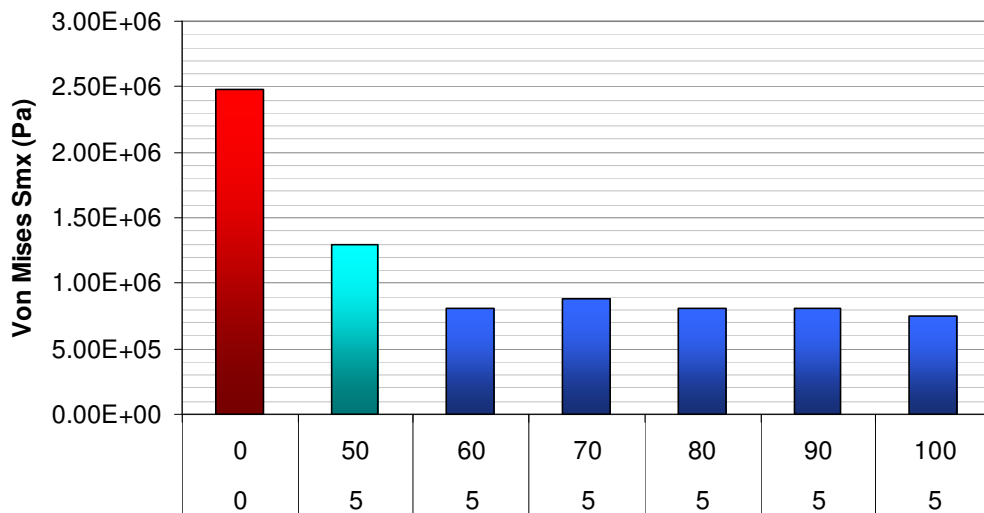


Fig. 8.17: Max. Von Mises Stress for varying chamfer geometry inc. original

### 8.2.2.2. Max. Friction Force

This can be seen as an indicator of the expected overall friction contribution for the panel geometry.

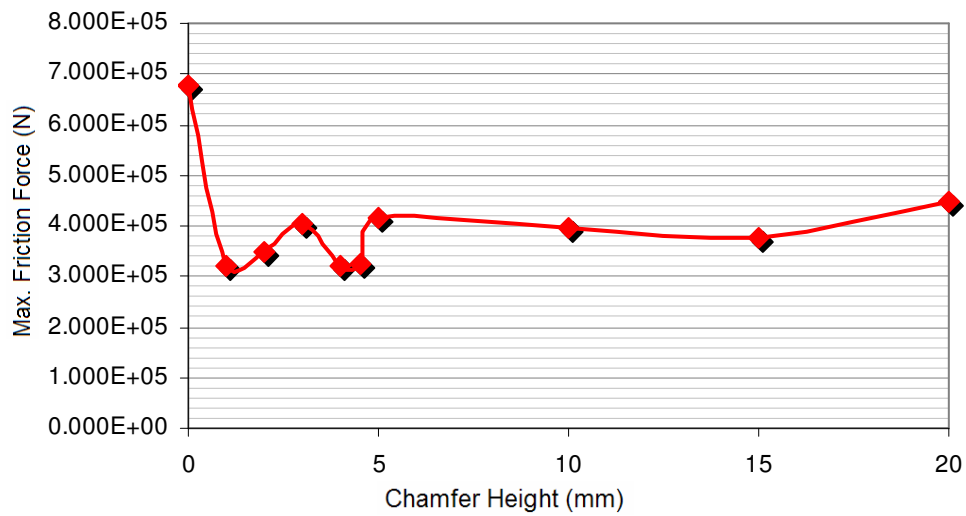


Fig. 8.18: Max. Friction Force for varying chamfer height ( $x=50$ ,  $y=1-20$ )

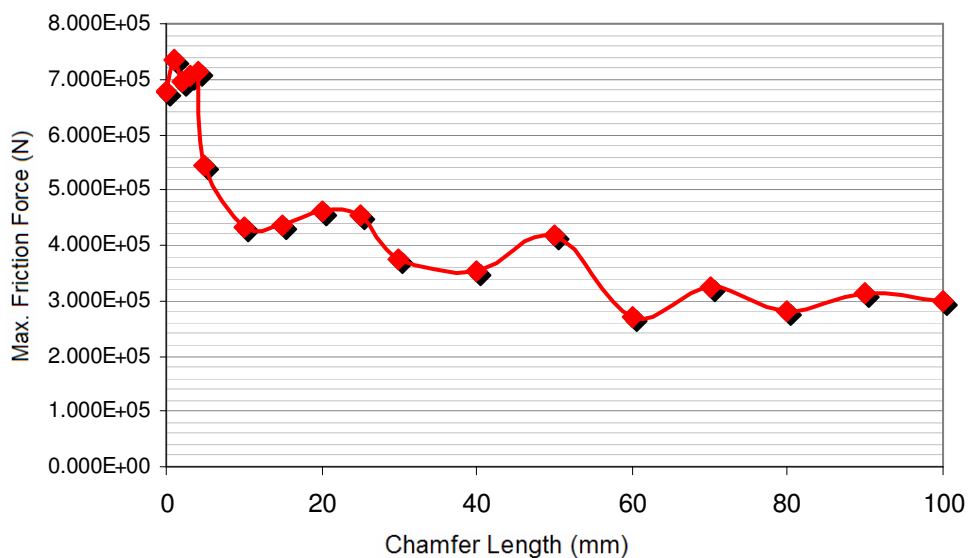


Fig. 8.19: Max. Friction Force for varying chamfer length ( $y=5$ ,  $x=1-100$ )

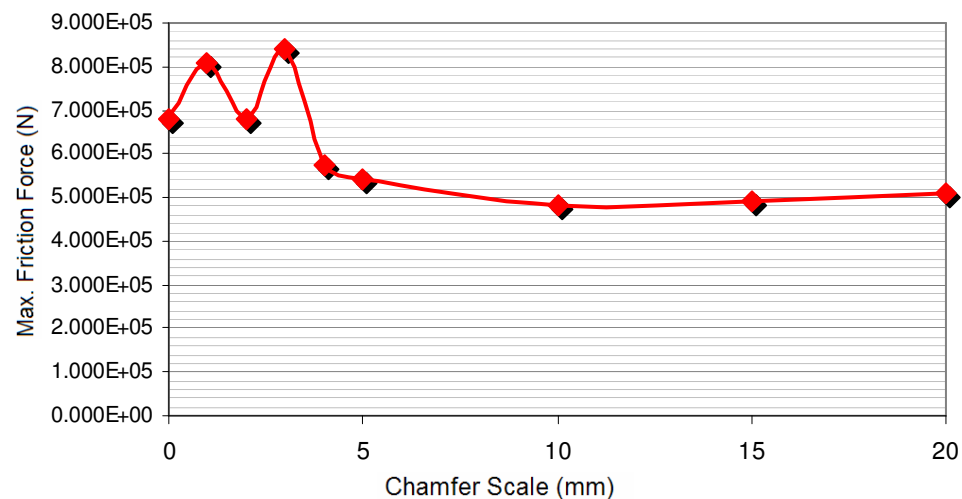


Fig. 8.20: Max. Friction Force for varying chamfer scale ( $x,y=0-20$ )

From these results it can be inferred that beyond a chamfer depth of 5mm the most significant contributor to a reduction in friction force is the chamfer length, varying the scale and depth beyond 5mm has little additional impact on the friction force. Chamfer lengths beyond 60mm show significant reductions in friction force compared with both the original panel geometry and the 5x50mm chamfer investigated; consequently these would appear to be the best selection for reducing the apparent friction along the slipway. A comparison of results is shown below.

y	x	angle	area	Friction Force Max.	% Original
0	0	0	0	6.78E+05	100.00%
5	50	5.710593	125	4.18E+05	61.62%
5	60	4.763642	150	2.700E+05	39.85%
5	70	4.085617	175	3.250E+05	47.97%
5	80	3.576334	200	2.825E+05	41.70%
5	90	3.17983	225	3.150E+05	46.49%
5	100	2.862405	250	2.975E+05	43.91%

Table 8.9: Best Chamfer Geometry comparison

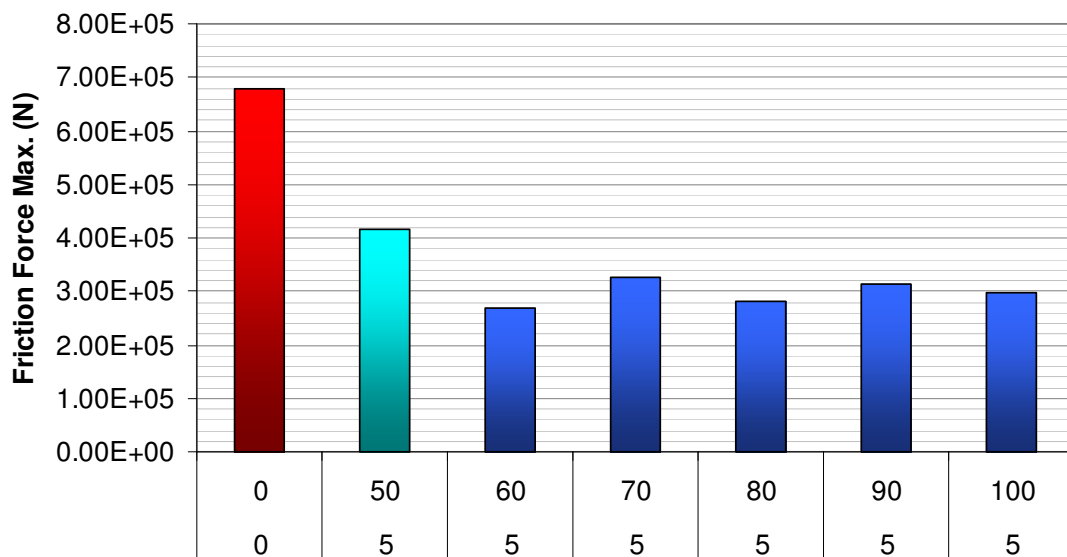


Fig. 8.21: Max. Friction Force for varying chamfer geometry inc. original



8.2.2.3. Max. Wear Rate

The maximum wear rate is shown below for the various panel chamfers tested.

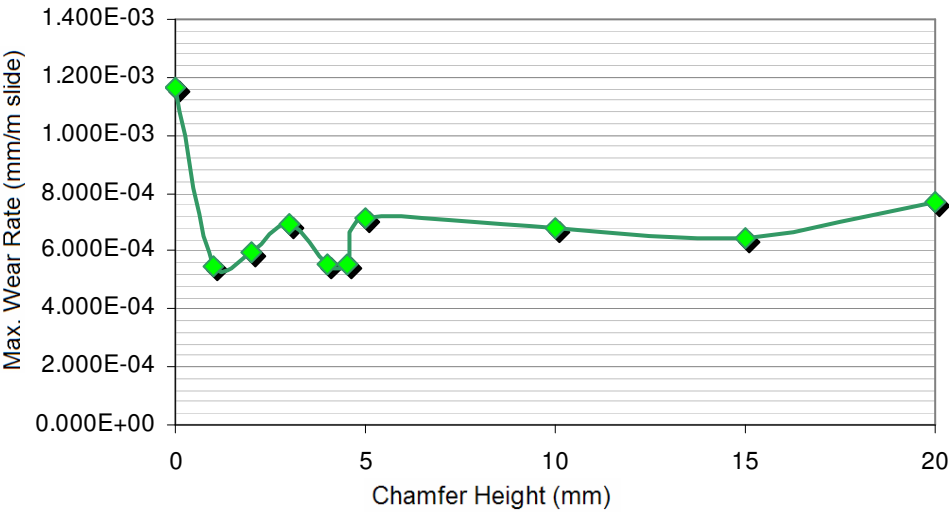


Fig. 8.22: Max. Wear rate for varying chamfer depth (x=50, y=1-20)

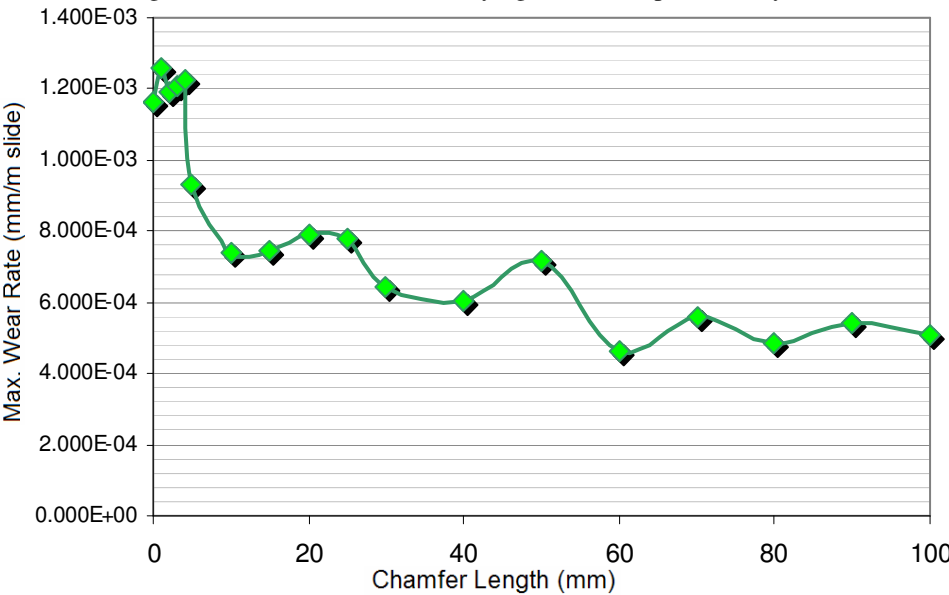


Fig. 8.23: Max. Wear rate for varying chamfer length (y=5, x=1-100)

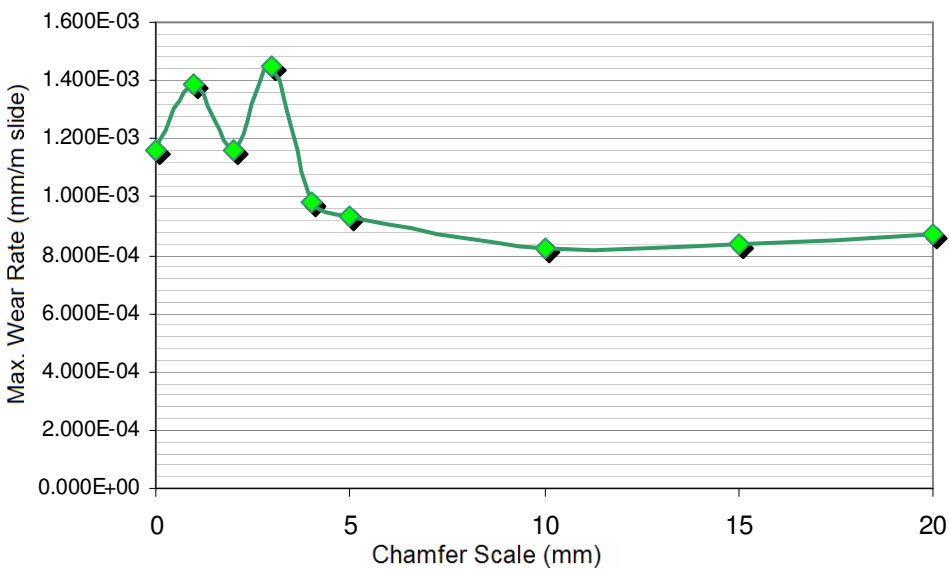


Fig. 8.24: Max. Wear rate for varying chamfer scale (x,y=0-20)

These results again show that the most significant contributor to a reduction in the maximum wear rate on the panel is the chamfer length, with chamfer lengths beyond 60mm showing significant reductions in wear rates at the raised panel edge compared with both the original panel geometry and the initial 5x50mm chamfer investigated. Subsequently, these are selected as the best performing chamfers with regards to wear rate reduction. A comparison of results is shown below.

y	x	angle	area	Wear Rate Max.	% Original
0	0	0.0000	0	1.16E-03	100.00%
5	50	5.7106	125	7.163E-04	61.62%
5	60	4.7636	150	4.633E-04	39.85%
5	70	4.0856	175	5.576E-04	47.97%
5	80	3.5763	200	4.847E-04	41.70%
5	90	3.1798	225	5.405E-04	46.49%
5	100	2.8624	250	5.104E-04	43.91%

Table 8.10: Best Chamfer Geometry comparison

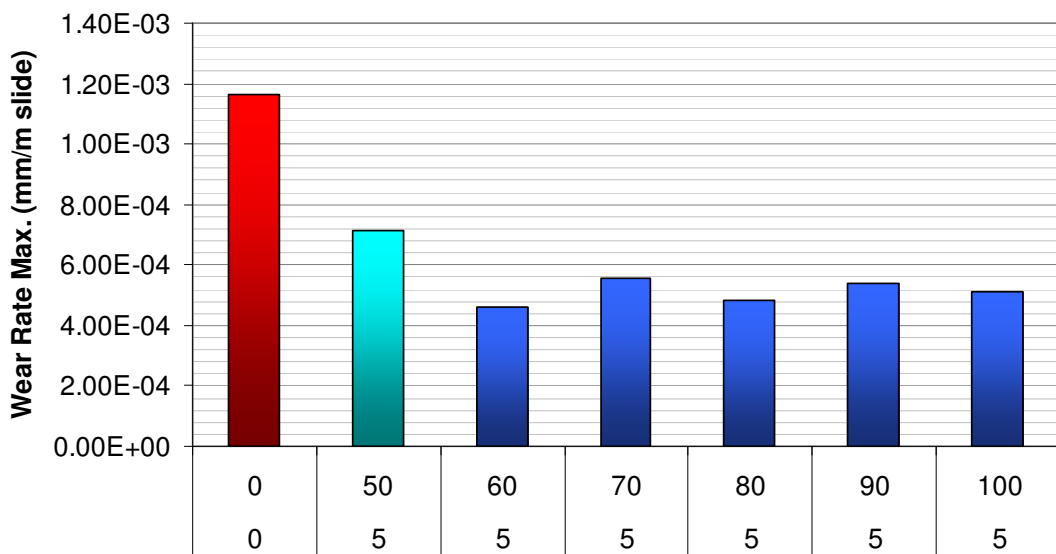


Fig. 8.25: Max. Wear rate for varying chamfer geometry inc. original

### 8.2.3. Conclusions

The above results show that chamfers of geometry  $y=5$ ,  $x=60-100$  exhibit significant reductions in the Max. Von Mises stress, friction force and wear rates compared with both the original geometry, and the 5x50 mm chamfer initially investigated. Results indicate that by optimising the panel chamfer reductions of around a further 20% in Von Mises stresses, friction forces and wear rates compared to the initial chamfer modification; these equate to savings of 70% in Von Mises stress and 60% in friction forces and wear rates compared to the original geometry. This research would imply that friction and wear savings are most

directly affected by the chamfer length and steer the designer towards the largest chamfer length in order to achieve the largest reductions, however further investigations into the possible effect these large chamfers and the associated chamfer angles may have on the kinematics of lifeboat recovery during slipway mounting and hauling are required before a fully informed recommendation can be made.

### 8.3. Kinematic Analysis of Slipway Panel Chamfer Effects

#### 8.3.1. Effects on Winch Loading During Recovery

The lifeboat is recovered to the top of the slipway following a launch using a winch; the load on the winch cable is proportional to the angle of the slipway. By incorporating a chamfer into the slipway panel design it is possible that the lifeboat keel will meet the slipway at a chamfered panel edge as it mounts the slipway, this would mean the initial apparent winch load would be higher as the chamfer effectively adds to the slipway angle until the boat begins to mount the slipway fully. Although the effect would be rare (only apparent if the lifeboat hits the slipway at a chamfer edge) and short lived, only lasting until the keel clears the chamfer (~60-100mm worst case scenario) it is important to assess this effect in selecting an appropriate slipway panel geometry.

To calculate the effect of the panel chamfer on the initial winch loading we can simply model the chamfer region as a steeper section of slipway, increasing the slipway angle by the chamfer angle. The following model is developed:

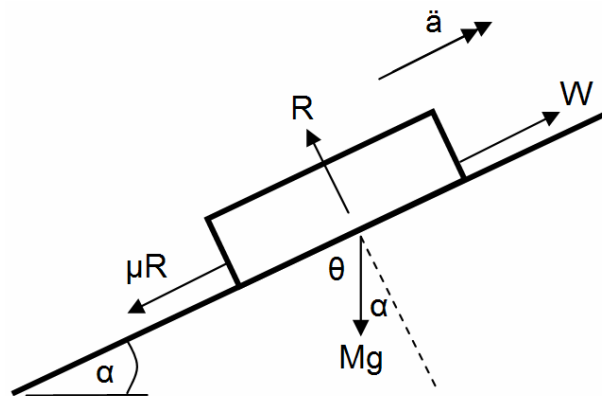


Fig. 8.26: Free body diagram of Selsey slipway

The apparent slipway angle  $\alpha$  is the original slipway angle ( $11.3^\circ$  from a 1 in 5 gradient) plus the chamfer angle. Results are developed for the static case,  $\ddot{a} = 0$  so that:

$$R(\uparrow) \quad W \sin \alpha + R \sin \theta - \mu R \sin \alpha - Mg = 0 \quad -\textcircled{1}$$

$$R(\rightarrow) \quad W \cos \alpha - R \cos \theta - \mu R \cos \alpha = 0 \quad -\textcircled{2}$$

So;

$$W = R \left( \frac{\cos\theta}{\cos\alpha} + \mu \right)$$

$$R = \frac{Mg}{[(\cos\theta/\cos\alpha) + \mu]\sin\alpha + \sin\theta - \mu\sin\alpha}$$

$\mu$  is set to 0.252 as recorded during the long dry sliding reciprocating tribometer tests.

$M$  is set to  $35 / 2 = 17.5$  tonnes as the lifeboat is modelled with half its mass being supported by its own buoyancy in the water at the point of mounting the slipway.

Winch loads are calculated for the original panel, the 5x50mm chamfer and for the 5x60-100mm chamfers identified for their wear and friction performance in the previous section.

Chamfer	$\theta$	$\alpha$	R	W	W%
Original	11.30993	78.69007	168341.2	75753.53	100.00%
50x5	17.02053	72.97947	164155.6	91290.63	120.51%
60x5	16.07357	73.92643	164963.7	88772.84	117.19%
70x5	15.39555	74.60445	165514.6	86955.14	114.79%
80x5	14.88627	75.11373	165913.2	85581.8	112.97%
90x5	14.48976	75.51024	166214.4	84507.9	111.56%
100x5	14.17234	75.82766	166449.8	83645.25	110.42%

Table 8.11: Best Chamfer effects on winch loading

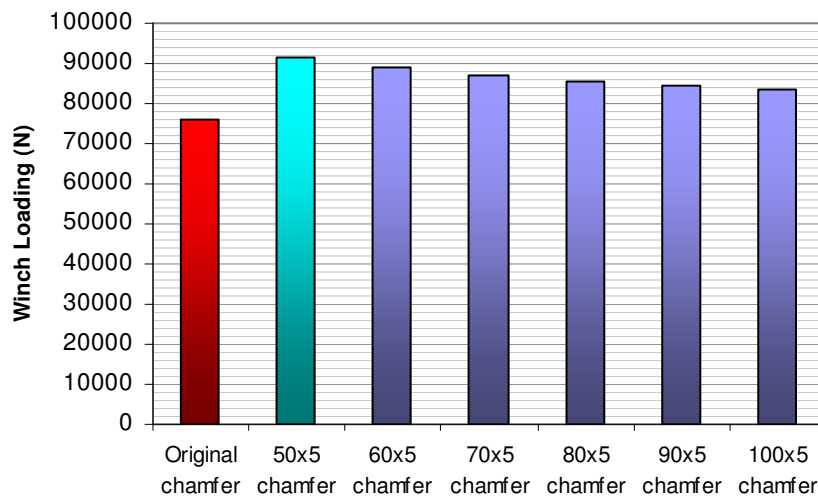


Fig. 8.27: Best Chamfer effects on winch loading

These results show that the effects of adding a chamfer to the slipway could lead to an initial increase in winch loading as the lifeboat mounts the slipway. It should be noted however that this increase of 10-20% is short lived and occurs while the lifeboat is partially supported by its own buoyancy; the increase is also small compared with the overall friction force reductions of up to 60%. It is also true that as the lifeboat mass is partially supported by the water at this point the winch loads will still remain below the design limit of 12 tonnes in all cases.

### 8.3.2. Effects on Lifeboat mounting the slipway

As the lifeboat mounts the slipway for recovery it is first necessary to manoeuvre the keel onto the slipway so that it 'sticks' before the winch line can be attached. With the lower friction composite slipway panels this has in the past proved difficult as the low friction contact between keel and slipway panel does not always hold. This can further increase the time and difficulty in recovering the lifeboat to the top of the slipway. Adding a chamfer to the slipway panels will, at the chamfer edge, provide a shallower angled region for the lifeboat keel to 'stick' on. The effect of this is analysed below in a similar way to the analysis of initial winch loading, however this time the lifeboat keel is assumed to lie on the top chamfer of the panel, effectively reducing the slipway angle. Friction force is calculated using  $\mu = 0.252$  as derived from tribometer tests.

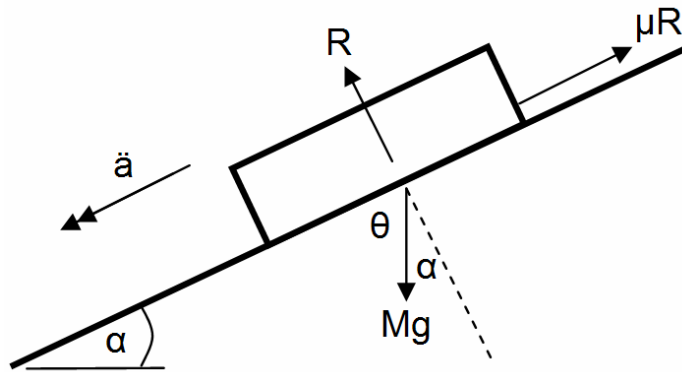


Fig. 8.28: Free body diagram of Selsey slipway

The apparent slipway angle  $\alpha$  is the original slipway angle ( $11.3^\circ$  from a 1 in 5 gradient) minus the chamfer angle as this effectively shallows the slipway at this point.

$$\sum F(\perp) \quad R - Mg \cos \alpha = 0 \quad -\textcircled{1}$$

$$\sum F(\parallel) \quad Mg \sin \alpha - \mu R = M \ddot{a} \quad -\textcircled{2}$$

So;

$$R = Mg \cos \alpha$$

And friction force  $F_{\max}$  is:

$$F = \mu R$$

$\mu$  is set to 0.252 as recorded during the long dry sliding reciprocating tribometer tests.

$M$  is again set to  $35 / 2 = 17.5$  tonnes as the lifeboat is modelled with half its mass being supported by its own buoyancy in the water.

Chamfer	$\theta$	$\alpha$	R	$\mu R$	$\mu R\%$
Original	11.30993	78.69007	168341.2	42085.3	100.00%
50x5	17.02053	72.97947	170855.9	42713.96	101.49%
60x5	16.07357	73.92643	170555.7	42638.92	101.32%
70x5	15.39555	74.60445	170312.1	42578.04	101.17%
80x5	14.88627	75.11373	170113.5	42528.38	101.05%
90x5	14.48976	75.51024	169949.6	42487.39	100.96%
100x5	14.17234	75.82766	169812.5	42453.12	100.87%

Table 8.12: Best Chamfer  $F_{\max}$  for keel 'stick'

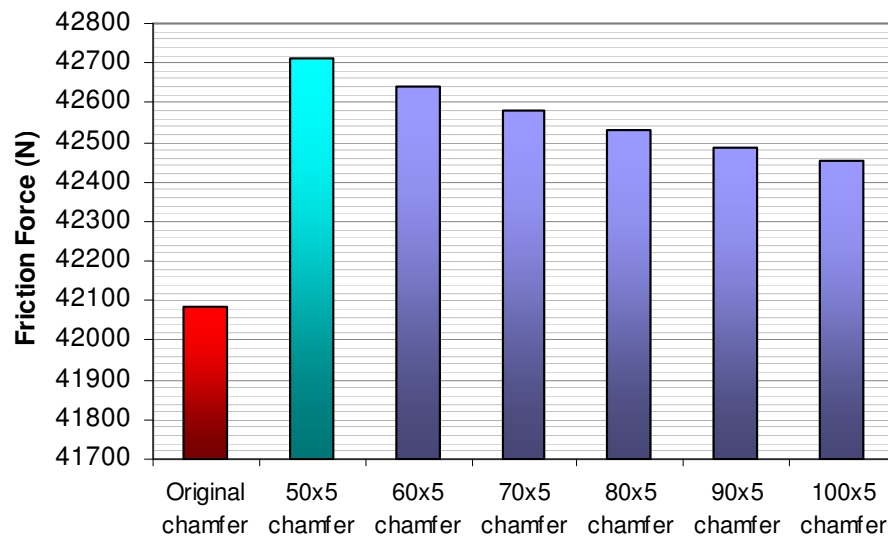


Fig. 8.29: Best Chamfer  $F_{\max}$  for keel 'stick'

The effects of adding a chamfer to the 'keel stick' properties of the slipway would appear to be negligible, with only a maximum beneficial effect of 1.49% for the 50mm chamfer, decreasing with increased chamfer length.

### 8.3.3. Effects of reduced contact area on friction

By adding a chamfer to the slipway panels the effective contact area between the slipway and the keel is decreased. This will lead to slightly higher contact pressures and consequently higher friction with the greater effects occurring with longer chamfers. This effect is investigated below with  $\mu = 0.252$  as recorded in the dry sliding tribometer tests:

Chamfer	Effective Panel length (m)	Contact Area (m <sup>2</sup> )	Comparison with original	Contact Pressure (MPa)	Friction Force/ Unit Area (N/m <sup>2</sup> )	Comparison with original
Original Panel	1.22	0.183	100.00%	176076.9231	44019.23077	100.00%
50x5 chamfer	1.17	0.1755	95.90%	183601.5779	45900.39448	104.27%
60x5 chamfer	1.16	0.174	95.08%	185184.3501	46296.08753	105.17%
70x5 chamfer	1.15	0.1725	94.26%	186794.6488	46698.66221	106.09%
80x5 chamfer	1.14	0.171	93.44%	188433.1984	47108.2996	107.02%
90x5 chamfer	1.13	0.1695	92.62%	190100.7488	47525.1872	107.96%
100x5 chamfer	1.12	0.168	91.80%	191798.0769	47949.51923	108.93%

Table 8.13: Best Chamfer Effects of reduced contact area on friction force

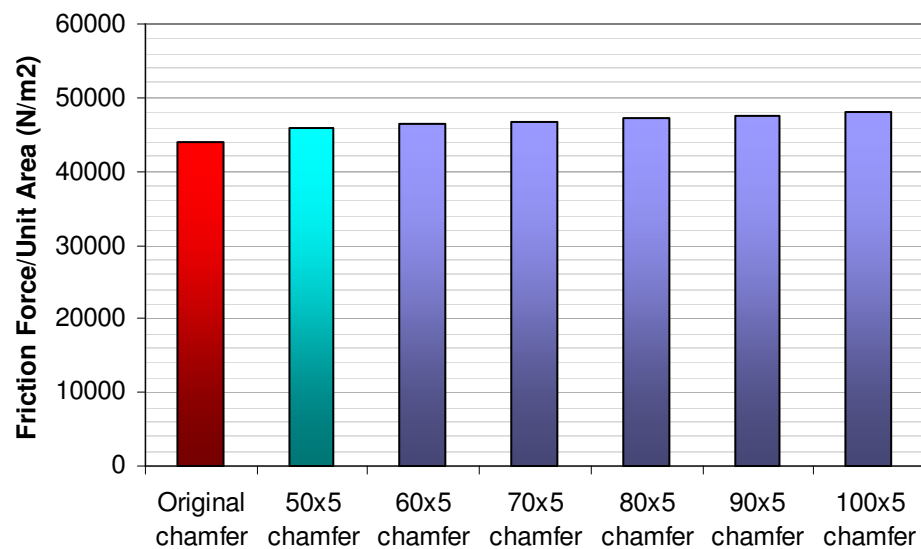


Fig. 8.30: Best Chamfer Effects of reduced contact area on friction force

The results of this analysis show that the increased contact pressure associated with larger chamfers could be a significant effect and maybe useful in selecting an appropriate chamfer geometry. Contact pressure increases range from 4-9% increasing with chamfer length, again this must be compared with overall friction savings compared with the original panel geometry of over 60%.



### 8.3. FEA Conclusions

---

The above research shows that fitting a modified, chamfered slipway panel in place of the original geometry slipway panel can considerably reduce the wear and friction on the panel. The chamfer optimisation tests indicate that chamfer geometries of  $y=5$ ,  $x=60-100$  mm have the most significant effect with stress reductions of around 70% and wear and friction reductions of around 60% compared with the original panel. However, the kinematic analyses show that these are not the only considerations when selecting an appropriate chamfer geometry. For example a chamfer of 5x100 mm shows the lowest stress, friction and wear rate properties, and performs best in the initial keel load analysis but also has the highest contribution to the increased contact pressure due to reduced contact area and the lowest beneficial contribution to the 'keel stick' effect. The relative real world importance of these factors should guide any selection of an appropriate chamfer geometry, however for general all round performance chamfers of 50 x 5 and 60 x 5 are recommended here as the most suitable for real world slipway applications.

The fitting of chamfered panels to existing slipways will also increase the misalignment tolerance along the slipway as they show lower stress factors at misaligned panel interfaces compared with the original panel. This allows current panel alignment standards to be maintained without significant adverse effects on friction and wear along the slipway, this is important as upgrading the panel alignment standards to prevent the friction and wear peaks identified in section 7 for all future slipway panel fitting and replacement may prove impractical as there is always likely to be some systemic misalignment during fitting.

## 9 APPLIED RESULTS

---

### 9.1. Expected panel lifespan for varying conditions

---

It is now possible to develop wear predictions and failure criteria based on the wear coefficients generated by the tribometer tests and on the stress concentrations from the FEA and slipway survey data.

The experimental tests, FEA simulations and slipway surveys conducted above show that while the sliding wear coefficient between the lifeboat keel and the jute/phenolic composite is low enough to cause little concern under ideal sliding conditions, in the real world the stress concentration effects of even slight panel misalignments can result in a serious increase in slipway panel wear. Slipway surveys show that the average panel parallel offset was 0.88mm; with a maximum of over 4mm. FEA Analysis of the stress concentrations presented by this misalignment from the plane sliding case reveal that edge stresses resulting from this misalignment can increase up to 25 times that encountered in the perfectly aligned case. The contact pressure tests conducted above indicate a linear relationship between contact pressure and wear and so it would be reasonable to conclude that this would also result in a corresponding 25-fold increase in the wear rate at these high stress regions. If we then use

the wear rates found from the tribometer tests and the maximum stress concentrations found from the FE Analysis for each misalignment case, the number of launches that will generate a wear scar depth of 19mm, the entire depth of the composite slipway panel can be calculated for these high stress regions.

Lubricant	Eq. No of Launches & Recoveries for 19mm Wear Scar Depth
Seawater	19.65
Freshwater	21.83
Silicon Microball Lub.	26.49
Marine Grease	58.35
Biogrease	65.86
Dry	98.94

Table 9.1: Equivalent number of lifeboat launches/recoveries required to generate a 19mm wear scar on a 4mm parallel offset misaligned slipway panel by lubricant used

It is found that for the seawater lubricated case a wear scar depth equal to the 19mm panel thickness will occur after just 19 launches and recoveries. This would support the experience at Tenby where initial slipway hauling trials resulted in 10 launches and recoveries during the trial; this may well have contributed to the subsequent wear failure of slipway panels.

## Conclusions

The tests and slipway surveys conducted above show that while the sliding wear coefficient between the lifeboat keel and the jute/phenolic composite is low enough to cause little cause for concern under ideal sliding conditions, in the real world even slight panel misalignments can result in a serious increase in slipway panel wear. This increase in wear due to panel misalignment would be sufficient to explain the high wear observed at Tenby and Padstow with the introduction of the new Tamar class lifeboat, particularly when the initial extended slipway line trials involving ten or more ascents/descents of the slipway under winch loading are considered. While these would have had little contribution to the wear under ideal conditions, panel misalignment effects show that they constitute over 50% of the number of launches required for the most seriously misaligned panels to fail.

As can be seen in the table above, the lubricant selection can have a significant impact on the wear rates for a misaligned panel. It should be noted however that previous reciprocating tribometer testing indicates that for the consistently low friction required for successful lifeboat launch and recovery it is necessary to use some form of lubrication. It is also shown in the FE analysis that the increased edge stresses associated with panel misalignment will also result in increased friction at these points, further emphasising the need for lubrication to reduce friction. For this reason it is more sensible to examine and reduce the causes of

slipway panel misalignment than to select a lubricant based on the high wear rates encountered with misaligned panels.

## 9.2. Comparison of Original and Modified Slipway Panel Expected Lifespan

By the same process the original and modified slipway panels are compared across the misalignment scenarios examined in the FE Analysis. The chamfer panel shows a very considerable increase in panel lifespan compared to the original panel when the more common Parallel and Angled panel misalignment scenarios are examined and also shows a significant increase for the skewed panel misalignment scenario. For example, at a panel misalignment of 1mm, close to the average misalignment found on both Tenby and Padstow slipways, and under a freshwater lubrication regime, as used at both these slipways, the original panel will wear a depth of 19mm at the peak wear rate after 37, 41 and 49 lifeboat launches and recoveries for the Parallel, Angled and Skewed scenarios respectively. A panel featuring a chamfer of 5 x 50mm, as described in the FE Analysis of the modified slipway panel will wear a depth of 19mm at the peak wear rate after 78, 89 and 123 lifeboat launches and recoveries for the Parallel, Angled and Skewed scenarios respectively. Assuming one lifeboat launch/recovery per week this represents a lifespan increase from approximately 10 months in the Parallel and Angled misalignment cases to around 20 months. Similarly for the Skewed scenario the lifespan increases with the original panel wearing 19mm at the maximum wear rate after almost 12 months and the modified panel lasting around 30 months. These results are shown below for the preferred dry, freshwater, seawater and biogrease #1 lubrication regimes and for marine grease lubrication:

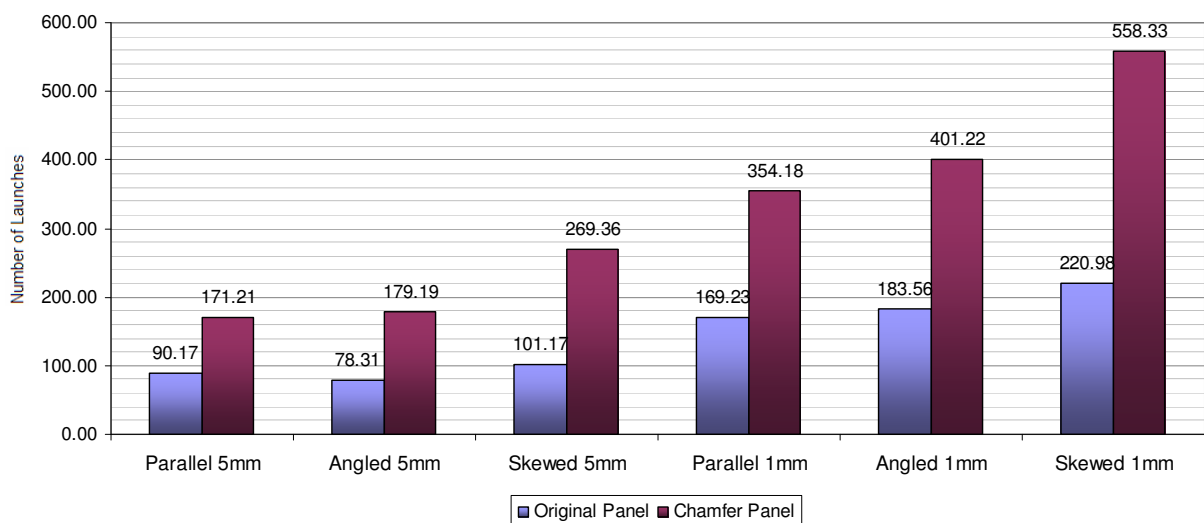
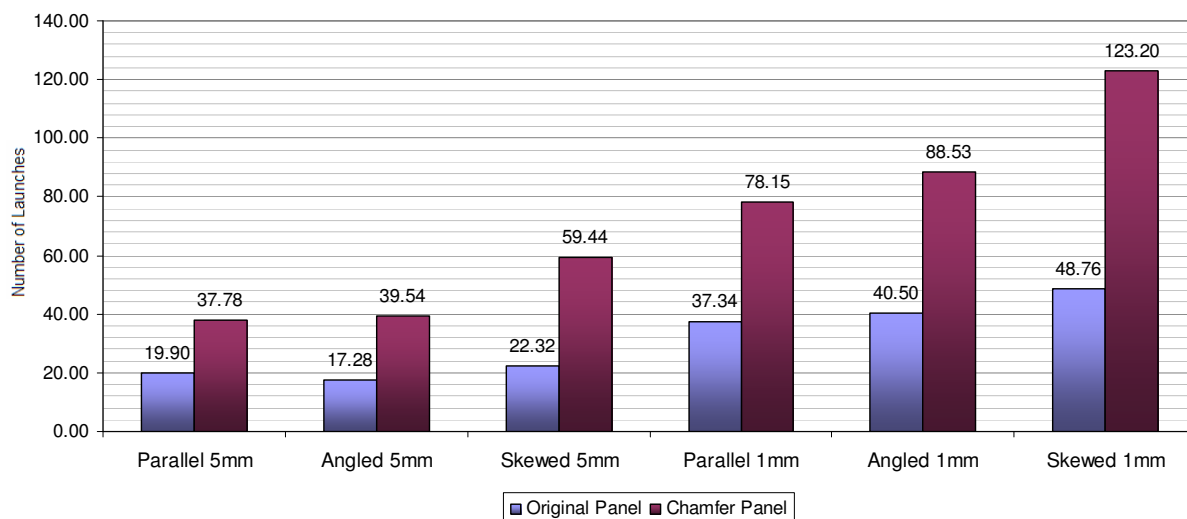
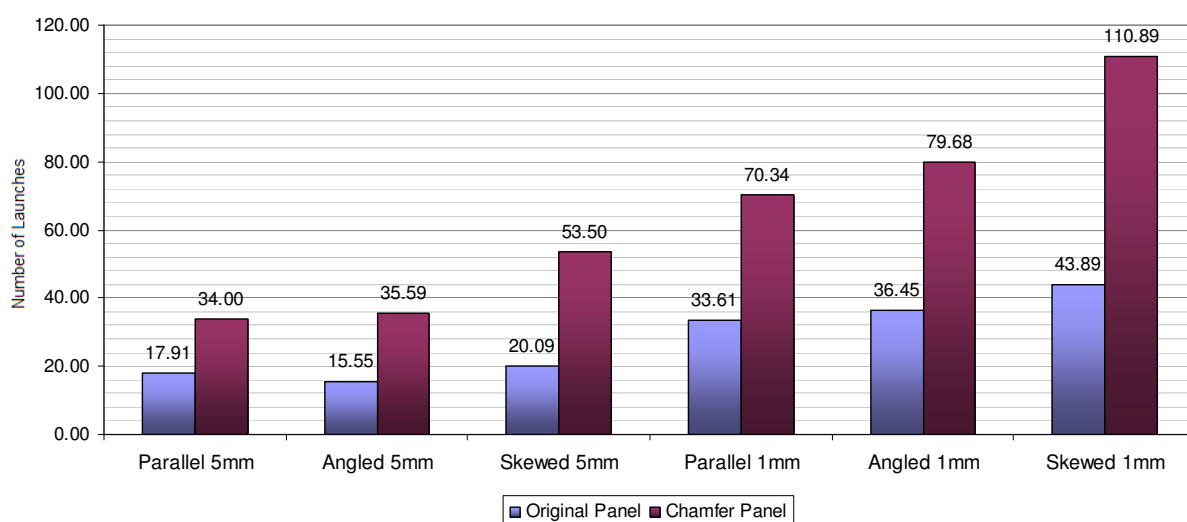


Fig. 9.1: Equivalent number of lifeboat launches/recoveries required to generate a 19mm wear scar on a composite slipway panel for original and modified slipway panels without lubrication



**Fig. 9.2: Equivalent number of lifeboat launches/recoveries required to generate a 19mm wear scar on a composite slipway panel for original and modified slipway panels using freshwater lubrication**



**Fig. 9.3: Equivalent number of lifeboat launches/recoveries required to generate a 19mm wear scar on a composite slipway panel for original and modified slipway panels using seawater lubrication**

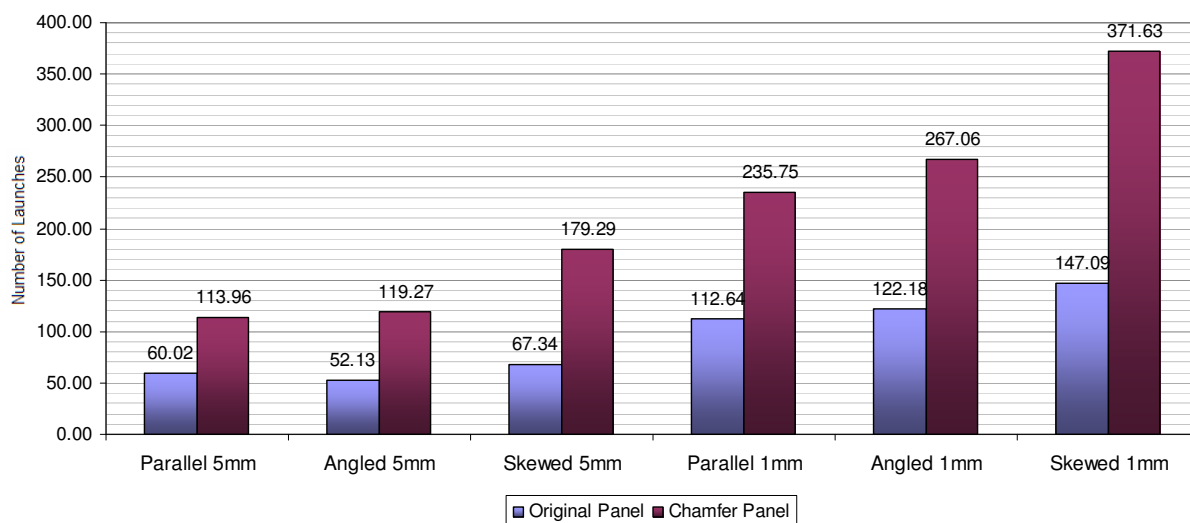


**Fig. 9.4: Equivalent number of lifeboat launches/recoveries required to generate a 19mm wear scar on a composite slipway panel for original and modified slipway panels using biogrease #1 lubrication**

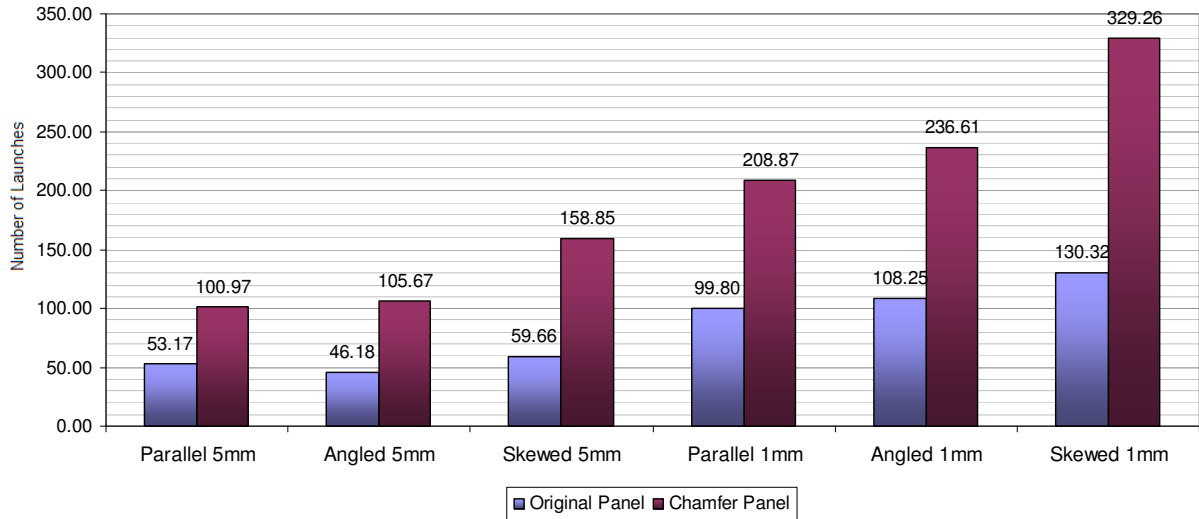


**Fig. 9.5: Equivalent number of lifeboat launches/recoveries required to generate a 19mm wear scar on a Composite slipway panel for original and modified slipway panels using marine grease lubrication**

These results are very promising but the following assumptions in the calculations should be noted, firstly the results are based on the maximum contact stresses found in the slipway panels, it is likely that as the areas of the panel under higher contact stresses wear away these peak contact stresses will reduce. The second assumption is that the panels will fail only when the entire depth of the panel wears away; it is likely that serious effects on the friction along the slipway will be observed before this happens due to the reduced bearing area of the panel, this effect is examined below. The third assumption is that erosive wear will remain the primary wear mechanism even when significantly reduced by the reduction in contact stresses resulting from the modified slipway panel geometry. It is likely that other wear mechanisms such as the panel surface wear identified in the aligned load panel simulations in section 7.1 will become more significant during this extended lifespan.

### 9.3. Friction Coefficient Based Slipway Panel Expected Lifespans

As a slipway panel wears, the bearing surface it presents to the lifeboat keel will reduce, this will affect the contact pressure and consequently the friction forces along the panel. Following on from the slipway panel lifespan results discussed above, and with regard to the wear patterns encountered during slipway panel surveys and similarly predicted by the FE Analysis it is thought that the effects of the reduced bearing area on the friction forces will cause the slipway panel to fail due to high friction rather than solely through wearing away. By analysis the limits of this reduced bearing area with regard to the maximum friction that will allow the lifeboat to proceed down the slipway can be found so that:

$$\tan \alpha > \mu \frac{A_n}{A_a}$$

Where  $A_n$  is the nominal panel bearing area,  $A_a$  is the actual panel bearing area,  $\mu$  is the friction coefficient along the slipway and  $\alpha$  is the slipway angle.

Similarly, in the lifeboat recovery case:

$$\mu \frac{A_n}{A_a} < \frac{F/Mg - \sin \alpha}{\cos \alpha}$$

Where  $A_n$  is the nominal panel bearing area,  $A_a$  is the actual panel bearing area,  $\mu$  is the friction coefficient along the slipway,  $\alpha$  is the slipway angle,  $F$  is the maximum winch line pull specification and  $M$  is the lifeboat mass.

Using these criteria in combination with the winch specifications calculated in section 2.2.1, a lifeboat mass for the Tamar of 35 tonnes and the friction coefficients from the tribometer tests the bearing area at which the friction coefficient exceeds the value that will allow the lifeboat to proceed down the slipway under its own mass can be calculated. Using the wear coefficients from the tribometer tests the predicted number of launches and recoveries to achieve this bearing area reduction can therefore be found. Results are presented below for preferred lubrication regimes: (note: The dry sliding friction coefficient of the composite already exceeds the friction coefficient necessary to allow the lifeboat to proceed down the slipway under its own mass, hence, it is not possible to show this data).

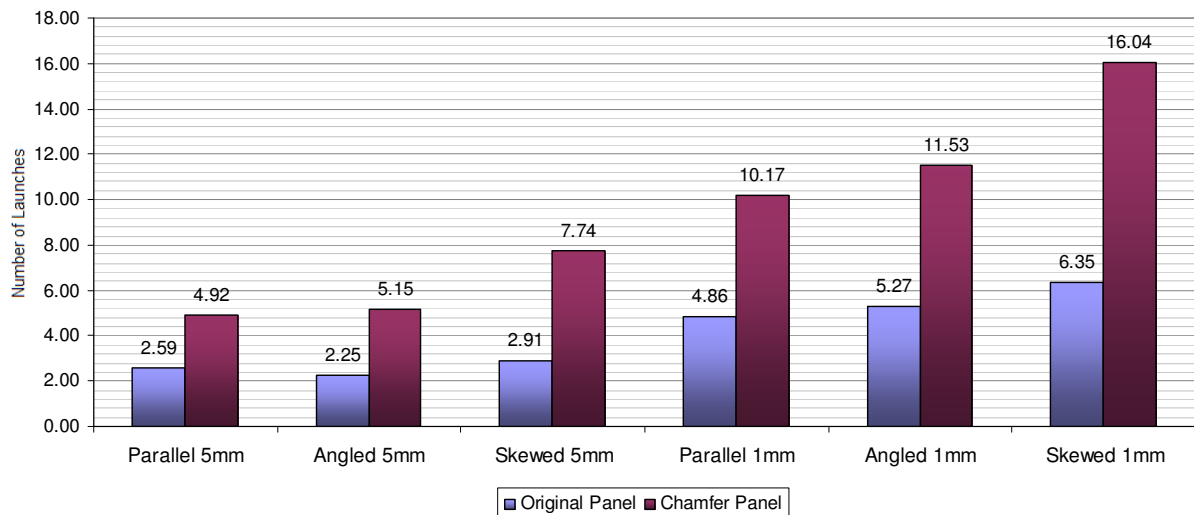


Fig. 9.6: Equivalent number of lifeboat launches/recoveries required for the slipway panel to fail due to friction criteria on a Composite slipway panel for original and modified slipway panels using seawater lubrication



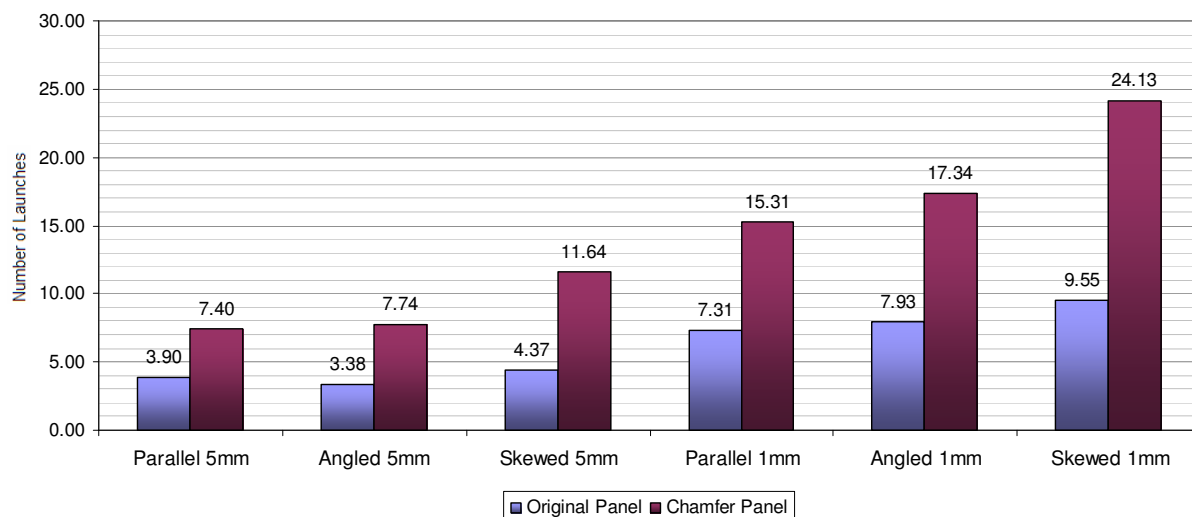


Fig. 9.7: Equivalent number of lifeboat launches/recoveries required for the slipway panel to fail due to friction criteria on a composite slipway panel for original and modified slipway panels using freshwater lubrication

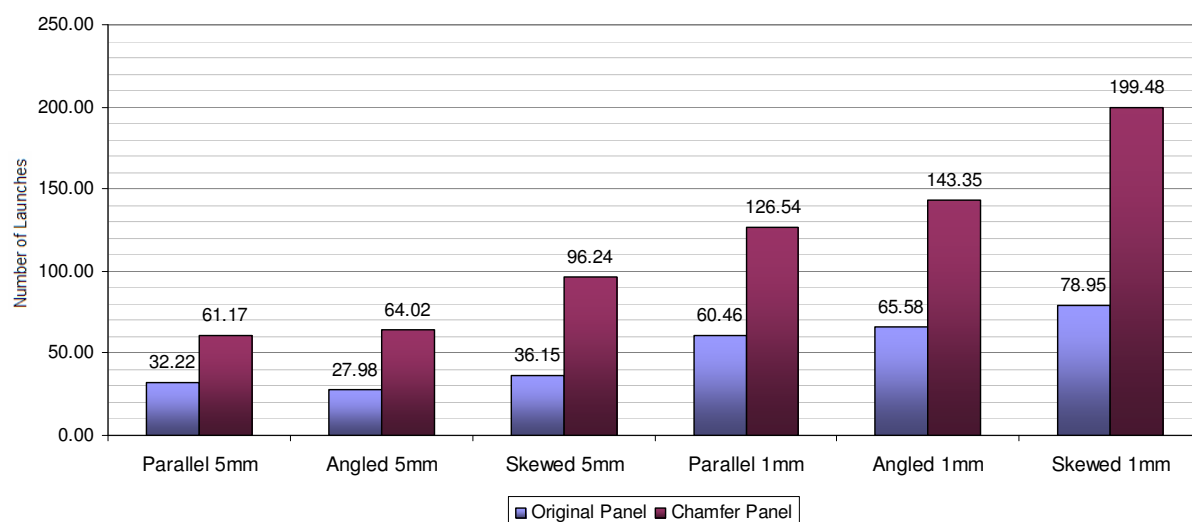


Fig. 9.8: Equivalent number of lifeboat launches/recoveries required for the slipway panel to fail due to friction criteria on a composite slipway panel for original and modified slipway panels using biogrease #1 lubrication

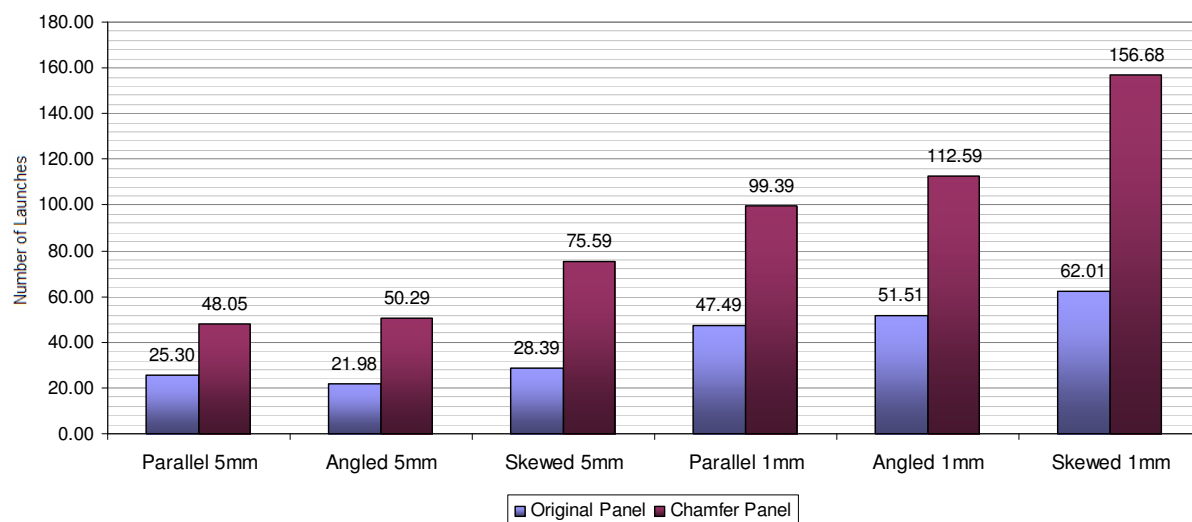


Fig. 9.9: Equivalent number of lifeboat launches/recoveries required for the slipway panel to fail due to friction criteria on a composite slipway panel for original and modified slipway panels using marine grease lubrication

These formulae can be adapted to provide panel failure criteria for any given slipway, slipway panel material and lifeboat mass once the slipway panel material friction and wear coefficients for the relevant lubrication regimes are found. When considering these results the same assumptions discussed in section 9.2 are present.

It is noted that the number of launches and recoveries necessary to cause panel failure by friction criteria is lower in all cases than the number required to cause full panel failure by wear criteria, it is thus reasonable to monitor the condition of the slipway panels as a whole by measuring the friction performance.

### Friction based slipway monitoring

Shown in Table 9.2 below are maximum launch friction coefficients and winch line pull loads for various slipway inclines, as calculated by slipway geometry inspection. This allows the winch operator to assess the condition of the slipway by monitoring the winch load during recovery; the table presents maximum winch load failure criteria for any slipway incline.

If the winch load is seen to exceed the value shown here for the relevant slipway angle it is indicative that the friction coefficient has exceeded that which will allow the lifeboat to proceed down the slipway under its own mass and a slipway panel wear inspection should be performed in order to investigate the causes as described in section 9.4.

Slipway incline		Angle	Launch Friction Coefficient Specification	Maximum Winch Specification (kg)	Maximum Winch Specification (tonnes)
1	4	14.04	0.25	1.70E+04	17.0
1	4.5	12.53	0.22	1.52E+04	15.2
1	5	11.31	0.20	1.37E+04	13.7
1	5.5	10.30	0.18	1.25E+04	12.5
1	6	9.46	0.17	1.15E+04	11.5
1	6.5	8.75	0.15	1.06E+04	10.6
1	7	8.13	0.14	9.90E+03	9.9
1	7.5	7.59	0.13	9.25E+03	9.3
1	8	7.13	0.13	8.68E+03	8.7
1	8.5	6.71	0.12	8.18E+03	8.2
1	9	6.34	0.11	7.73E+03	7.7
1	9.5	6.01	0.11	7.33E+03	7.3
1	10	5.71	0.10	6.97E+03	7.0
1	10.5	5.44	0.10	6.64E+03	6.6
1	11	5.19	0.09	6.34E+03	6.3
1	11.5	4.97	0.09	6.06E+03	6.1
1	12	4.76	0.08	5.81E+03	5.8

Table 9.2: High recovery winch loading failure criteria at various slipway inclines

## 9.4. Panel Failure Guidelines

Friction based replacement criteria are shown below in tables 9.3-5. The maximum friction coefficient on a particular slipway is determined by its geometry, the actual friction coefficient can be found by looking at the winch loading during recovery, if this is not possible the friction coefficient can be calculated by timing the lifeboat launch or by referring to tables 9.3-5 below to specify the likely friction coefficient by the lubricants in use. The replacement criteria are given as a percentage of the panel bearing area that remains; typical worn panel outlines for varying percentages of bearing area remaining are shown in appendix I.

Slipway Gradient	Winch Load (tonnes)	Actual Friction Coefficient	% Worn Surface Area
0.20	6.00	-0.03	-14.29%
0.20	6.50	-0.01	-7.14%
0.20	7.00	0.00	0.00%
0.20	7.50	0.01	7.14%
0.20	8.00	0.03	14.29%
0.20	8.50	0.04	21.43%
0.20	9.00	0.06	28.57%
0.20	9.50	0.07	35.71%
0.20	10.00	0.09	42.86%
0.20	10.50	0.10	50.00%
0.20	11.00	0.11	57.14%
0.20	11.50	0.13	64.29%
0.20	12.00	0.14	71.43%
0.20	12.50	0.16	78.57%
0.20	13.00	0.17	85.71%
0.20	13.50	0.19	92.86%
0.20	14.00	0.20	100.00%
0.20	14.50	0.21	107.14%
0.20	15.00	0.23	114.29%
0.20	15.50	0.24	121.43%

Table 9.3: Worn panel failure criteria for various recorded winch loads for a 1 in 5 Slipway Gradient

Slipway Gradient	Winch Load (tonnes)	Actual Friction Coefficient	% Worn Surface Area
0.18	5.50	-0.02	-13.57%
0.18	6.00	-0.01	-5.71%
0.18	6.50	0.00	2.14%
0.18	7.00	0.02	10.00%
0.18	7.50	0.03	17.86%
0.18	8.00	0.05	25.71%
0.18	8.50	0.06	33.57%
0.18	9.00	0.08	41.43%
0.18	9.50	0.09	49.29%
0.18	10.00	0.10	57.14%
0.18	10.50	0.12	65.00%
0.18	11.00	0.13	72.86%
0.18	11.50	0.15	80.71%
0.18	12.00	0.16	88.57%
0.18	12.50	0.18	96.43%
0.18	13.00	0.19	104.29%
0.18	13.50	0.20	112.14%
0.18	14.00	0.22	120.00%

Table 9.4: Worn panel failure criteria for various recorded winch loads for a 1 in 5.5 Slipway Gradient

Slipway Gradient	Winch Load (tonnes)	Actual Friction Coefficient	% Worn Surface Area
0.17	5.00	-0.02	-14.29%
0.17	5.50	-0.01	-5.71%
0.17	6.00	0.00	2.86%
0.17	6.50	0.02	11.43%
0.17	7.00	0.03	20.00%
0.17	7.50	0.05	28.57%
0.17	8.00	0.06	37.14%
0.17	8.50	0.08	45.71%
0.17	9.00	0.09	54.29%
0.17	9.50	0.10	62.86%
0.17	10.00	0.12	71.43%
0.17	10.50	0.13	80.00%
0.17	11.00	0.15	88.57%
0.17	11.50	0.16	97.14%
0.17	12.00	0.18	105.71%
0.17	12.50	0.19	114.29%

Table 9.5: Worn panel failure criteria for various recorded winch loads for a 1 in 6 Slipway Gradient

## 9.5. Panel replacement criteria

Following the above results visual panel replacement criteria, based on the reduced bearing surface friction failure criteria can be developed to allow the simple recognition of failing slipway panels before high friction incidents occur.

### 9.5.1. Wear – Visual Inspection for High Friction Prevention

Using the reduced bearing surface friction failure criteria from section 9.4 in which the panel wear at which the equivalent friction coefficient (derived from the tribometer tests for a given lubrication regime) exceeds the design maximum friction coefficient (derived in section 2.2.1) is determined, visual guides to slipway wear failure criteria based on the percentage of the panel surface that remains undamaged are determined.

These are shown below for the 1 in 5 slipway incline case and preferred slipway lubricants, a full list of visual panel failure criteria for all slipway angles and lubrication regimes is presented in appendix I and the related RNLI documents [84-6]. Selected visual inspection failure criteria are shown below:

Lubricant	Slipway Gradient	Friction Coefficient	Expected Launches to Failure*	% Worn Surface Area
Freshwater	0.2	0.15	10.04	73.11%
Seawater	0.2	0.16	7.47	77.76%
Biogrease #1	0.2	0.08	65.21	42.11%
Marine grease	0.2	0.10	52.24	47.65%
Microball lubricant	0.2	0.08	26.84	40.76%

\*from typical 1mm parallel offset

Table 9.6: Worn panel failure criteria for various lubrication regimes for a 1 in 5 Slipway Gradient

Lubricant	Slipway Gradient	Friction Coefficient	Expected Launches to Failure*	% Worn Surface Area
Freshwater	0.18	0.15	7.31	80.42%
Seawater	0.18	0.16	4.86	85.54%
Biogrease #1	0.18	0.08	60.46	46.32%
Marine grease	0.18	0.10	47.49	52.41%
Microball lubricant	0.18	0.08	25.00	44.83%

\*from typical 1mm parallel offset

Table 9.7: Worn panel failure criteria for various lubrication regimes for a 1 in 5.5 Slipway Gradient

Lubricant	Slipway Gradient	Friction Coefficient	Expected Launches to Failure*	% Worn Surface Area
Freshwater	0.17	0.15	4.58	87.73%
Seawater	0.17	0.16	2.25	93.31%
Biogrease #1	0.17	0.08	55.72	50.53%
Marine grease	0.17	0.10	42.73	57.18%
Microball lubricant	0.17	0.08	23.15	48.91%

\*from typical 1mm parallel offset

Table 9.8: Worn panel failure criteria for various lubrication regimes for a 1 in 6 Slipway Gradient

### 9.5.2. Other Visual Wear Failure Criteria

In addition to slipway panel wear criteria based on the erosion of the panel bearing area, the following cases should be considered:

#### Cracking Around Panel Fixing Holes

During slipway surveys a number of panels were observed to exhibit cracks around the fixing holes used to attach the panel to the slipway, an example of this is shown below in fig. 92. If the crack is seen to extend from the hole to the panel edge the panel insufficiently secured to the slipway and is in danger of breaking free, thus this condition also constitutes a panel failure.

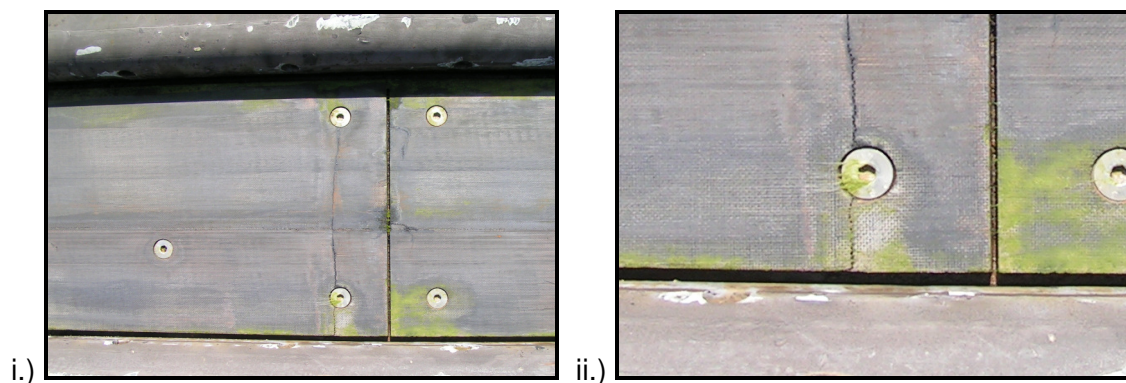


Fig 9.10: Worn Panel Failure Criteria by cracking around fixing hole area; ii.) shows a detail from image i.) where a crack can be clearly seen to extend from the fixing hole to the panel edge

#### Cracking to Leave Panel 'Islands'

From panel surveys it was noted that cracking on the panel often led to the creation of 'islands', where the crack fully describes a Composite region that is weakly held in place by remaining fibres or similar. Examples of these are shown below:

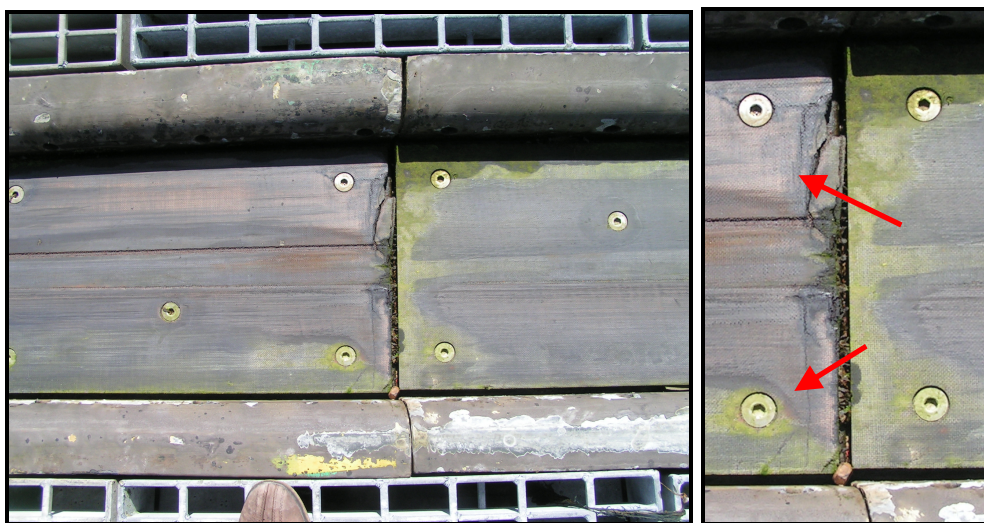


Fig 9.11: Worn Panel Failure Criteria – Islands shown on slipway panels from Padstow



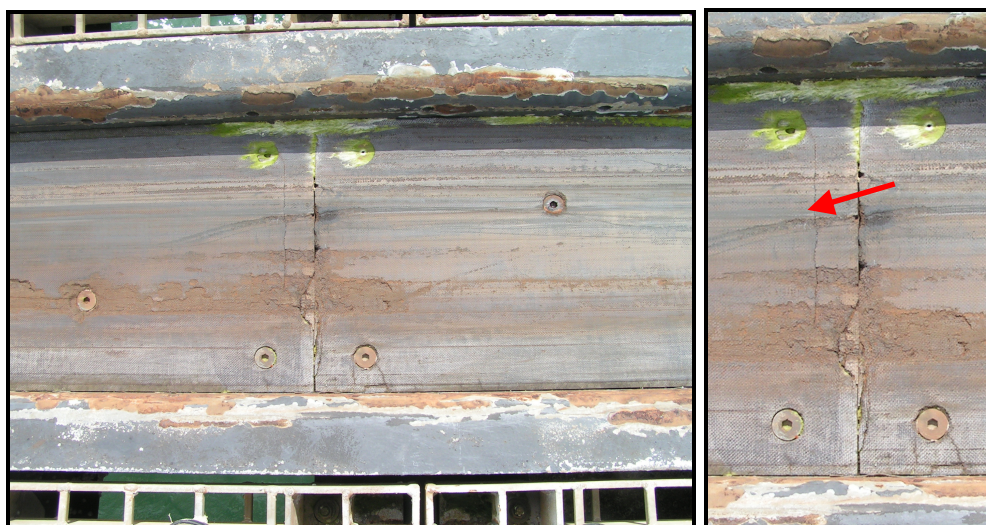


Fig 9.12: Worn Panel Failure Criteria – Islands shown on slipway panels from Tenby

These ‘islands’ are vulnerable to breaking free at any time and their weak bonding to the slipway can also result in vibration during slipway launch and recovery, with unpredictable friction results. Because of this ‘islands’ should be discounted when assessing the remaining slipway panel bearing area using the visual inspection criteria above.

### **9.5.3. Uneven Panel End Wear**

On real world slipways it is common for the panels to wear unevenly in places, when considering panel failure criteria, the furthest extent of the wear should be considered in order to evaluate the panel bearing area as shown below:

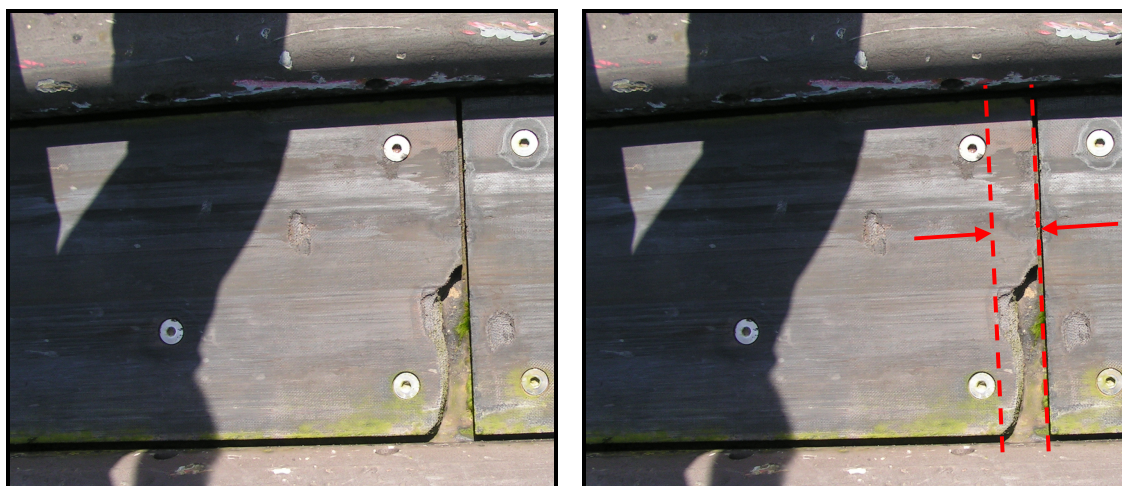


Fig 9.13: Worn Panel Failure Criteria – Uneven panel end wear from Padstow



#### 9.5.4. Other Visual Indicators of High Friction Causes

Scoring of the slipway panels as show below in fig. 9.14 indicates the presence of a raised a asperity or hard 3<sup>rd</sup> body particle in the contact. A straight scar along the slipway length indicates a raised asperity on the lifeboat keel, while a wavy scar indicates a 3<sup>rd</sup> body particle in the contact region.



Fig 9.14: Worn Panel Failure Criteria – i.) Scoring from raised keel section at Tenby, ii.) 3<sup>rd</sup> Body wear at Tenby

Scoring of the slipway panels due to raised sections on the lifeboat keel are a cause for immediate concern as repeated slipway launches in this condition will not only

result in high and unpredictable friction but also cause heavy wear to slipway panels. The friction contribution for a given keel imperfection can be assessed by analysing the size and shape of the wear scar using the formula shown. Slipway sections that have been worn in this way can continue to be used after the lifeboat keel imperfection is repaired, however the wear scar generated should be considered when assessing the slipway panel bearing area.

$$\mu_{\text{plough}} = (2/\pi) \cot \alpha$$

Where  $\alpha$  is the apex semi-angle of a conical asperity (10)

# 10 SUSTAINABILITY CONSIDERATIONS

---

## 10.1. Life Cycle Analysis

---

With the dwindling resources and environmental problems facing the world today the environmental performance of engineering products and systems is becoming an important aspect of the design process. This can be assessed using techniques such as Life Cycle Analysis (LCA) [87] which itemises the energy and material inputs and outputs of all stages in a system or design in order to calculate the overall impact. Due to the complexity involved in many real world design and systems it is common to set boundary conditions to limit the analysis to a level that can be successfully analysed using the available data.

In the case of slipway launched lifeboats this involves limiting the analysis to two aspects of the slipway operation, the environmental impacts of the materials consumed (e.g. worn slipway panels), and the environmental impacts of the lubricants used.

## 10.2. Materials Based Environmental Analysis

Materials based analysis involves an assessment of the environmental impacts involved in the manufacture and replacement of slipway lining panels over a 1 year period for a single slipway. This involves a number of assumptions; firstly the composite is modelled as a phenolic resin for assessment purposes as this is the bulk of the material. Secondly, environmental impacts are based on the wear rate recorded during tribometer experiments for each given lubricant regime including a stress factor of 1100% to simulate slipway panel misalignment effects. The stress factor is derived from FEA analysis for a parallel panel offset of 1mm. This reflects the real world situation where average panel misalignments at Tenby and Padstow recorded during slipway surveys are seen to approach this. Materials emissions data is compiled from the Cambridge Engineering Selector [88] software.

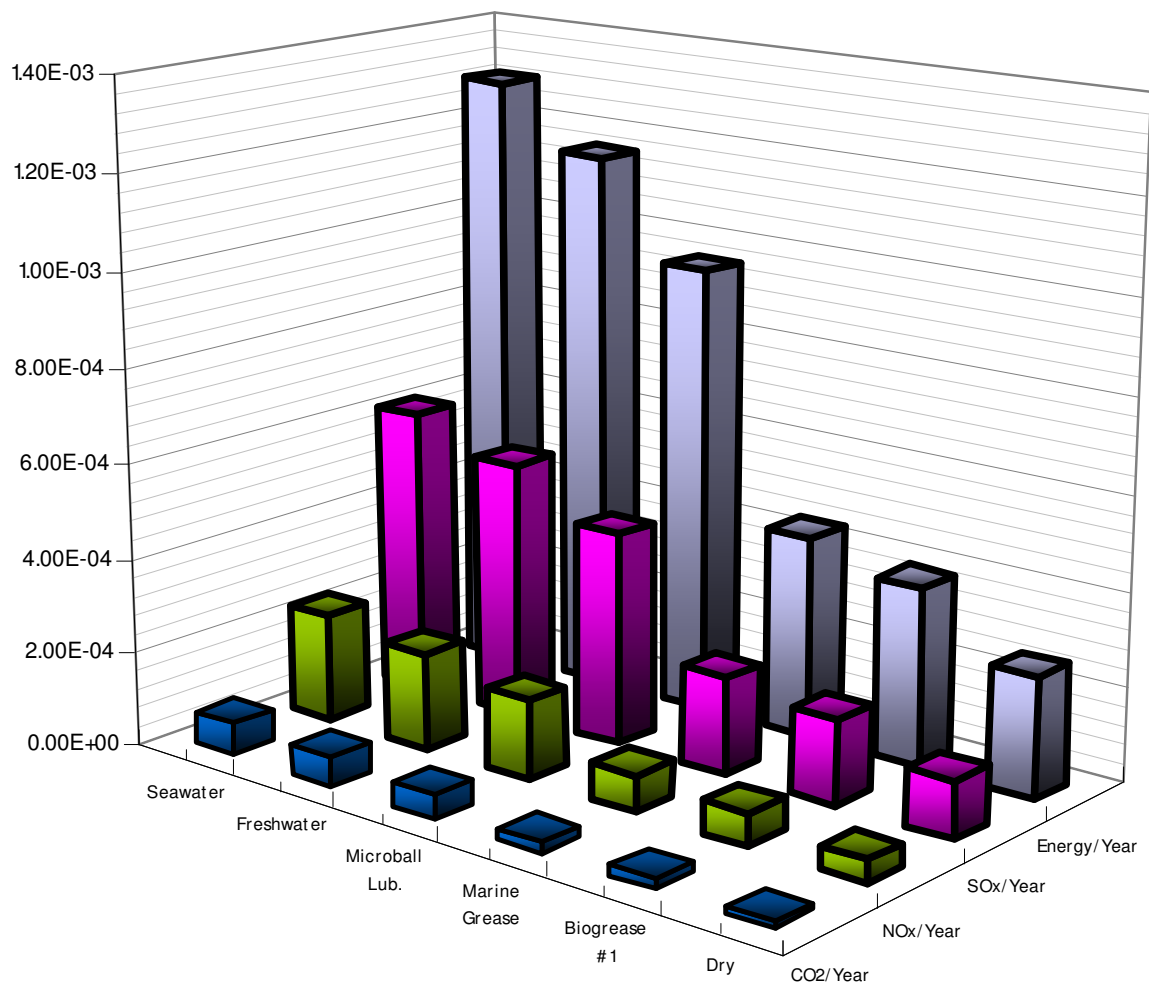


Fig. 10.1: Environmental Impacts due to material manufacture to replace slipway panel wear per year (CO<sub>2</sub> in kg/kg, NO<sub>x</sub>, SO<sub>x</sub> in g/kg, Energy in MJ/kg)

These results should be considered indicative rather than representing absolute values due to the variability of real world conditions and the approximations made during the calculations; however they are a useful tool for ranking the relative environmental

performance of slipway lubricants. It is also important to note that these results only represent the environmental impacts resulting from the manufacture of sufficient composite material to replace composite lining material loss and do not take into account the environmental impact resulting from the use of the lubricants themselves.

Lubricant	Specific Wear Rate (mm <sup>3</sup> /N.m)	Inc. 1mm Panel Misalignment						
		mm <sup>3</sup> / launch & recovery	W50	W500	CO <sub>2</sub> /Year	Energy/Year	NO <sub>x</sub> /Year	SO <sub>x</sub> /Year
Seawater	1.86E-04	2.05E-01	1.02E+01	1.02E+02	6.84E-05	1.29E-03	2.28E-04	6.08E-04
Freshwater	1.68E-04	1.84E-01	9.21E+00	9.21E+01	6.16E-05	1.16E-03	2.05E-04	5.47E-04
Microball Lub.	1.38E-04	1.52E-01	7.59E+00	7.59E+01	5.07E-05	9.53E-04	1.69E-04	4.51E-04
Marine Grease	6.28E-05	6.90E-02	3.45E+00	3.45E+01	2.30E-05	4.33E-04	7.68E-05	2.05E-04
Biogrease #1	5.56E-05	6.11E-02	3.05E+00	3.05E+01	2.04E-05	3.84E-04	6.80E-05	1.81E-04
Dry	3.70E-05	4.07E-02	2.03E+00	2.03E+01	1.36E-05	2.55E-04	4.53E-05	1.21E-04

Table 10.1: Environmental Impacts due to slipway panel wear per year

Use of the modified chamfer slipway panel is shown in section 8 to reduce edge stress effects by up to 55% of the original panel for a 1mm offset with a corresponding reduction in the wear at this point. This directly translates into the life cycle material analysis so that all emissions generated by material loss will be reduced by up to 45% when using the modified chamfer panel in preference to the original panel.

### 10.3. Lubricants based environmental analysis

Another area of in-use environmental impact is the lubricants used along the slipway, this is more difficult to assess, partly due to the difficulty in precisely calculating the amount of lubricant used on the slipway and partly due to the lack of life cycle database information on the impacts of the lubricants tested when released into a marine environment, however a rough environmental ranking can be inferred for the lubricants and this is shown below:

Lubricant	Mean Friction Coefficient: $\mu$	Wear Coefficient (Py)	Environmental Performance Rank
<b>Dry</b>	0.25	1.55E-12	1
<b>Seawater</b>	0.16	7.83E-12	2
<b>Freshwater</b>	0.15	7.04E-12	3
<b>Biogrease #1</b>	0.08	2.33E-12	4
<b>Marine grease</b>	0.10	2.64E-12	5
<b>Microball lubricant</b>	0.08	5.80E-12	6

Table 10.2: Slipway Lubricants Comparison Table

It should be noted that while dry sliding is recommended here due to its environmental performance, it is shown in chapter 6 to be unsuitable due to high friction performance.

## 10.4. Wider sustainability considerations

A true analysis of sustainability includes the wider issues of economic and social aspects, these two areas, combined with the environmental impacts make up the ‘three pillars’ of sustainability [89-90].

### 10.4.1. Economic Analysis

The economic aspect of this analysis assesses the monetary cost of the lubrication systems considered here per year, based on an assumption of 50 launches/recoveries per year. The materials cost of a freshwater lubrication system is calculated as £23.16 per year, based on a water cost of £1.28/m<sup>3</sup> [91], a flow rate of 0.2l/s and a running time of 30 minutes for each launch and recovery. The materials cost of a seawater lubrication system can be calculated by assessing the cost of the energy required to pump seawater from sea level to the top of the slipway. This is calculated as being £14.19 per year based on the same flow rate and running time as above, a mean lined slipway section height above sea level of 6m, a pump efficiency of 50% and an energy cost of £0.241/kWh [92].

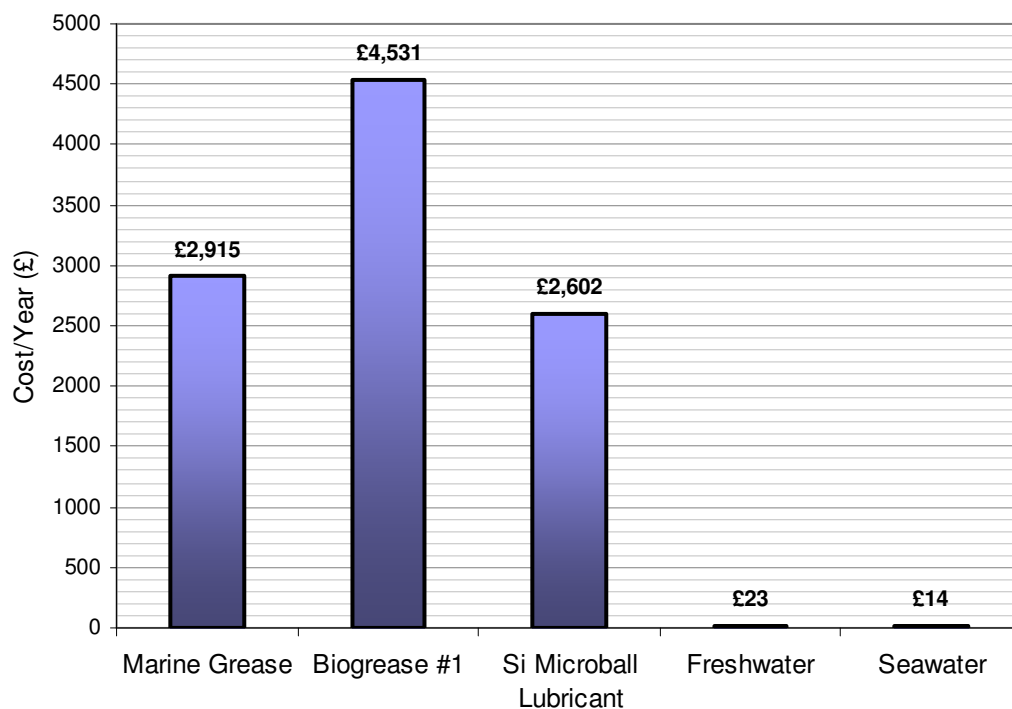


Fig. 10.2: Slipway lubricant costs / year

The cost of grease lubrication is assessed by considering the slipway to be coated with a layer of grease 1mm thick before each recovery (the grease remaining in place for launch as per current RNLI practice). In this way the volume of grease consumed during a year can be calculated and thus the cost of grease lubrication determined. This is calculated to be £2915

for marine grease, £2602 for the silicon microball lubricant, £4531 for biogrease #1. Biogrease #2 is shown to be unsuitable due to friction criteria in section 6. This analysis shows that there is an economic incentive to use water lubrication systems rather than grease lubrication systems as well as the environmental advantages identified in section 10.3. These lubricant costs, if applied to all non-roller RNLi slipway stations reveal that water lubrication systems have the potential to save the RNLi over £50k per year based on current marine grease practices, and over £80k per year if the current marine grease practice is directly replaced with biogrease #1.

The wear rate at a 1mm panel offset is shown to be reduced by 55% on average over all misalignment scenarios when using the modified chamfer panels developed in section 8. It is therefore reasonable to expect a corresponding reduction in the panel replacement costs; these are quoted as being £260k per year [12] extrapolating current panel failure rates across the whole RNLi slipway network. This would reduce to £117k per year using the modified chamfer panels, a saving of £133k per year.

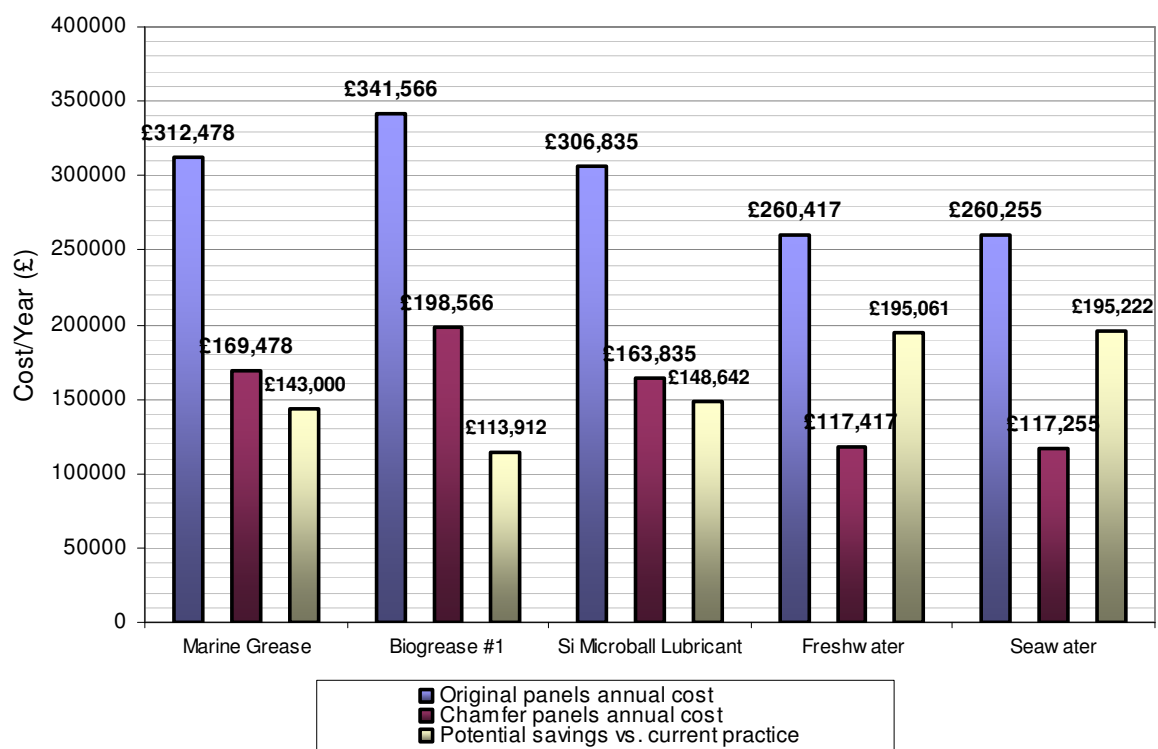


Fig. 10.3: Slipway operating costs/year – Original panel vs. chamfer panel

Combining the costs of marine grease lubrication and panel replacement gives a current annual operating cost of £312k, switching to chamfered slipway panels and a water based lubrication system will reduce this to £117k per year, a saving of £195k.

### **10.4.2. Social Considerations**

The third pillar of sustainability concerns social aspects; in this case this represents the importance to society of a well functioning search and rescue service. As an emergency service designed to protect human life and property rather than a consumer product the social aspects of RNLI slipway use are very important and these should be weighted accordingly in any overall life cycle analysis of lifeboat slipway operation. The implications of this are that any decisions regarding slipway lubrication and panel design must be made with primary regard to the successful operation of the RNLI search and rescue service, with friction and wear performance taking precedence.

### **10.5. Discussion**

---

In the case of slipway launched lifeboats the charitable status of the RNLI and its operation as a service rather than a business reduce the importance of the economic pillar as the service offered must always take precedence over financial considerations. This is similarly true for the environmental impacts; they must be set against the wider importance to society of a fully functioning lifeboat service. This said, the environmental impacts are noted to be very low, by way of comparison the CO<sub>2</sub> emission from one Tamar lifeboat fuel tank of marine diesel is  $1.79 \times 10^8$  times [93] the annual CO<sub>2</sub> emissions of the worst performing slipway lubricant. This shows that the environmental impacts of slipway operation are a tiny fraction of the impacts resulting from lifeboat use, to the point that they can be discounted from any full life cycle analysis of lifeboat operation.

Because of the very low environmental impacts and the significant social importance of a well functioning RNLI search and rescue service it is proposed that selection of slipway lubricants be conducted solely according to their friction and wear performance rather than by their life cycle performance ranking. It does however appear that biogrease #1 is able to match the performance of the marine grease while reducing the environmental impacts due to its increased biodegradability and is therefore a good candidate for substitution.

The economic aspects of this analysis are less clear, there are significant financial savings to be made from a switch to chamfered slipway panels and a water lubrication system, however the same caveats regarding social aspects discussed above apply, and any selection of lubrication regimes must be made with a high regard to protecting the functionality of the RNLI lifesaving service, i.e. friction and wear performance should take precedence over financial considerations. The experimental and FEA results above however indicate that water lubrication should be suitable in most cases.



The increased costs of biogreases in comparison with current marine greases is significant, and careful consideration of the relative importance of environmental and economic aspects should be made before biogreases are adopted for systemic use on lifeboat slipways. The more limited use of biogreases as a backup system for water lubricated slipways in preference to current marine grease practice should be considered however, as this will offer far lower financial disadvantages due to the reduced grease volumes likely to be used.

# 11 DISCUSSION

---

## 11.1. Contact Mechanisms

---

The contact is determined to be cohesive and abrasive, where asperities on relatively rough materials induce stresses deep into the sample material bulk. This is indicated by using the Plasticity Index to assess the degree of plastic deformation and by examining the contact behaviour under varying load, for cohesive contacts the friction coefficient will be roughly proportional to  $W$  the contact load, for adhesive contact the relationship will be closer to  $W^{1/3}$ .

### Plasticity Index

The plasticity index is calculated to be  $\psi = 14.4$  for the composite/keel contact, this is far higher than the  $\psi = 0.6$  values usually associated with adhesive contact and indicates that the composite will deform plastically and that cohesive wear mechanisms will dominate.

### Proportionality to Contact Load

Tribometer contact test results show direct proportionality between the friction force,  $F$  and  $W$ , the contact load. This indicates that cohesive, abrasive contact conditions are present.

## **Roughness and Transfer Layer Formation**

Microscope images of tribometer samples indicate that a reflective, smooth surface has been formed on the wear scar; this indicates the presence of a graphite transfer layer formed from the abrasion of the embedded graphite in the phenolic resin. This layer acts to reduce both the friction and wear on the sample compared to the plain phenolic resin case and also acts as a filler, smoothing the wear scar area and reducing the measured roughness. This accounts for the very low wear rates recorded and the decreasing roughness during the contact tests also shows the development of the contact film. The smooth surface is again indicative of cohesive abrasive wear without the larger pits and flakes usually associated with fatigue wear mechanisms.

### **11.2. Lubrication regime determination**

---

The tribometer contact tests conducted under lubricated conditions again show a direct correlation between the contact load,  $W$  and the friction force,  $F$  indicating that cohesive, abrasive contact mechanisms are present.

The lubrication regime is determined to be boundary film as indicated by the low sliding speeds on recovery. This is confirmed by the tribometer lubricated contact tests which indicate that the friction coefficient remains constant regardless of contact pressure variations as indicated by the boundary lubrication region of the Stribeck curve.

### **11.3. Dry Wear**

---

Dry sliding wear on the composite is observed to be consistent and directly proportional to the contact load,  $W$  which indicates that the contact is behaving as described by the Archard wear equation. This direct proportionality to  $W$  also indicates that the wear regime is consistent for these contact load and velocity values.

Under dry sliding conditions the wear rates recorded are noted to be very low, this is due to the formation of an abraded graphite transfer layer which acts to reduce both the friction and wear on the composite. The transfer layer is visible from light microscope images and is also inferred from profile interferometry results. The low wear rates recorded show that under these conditions sliding wear would not be sufficient to cause panel failure. As real world panels are noted to be failing this indicates that the real world contact conditions do not match those simulated in the laboratory. Slipway surveys and FEA analysis confirms that panel misalignment is present on lifeboat slipways and that this is an important contributor to wear,

further FEA analysis shows that this is likely to be the reason for the increased wear on real-world slipways with stress concentrations up to 25 times the aligned case encountered for the maximum offset of 5mm.

#### **11.4. Lubricated Wear**

---

Lubricated wear occurs here under boundary lubricated conditions. It is noted that the wear rates for lubricated sliding contact exceed those for dry sliding contact on the composite, which contrasts with the typical result of decreasing wear under lubricated conditions. This is due to the lubricants interfering with the formation of an abraded graphite transfer layer, the transfer layer acts to reduce both the friction and the wear in the contact and by interfering with its development this protection is lost under lubricated conditions. This also means that the use of the fractional film defect to analyse mixed lubrication conditions is not possible since this assumes that the wear decreases with the addition of lubricants.

The presence of a transfer layer acts to smooth the wear scar area and by recording the scar roughness a measure of the transfer layer development is formed. By comparing the wear scar surface roughness for lubricated contacts it can be seen that there is a good correlation between the scar roughness and the wear rate, supporting the theory that the addition of a lubricant affects the formation of a protective transfer layer.

#### **11.5. Contaminated Wear**

---

Contaminated wear refers to the case where particles such as sand are present in the contact. Screening wear tests indicate that the addition of sand to the contact has a severe adverse effect on the wear rate, up to 200 times the uncontaminated case for seawater lubrication.

The impact of adding sand to the contact was investigated following concerns expressed at Sennen Cove that the presence of wind blown sand on the recovery slipway may be affecting the friction and wear of the slipway lining. While it is shown that the wear and friction performance of the lining is adversely affected by sand particles the expected wear does not match any slipway survey observations. In fact the presence of third body particles along the slipways was infrequent and, if present usually consisted of isolated animal shells rather than sand. For this reason, systemic real world contaminated wear is discounted here.

## 11.6. Real World Wear

---

Slipway panel surveys conducted at Tenby and Padstow confirm observations from other slipways that panel misalignment is present and significant. FE analysis in section 7 develops the implications of these panel misalignments with wear rates at the stress concentrations caused by panel misalignments reaching 25 times the aligned case for the maximum 5mm offset tested, and over 11 times the aligned wear rate for a 1mm panel offset that matches the mean panel misalignment from slipway panel surveys.

Slipway panel misalignment height distributions are found to be heavily skewed with only two instances of misalignments greater than 2mm on all panels surveyed. These highly misaligned panels will have a disproportionately adverse impact on friction and wear along the whole slipway and this immediately prompts a recommendation for a maximum slipway panel offset of 2mm to be adopted. This should be achievable without significantly altering panel fitting procedures.

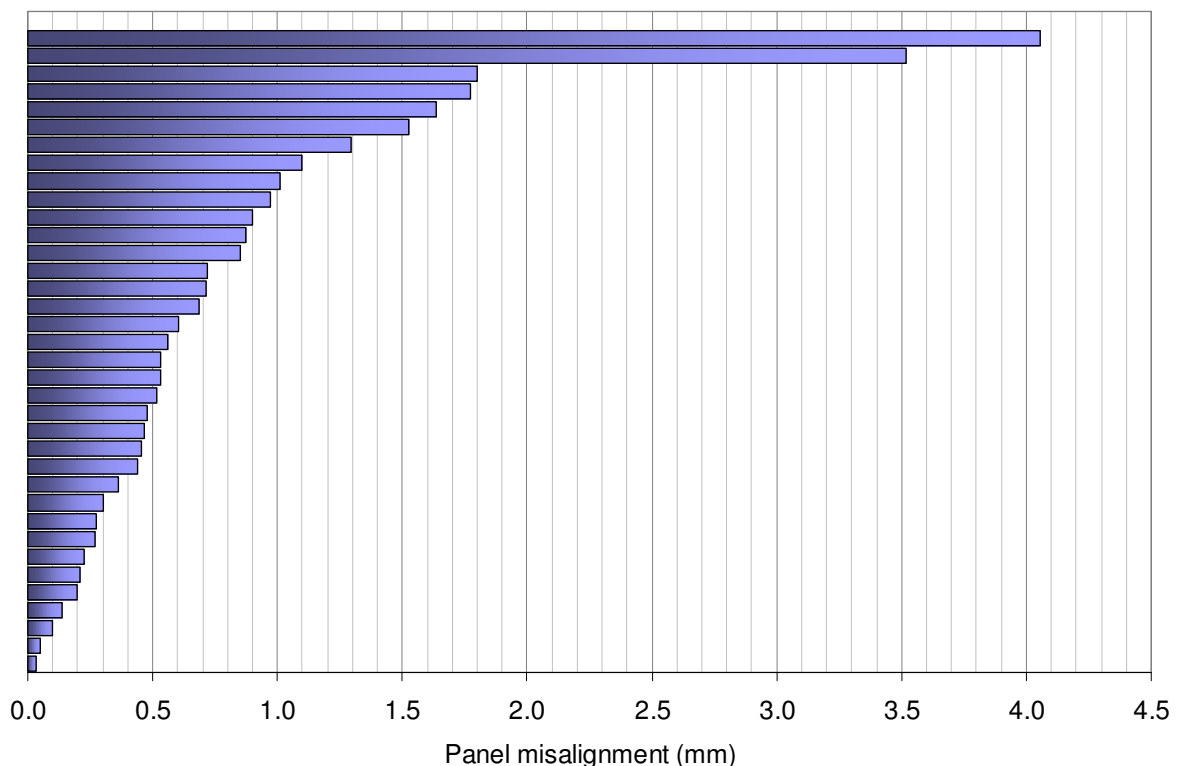


Fig. 11.1: All slipway panels misalignment heights

### **11.7. Dry Sliding Friction**

---

Tribometer friction tests show the friction coefficient,  $\mu$  to be directly proportional to the applied load,  $W$  this indicates that deformation is the primary friction mechanism. Adhesive friction mechanisms would typically be proportional to  $W^{1/3}$  rather than  $W$ .

From slipway geometry analysis it is shown that increasing the winch line pull specification from 12 to 13.7 tonnes allows the limiting friction to rise to  $\mu=0.2$  from  $\mu=0.15$  for a 1 in 5 slipway. From winch load analysis it is shown that  $\mu=0.167$  presents the limiting friction coefficient for a 1 in 6 slipway, for a 1 in 5 slipway this is shown to be 0.2. Tribometer friction tests show the composite recording a friction coefficient of 0.25 during the extended tests with a mean of 0.2 during the contact load testing. These results exceed the friction specifications calculated above making the composite unsuitable for unlubricated use.

Further evidence against the unlubricated use of the composite is provided by observations at Padstow, which indicates that under dry sliding conditions launch velocities can cause the keel/composite contact to exceed the Pressure-Velocity limit of the material. This leads to a severe adverse change in both friction and wear regimes and may cause both to exceed specified limits. The use of lubricants on the slipway will reduce this effect in two ways, the reduction in friction coefficient will reduce the heat energy generated from sliding and the presence of lubricant will also improve heat dissipation from the contact surface.

### **11.8. Lubricated Sliding Friction**

---

Tribometer results show that all lubricants except biogrease #2 will meet the friction specification of  $\mu=0.167$  on a 1 in 6 slipway and are thus suitable for slipway use. The silicon microball lubricant is determined to be unsuitable for use due to the dangers of microball accumulation on or around the slipway and the unexceptional friction and wear performance exhibited. This leaves seawater and freshwater lubrication, and two greases for direct application to the slipway. It is recommended to use either fresh or seawater lubrication on slipways due to the reduced environmental and safety impacts compared with manually applied grease. As this research has shown, friction and wear can vary significantly from laboratory test values in the real world, for this reason it is recommended to use biogrease #1 as a direct substitute for the marine grease should friction coefficients outside of the specification be encountered while using water lubrication. The biogrease #1 is selected in preference to the marine grease due to its reduced environmental impact and comparable performance.

## 11.9. Contaminated Friction

---

The effects of third party particles and lubricant contamination at the keel / slipway contact are assessed using tribometer testing.

### **Sand Contamination**

The effects of third party particles and lubricant contamination at the keel / slipway contact are assessed using tribometer testing. The coxswain at Sennen Cove had expressed concern that wind-blown sand along the slipway lining may be having an adverse effect on the slipway performance and thus tests were conducted into the effects of this on friction and wear. It was found that the presence of sand had a serious effect on the wear rate of the composite, screening tests indicate this is between 30-200 times the uncontaminated case for a given lubricant regime. Friction results were less clear with the marine grease/sand mixture actually showing reduced friction compared with the uncontaminated case. All other lubricant/sand combinations tested showed an increase in the friction coefficient to beyond the  $\mu=0.167$  maximum specification for a 1 in 6 slipway. Also noteworthy is the standard deviation of the friction coefficient under contaminated conditions, this is shown to be far higher than the uncontaminated contact in all but the marine grease/sand case which indicates that while the friction coefficient recorded may not substantially exceed the 1 in 5 slipway specification of  $\mu=0.2$ , the friction variability is far worse.

Slipway surveys however failed to identify any instances of wind-blown sand, or the high plane wear on panels that would be expected if this was the case. Because of the seemingly low incidence of sand contaminated contact it is likely that this can be discounted as a systemic factor in slipway lining performance however, the tribometer tests indicate that should sand contamination be encountered the use of grease on the slipway is most effective at mitigating the adverse effects.

### **Water Contamination**

Water contamination is likely under grease lubricated conditions as the lifeboat nears sea level at the end of the slipway. Consequently a marine grease/water mixture is tribometer tested. The results indicate that while water contamination does have an adverse effect on the friction performance of marine grease it remains well inside the  $\mu=0.167$  friction specification.



## 11.10. Real world friction

Friction in the real world case is shown in the FE analysis in section 7 to be dependant on slipway panel geometry and alignment effects as well as the lubricant regimes in place. This manifests as an additional contribution to the friction coefficient so that the overall friction coefficient along the slipway can be expressed as:

$$\mu_{\text{overall}} = \mu_{\text{lubrication}} + \mu_{\text{misalignment}} + (\mu_{\text{ploughing}} + \mu_{\text{contaminant}}) \quad (17)$$

Where  $\mu_{\text{overall}}$  is the overall friction coefficient along the slipway,  $\mu_{\text{lubrication}}$  is the friction coefficient derived from the lubricated sliding tribometer tests,  $\mu_{\text{misalignment}}$  is the friction coefficient contribution resulting from the panel geometry and panel misalignment. The terms  $\mu_{\text{ploughing}}$  and  $\mu_{\text{contaminant}}$  represent the friction contributions of ploughing keel imperfections and 3<sup>rd</sup> body wear particles such as sand respectively, these may or may not be present along any given slipway.

Lubrication regime friction coefficient contribution:  $\mu_{\text{lubrication}}$

Lubricant	Dry	Marine Grease	Microball Lub.	Seawater	Freshwater	Biogrease #1	Biogrease #2
Mean Friction Coefficient: $\mu$	0.252	0.095	0.082	0.156	0.146	0.084	0.171

Panel Misalignment friction coefficient contribution:  $\mu_{\text{misalignment}}$

Offset dist. (mm)	Parallel Misalignment		Angled Misalignment		Skewed Misalignment	
	Original	Chamfer	Original	Chamfer	Original	Chamfer
0	0.028	0.054	0.028	0.054	0.028	0.054
1	0.503	0.109	0.247	0.227	0.164	0.107
2	1.035	0.210	0.492	0.464	0.368	0.265
3	1.565	0.313	0.742	0.520	0.582	0.385
4	1.752	0.417	0.984	0.662	0.827	0.606
5	2.194	0.519	1.215	1.123	1.042	0.806

Table 11.1: Lubricant and panel misalignment effects on friction coefficients

Using the data in table 11.1 the overall friction coefficient can be calculated for any given lubricant regime and panel misalignment scenario. The additional potential contribution from a raised keel section as initially found on the Tamar lifeboat prototype can be calculated using the ploughing friction formula in section 1.6.2.2. if the slope of the raised asperity is known. For the Tamar prototype case this was calculated as:  $\mu_{\text{ploughing}} = 0.408$ .

Asperity semi-angle (°)	0	5	10	15	20	25	30	35	40	45
$\mu_{\text{ploughing}}$	0.000	0.056	0.112	0.171	0.232	0.297	0.368	0.446	0.534	0.637

Table 11.2: Asperity ploughing contribution to friction coefficient by asperity semi-angle

Contaminated friction effects are harder to evaluate, however these are unlikely to occur regularly as no significant debris was seen on any of the slipways surveyed and there are no reports of the systemic high friction and wear that would be expected if this were a systemic feature of the keel/slipway contact. Friction effects can be assessed to some extent however using the table below which summarises the contaminated lubrication tribometer contact tests. These are for guidance only however as real world contaminated friction will depend on the amount and nature of the debris concerned.

Lubricant	Uncontaminated friction coefficient	Contaminated friction coefficient	Contaminant contribution to friction: $\mu_{\text{contaminant}}$
Dry	0.253	0.336	0.083
Marine Grease	0.095	0.071	-0.025
Microball Lub.	0.082	0.189	0.107
Seawater	0.156	0.212	0.056
Freshwater	0.146	0.217	0.071
<b>Mean:</b>			<b>0.058</b>

Table 11.3: Contaminant contribution to friction coefficient by lubrication regime

### 11.11. Sustainability Considerations

The life cycle analysis in section 10 indicates that the environmental impacts of using lubricants along the slipway are low in comparison with the impacts inherent in running a diesel powered lifeboat. It is also noted that the social aspects of a well functioning search and rescue service around the coast of the UK and Ireland far outweigh these impacts in any full sustainability analysis. For these reasons it is not recommended that lubricant selection be made on the basis of environmental performance but rather on the functional friction and wear performance.

Economic analyses in section 10.4.1 shows large variations in the annual operating costs associated with slipway operation, for an organisation entirely funded by charitable donations such as the RNLI this may prove an important aspect of any solution adopted. If grease lubrication is to be used systemically along the slipway as currently practiced at Selsey, Bembridge and the majority of composite lined slipway stations then there is a significant cost increase of over 50% associated in switching to the more eco-friendly biogrease #1 compared with the marine grease currently used. For this reason the systemic use of biogrease along the composite slipway as a direct replacement for the use of marine grease cannot be recommended as the environmental benefits are not adjudged to justify the increase in cost. This is especially valid when comparing the very low environmental impacts

and annual operating costs of water lubrication systems, which should also offer suitable slipway performance. If, as recommended, the use of grease along the slipway be restricted to a backup for predominately water lubrication systems the net annual associated cost of using biogreases is likely to be far less and so substitution can be recommended.

The annual costs of current slipway operating procedures using marine grease and normal composite panels is estimated to be around £312k per year across all slipway stations. By adopting the chamfered slipway panels developed in section 8 the reduction in friction concentrations along the slipway will allow water lubrication to be used reliably. The combination of the lower wear rates due to inherent panel misalignment offered by the chamfered slipway panels and the elimination of expensive greases used regularly along the slipway can reduce this cost to £117k per year. This represents a saving of £195k per year and thus provides an additional motivation for adopting chamfered panels and water lubrication systems.

## **11.12. Implications**

---

### **Implications for Slipway Lubricant Practice**

The reciprocating tribometer experiments in section 6 indicate that under good contact conditions the composite lining is only able to reliably exceed the friction specifications developed in section 2.2.1 if a lubricant is used. All lubricants tested were able to reduce the friction coefficient to below this level.

Wear results were seen to be uniformly low under ideal conditions for all lubricants tested, even when contaminated with sand. Wear is seen to be a problem along real world slipways however, and the FE analysis in section 7 details the effects of the contact moving away from the perfectly aligned plane sliding case which would seem to account for much of the wear exhibited by real world slipways rather than the choice of lubricants.

With all lubricants tested performing up to the required friction standard selection criteria and wear determined to be more dependant on panel alignment than lubricants used, selection is now based on safety and sustainability factors. When considering sustainability aspects and the dangers of manual application of grease to the slipway which in part prompted this research, the lubrication regimes of freshwater and seawater are proposed, as these are the only lubricants that can be applied to the slipway without manual aid. Of the two, seawater has the slightly lower environmental impact, though the impacts of both are low and practical considerations should take precedence when choosing between the two.

The use of greases or other lubricants manually applied to the slipway is shown to be unnecessary here as freshwater or seawater lubrication performs sufficiently well. Manually applied slipway lubricants are shown to function well at reducing friction coefficients, but doubts are expressed as to the environmental impact of using some of these long term. Microball lubricant is considered to be particularly unsuitable as it contains silicon 'microspheres' these were shown to accumulate into a hard mass during testing and it is felt that the accumulation of these microspheres could affect the friction reliability of the slipway as well as the local environment. Marine grease also shows excellent friction characteristics but the guidelines for use imply that it is not particularly suitable for open water use and the low biodegradability means that there is an increased chance of bioaccumulation. The biogreases tested are shown to perform well, with biogrease #1 in particular exceeding the performance of the marine grease currently used. This suggests the possibility of direct substitution with the marine grease, with the greater biodegradability of biogrease #1 reducing the overall environmental impact in this way. Freshwater and seawater lubrication are shown to be effective here and the manner of their use addresses the safety problems associated with manually applying grease to the length of the slipway. An added benefit of using running water along the slipway is that this will help to clear the slipway of debris, reducing the friction and wear effects of 3<sup>rd</sup> body abrasion.

Following this research it is recommended that freshwater or seawater lubrication is adopted for all slipways. In isolated incidences of high friction along the slipway the use of marine biogrease #1, in a similar manner to existing marine grease application procedures is recommended, however, this should only be used in isolated incidents, if high friction consistently persists along the slipway consideration should be given to slipway panel inspection for wear and misalignment as detailed in section 9.5.

### **Implications for panel lifespan & replacement procedure**

Slipway panel lifespan and replacement criteria are detailed in section 9.5 and appendix I. Due to the relatively low panel lifespan predicted at the maximum wear rate for standard slipway panels the slipway should be inspected before each recovery in this case. This allows potential problems to be identified before the lifeboat mounts the slipway and mitigative measures such as grease application to be taken if potential high friction is expected.

Section 8 indicates that the wear on chamfered panels is significantly lower than on the original panels and so the inspection schedule can be relaxed here, it is hoped that by using

these panels slipway inspection will only be necessary as high friction becomes apparent due to high winch loadings during recovery. However, in the initial stages of assessment these panels should be inspected before each recovery in the same way as for standard slipway panels until the slipway performance prompts confidence in relaxing the inspection schedule.

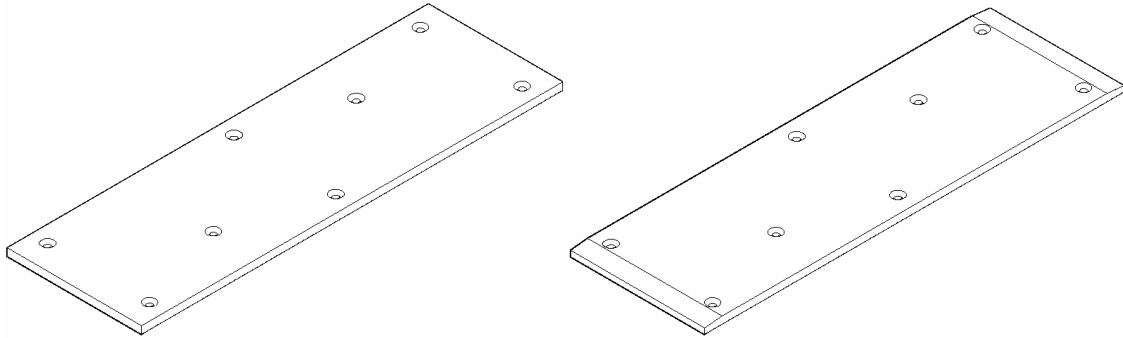


Fig. 11.2: Original (left) and Modified (right) Slipway Panels

# 12 CONCLUSIONS

---

The research conclusions can be summarised as follows:

- It is shown that consistent, low friction using composite slipway panels is only reliably achievable using lubricants.
- Lubrication can take two main forms, the manual application of grease to the slipway before each launch and recovery, or the use of running water along the slipway.
- The use of biogrease #1 is shown to be as effective as current marine grease practice and this can be considered a candidate for direct substitution with due consideration given to the increased cost of biogrease #1.
- The use of water lubrication is shown to be effective under good slipway alignment conditions and is also shown to offer significant environmental and economic benefits.
- Current slipway winch specifications are shown to be the limiting factor when calculating friction specifications on 1 in 5 slipways and these should be increased as described in section 2.2.1.
- The effects of contaminated contact conditions (i.e. wind blown sand) are shown to be severe, however real world instances of this were rare and this can be discounted as a systemic factor in slipway panel wear.
- Slipway panel geometry and alignment is shown to be an important factor in determining the real world friction and wear performance of composite slipway panels.
- The use of a modified chamfer panel in place of the current panel design is shown to reduce the effects of panel misalignments leading to reduced wear and friction on slipway panels.
- Slipway panels are shown to fail due to friction specifications rather than panel material failure so that slipway wear performance can be assessed at each slipway station using winch loads criteria.
- Slipway panel failure criteria can be developed by assessing the bearing area of the panel surface.
- Reducing panel misalignment and using chamfered slipway panels is shown to more than double current panel lifespans.
- Using water lubrication and chamfered slipway panels could potentially save up to £195k per year whilst improving the safety, reliability and panel lifespan of slipway launched lifeboat operation.

# 13 RECOMMENDATIONS

---

Recommendations for slipway lifeboat operation derived from this research are shown below:

- Winch specifications for various slipway angles should be assessed using calculations outlined in section 2.2.1. This shows that increasing the winch line pull specification from 12 tonnes to 13.7 tonnes for 1 in 5 gradient slipways will allow for a far greater friction coefficient tolerance. By the same analysis, for shallower 1 in 6 slipways the winch specification can be relaxed to 11.5 tonnes.
- It is recommended to adopt water lubrication systems across the RNLI slipway station network as this is shown to be effective and reliable while also reducing operating costs.
- It is recommended that the use of greases along the slipway be relegated to a backup system for water lubrication due to the economic, environmental and safety implications inherent in direct grease application to the slipway.
- The direct substitution of marine grease with biogrease #1 is shown to be feasible and this should be considered with appropriate assessment of the relative importance of economic and environmental factors.
- Panel misalignments are shown to be a significant factor in real world slipway friction and a maximum panel alignment specification of 2mm is recommended to prevent high friction and wear occurrences.
- Slipway condition monitoring using winch loading is shown to be effective at assessing slipway performance and it is recommended that this practice be adopted across all slipway stations.
- Individual slipway panel condition can be assessed using the bearing area failure criteria developed in section 9 and this is recommended for adoption in conjunction with winch load monitoring.



# REFERENCES

---

1. **Warner, O:** 'The lifeboat service: a history of the Royal National Lifeboat Institution, 1824-1974' London : Cassell, (1974)
2. **Hudson, F, D:** 'The design and development of modern SAR craft - A personal view' The Royal Institution of Naval Architects, Drydocks, Launching, and Shiplift Conference, pp79-82. (2003)
3. **Leach, N:** 'A Century of RNLI Motor Lifeboats' Landmark Publishing Ltd. (2007)
4. **Clayton Engineering:** 'Trial Results: New Tenby Boathouse Winch Instrumented Line Pulls – 10/05/05'. A study for the RNLI (2005)
5. **Clayton Engineering:** '2<sup>nd</sup> Instrumented Line Pull Trial Results: New Tenby Boathouse Winch - 10/08/07'. A study for the RNLI (2007)
6. **Clayton Engineering:** 'Trial Results: New Padstow Boathouse Winch Instrumented Line Pulls – 06/06/06'. A study for the RNLI (2006)
7. **RNLI:** 'Bembridge Slipway Trial: April 1999'. Internal RNLI Document (1999)
8. **RNLI:** 'Bembridge Slipway Trial: October 2001'. Internal RNLI Document (2001)
9. **Clayton Engineering:** 'Instrumented Line Pull Trial Results: Mumbles Boathouse Winch – 10/08/07'. A study for the RNLI (2007)
10. **RNLI:** 'Selsey Slipway Winch Load & Keelway Lining Trial Report: March 2002'. Internal RNLI Document (2002)
11. **RNLI:** 'Selsey Slipway Trial: November 2002'. Internal RNLI Document (2002)
12. **Austen, S:** RNLI Head of Engineering Support - Private communication, 5<sup>th</sup> June (2008)
13. **Plint, G:** 'Specification and Design of Tribological Tests'. Cambridge University Tribology Course. Plint and Partners Ltd. (2000)
14. **Williams, J. A:** 'Engineering Tribology', Oxford Science Publications, p166 (1998)
15. **Archard, J.F:** 'Contact and Rubbing of Flat Surfaces'. Journal of Applied Physics 24(8) pp981-988 (1953)
16. **Hutchings, I:** 'Tribology – Friction and Wear of Engineering Materials', Arnold, p86 (1992)
17. **Bhusan, B:** 'Introduction to tribology' Wiley, p346 (2002)
18. **Hutchings, I:** 'Tribology – Friction and Wear of Engineering Materials', Arnold, p122 (1992)
19. **Stolarski, T.A:** 'Tribology in machine design', Butterworth-Heinemann, p14 (2000)
20. **Sinha, Sujeet, K:** 'Wear Failures of Plastics' p1019-27, in 'ASM Handbook: Failure Analysis and Prevention Vol. 11: Failure Analysis and Prevention', ASM International (2002)
21. **Dowson, D:** 'History of Tribology' Professional Engineering Publishing Limited, p187-90 (1998)
22. **Ludema, K.C:** 'Friction, Wear, Lubrication: A Textbook in Tribology' CRC Press, pp73-81 (1996)
23. **Hutchings, I:** 'Tribology – Friction and Wear of Engineering Materials', Arnold, p29 (1992)
24. **Archard, J.F. and Kirk, M.T:** 'Lubrication at Point Contacts'. Proceedings of the Royal Society: pp532-549 (1960)
25. **Rowe, CN:** 'Some Aspects of the Heat of Absorbtion in the Function of a Boundary Lubricant'. ALSE Trans. 9, pp101-111. (1966)

- 26. Thompson, R.A, Bocchi, W:** 'A Model for Asperity Load Sharing in Lubricated Contacts'. ALSE Trans. 15, pp67-69. (1972)
- 27. Stolarski, T.A:** 'Adhesive Wear of Lubricated Contacts'. TRIBOLOGY International – August 1979: pp169-179, IPC Business Press. (1979)
- 28. Stolarski, T.A:** 'Probability of Scuffing in Lubricated Contacts'. Proceedings of the Institute of Mechanical Engineers 203: pp361-369. (1987)
- 29. Stolarski, T.A:** 'A System for Wear Prediction in Lubricated Sliding Contacts'. Lubrication Science 8(4): pp315-350. (1996)
- 30. Stachowiak, G. W, Batchelor, A:** 'Engineering Tribology' Butterworth-Heinemann, pp305-18 (2001)
- 31. Stolarski, T.A:** 'Tribology in machine design', Butterworth-Heinemann, pp35-8 (2000)
- 32. Hutchings, I:** 'Tribology – Friction and Wear of Engineering Materials', Arnold, p58 (1992)
- 33. Bhusan, B:** 'Introduction to tribology' Wiley, p425-6 (2002)
- 34. Hegadekatte, V, Huber, N, Kraft, O:** 'Finite element based simulation of dry sliding wear' Modelling and Simulation in Materials Science and Engineering issue 13, Institute of Physics Publishing, pp57-75 (2005)
- 35. Pödra, P, Andersson, S:** 'Finite element analysis wear simulation of a conical spinning contact considering surface topography' WEAR, Vol. 224, pp13-21. (1999)
- 36. Molinari, J. F, Ortiz, M, Radovitzky, R and Repetto, E, A:** 'Finite-element modelling of dry sliding wear in metals' Engineering Computations, Vol. 18 No.3/4 pp592-609 (2001)
- 37. Bilkay, O, Anlagen, O:** Computer simulation of stick-slip motion in machine tool slideways' Tribology International, Vol. 37, pp347-351 (2004)
- 38. Wriggers, P:** 'Finite element methods for contact problems with friction' Tribology International, Vol. 29 No. 8, pp651-658 (1996)
- 39. Pödra, P, Andersson, S:** 'Wear simulation with the Winkler surface model' WEAR, Vol. 207, pp79-85. (1997)
- 40. Pödra, P, Andersson, S:** 'Simulating sliding wear with finite element method' Tribology International, Vol. 32, p71-81. (1999)
- 41. Öqvist, M:** 'Numerical simulations of mild wear using updated geometry with different step size approaches' WEAR, Vol. 249, pp6-11. (2001)
- 42. Kim, N, H, Dongki, W, Burris, D, Holtkamp, B, Gessel, G, Swanson, P, Sawyer, W, G:** 'Finite element analysis and experiments of metal/metal wear in oscillatory contacts' WEAR, Vol. 258, pp1787-1793. (2005)
- 43. Popov, V, Ostermeyer, G:** 'Numerical Simulation Methods in Tribology: possibilities and limitations' Tribology International, Vol. 40, p915 (2007)
- 44. Popov, V, Psakhie, S, G:** 'Numerical Simulation Methods in Tribology' Tribology International, Vol. 40, pp916-923 (2007)
- 45. Andersson, S, Söderberg, A, Björklund, S:** 'Friction models for sliding dry, boundary and mixed lubricated contacts' Tribology International, Vol. 40, p580-587. (2007)
- 46. Walker, F:** 'An overview of ship launching' The Royal Institution of Naval Architects, Drydocks, Launching, and Shiplift Conference, pp79-82. (2003)
- 47. Salisbury, J, Dobb, J. M:** 'Recent dynamic launches at Barrow-in-Furness: Prediction and Reality' The Royal Institution of Naval Architects, Drydocks, Launching, and Shiplift Conference, pp93-109. (2003)

48. **Bull, S.J. and Birmingham, R.W:** 'Slip Launched Lifeboats: Materials for Keel and Keelway'. A study for the RNLI (1997)
49. **Bull, S.J, Diebel, T, Malkow, T and Birmingham, R. W:** 'Friction and Wear of Composite Materials for Keels of Slip Launched Lifeboats'. A study for the RNLI (1999)
50. **Bull, S.J, Horvathova, K, McNaught, R and Birmingham, R:** 'Friction and Wear of Alternative Composite Materials for Keels of Slip Launched Lifeboats'. A study for the RNLI (1999)
51. **Sauter, B:** RNLI Shoreworks Projects Engineer - Private communication (2008)
52. **Hudson, F, D:** 'The design and development of modern SAR craft - A personal view' The Royal Institution of Naval Architects, Drydocks, Launching, and Shiplift Conference, pp1-17. (2003)
53. **Wake-Walker, E:** 'The Lifeboats Story', Sutton Publishing Ltd (2007)
54. **Bailey, D:** 'A New RNLI Lifeboat: The Tyne Class Fast Slipway boat' RINA Spring Meeting (1993)
55. **Padstow Slipway Station:** Website, accessed (06/2008)
56. **Tamar Lifeboat Schematics:** DML Devonport Shipbuilding (2003)
57. **RNLI:** Draft Doc. No. TSK2539-0001, (2005)
58. **Low Friction Coated Steel:** Manufacturers data sheet (2006)
59. **Jute / Phenolic Composite:** Factory site visit (06/2005)
60. **Sinha, Sujeet, K:** 'Wear Failures of Plastics' in 'ASM Handbook: Failure Analysis and Prevention Vol. 11: Failure Analysis and Prevention', ASM International, p1022 (2002)
61. **RNLI Slipway Lifeboat Coxswains:** 'Slipway Lifeboat Launch and Recovery Procedure' Internal RNLI document (2002)
62. **Rudwick, M:** RNLI Selsey slipway station coxswain – private interview (09/10/06)
63. **Simmonds, S:** RNLI Bembridge slipway station coxswain – private interview (02/11/06)
64. **George, T:** RNLI Sennen Cove slipway station coxswain – private interview (23/08/06)
65. **Greenslade, P:** RNLI The Lizard slipway station coxswain – private interview (23/08/06)
66. **Thomas, A:** RNLI Tenby slipway station coxswain – private interview (27/07/07)
67. **Tarby, A:** RNLI Padstow slipway station coxswain – private interview (24/08/06)
68. **Dunn, T, Kennedy, A and Tibbs, J:** 'Launching in the 21st Century'. Drydocks Launching and Shiplift, London, UK: 87-91. Royal Institute of Naval Architects. (2003)
69. **Pattison, N, Dixon, M and Hodder, C:** 'Launching and Docking: Experiences at VT Shipbuilding'. The Royal Institution of Naval Architects, Drydocks, Launching, and Shiplift Conference, pp35-40. (2003)
70. **Composite Slipway Lining Manufacturers:** 'Summary of Static Friction Load Testing' Internal Document (2006)
71. **Composite Slipway Lining Manufacturers:** 'Summary of Dynamic Friction Load Testing' Internal Document (2006)
72. **Composite Slipway Lining Manufacturers:** 'Scar Wear Testing' Internal Document (2006)
73. **Plint, G:** 'TE57 Pressurised Lubricity Tester: Operating Instructions' Phoenix Tribology Ltd (2002)
74. **Plint, G:** 'TE92 Rotary Tribometer: Operating Instructions' Phoenix Tribology Ltd (2002)
75. **Zygo Corporation:** 'MetroPro Reference Guide' Zygo Corporation (2004)

- 76. Garland, N and Hadfield, M:** 'In-use Tribological Analysis of Hydrocarbon Refrigerants applied to the Hermetic Compressor' Proceedings of the second International Conference on Tribology in Environmental Design, Bournemouth, Professional Engineering Publishing, pp. 193-203 (2003)
- 77. Garland, N and Hadfield, M:** 'Tribological Analysis of Hydrocarbon Refrigerants applied to the Hermetic Compressor' International Journal of Materials and Design (2003)
- 78. Sheasby, J. S, Caughlin, T. A, Blahey, A. G, Laycock, K. F:** 'A Reciprocating Wear Test for Evaluating Boundary Lubrication' Tribology International 23(5) pp 301-307 (1990)
- 79. Johanssen, E, Hogmark, S, Nilsson, H, Redelius, P:** 'Compositional Changes in Lubricated Sliding Metal Surfaces Related to Seizure' Proc. 5th Int. Congress on Tribology, Eurotrib Vol. 1, pp 174-180 (1989)
- 80. Samuels, B, Richards, M. N:** 'The Transition Between Mild and Severe Wear for Boundary Lubricated Steels' ASME Journal Of Tribology, 113, pp 65-72 (1991)
- 81. Hutchings, I:** 'Tribology – Friction and Wear of Engineering Materials', Arnold, pp52-55 (1992)
- 82. Sinha, Sujeet, K:** 'Wear Failures of Plastics' p1022, in 'ASM Handbook: Failure Analysis and Prevention Vol. 11: Failure Analysis and Prevention', ASM International (2002)
- 83. Sinha, Sujeet, K:** 'Wear Failures of Plastics' p1025, in 'ASM Handbook: Failure Analysis and Prevention Vol. 11: Failure Analysis and Prevention', ASM International (2002)
- 84. Thomas, B:** 'Lifeboat Slipway Usage Guidelines' RNLI internal document (2008)
- 85. Thomas, B:** 'Design of Lifeboat Slipway Linings: Methodology' RNLI internal document (2008)
- 86. Thomas, B:** 'Design of Lifeboat Slipways' RNLI internal document (2008)
- 87. ISO 14040:** 'Environmental management - Life cycle assessment -Principles and framework' International Organisation for Standardisation (ISO), Geneve (2006)
- 88. Granta Design:** 'Cambridge Engineering Selector 2009 – EduPack' Granta Design (2009)
- 89. Adams, W.M:** 'The Future of Sustainability: Re-thinking Environment and Development in the Twenty-first Century.' Report of the IUCN Renowned Thinkers Meeting, 29–31 January, 2006. (2006)
- 90. United Nations General Assembly:** 2005 World Summit Outcome, Resolution A/60/1, adopted by the General Assembly on 15 September 2005 (2005)
- 91. Anglian Water:** '<http://www.anglianwater.co.uk/household/your-account/tariffs/standard-rates/>' Accessed (07/2009)
- 92. British Gas:** 'Electricity Prices: 2009' (2009)
- 93. Environmental Protection Agency:** '<http://www.epa.gov/OMS/climate/420f05001.htm#calculating>' Accessed (10/2008)
- 94. Lignum Vitae:** 'Lignum Vitae (greenheart wood)' [http://en.wikipedia.org/wiki/Lignum\\_vitae](http://en.wikipedia.org/wiki/Lignum_vitae) accessed (05/09)

# A SLIPWAY SCHEMATICS

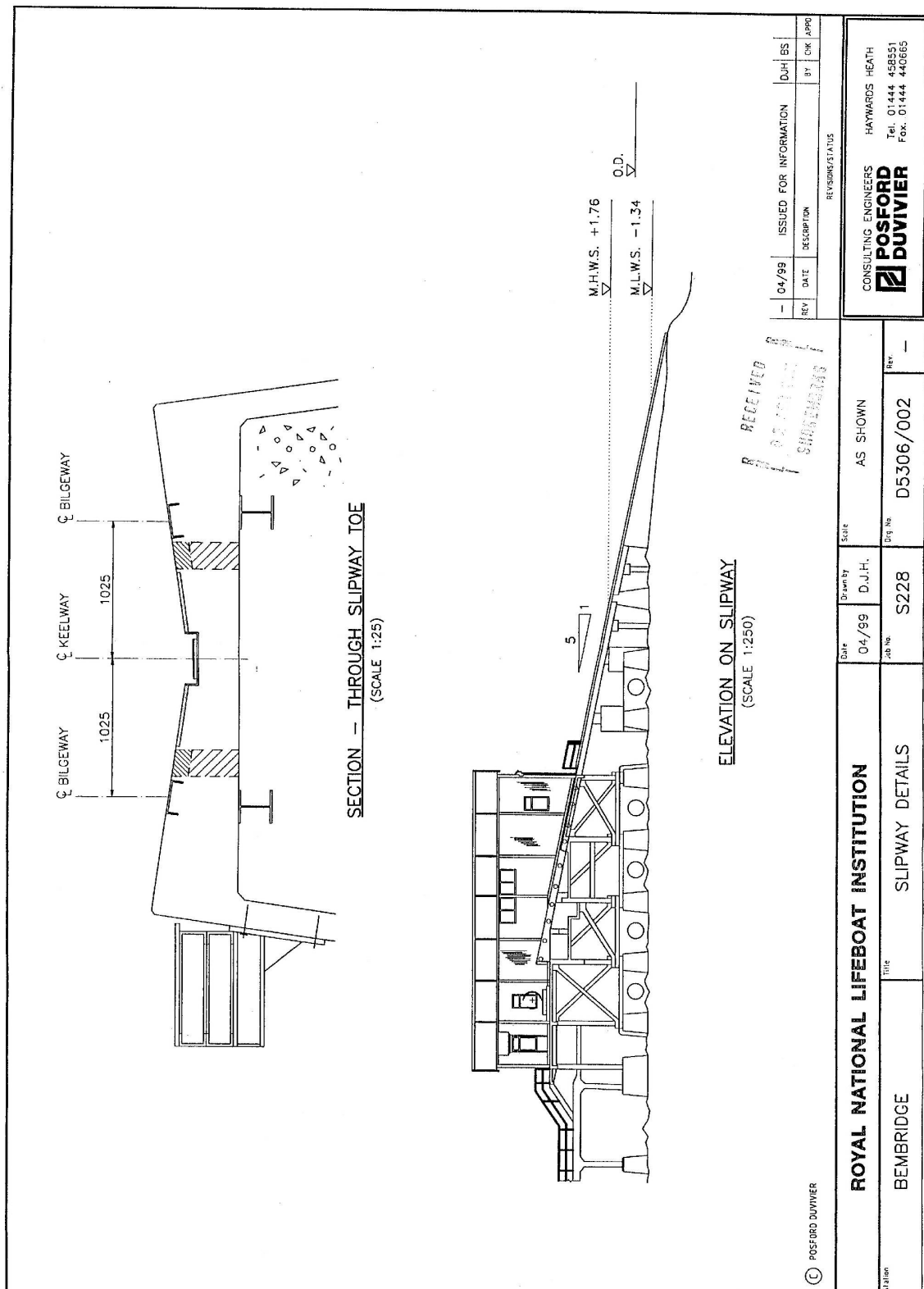
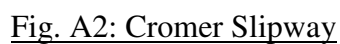


Fig. A1: Bembridge Slipway



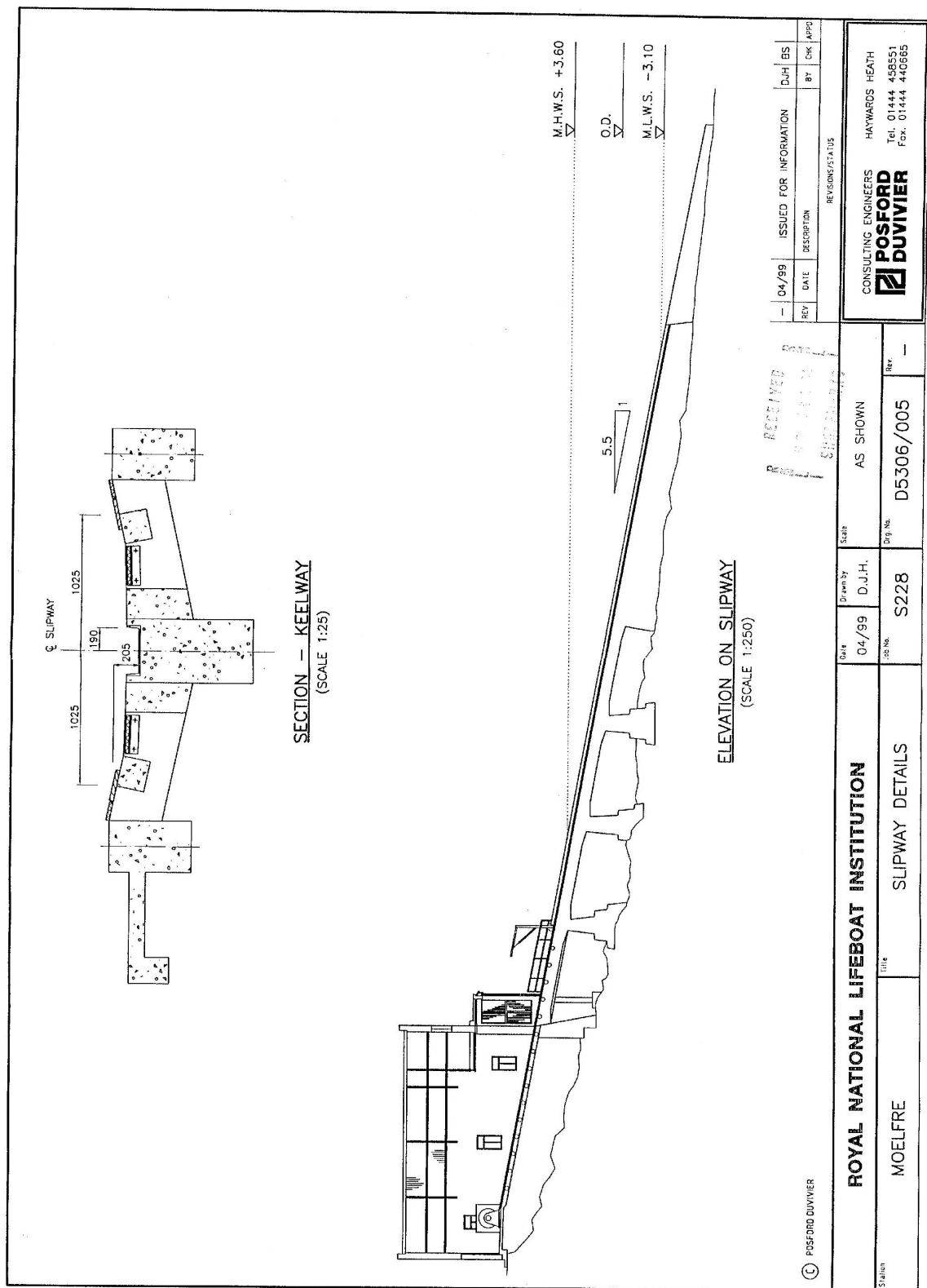
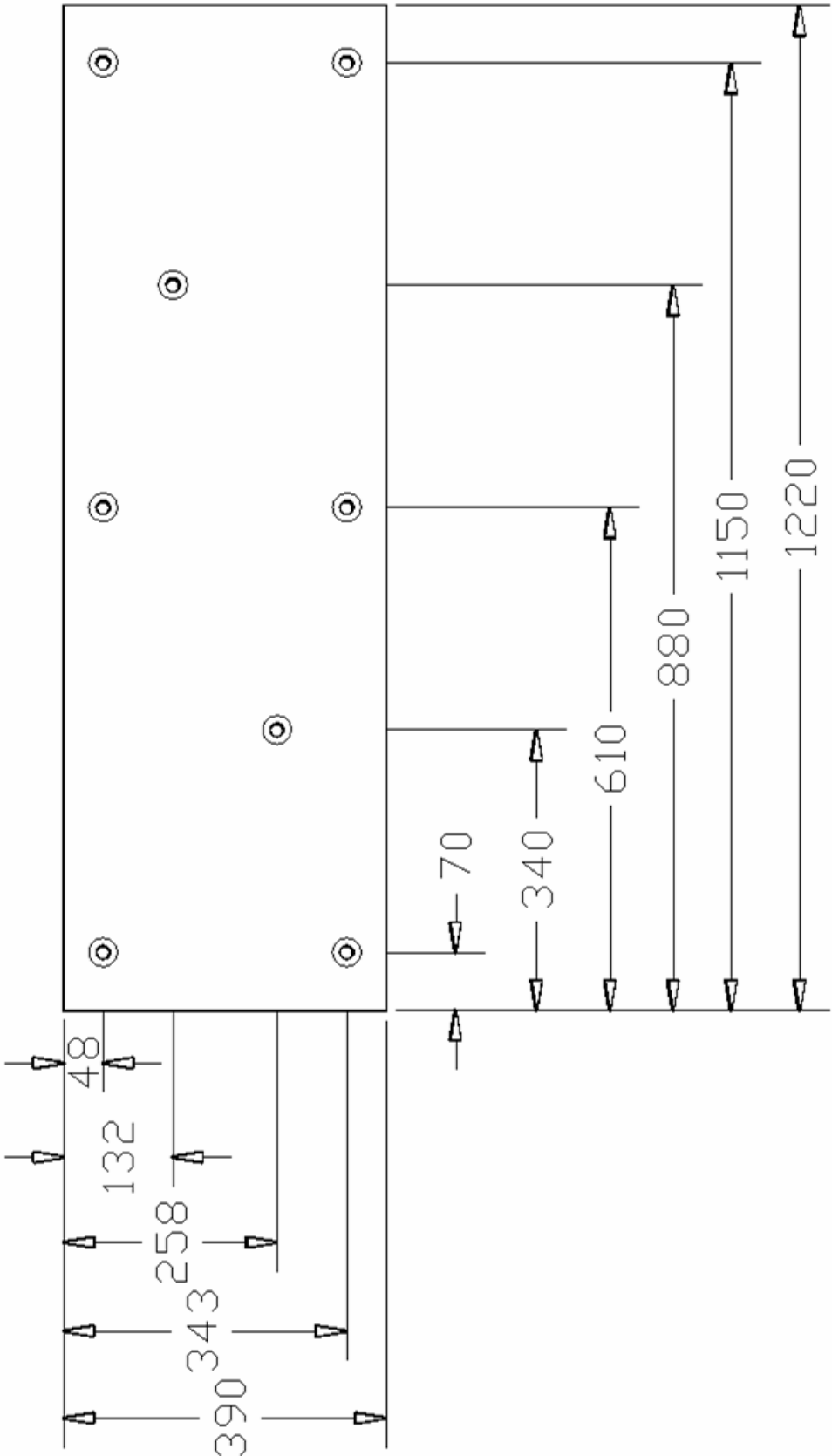


Fig. A3: Moelfre Slipway



# SLIPWAY PANEL SCHEMATIC



**Fig. B1: Slipway Panel Schematic**

# C MATERIAL DATA

## Keel Steel

### Stainless Steel S275J2G3

Name	Number	C	Mn	Si(max)	P	S	Ni	Yield Stress R <sub>eH</sub>	Tensile Strength R <sub>m</sub>	Equivalent BS	Code
								MPa	MPa		
S275J2G3	1.0144	0,18	1,50	-	0,035	0,035	-	205 - 275	380 - 580	BS4360	43D

## Slipway Linings

### Jute / Graphite infused phenolic resin composite

**Class** Composite

**Material** Phenolic

**Type** Semi-finished product

**Applications** It is used in Railway industry and Marine industry. Because of its wear resistance and stability with oil and water lubrication primary applications include propeller shaft and rudder bearings. It is also used in chemical industry, aerospace industry, automotive industry and industries handling fluids. Other uses include:

In Civil Engineering to make bridge bearings and expansion pads, jetty fender bearings, lifeboat launching slipways pads, lock gate hinge bushes etc.

In Food Processing to make filter plates, food extrusion screws, scrapers, conveyor guide strips.

In Machine Tools for making saw guides, slideway facings, IM Machine platen tie bar bushes etc.

In Mechanical Handling to make conveyor bearings, crane jib boom extension pads and wheel bearings.

In Mining and Oil Production to make cable guide rollers, anchor sheave bearings, derrick bushes, hydraulic cylinder wearings etc.

In Steel Manufacturing to make roll mill bearings, thrust collars, table guides and continuous steel casting chain link bushes.

In Textiles and Paper Production to make felting rollers, doctor blades, stenter guides, dye vat bearings, steam joint rings etc.

**Form** Sheet, Rod, Tube, Profile

### Mechanical Properties

Property	Parameter	Unit	Min	Max
Flexural Strength		MPa	88	
Tensile Strength		MPa	57	
Shear Strength		MPa	53	
Compressive Strength	Ultimate	MPa	195	
Normal Working Strength		MPa	48	
Impact Strength		KJ/m <sup>2</sup>	8	
Bond Strength	Interlaminae, 10mm ball	lb	5.62E-4	
Brinell Hardness	500 kg, 10mm ball	HB	30	
Coefficient of Friction	Unlubricated, 20-200 kg/cm <sup>2</sup>	μ	0.12	0.25
Compressive Yield	Under 68.9 MPa Pressure	%	1.8	

### Physical Properties

Property	Parameter	Unit	Min	Max
Density		g/cm <sup>3</sup>	1.35	
Swell in Water	normal to laminae @20°C	%	1.1	3.1

### Thermal Properties

Property	Parameter	Unit	Min	Max
Coefficient of Linear Thermal Expansion	Parallel	/°C	2.00E-5	
Coefficient of Linear Thermal Expansion	Normal	/°C	6.00E-5	
Normal Maximum Temperature Capability		°C	130	
Intermittent Maximum Temperature Capability		°C	150	

### Impact Properties

Property	Parameter	Unit	Min	Max
Charpy Notched Impact Strength		ft.lb/in <sup>2</sup>	2.10E+7	

## Low friction coated steel

#### DESCRIPTION

is a unique alloy containing fine, multiple hard phases which are uniformly distributed throughout a Ni-Cr-B matrix. These hard phases, comprised of complex bi- and tri-metallic borides and carbides, are precipitated during manufacturing, and are therefore an inherent part of the microstructure and not added externally as in conventional composite powders. The hard phases remain uniformly distributed during shipping, spraying and fusing to ensure consistent performance throughout the coating. They are an intimate part of the matrix and will not erode prematurely. Their fine size (5-10 microns) contributes to better finishing characteristics. The hard phases, along with the high-hardness Ni-Cr-B matrix, resist extreme abrasion and corrosion.

#### TYPICAL USES

has proved successful in increasing the service life of glass mould plungers, where the alloy withstands wear from hot (1800°F), extremely abrasive, molten silica. Other applications include:

pump plungers and sleeves, valve seats, thermowells, centrifuges, plastics processing screws and barrels, wire drawing capstans, catalytic cracker components.

#### NOMINAL COMPOSITION

Carbon	0.8%
Chromium	15.0
Boron	3.0
Silicon	4.0
Iron	3.5
Tungsten	17.3
Nickel	Balance

#### PHYSICAL PROPERTIES

Hardness (Rockwell C)	59-64
Melting Point (approx):	
Solidus	1810°F (990°C)
Liquidus	2160°F (1180°C)
Density	9.89 gm/cc
Apparent Density	4.78 gm/cc

## Greenheart weather treated wood


Lignum vitae is a trade wood, from trees of the genus Guaiacum, also called guayacan. This wood was once very important for uses requiring strength, weight, and hardness.

It is a hard, dense and durable wood, the most dense wood traded; it will easily sink in water. On the Janka Scale of Hardness, which measures hardness of woods, lignum vitae ranks highest of the trade woods, with a Janka hardness of 4500 (compared with Hickory at 1820, red oak at 1290, and Yellow Pine at 690). The heartwood is green in colour leading to the common name Greenheart. In the shipbuilding, cabinetry, and woodturning crafts the term greenheart refers to the green heartwood of Chlorocardium rodiei, commonly used in ship's propeller stern-tube bearings, due to its self-lubricating qualities, until the 1960s with the introduction of sealed white metal bearings [94].

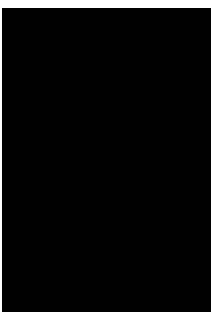
## Lubricants

### Marine Grease

#### 1. IDENTIFICATION OF THE SUBSTANCE / PREPARATION AND OF THE COMPANY / UNDERTAKING

Product name: 

Use / description of product: Marine lubricant.

Company name: 

#### 2. COMPOSITION / INFORMATION ON INGREDIENTS

Ingredients: HIGHLY SOLVENT-REFINED MINERAL OIL >75%

#### 3. HAZARDS IDENTIFICATION

Main hazards: No significant hazard.

#### 4. FIRST AID MEASURES (SYMPTOMS)

**Skin contact:** Prolonged or repeated contact may cause irritation.

**Eye contact:** May be irritating to the eyes.

**Ingestion:** May be harmful by ingestion. Ingestion may cause sickness and vomiting.

**Inhalation:** Inhalation of oil mist or vapour may cause irritation of the respiratory tract.

#### 4. FIRST AID MEASURES (ACTION)

**Skin contact:** Wash immediately with soap and water. Remove contaminated clothing and wash before re-use.

**Eye contact:** In case of contact with eyes, rinse immediately with plenty of water and seek medical advice.

**Ingestion:** Do not induce vomiting. Wash out mouth with water. Seek medical attention, showing this sheet.

**Inhalation:** Not anticipated to be a problem under normal conditions of use. In extreme cases, remove from exposure. If patient is feeling ill, seek medical attention.

#### 5. FIRE-FIGHTING MEASURES

**Extinguishing media:** Dry chemical, CO<sub>2</sub>, water fog, foam and sand.

**Exposure hazards:** Carbon Dioxide and Carbon Monoxide. Partially oxidised organic fragments of the product's ingredients.

#### 6. ACCIDENTAL RELEASE MEASURES

**Personal precautions:** Refer to section 8 of SDS for personal protection details.

**Environmental precautions:** Contain the spillage using bunding. Do not allow the spillage to enter sewers, rivers or open water.

**Clean-up procedures:** Absorb into dry earth or sand. Transfer to a closable, labelled salvage container for disposal by an appropriate method.

#### 7. HANDLING AND STORAGE

**Handling requirements:** No special conditions.

**Storage conditions:** Keep container tightly closed. Containers should preferably be stored under cover.

#### 8. EXPOSURE CONTROLS / PERSONAL PROTECTION

Ingredients: HIGHLY SOLVENT-REFINED MINERAL OIL  
5mg/m<sup>3</sup> 10mg/m<sup>3</sup> (OES)

**Engineering measures:** Local exhaust ventilation is recommended when excessive product misting occurs. Care should be taken to keep exposures below applicable occupational exposure limits.

**Hand protection:** Gloves (oil-resistant).

**Eye protection:** Goggles are recommended where the material may be splashed.

**Skin protection:** No specific protective clothing normally required. High standards of industrial and personal hygiene are recommended while using this product.

#### 9. PHYSICAL AND CHEMICAL PROPERTIES

**State:** Grease.

**Colour:** Dark green

**Solubility in water:** Not miscible

**Viscosity value:** N/A

**Flash point°C:** Seta >170°C

**Relative density:** 1.11kg/l @ 15°C

**pH:** N/A

#### 10. STABILITY AND REACTIVITY

**Stability:** Stable under normal conditions.

**Conditions to avoid:** Extreme heat.

**Materials to avoid:** Strong oxidising agents. Strong acids.

**Haz. decomp. products:** In combustion emits toxic fumes of carbon dioxide / carbon monoxide. Partially oxidised organic fragments of the product's ingredients.

#### 11. TOXICOLOGICAL INFORMATION

**Acute toxicity:** [REDACTED]

Not tested

**Ingredients:** HIGHLY SOLVENT-REFINED MINERAL OIL

ORAL RAT LD50 >5000 mg/kg

**Routes of exposure:** Refer to section 4 of SDS for routes of exposure and corresponding symptoms.

#### 12. ECOLOGICAL INFORMATION

**Ecotoxicity:** [REDACTED]

Not tested

**Mobility:** Insoluble in water. Non-volatile at ambient temperature.

**Persistence and degradability:** Mineral oil component biodegrades slowly.

**Bioaccumulative potential:** Mineral oil component has the potential to bioaccumulate.

#### 13. DISPOSAL CONSIDERATIONS

**Disposal operations:** The product can be burned under controlled conditions or removed by approved waste contractors.

**Disposal of packaging:** May be reused following decontamination. Dispose of as normal industrial waste.

**NB:** The user's attention is drawn to the possible existence of regional or national regulations regarding disposal.

#### 14. TRANSPORT INFORMATION

##### ADR / RID

**Labelling:** Not classified.

##### IMDG / IMO

**Labelling:** Not classified.

##### IATA / ICAO


**Labelling:** Not classified.

#### 15. REGULATORY INFORMATION

**Hazard symbols:** No significant hazard.

**Note:** The regulatory information given above only indicates the principal regulations specifically applicable to the product described in the safety data sheet. The user's attention is drawn to the possible existence of additional provisions which complete these regulations. Refer to all applicable national, international and local regulations or provisions.

## Biogrease #1

 BIOGREASE is a green, partsynthetic multipurpose grease based on lithium-calcium soap. BIOGREASE is biologically degradable. BIOGREASE has following characteristics:

- good mechanical stability
- high oxidation stability
- good anti-wear and anti-corrosion behavior
- good water resistance
- wide temperature range
- compatible with greases based on lithium soap

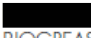
### Applications (follow manufacturer's instructions)

- where greasepollution to the environment is possible, e.g. earth moving equipment and vehicles (excl. wheel bearings)
- water turbines
- bearings of spiral pumps used in sewerage plant

### Biological degradability

> 90 % to CEC-L-33-T-82

### Technical data (mean values, subject to normal tolerances)

 BIOGREASE	Prod.Nr.	Base oil	NLGI-class	Worked penetration in 1/10 mm	Dropping point in °C	Temperature-range in °C
2	7258	Synthetic oil / vegetable oil	2	265 – 295	170	-20/110

\* for short periods and with a higher frequency of regreasing up to 200 °C

## 1. IDENTIFICATION OF THE SUBSTANCE/PREPARATION AND THE COMPANY/UNDERTAKING

### Chemical characterization

Grease based on synthtetic esters with soaps and additives.

## 2. COMPOSITION/INFORMATION ON INGREDIENTS

### Hazardous components

The product contains no substances which at their given concentration, are considered to be hazardous to health.

## 3. HAZARDS IDENTIFICATION

None.

## 4. FIRST AID MEASURES

### Inhalation

Move to fresh air in case of accidental inhalation of vapours.

### Skin contact

Wash with water and soap as a precaution.

### Eye contact

Rinse immediately with plenty of water, also under the eyelids, for at least 15 minutes.

### Ingestion

Do not induce vomiting. Drink water as a precaution. Obtain medical attention.

## 5. FIRE-FIGHTING MEASURES

<b>Suitable extinguishing media</b>	Foam. Dry chemical. Carbon dioxide (CO <sub>2</sub> ).
<b>Extinguishing media which must not be used for safety reasons</b>	High volume water jet.
<b>Special protective equipment for firefighters</b>	In case of fire, wear a self contained breathing apparatus.
<b>Specific methods</b>	Do not use a solid water stream as it may scatter and spread fire.

---

## 6. ACCIDENTAL RELEASE MEASURES

<b>Personal precautions</b>	Sweep up to prevent slipping hazard.
<b>Environmental precautions</b>	Do not flush into surface water or sanitary sewer system.
<b>Methods for cleaning up</b>	Take up mechanically and collect in suitable container for disposal.

---

## 7. HANDLING AND STORAGE

<b>Handling</b>	Spilling onto the container's outside will make container slippery.
<b>Storage</b>	Keep containers dry and tightly closed to avoid moisture absorption and contamination. Store at room temperature in the original container.

---

## 8. EXPOSURE CONTROLS / PERSONAL PROTECTION

<b>Engineering measures to reduce exposure</b>	General industrial hygiene practice.
<b>Personal protection equipment</b>	
<b>Respiratory protection</b>	No personal respiratory protective equipment normally required.
<b>Hand protection</b>	Rubber or plastic gloves.
<b>Eye protection</b>	Safety glasses with side-shields.
<b>Skin and body protection</b>	Remove and wash contaminated clothing before re-use.

---

## 9. PHYSICAL AND CHEMICAL PROPERTIES

Form	Paste.	
Colour	Beige. Brown.	
Odour	Characteristic.	
<b>Physical and chemical properties</b>		
	Flash point	> 130 °C.
	NLGI	2
	Drop point (TAB)	none.
	Water solubility:	insoluble.

## 10. STABILITY AND REACTIVITY

<b>Stability</b>	No decomposition if stored and applied as directed.
<b>Conditions to avoid</b>	Fire or intense heat may cause violent rupture of packages.
<b>Materials to avoid</b>	Strong oxidizing agents.
<b>Hazardous decomposition products</b>	None under normal use. When the substance is heated the formation of Acrolein is possible.



## 11. TOXICOLOGICAL INFORMATION

<b>Acute toxicity</b>	ALD/oral/rat = > 2'000 mg/kg. Estimated from the datas of the components or similar substances.
<b>Local effects</b>	Negligible.
<b>Long term toxicity</b>	Negligible.
<b>Sensitization</b>	Negligible.
<b>Further information</b>	The product contains no substances which at their given concentration, are considered to be hazardous to health. Health injuries are not known or expected under normal use. No persistent or cumulative effects were observed.

---

## 12. ECOLOGICAL INFORMATION

<b>Ecotoxicity</b>	Ecological injuries are not known or expected under normal use.
<b>Persistence / degradability</b>	Biological degradability (CEC L-33-A-94): > 90 %.

---

## 13. DISPOSAL CONSIDERATIONS

<b>Waste from residues / unused products</b>	Can be incinerated, when in compliance with local regulations. Where possible recycling is preferred to disposal or incineration. In accordance with local and national regulations. waste-code (VVS): (CH): 1740
<b>Contaminated packaging</b>	Empty containers should be taken for local recycling, recovery or waste disposal. Empty containers can be returned to the supplier. Partly empties containers won't be accepted by the supplier. It doesn't exist a duty for return.

---

## 14. TRANSPORT INFORMATION

<b>Further Information</b>	Not classified as dangerous in the meaning of transport regulations.
----------------------------	--

---

## 15. REGULATORY INFORMATION

<b>Regulatory Information</b>	The product does not need to be labelled in accordance with (national equivalent of EC-Directive 88/379). This product is not a hazardous article and need not to be labelled according to EC-Directive 67/548, as amended.
<b>Symbol(s)</b>	None.
<b>R-phrases(s)</b>	None.
<b>S-phrases(s)</b>	S26: In case of contact with eyes, rinse immediately with plenty of water and seek medical advice. S37: Wear suitable gloves.

---

## 16. OTHER INFORMATION

<b>Recommended use</b>	According to datasheet.
------------------------	-------------------------

## Biogrease #2

### **FOOD GRADE BIODEGRADABLE WATER RESISTANT GREASE**

Will be applied whenever a lubricant provided with high biodegradability, high anticorrosive capacity and water resistance is needed.

Biogrease #2 is formulated with an environmentally friendly additive package to obtain excellent an balance between environmental requirements and lubricating-anticorrosive capacity.

Biogrease #2 has got superior sealing capacity and very good resistance to water action, combined with a high adhesion to the mechanism to be lubricated.

Biogrease #2 is must be used wherever the lubricant is an important contaminating factor and whenever it is possible that uncontrolled lubricant losses pass to the soil or to water.

Thanks to their biodegradable properties they will have better performances and higher efficiency in further water treatments, whatsoever physico-chemical or biological they might be.

The eventual contamination of soils, cultures, forests, water, will have a lower effect, due to the high biodegrading velocity, specially when compared to the conventional greases.

Biogrease #2 is intended for:

- ☐ Forest machinery.
- ☐ Public Works machinery.
- ☐ Nautic mechanisms.
- ☐ Various mechanisms in water treatment plants.
- ☐ Water pumping installations.
- ☐ Mechanisms in contact with water.
- ☐ Protection of carbodies

### **BENEFITS**

The most significant benefits of Biogrease #2 is:

- ⇒ Anticorrosive capacity.
- ⇒ Outstanding water resistance.
- ⇒ High adherence.
- ⇒ Biodegradability.

### **SPECIFIED CHARACTERISTICS**

Characteristics	Test Method	Biogrease #2
<input type="checkbox"/> Thickener (soap type)	-	calcium
<input type="checkbox"/> Base oil nature	-	natural ester
<input type="checkbox"/> Worked penetration 60 W, 0,1 mm	ASTM D-217	265 - 295
<input type="checkbox"/> Drop point	ASTM D-566	120° C min.

### **GENERAL CHARACTERISTICS**

Characteristics	Test Method	Biogrease #2
<input type="checkbox"/> Colour	-	brown
<input type="checkbox"/> NLGI Consistency Class	(DIN 51818)	2
<input type="checkbox"/> Copper corrosion, 24hr/100°C	(ASTM D-4048)	max. 1b
<input type="checkbox"/> Water washout, 40°C	(ASTM D-1264)	max. 1%
<input type="checkbox"/> Flow pressure at -25°C	(DIN 51805)	max. 1000 mbar
<input type="checkbox"/> 4 balls test		
⇒ welding load	(IP-239)	min. 120 kg
⇒ Wear scar diameter 1'/80 kg		max. 0,50 mm
<input type="checkbox"/> EMCOR corrosion test	(DIN 51802)	Degree 0

☐ Oil separation, 7 days/40°C	(IP-121).	3,5% max.
☐ Water washout (3hr/90°C)	(DIN-51807	0
☐ Oxidation stability, 100°C	(ASTM D-972)	max. 0,8kg/cm <sup>2</sup>
☐ Evaporation loss, 22 hr/100°C,% weight	(ASTM D-942)	max. 0,7%
☐ Biodegradability test	(CEC-L-33-A-93)	88,90%
☐ Resistance to hydrocarbons	-	resists
☐ Operating temperatures	-	- 25 / +80°C

## CAUTIONS

- ☼ The usual ones when handling and using lubricants.
- ☼ Keep the can closed to avoid contamination.
- ☼ Do not mix with different nature greases.

## Silicon Microball Lubricant

### MATERIAL SAFETY DATA SHEET

1. Product :		
2. Composition / Information on Hazardous Ingredients		
Material	%	CAS No.
	Water emulsion with silicone and other additives.	
3. Hazards Identification		
This product is not hazardous according to the EEC criteria.		
4.0 First Aid		
Eye Contact:	NEVER give fluids or induce vomiting if patient is unconscious or having convulsions.	
Skin Contact:	Irrigate with flowing water immediately and continuously for 15 minutes.	
Ingestion:	Wash thoroughly with soap and water. If irritation persists, seek medical advice.	
	Except as a deliberate act, the ingestion of large quantities is unlikely.	
	If it should occur, do not induce vomiting; obtain medical advice.	
Inhalation:	Remove patient from exposure. Obtain medical attention if ill effects occur.	
5.0 Fire-Fighting Measures		
Extinguishing	Water, Carbon Dioxide, Dry Chemical, Foam.	
Media:		
Special Protective	Fires in confined spaces should be dealt with by trained personnel wearing	
Equipment:	Approved breathing apparatus.	
Hazardous		
Decomposition		
Products:	Oxides of carbon, sulphur and silicone may be evolved on burning.	
6.0 Accidental Release Measures		
Spills may cause very slippery surfaces.		
Personal Precautions:	Prevent skin and eye contact.	
Environmental Precautions:	Prevent contamination of surface and groundwater.	
Spill Clean-up Methods:	Soak up with inert absorbent material (e.g. sand, silica gel, universal binder).	
	Wash away residues with soap and water.	
7.0 Handling and Storage		
Usage/Handling Precautions:	Wear suitable protective clothing and equipment. Gloves are not normally require	
Storage Precautions:	Store in dry conditions away from heat sources. Do not expose to frost.	
Handling Precautions:	Handle in accordance with good industrial hygiene and safety practice.	
8.0 Exposure Controls / Personal Protection		
Engineering Controls:	Good general ventilation should be sufficient for most conditions.	
Exposure Limits:	There are no mandatory limits. Users should carry out a COSHH assessment.	
Protective Equipment/		
Industrial Hygiene:	Adopt normal good working practices and personal hygiene standards. Wash	
	hands after use, before eating, drinking, or smoking and before and after	
	using the toilet. Contaminated clothing should be laundered before re-use.	

## Contaminants

---

Sand from Sennen Cove slipway station is used for sand contamination tribometer tests. This is a sand comprised of hard silica particles approx. 0.3mm in size as show in fig. C1.

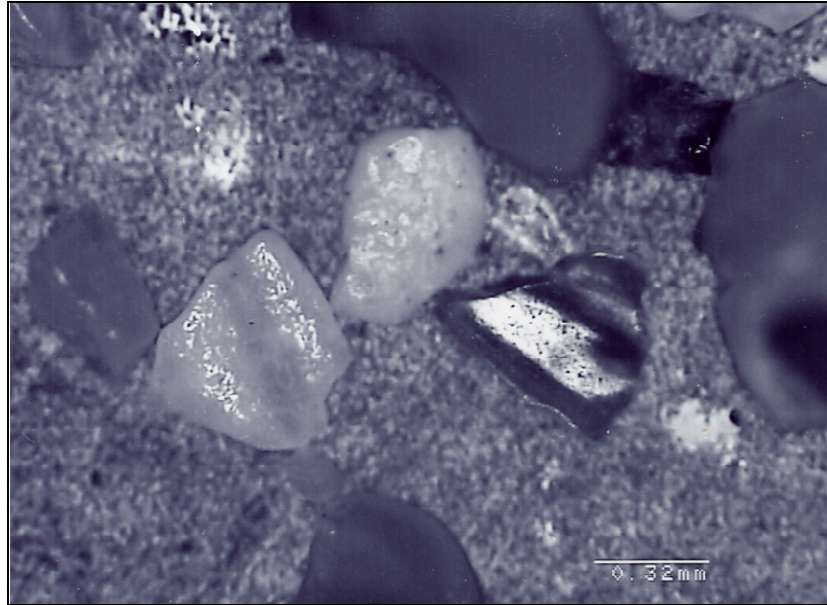


Fig. C1: Sennen Cove Sand

# D COMPOSITE TENSILE TEST

## FF tensile test

Ref 1 :  
 Ref 2 :  
 Ref 3 :  
 Test Name : BEN\_FF2  
 Test Type : Tensile  
 Test Date : 05/07/2007 14:02

Test Speed : 26.00 mm/min  
 Width : 14.400 mm  
 Thickness : 3.045 mm  
 Pretension : Off  
 Sample Length : 37.940 mm

Test No	Elong. @ Break (mm)	Elong. @ Yield (mm)	Energy to Break (N.m)	Strain @ Break (%)	Strain @ Yield (%)	Stress @ Break (N/mm <sup>2</sup> )	Stress @ Yield (N/mm <sup>2</sup> )	Youngs Modulus (N/mm <sup>2</sup> )
1	1.3700	1.3200	1.4737	3.6110	3.4792	17.205	41.964	1889.8

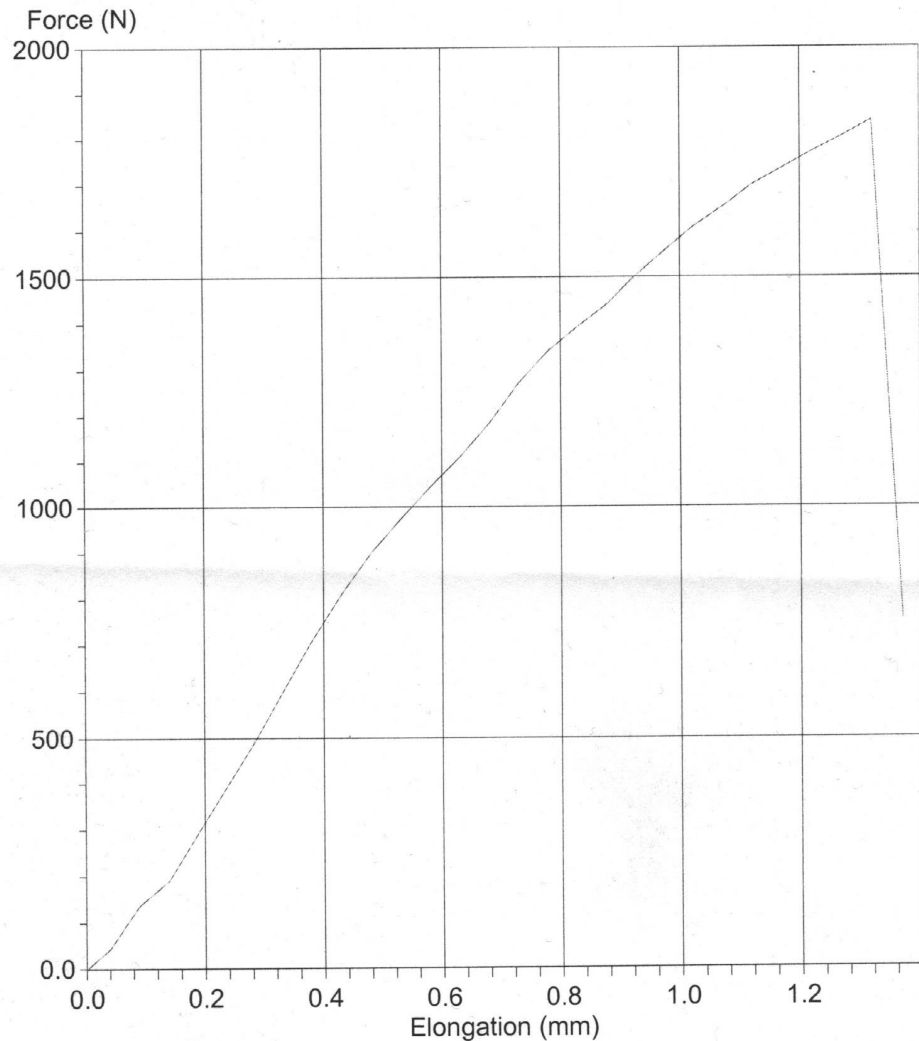


Fig. D1: Composite Tensile Test

# E SLIPWAY SURVEY DATA

Tenby Slipway Station



**Panel 1**



**Corner Heights**

A	1.23
B	6.42 (From Steel Channel)
C	-0.3
D	9.6 (From Steel Channel)
Average height difference to next panel: 0.465	

**Panel 2**



**Corner Heights**

A	-0.36
B	-1.23
C	3.96
D	0.3
Average height difference to next panel: 1.8	



### Panel 3



Corner Heights

A	-0.11
B	0.36
C	-0.29
D	-3.96
Average height difference to next panel: -0.2	


### Panel 4




Corner Heights

A	-0.1
B	0.11
C	0.03
D	0.29
Average height difference to next panel: -0.035	



Panel 5		
		
Corner Heights		
A		-0.41
B		0.1
C		-0.13
D		-0.03
Average height difference to next panel:		-0.27

Panel 6		
		
Corner Heights		
A		0.01
B		0.41
C		0.01
D		0.13
Average height difference to next panel:		0.01

### Panel 7



Corner Heights

A	0.83
B	-0.01
C	0.91
D	-0.01
Average height difference to next panel: 0.87	

### Panel 8



Corner Heights

A	-0.49
B	-0.83
C	-0.42
D	-0.91
Average height difference to next panel: -0.455	

### Panel 9

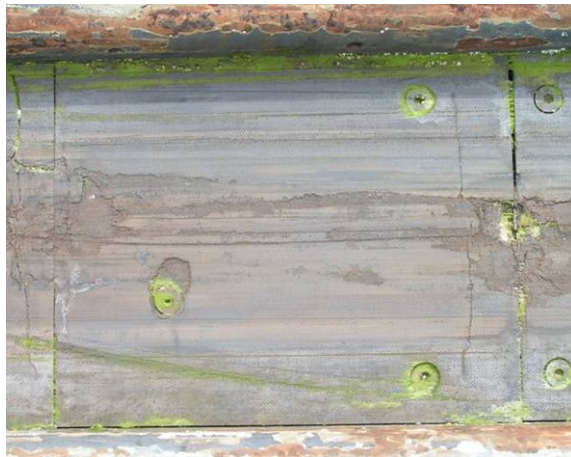


Corner Heights

A	1.14
B	0.49
C	0.88
D	0.42

Average height difference to next panel: 1.01

### Panel 10



Corner Heights

A	-0.91
B	-1.14
C	-0.89
D	-0.88

Average height difference to next panel: -0.9



### Panel 11



Corner Heights

A	-0.21
B	0.91
C	-0.91
D	0.89

Average height difference to next panel: -0.56

### Panel 12



Corner Heights

A	2.34
B	0.21
C	0.93
D	0.91

Average height difference to next panel: 1.635

### Panel 13



Corner Heights

A	1.21
B	-2.34
C	0.23
D	-0.93

Average height difference to next panel: 0.72


### Panel 14




Corner Heights

A	-0.71
B	-1.21
C	-0.72
D	-0.23

Average height difference to next panel: -0.715

Panel 15		
		
Corner Heights		
A		-1.46
B		0.71
C		-1.13
D		0.72
Average height difference to next panel:		-1.295

Panel 16		
		
Corner Heights		
A		1.24
B		1.46
C		0.7
D		1.13
Average height difference to next panel:		0.97



### Panel 17



Corner Heights

A	-1.16
B	-1.24
C	0.61
D	-0.7

Average height difference to next panel: -0.275

### Panel 18



Corner Heights

A	-4.26
B	1.16
C	-2.78
D	-0.61

Average height difference to next panel: -3.52



### Panel 19



Corner Heights


A	1.93
B	4.26
C	1.62
D	2.78
Average height difference to next panel: 1.775	


### Panel 20



Corner Heights

A	1.19
B	-1.93
C	0.51
D	-1.62
Average height difference to next panel: 0.85	

Panel 21		
		
Corner Heights		
A		-0.33
B		-1.19
C		-0.12
D		-0.51
Average height difference to next panel:		-0.225

Panel 22		
		
Corner Heights		
A	-	
B		0.33
C	-	
D		0.12
Average height difference to next panel:		-

**Panel 23**



**Panel 24**



**Panel 25**

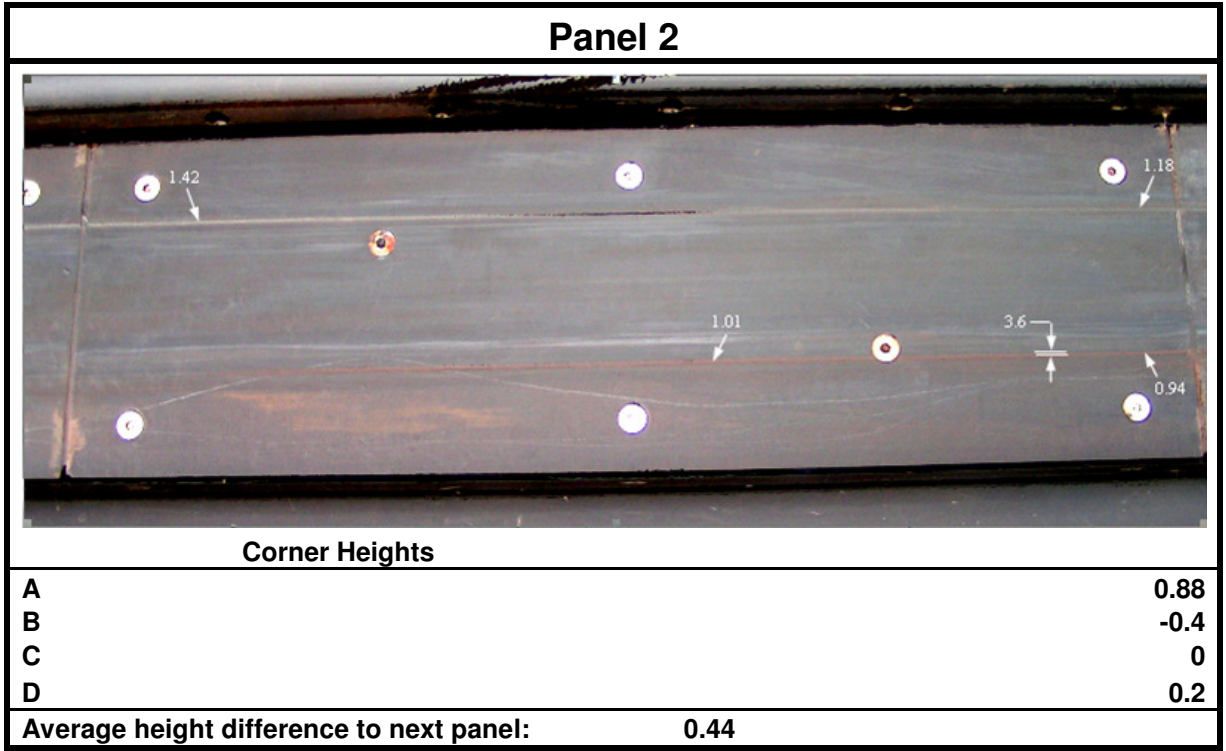
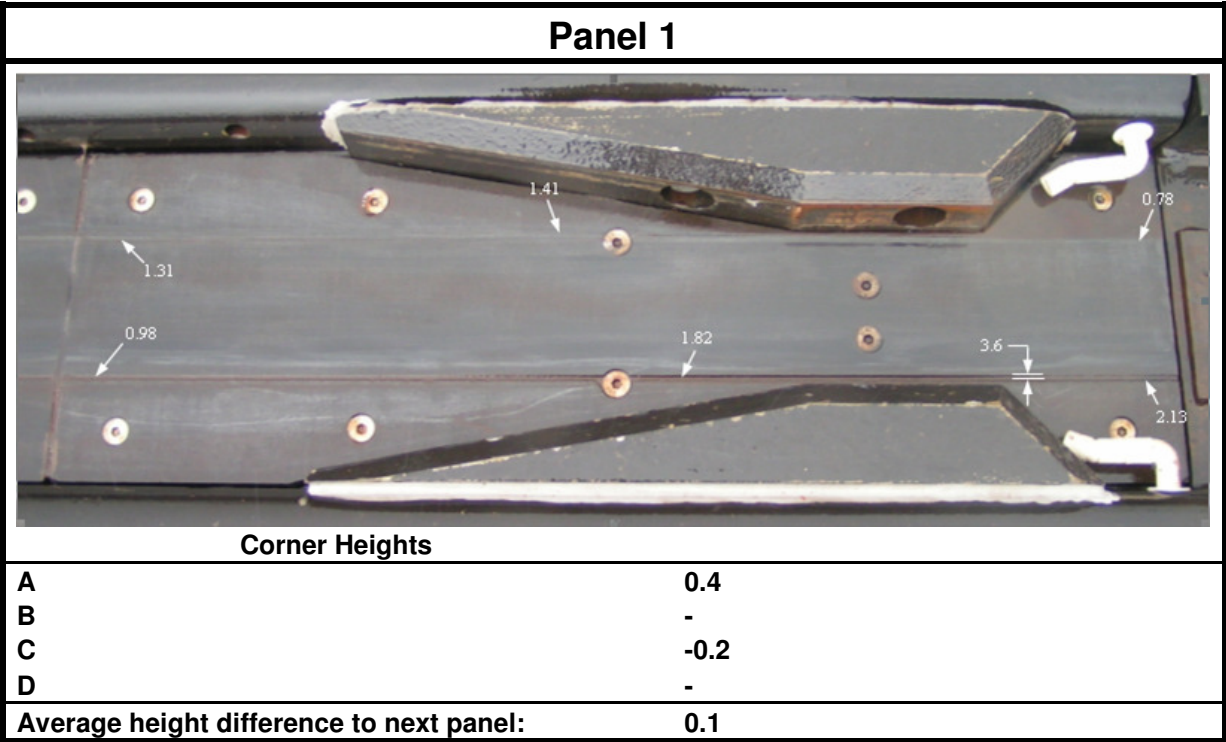


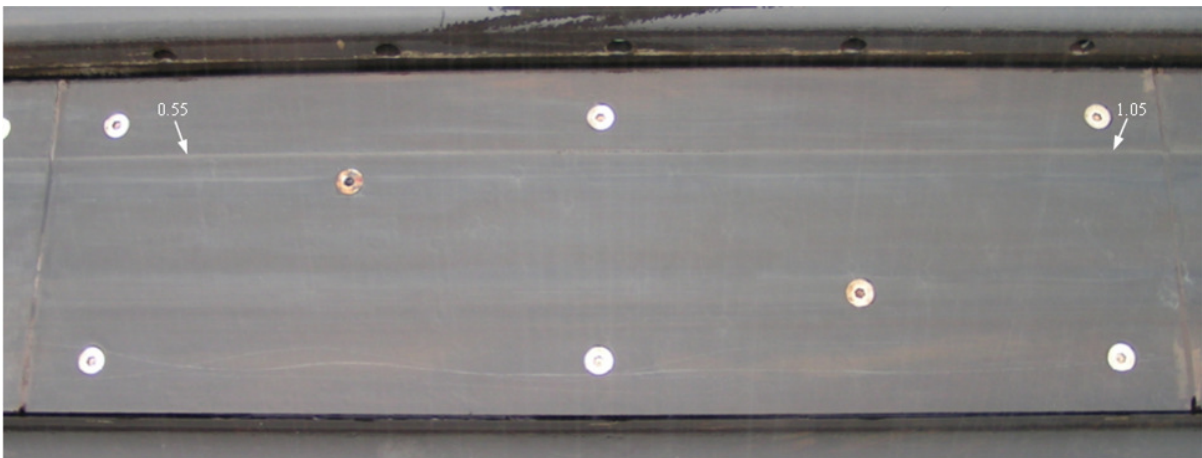


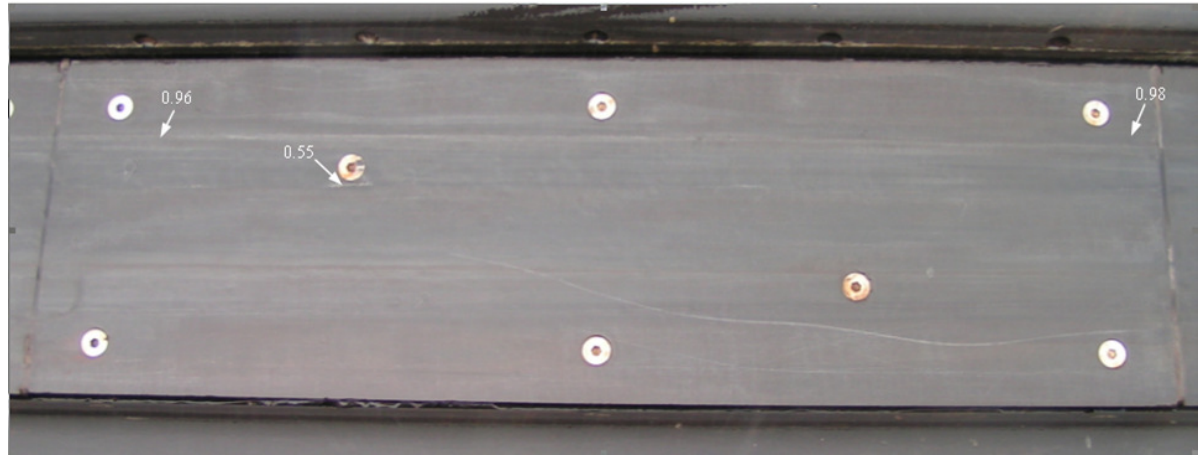
Panel No.	Average height difference to next panel (mm):	Mod. average height difference to next panel (mm):	Average distance to next panel (mm):	Panel end height difference*	Misalignment Scenario	Misalignment angle	Skewed A - C Height Difference	Mod. Skewed A - C Height Difference	Skewed?	Mod. Skew Angle
1	0.465	0.465	5.235	-1.335	Angled	0.062696624	1.53	1.53	Yes	0.224776
2	1.8	1.8	5.285				-4.32	4.32	Yes	0.634674
3	-0.2	0.2	3.725	0.165	Parallel	0.007749019	0.18	0.18	No	0.026444
4	-0.035	0.035	5.585				-0.13	0.13	No	0.019099
5	-0.27	0.27	7.49	0.26	Parallel	0.012210576	-0.28	0.28	No	0.041135
6	0.01	0.01	6.185				0	0	No	0
7	0.87	0.87	6.189	0.415	Parallel	0.019489958	-0.08	0.08	No	0.011753
8	-0.455	0.455	4.785				-0.07	0.07	No	0.010284
9	1.01	1.01	5.895	0.11	Parallel	0.005166013	0.26	0.26	No	0.038197
10	-0.9	0.9	7.33				-0.02	0.02	No	0.002938
11	-0.56	0.56	4.04	-1.075	Angled	0.050486042	0.7	0.7	No	0.102839
12	1.635	1.635	4.645				1.41	1.41	Yes	0.207147
13	0.72	0.72	4.885	0.005	Parallel	0.000234819	0.98	0.98	No	0.143974
14	-0.715	0.715	5.47				0.01	0.01	No	0.001469
15	-1.295	1.295	10.64	0.325	Parallel	0.01526322	-0.33	0.33	No	0.048481
16	0.97	0.97	5.64				0.54	0.54	No	0.079333
17	-0.275	0.275	No Data	-3.245	Angled	0.15239756	-1.77	1.77	Yes	0.260036
18	-3.52	3.52	No Data				-1.48	1.48	Yes	0.217431
19	1.775	1.775	No Data	0.925	Parallel	0.043441476	0.31	0.31	No	0.045543
20	0.85	0.85	No Data				0.68	0.68	No	0.0999
21	-0.225	0.225	No Data	No Data	No Data	No Data	-0.21	0.21	No	0.030852
22	No Data	No Data	No Data				No Data	No Data	No Data	No Data
Mean	0.079	0.884	5.814	*0 implies parallel misalignment, integer implies angled misalignment						
Max.	1.8	3.52	10.64							
Min.	-3.52	0.01	3.725							

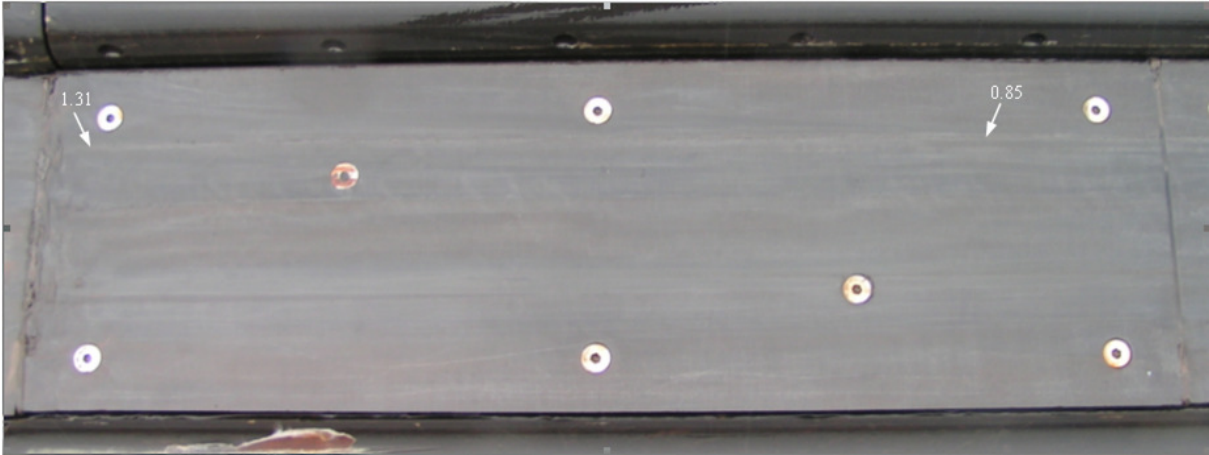
Table E1: Tenby Slipway Survey Data

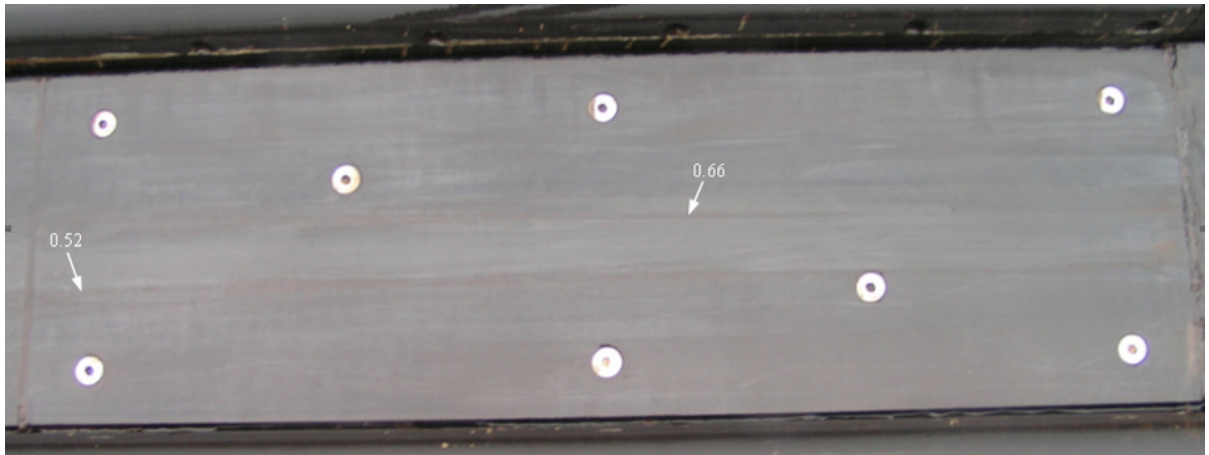
**Padstow Slipway Station**



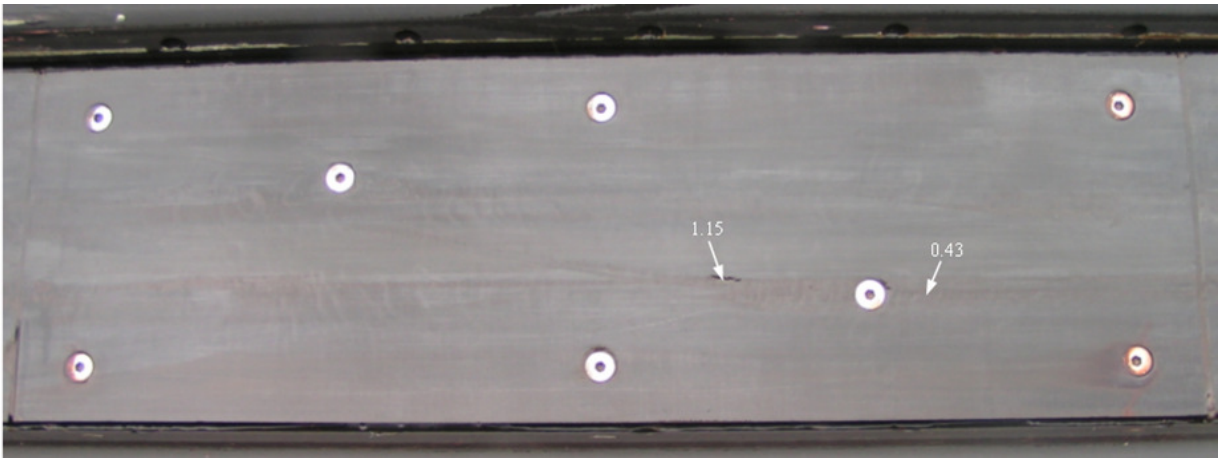
Panel 3		
		
Corner Heights		
A		0.2
B		-0.88
C		0.4
D		0
Average height difference to next panel:		0.3

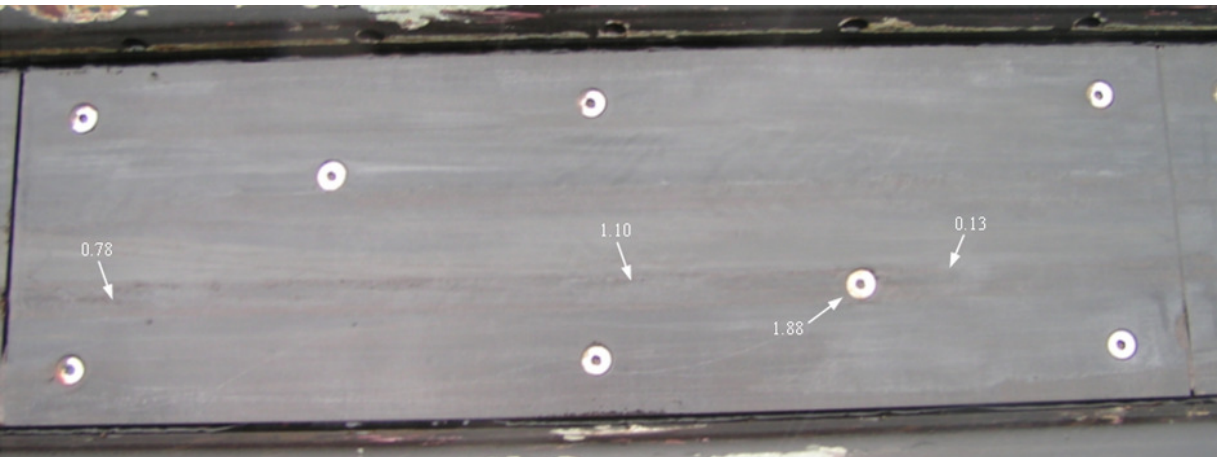
Panel 4		
		
Corner Heights		
A		-0.2
B		-0.2
C		0.1
D		-0.4
Average height difference to next panel:		-0.05

Panel 5		
		
Corner Heights		
A		3.31
B		0.2
C		4.8
D		-0.1
Average height difference to next panel:		4.055

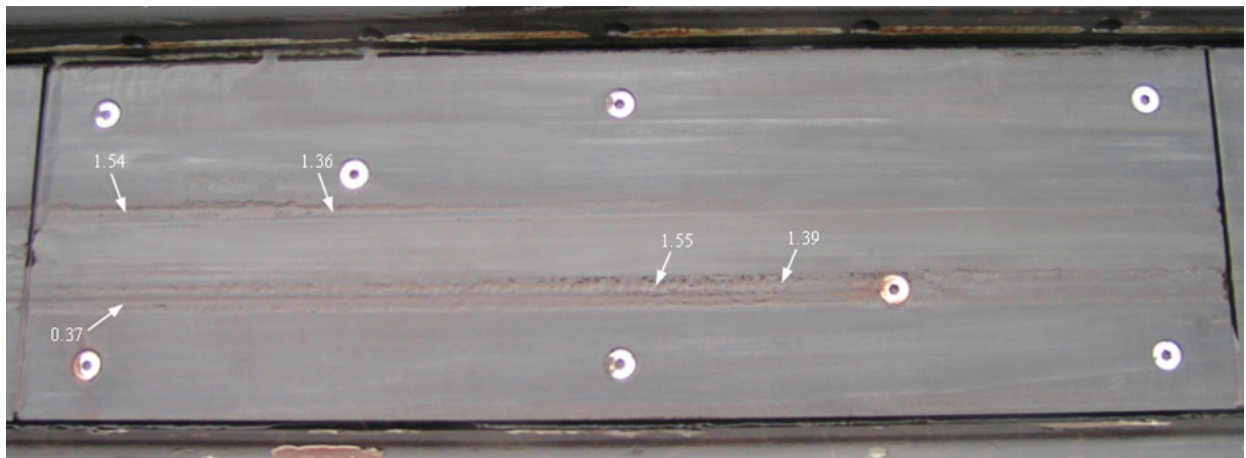
Panel 6		
		
Corner Heights		
A		0.87
B		-3.31
C		-0.6
D		-4.8
Average height difference to next panel:		0.135



Panel 7		
		
Corner Heights		
A		0.19
B		-0.87
C		0.53
D		0.6
Average height difference to next panel:		0.36

Panel 8		
		
Corner Heights		
A		0.77
B		-0.19
C		0.44
D		-0.53
Average height difference to next panel:		0.605

### Panel 9

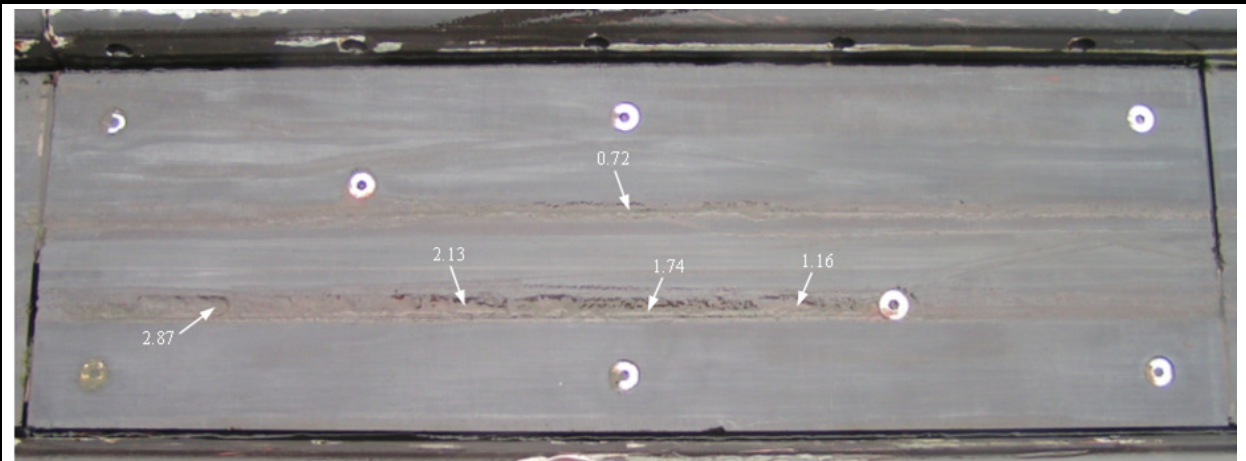


Corner Heights

A	0.45
B	-0.77
C	0.92
D	-0.44

Average height difference to next panel: 0.685

### Panel 10

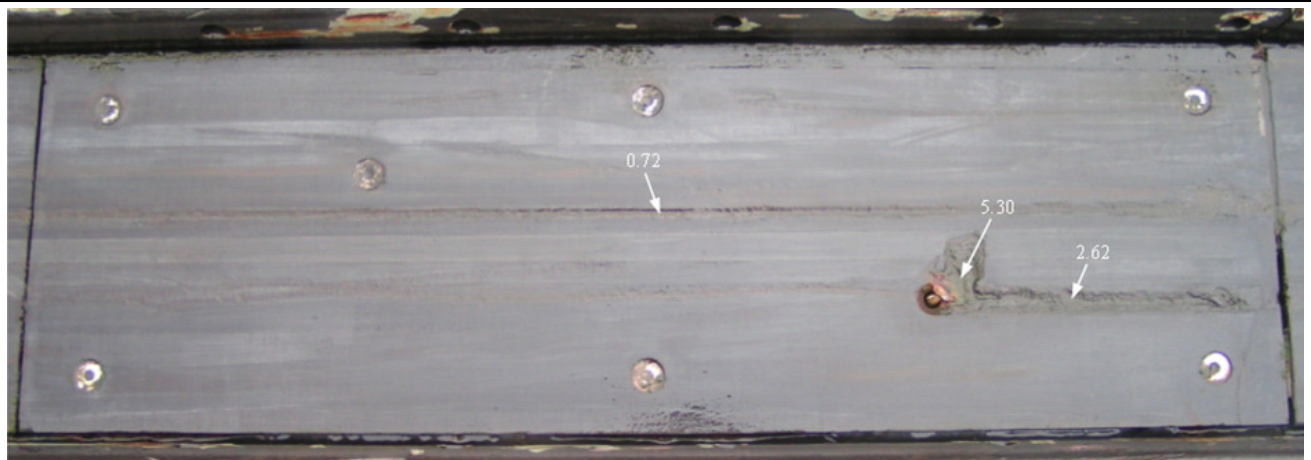


Corner Heights

A	2.25
B	-0.45
C	0.8
D	-0.92

Average height difference to next panel: 1.525

### Panel 11

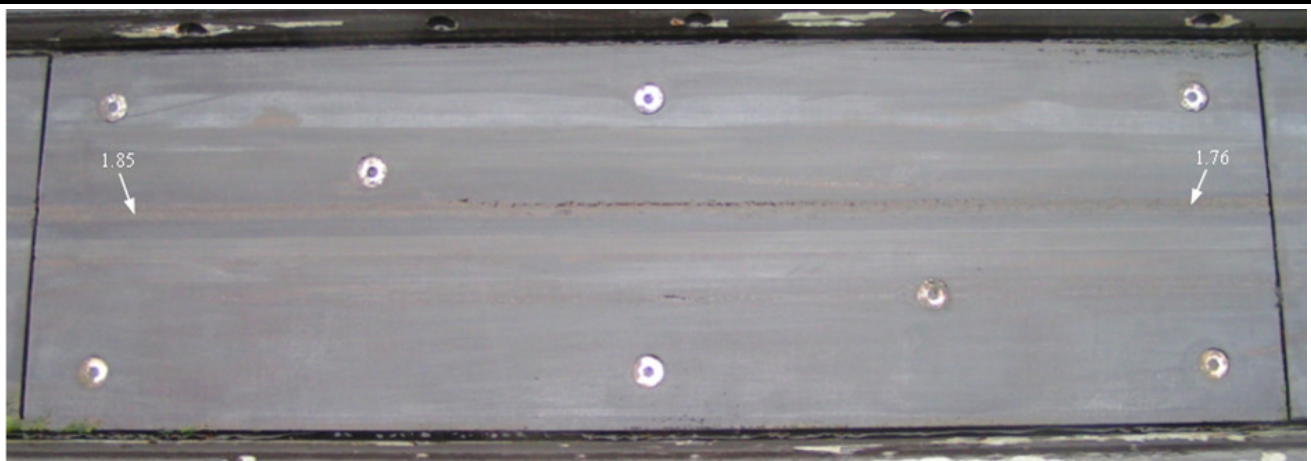


#### Corner Heights

A	0.51
B	-2.25
C	0.45
D	-0.8

Average height difference to next panel: 0.48

### Panel 12



#### Corner Heights

A	0.59
B	-0.51
C	0.44
D	-0.45

Average height difference to next panel: 0.515



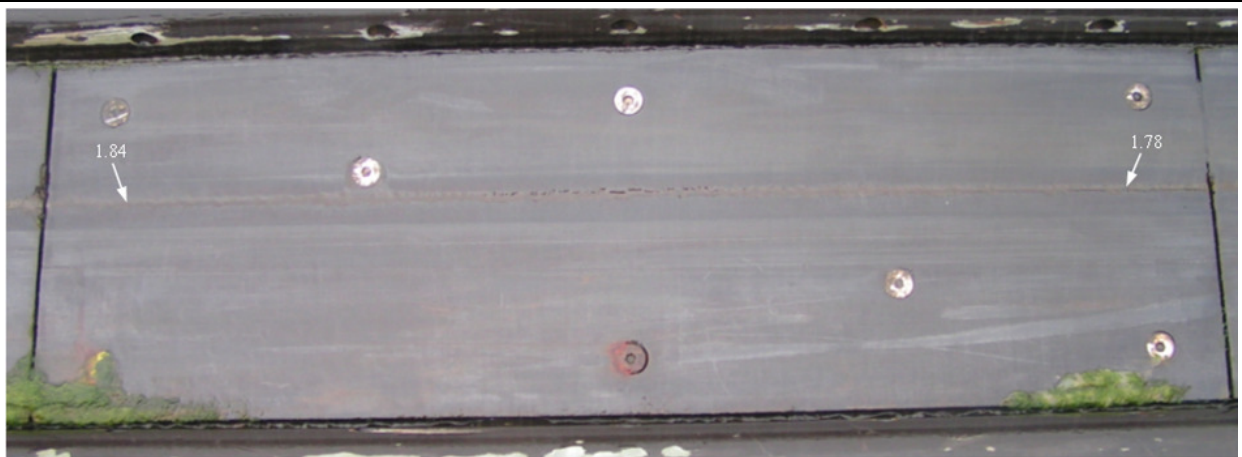
### Panel 13



Corner Heights

A	0.41
B	-0.59
C	0.65
D	-0.44
Average height difference to next panel: 0.53	

### Panel 14



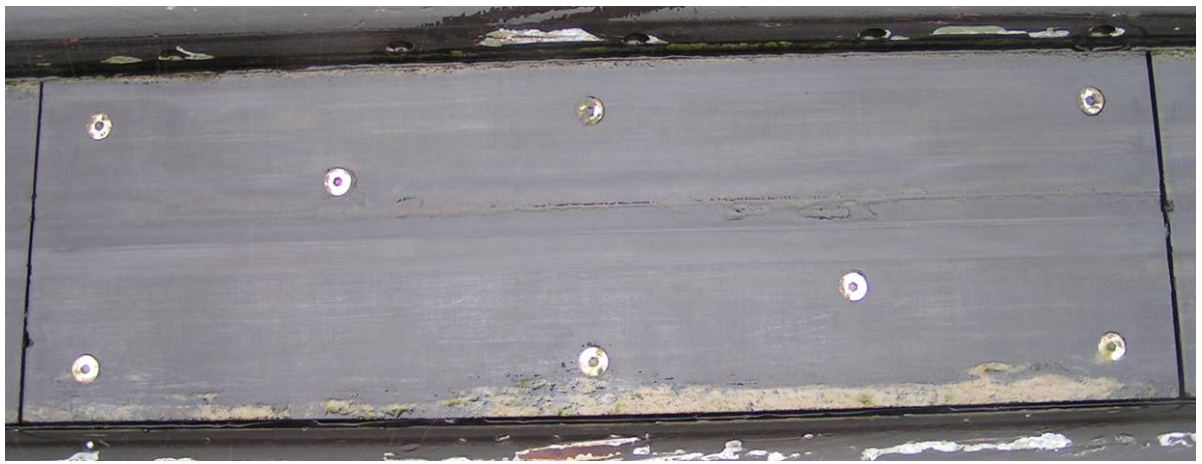
Corner Heights

A	0.58
B	-0.41
C	0.48
D	-0.65
Average height difference to next panel: 0.53	

Panel 15	
Corner Heights	
A	-1
B	-0.58
C	-1.2
D	-0.48
Average height difference to next panel: -1.1	

Panel 16	
Corner Heights	
A	0.38
B	1
C	0.04
D	1.2
Average height difference to next panel: 0.21	

**Panel 17**



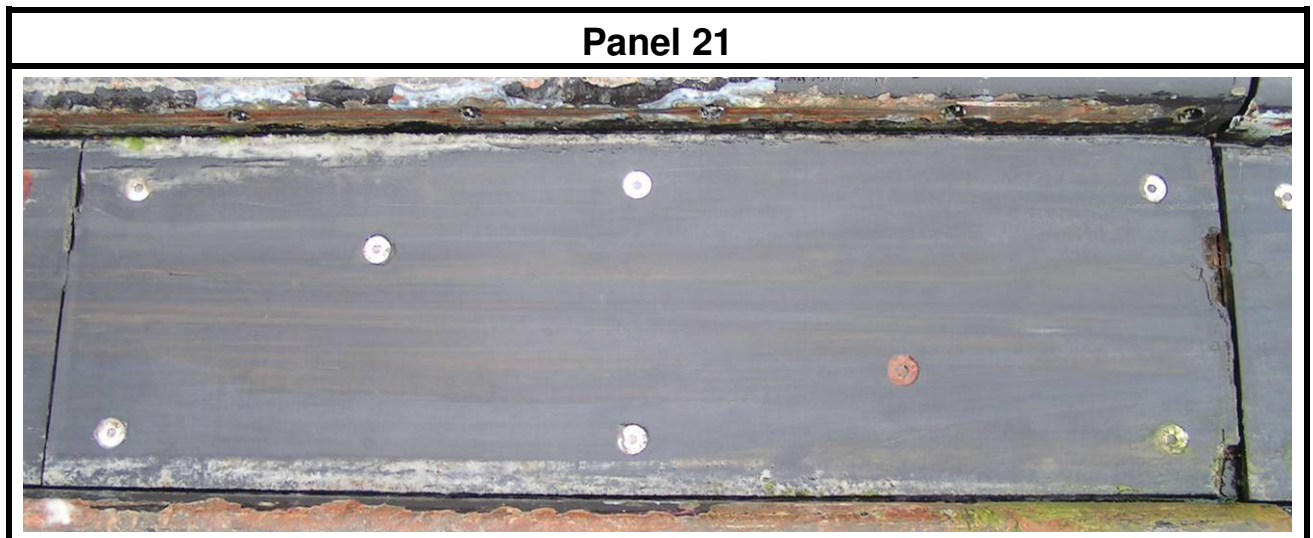
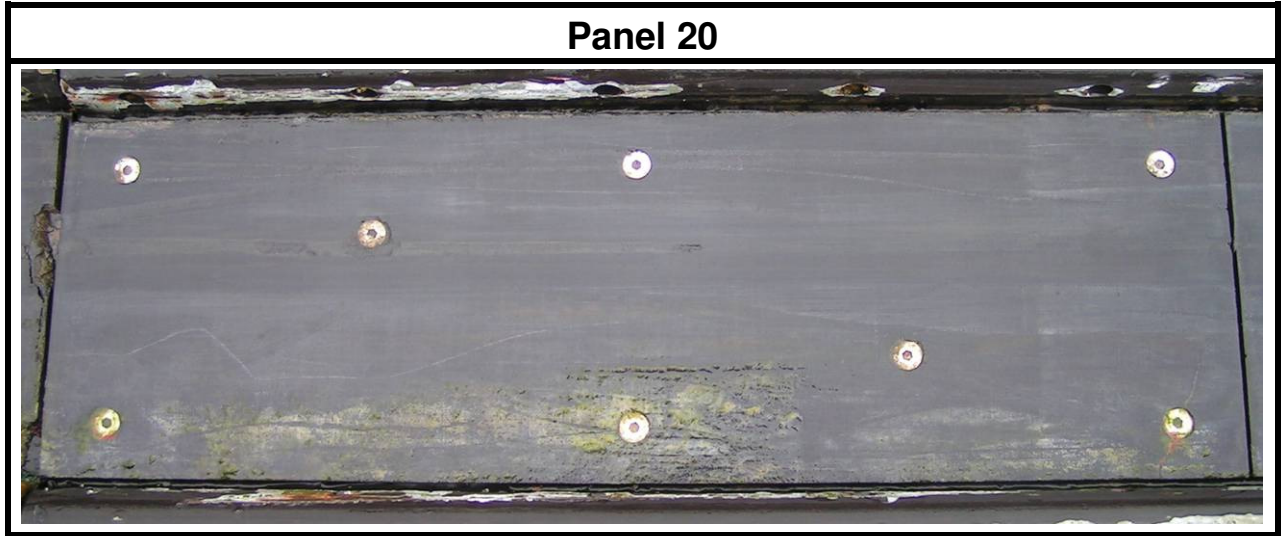
**Panel 18**



**Panel 19**







Misalignment Scenario	Padstow	Tenby	Total
% Parallel	62.50%	70.00%	66.67%
% Skewed	18.75%	23.81%	21.62%
% Angled	37.50%	30.00%	33.33%

Table E2: All panels misalignment scenarios



Panel No.	Average height difference to next panel (mm):	Mod. average height difference to next panel (mm):	Average distance to next panel (mm):	Panel end height difference*	Misalignment Scenario	Misalignment angle	Skewed A - C Height Difference	Mod. Skewed A - C Height Difference	Skewed?	Mod. Skew Angle
1	0.1	0.1	5.235	-0.34	Parallel	0.015967676	0.6	No	1	0.1
2	0.44	0.44	5.285				0.88	No	2	0.44
3	0.3	0.3	3.725	0.25	Parallel	0.011740939	-0.2	No	3	0.3
4	-0.05	0.05	5.585				-0.3	No	4	-0.05
5	4.055	4.055	7.49	3.92	Angled	0.184098231	-1.49	Yes	5	4.055
6	0.135	0.135	6.185				1.47	Yes	6	0.135
7	0.36	0.36	6.189	-0.245	Parallel	0.01150612	-0.34	No	7	0.36
8	0.605	0.605	4.785				0.33	No	8	0.605
9	0.685	0.685	5.895	-0.84	Angled	0.039449556	-0.47	No	9	0.685
10	1.525	1.525	7.33				1.45	Yes	10	1.525
11	0.48	0.48	4.04	-0.035	Parallel	0.001643731	0.06	No	11	0.48
12	0.515	0.515	4.645				0.15	No	12	0.515
13	0.53	0.53	4.885	0	Parallel	0	-0.24	No	13	0.53
14	0.53	0.53	5.47				0.1	No	14	0.53
15	-1.1	1.1	10.64	0.89	Angled	0.041797744	0.2	No	15	-1.1
16	0.21	0.21	5.64				0.34	No	16	0.21
17	No Data	No Data	No Data	No Data	No Data	No Data	No Data	No Data	17	No Data
18	No Data	No Data	No Data				No Data	No Data	18	No Data
19	No Data	No Data	No Data	No Data	No Data	No Data	No Data	No Data	19	No Data
20	No Data	No Data	No Data				No Data	No Data	20	No Data
21	No Data	No Data	No Data	No Data	No Data	No Data	No Data	No Data	21	No Data
22	No Data	No Data	No Data				No Data	No Data	22	No Data
Mean	0.5825	0.72625	5.814							
Max.	4.055	4.055	10.64							
Min.	-1.1	0.05	3.725							

\*0 implies parallel misalignment, integer implies angled misalignment

Table E3: Padstow Slipway Survey Data



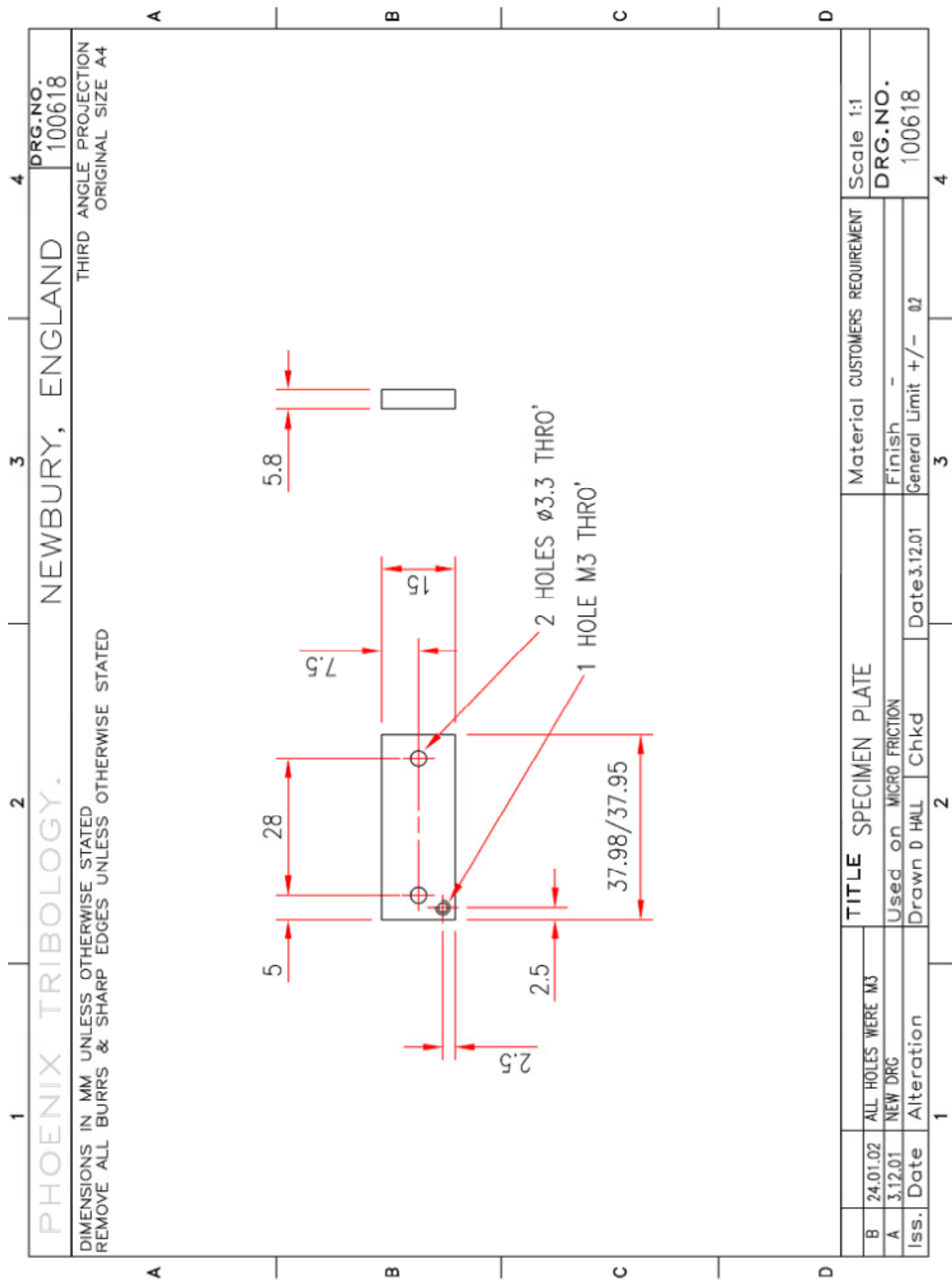


Fig. F2: TE57 Reciprocating Tribometer: Sample specification

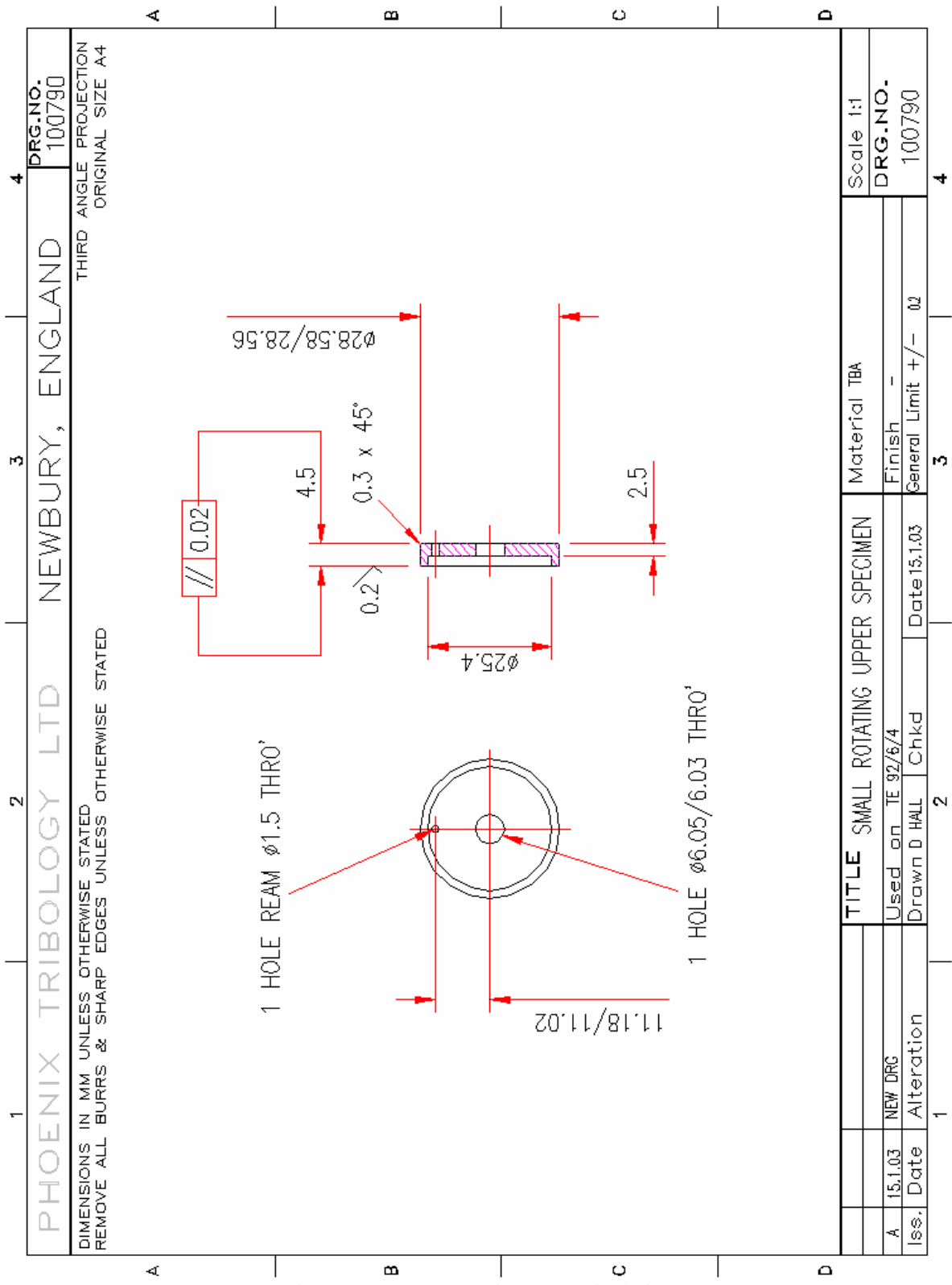


Fig. F3: TE92 Rotary Tribometer: Pin design

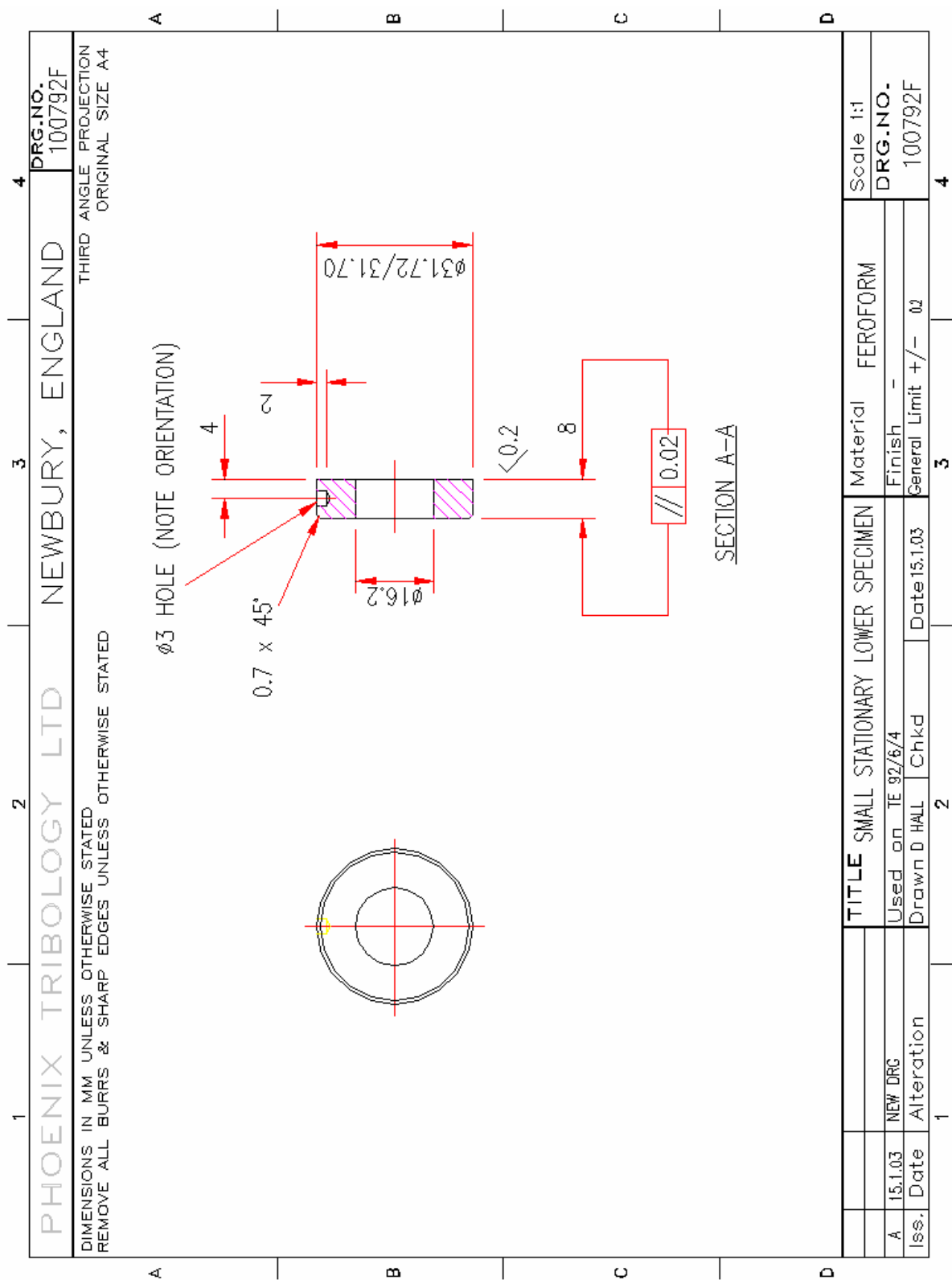
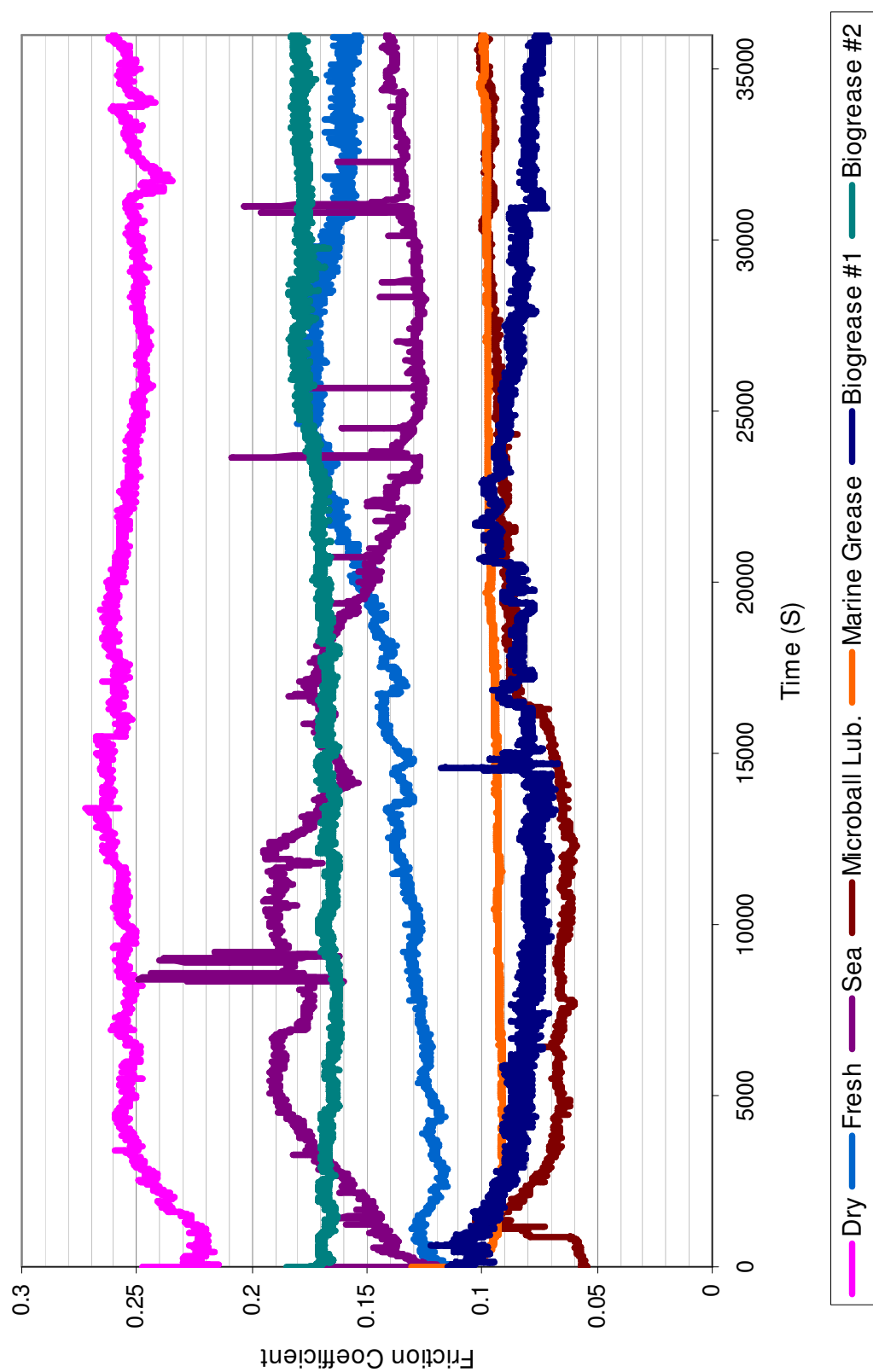
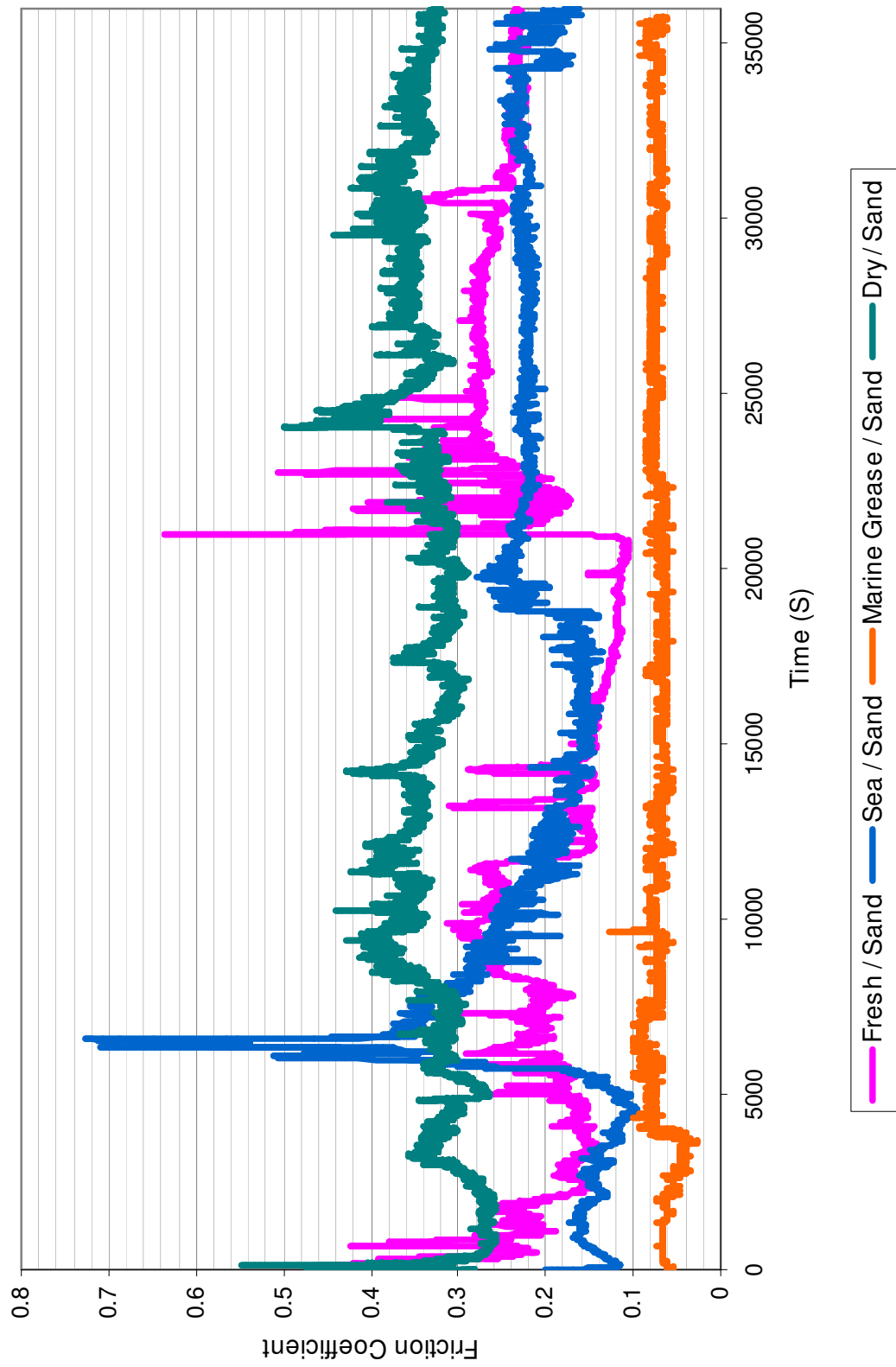


Fig. F4: TE92 Rotary Tribometer: Sample design

# G TRIBOMETER RESULTS







# H FINITE ELEMENT SIMULATION RESULTS

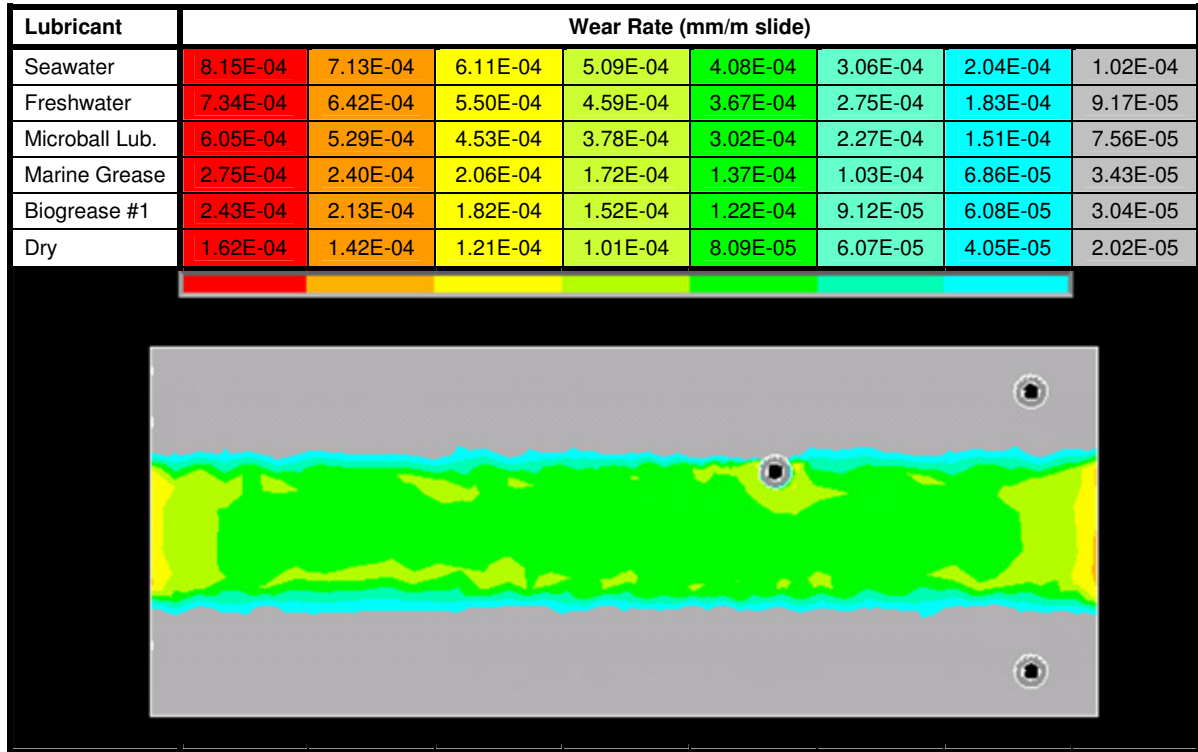


Fig. H1: Wear map for aligned contact conditions and various lubricants

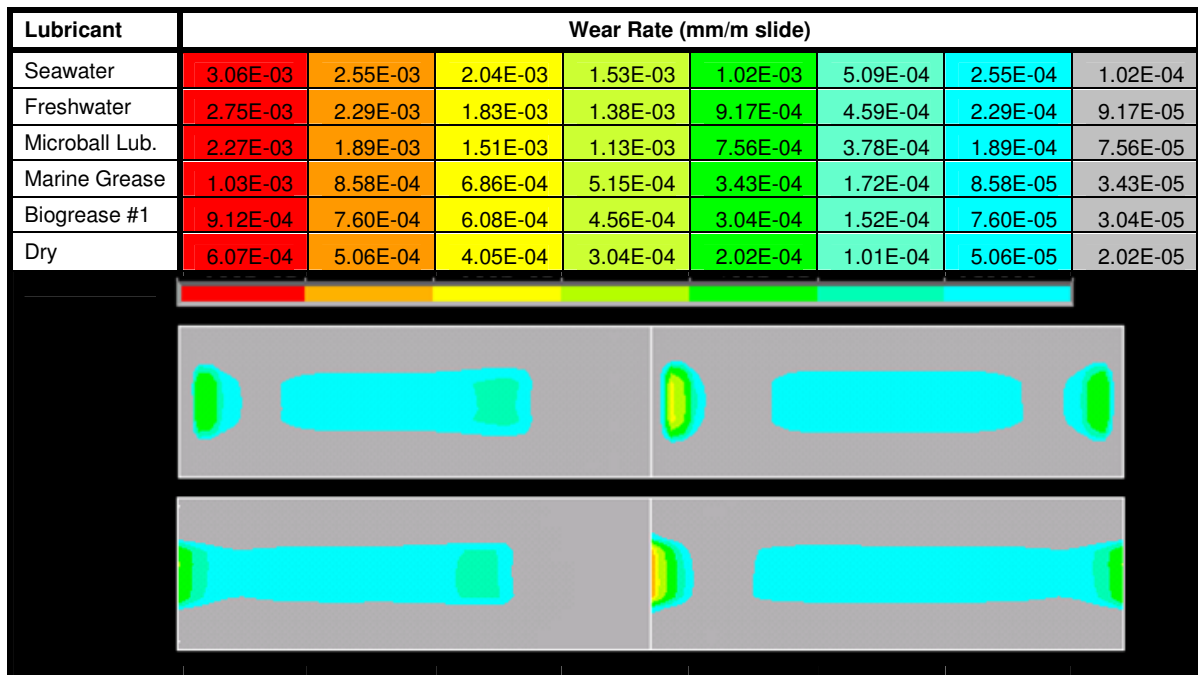


Fig. H2: Wear map for 1mm parallel offset – Chamfer panel (top), Original panel (bottom)

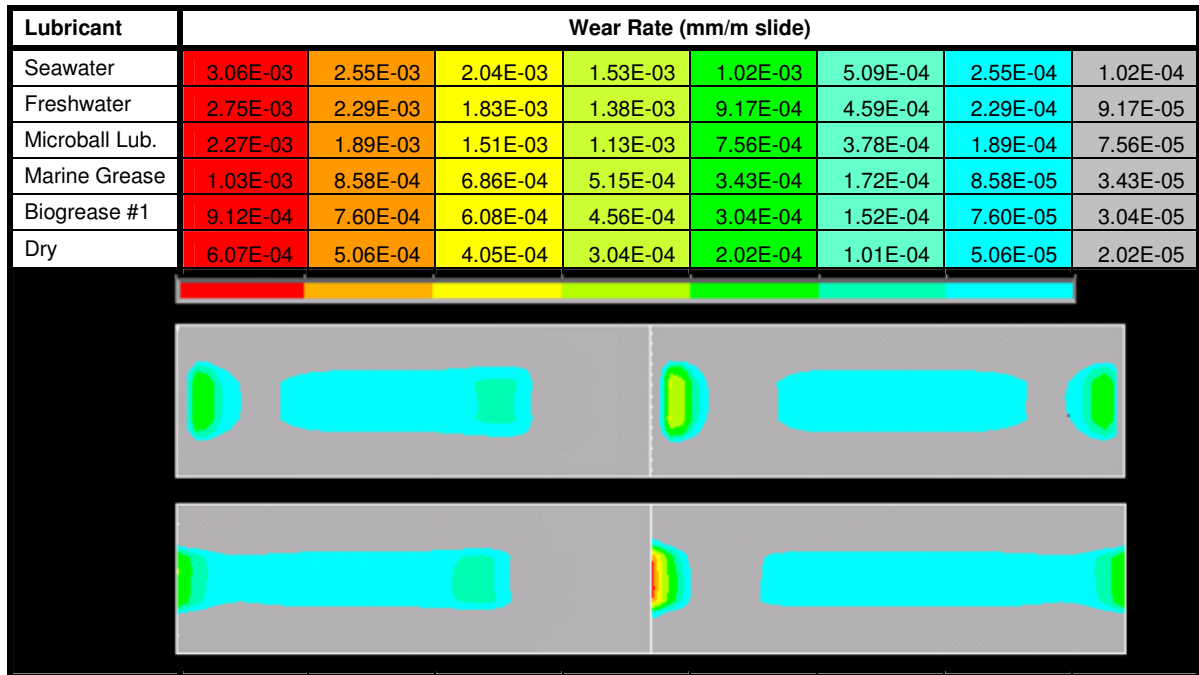


Fig. H3: Wear map for 1mm angled offset – Chamfer panel (top), Original panel (bottom)

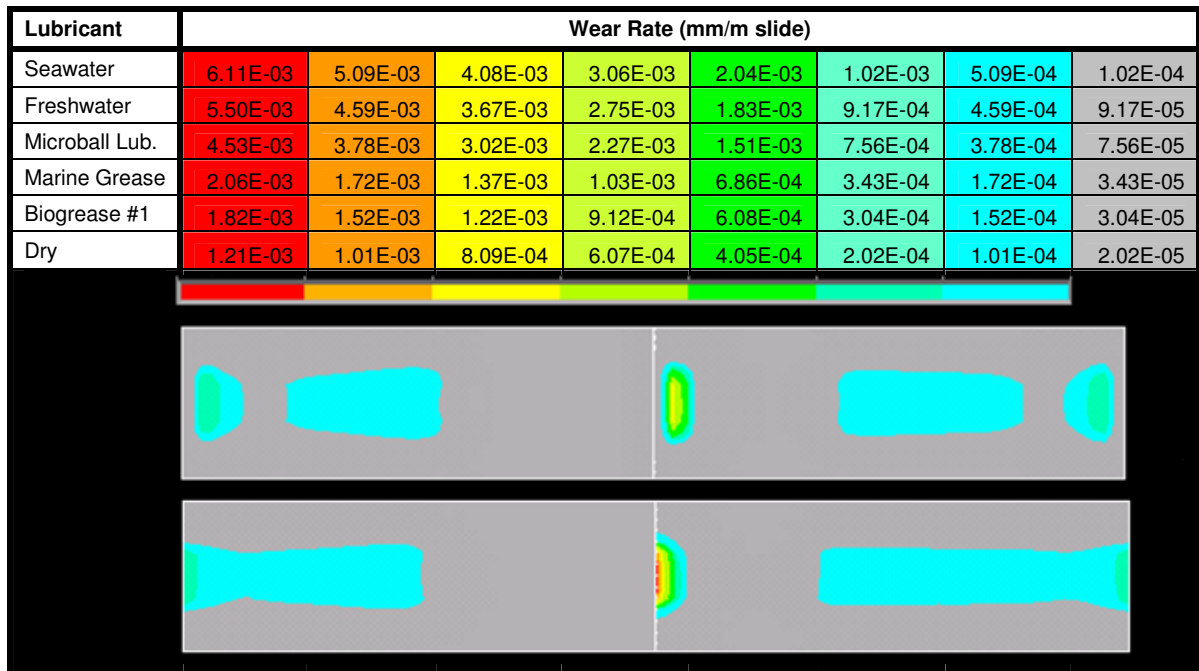


Fig. H4: Wear map for 5mm parallel offset – Chamfer panel (top), Original panel (bottom)

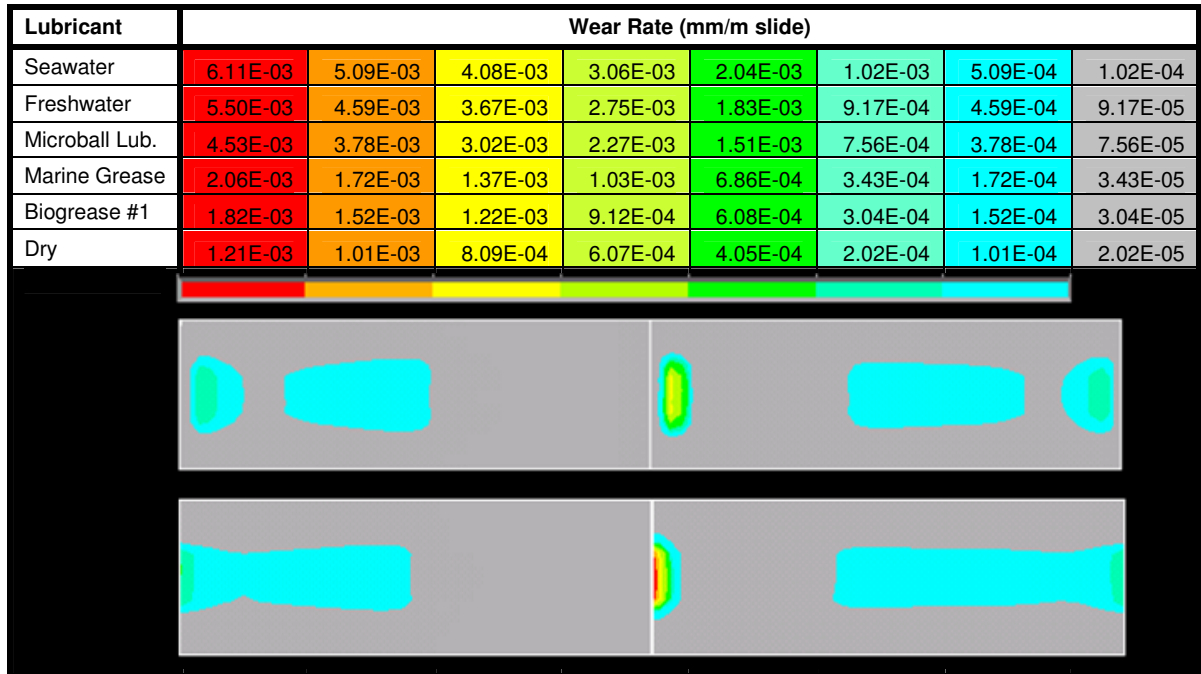


Fig. H4: Wear map for 5mm angled offset – Chamfer panel (top), Original panel (bottom)

## SLIPWAY PANEL WEAR CRITERIA

Slipway panel wear criteria is given here as a representation of panel surface area remaining. An example of how to assess real world panel surface area is shown below for a panel suffering severe delamination wear.

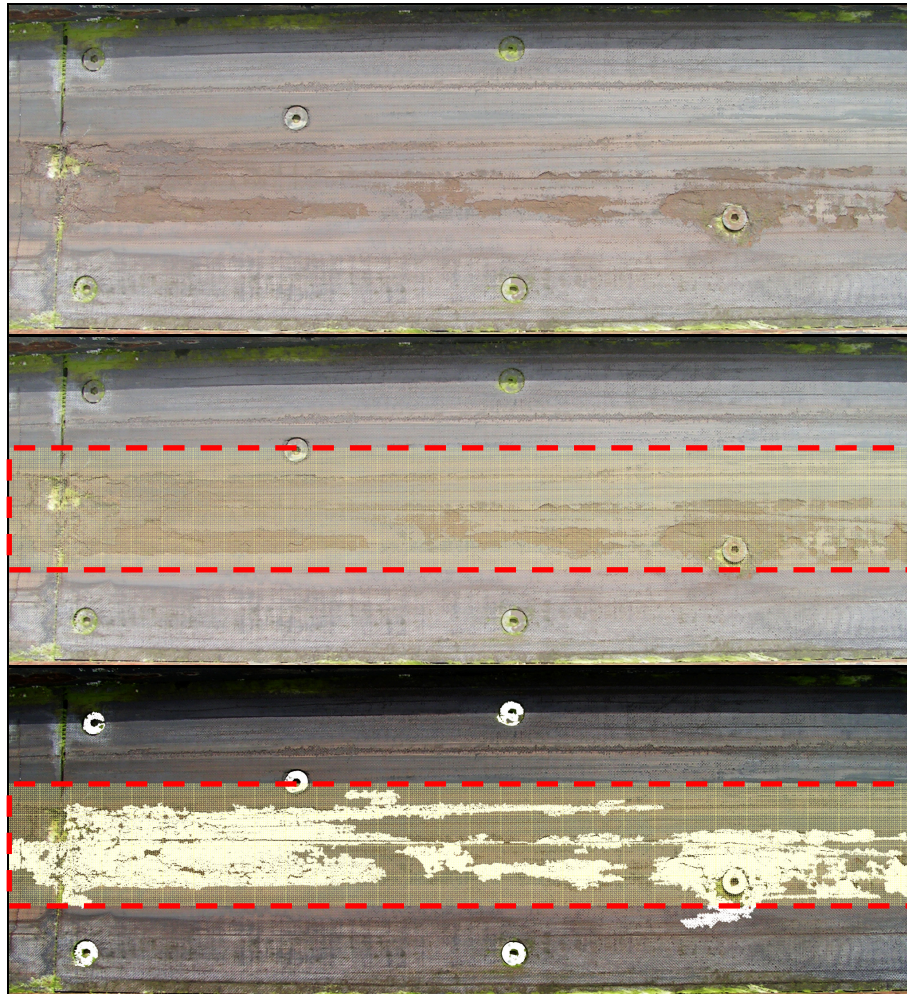
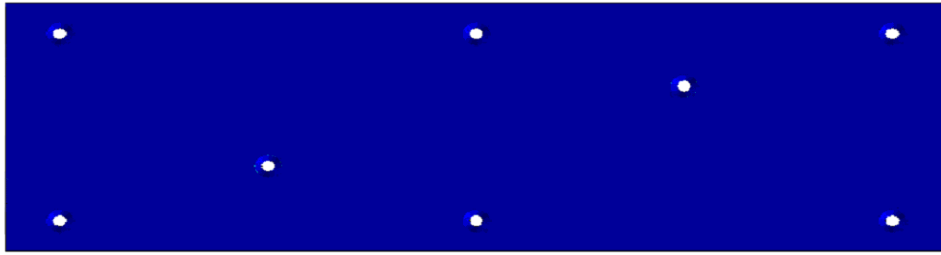
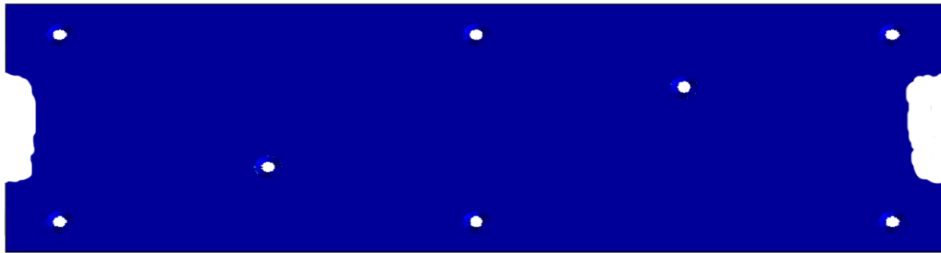


Fig. I1: Real world wear assessment – i.) original panel, ii.) panel bearing area (150mm wide central keel track), iii.)  
Worn surface discounted from panel bearing area

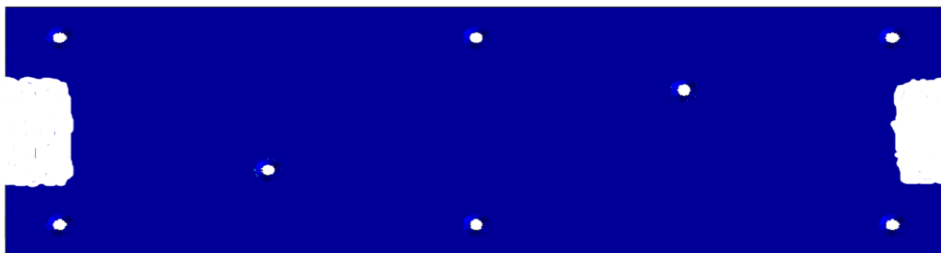
Here, the panel areas suffering delamination wear are discounted from the panel bearing area for assessment of panel condition. The images shown below represent guidelines for panel replacement based on remaining surface area for all preferred lubrication regimes and common slipway gradients. These images represent typical wear progression only; the variability of panel alignments and local conditions may mean that real world wear will vary considerably. Panel replacement criteria are also given as a percentage of the bearing area remaining allowing slipway panel assessment even when the wear scar may not match those shown here.



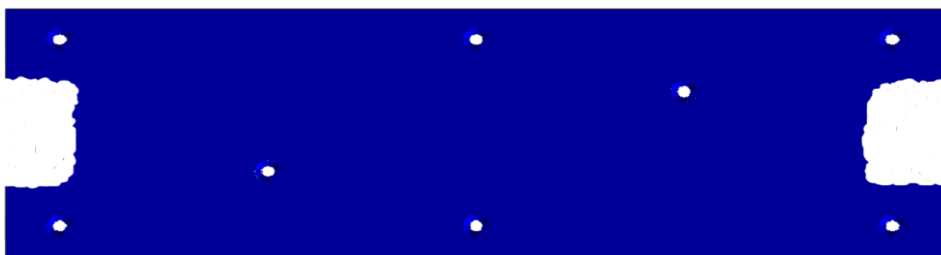
Original Panel 100%



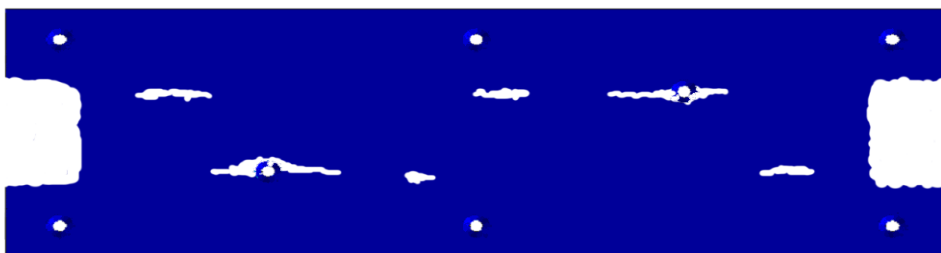
1 in 6 Gradient: Seawater Lubrication 93.31%



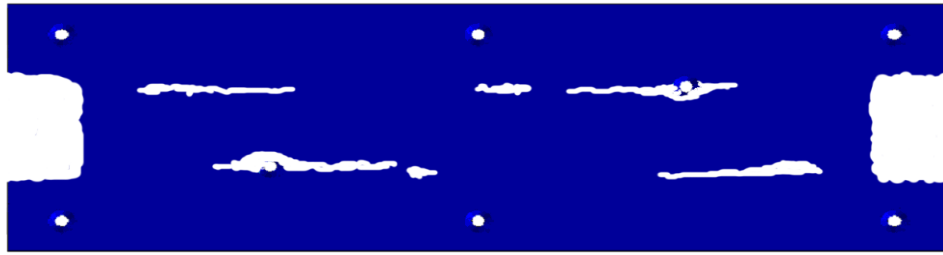
1 in 6 Gradient: Freshwater Lubrication 87.73%



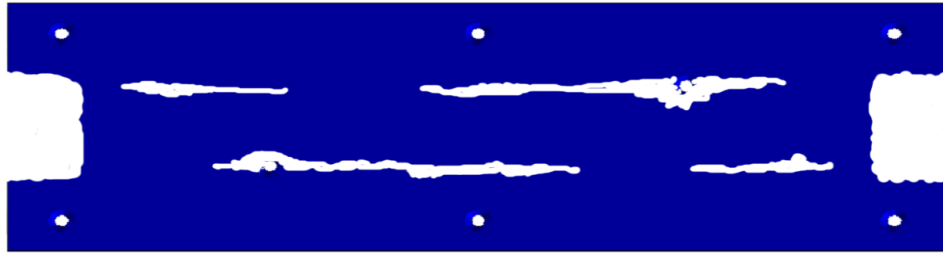
1 in 5.5 Gradient: Seawater Lubrication 85.54%



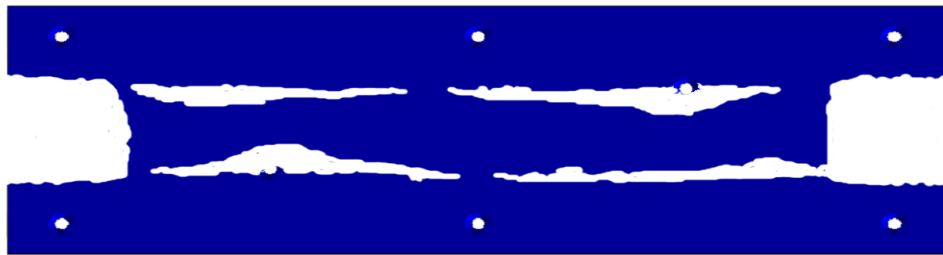
1 in 5.5 Gradient: Freshwater Lubrication 80.42%



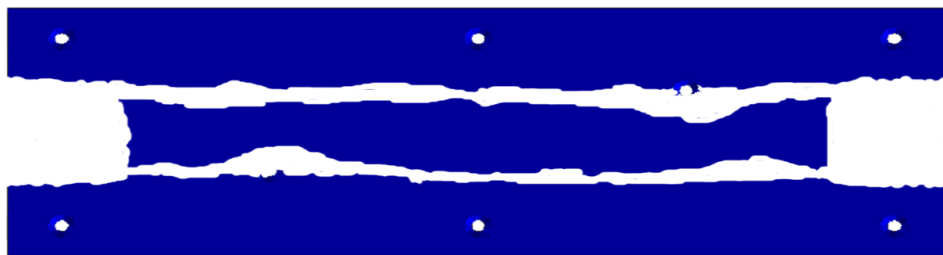
1 in 5 Gradient: Seawater Lubrication **77.76%**



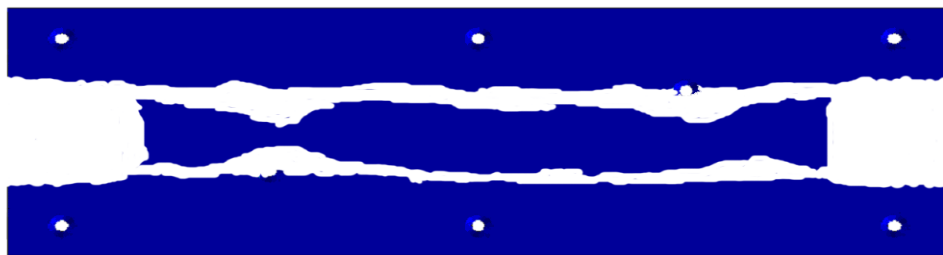
1 in 5 Gradient: Freshwater Lubrication **73.11%**



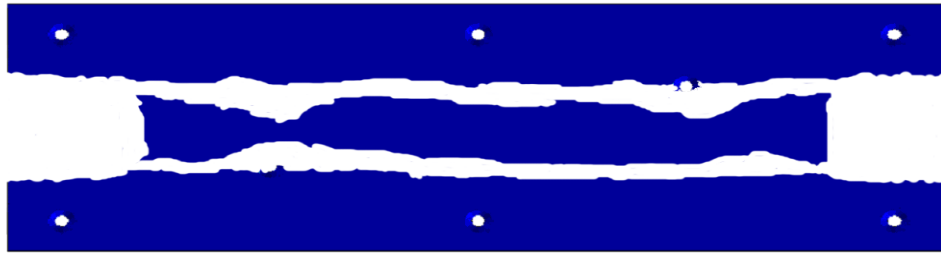
1 in 6 Gradient: Marine Grease Lubrication **57.18%**



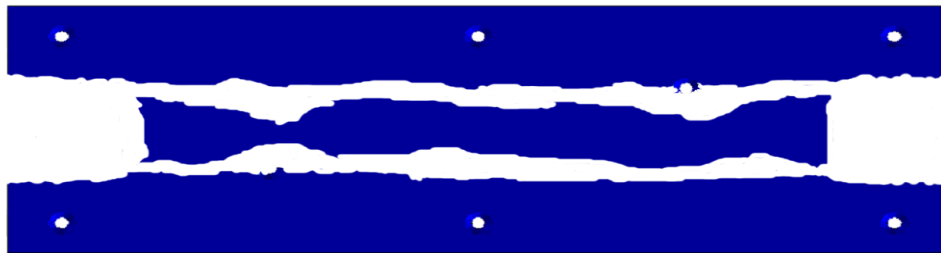
1 in 5.5 Gradient: Marine Grease Lubrication **52.41%**



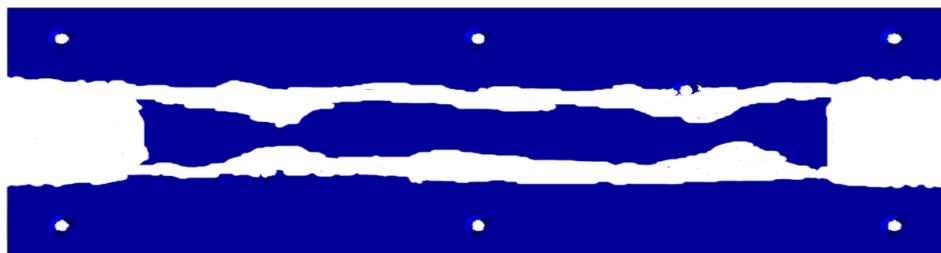
1 in 6 Gradient: Biogrease #1 Lubrication **50.53%**



1 in 5 Gradient: Marine Grease Lubrication      **47.65%**



1 in 5.5 Gradient: Biogrease #1 Lubrication      **46.32%**



1 in 5 Gradient: Biogrease #1 Lubrication      **42.11%**